INFORMATION TO USERS

This manuscript has been reproduced from the microfilm master. UMI films the text directly from the original or copy submitted. Thus, some thesis and dissertation copies are in typewriter face, while others may be from any type of computer printer.

The quality of this reproduction is dependent upon the quality of the copy submitted. Broken or indistinct print, colored or poor quality illustrations and photographs, print bleedthrough, substandard margins, and improper alignment can adversely affect reproduction.

In the unlikely event that the author did not send UMI a complete manuscript and there are missing pages, these will be noted. Also, if unauthorized copyright material had to be removed, a note will indicate the deletion.

Oversize materials (e.g., maps, drawings, charts) are reproduced by sectioning the original, beginning at the upper left-hand corner and continuing from left to right in equal sections with small overlaps.

Photographs included in the original manuscript have been reproduced xerographically in this copy. Higher quality 6" x 9" black and white photographic prints are available for any photographs or illustrations appearing in this copy for an additional charge. Contact UMI directly to order.

Bell & Howell Information and Learning
300 North Zeeb Road, Ann Arbor, MI 48106-1346 USA

UMI®
800-521-0600

WIND-INDUCED INTERFERENCE EFFECTS ON BUILDINGS - INTEGRATING EXPERIMENTAL AND COMPUTERIZED APPROACHES

Atul C. Khanduri

A Thesis

in

The Centre for
Building Studies

Presented in Partial Fulfilment of the Requirements
for the Degree of Doctor of Philosophy at
Concordia University
Montreal, Quebec, Canada

May 1997

ABSTRACT

Wind-Induced Interference Effects on Buildings - Integrating Experimental and Computerized Approaches

Atul C. Khanduri, Ph.D.
Concordia University, 1997

Wind-induced interference effects are caused by the presence of adjacent structures, resulting in an increase or a decrease in the wind loads on a building depending mainly on the geometry and arrangement of these buildings, their orientation with respect to the direction of wind and upstream exposure. A comprehensive analysis of literature underscores the seriousness of the problem whilst exposing the inadequacy of existing research efforts in explaining and solving the problems of wind interference. The overriding reason for this is the complex nature of the problem and the large number of variables involved, even for the basic two-interfering buildings situation.

The main aim of this research is to tackle the problem of interference in a systematic manner in order to establish a generalized set of guidelines that will be of practical use to building designers and planners. An extensive experimental program is developed to quantify interference effects and a methodology employing neural network representations is developed to model these effects, to define the complex relationships among the various parameters involved and to provide knowledgeable assistance to building designers.

Extensive wind tunnel experiments have been conducted to find the mean and fluctuating forces as well as their spectra on a building due to an adjacent building of small, medium and

large sizes, for several wind directions and various upstream exposure conditions, including city-centre situations. Interference effects are presented in the form of non-dimensional Interference Factors that represent the aerodynamic forces on a building with interference from an adjacent building, relative to the forces on a single free-standing building. The detailed experimental results have been analyzed and simplified to yield simple Interference Influence Grids, generalized guidelines and regression equations.

Finally, a database of experimental cases has been constituted and integrated with the qualitative knowledge-base developed during the course of this study, in order to provide valuable assistance to building designers at an early design stage. The database is used to model interference effects via a novel technique based on Neural Network representations. The methodology is capable of developing functional relationships among limited experimental data and documented cases. The ability of Neural Networks to generalize when presented with limited data makes them an attractive tool for knowledge acquisition on wind-induced interference effects for which there is no theory or empirical generalization at present. The developed knowledge-based design adviser is effective in analyzing wind interference situations and in suggesting suitable remedial measures to alleviate problematic interference effects.

To

My Parents

Acknowledgments

I wish to express my sincere appreciation and profound gratitude to Dr. Claude Bédard and Dr. Theodore Stathopoulos for their expert guidance, valuable suggestions and continued encouragement throughout the course of this study.

A special note of appreciation and thanks are due to fellow doctoral candidate and friend Mr. Suresh Kumar, for numerous valuable discussions and for his insightful and objective commentary on the evolving framework of this dissertation.

Thanks are also due to Dr. Patrick Saathoff and Dr. Hanquing Wu for many useful discussions and help during this study.

The technical craftsmanship of Messers Hans Obermeir, Joe Hrib and Joseph Zilka in the fabrication of the force balance and experimental models is deeply appreciated. Many thanks to Mr. Sylvain Bélanger for assistance with computer facilities.

The financial support provided by the Canadian Commonwealth Scholarship and Fellowship Plan and study leave granted by the University of Roorkee, Roorkee, India is gratefully acknowledged.

The spiritual, moral and emotional support, love and encouragement of my parents and brothers contributed immensely to my efforts.

Finally, a very special note of thanks to my wife Archana for her love, patience, encouragement and support and to my son Amit and daughter Pooja, for showing me how to look at the world around me with the wonder of a child.

Table of Contents

List of Figures

List of Tables

Nomenclature

A	projected area of building face normal to the direction of wind
BF	buffeting factor
b	width of square plan shaped principal building
	width of the building in the across-wind direction
b_i	width of the interfering building
b_p	width of the principal building
C	force coefficient for a particular interfering building location
$\overline{C}_d$	mean drag coefficient
$\widetilde{C}_d$	fluctuating drag coefficient
$\hat{C}_d$	peak drag coefficient
$\overline{C}_l$	mean lift coefficient
$\widetilde{C}_l$	fluctuating lift coefficient
$\hat{C}_l$	peak lift coefficient
C_{M_x}	moment coefficient in the across-wind direction
C_{M_y}	moment coefficient in the along-wind direction
$\overline{C}_p$	mean pressure coefficient
$\widetilde{C}_p$	root-mean-square pressure coefficient
$[C]_v$	cumulative force coefficient for a wind velocity of v

D width of the building in the across-wind direction

E evaluation factor

average mean square error

$|\overline{E}|$ mean absolute error

$|\hat{E}|$ maximum absolute error

E_f exposure factor

F activation or transfer function

$\overline{F}_d$ mean drag force

$\widetilde{F}_d$ fluctuating drag force

$\overline{F}_l$ mean lift force

$\widetilde{F}_l$ fluctuating lift force

f frequency

g statistical peak factor

h height of the building

h_i height of the interfering building

h_p height of the principal building

I interfering building model number

importance factor

IF interference factor

I_q input function for the qth hidden layer neuron

I_v longitudinal turbulence intensity of the approach wind at building height

i	number of input variables
	ith sector in a 16-direction compass
L_x	length scale of turbulence of wind in the longitudinal direction
l	length of the building in the along-wind direction
	number of training examples
M	modification factor
M_x	overturning moment in the across-wind direction
M_y	overturning moment in the along-wind direction
M_z	torsional moment
m	number of training iterations
N_i	number of input nodes
N_o	number of output nodes
N_{pat}	number of data patterns
N_{trn}	number of training patterns
n	frequency
	total number of sectors or compass directions
	number of outputs of each training example
n''	number of neurons in the output layer
O_{ij}	network output at the i^{th} output neuron of the j^{th} training example set
O_p	value of output for neuron p (input layer)
O_q	value of output for neuron q (hidden layer)
P	principal building model number

$\overline{P}$	local mean surface pressure
$\widetilde{P}$	root-mean-square of the fluctuating component of surface pressure
P_s	free stream static or atmospheric pressure
p_i	probability of wind speed exceedance for sector i
R^2	criterion used for evaluating "goodness of fit" of the model
R_v	auto-covariance
S	clear spacing between two buildings
	summation of the weighted inputs at each neuron
SF	shielding factor
$S(n)$	power spectral density of the longitudinal turbulence component of wind velocity
Sx	centre-to-centre distance between two buildings along the X-axis
Sy	centre-to-centre distance between two buildings along the Y-axis
s	normalized separation variable
T_{ij}	i^{th} output of the j^{th} training example set
t	time
U	free-stream mean velocity at the top of the building
v	wind velocity
$\bar{v}$	mean wind velocity at a given height
W_{qr}	value of weight of connection from neuron q in the hidden layer to neuron r in the output layer
W_{qi}	value of weight of connection from neuron q in the hidden layer to neuron i in the output layer

W_{pq} value of weight from neuron p in the input layer to neuron q in the hidden layer

$\bar{x}$ mean value of a random variable x

$\hat{x}$ peak response of a random variable x

y actual value of a variable

$\hat{y}$ predicted value of y

$\bar{y}$ mean of the y values

z height above ground

z_g gradient height

Greek Symbols

α power law exponent of the boundary-layer wind profile

δ_i error for neuron i in the output layer

δ_q error for neuron q in the hidden layer

δ_r error for neuron r in the output layer

θ incident wind direction,

η training rate coefficient

ρ density of air

σ_x standard deviation of x

σ^2 variance

τ time lag

$\bar{\tau}$ time scale of a random process

ω smoothing constant

Subscripts

d	drag
f	factor
g	gradient
i	interfering building
ij	*i*th neuron of *j*th training example set
l	lift
p	principal building
	pressure
	neuron *p*
pat	data patterns
pq	from neuron *p* to neuron *q*
q	neuron *q*
qi	from neuron *q* to neuron *i*
qr	from neuron *q* to neuron *r*
s	static or free stream
trn	training patterns
v	wind velocity
x	across-wind direction
	longitudinal direction
y	along-wind direction
z	height
10	10m height

Abbreviations

BPNN	Back-Propagation Neural Network
CAM	Conclusion-Analysis Module
CPU	Central Processing Unit
DCM	Data Collection Module
DEM	Data Evaluation Module
ESDU	Engineering Sciences Data Unit
GRNN	General Regression Neural Network
IIG	Interference Influence Grids
ISD	Interference Spectral Diagrams
KBS	Knowledge-Based Systems
MSE	Mean Squared Error
NN	Neural Networks
NETWIND	Hybrid knowledge-based design adviser for wind-induced interference effects
Rms	root mean square
SSE	Sum Squared Error

1

Introduction

1.1 Overview

The evaluation of wind loads on buildings is carried out mainly by using codes and standards, whose specifications are generally based on wind tunnel tests performed on isolated structures. In reality however, buildings seldom exist in isolation. It has been shown by several researchers that wind loads on buildings in realistic environments may be considerably different from those measured on isolated buildings. Neighbouring buildings may either decrease or increase the flow-induced forces on a structure, depending mainly on the geometry and arrangement of these buildings, their orientation with respect to the direction of flow and upstream terrain conditions. This effect, commonly known as interference, must therefore be properly assessed by designers and planners.

Wind Engineering Standards and Codes offer little guidance to the designer for assessing the effects of interference. In a study on the evaluation of wind loads acting on low-rise buildings in the presence of a large nearby building by Stathopoulos (1984a), comparisons with the National Building Code of Canada (NBCC 1985) and the ANSI Standard (ANSI 1982) show underestimation (up to 46%) or overestimation (up to 525%) of the code specifications, which are generally for isolated prismatic buildings. These results indicate that code recommendations may be significantly low (unsafe) or uneconomically conservative; therefore, the effect of adjacent structures on wind loads should be evaluated properly for realistic wind load design of buildings.

The problems arising out of the undesirable effects of interference have caused several cases of litigation. In a relevant lawsuit of Metropolitan Life Insurance Company vs. the Port Authority of New York and New Jersey, the World Trade Centre has allegedly caused "unusual, increased and unnatural wind pressures" on the plaintiffs' buildings nearby (Kwok 1989). Recognizing the importance of accounting for interference effects due to adjacent structures, the Australian Standard for Minimum Design Loads on Structures (SAA 1989) has incorporated a brief guideline on interference, but only as a general warning note: *".....The flow around any structure in a group will usually differ from that around a similar isolated structure leading to different forces.....Interference effects are prevalent in structures located less than 10b apart, where b is the dimension of the structure normal to wind....."*

Three main reasons appear to explain the lack of a comprehensive and generalized set of guidelines for wind load modifications caused by adjacent buildings. First, the complex nature of the problem even for a single additional building, since there are a large number of variables involved including the size and shape of buildings, their relative positions, wind direction and topographical conditions; second, the scarcity of adequate experimental data; and third, the widely held notion that wind loads on a building are expected to be generally less severe if surrounded by other structures than when it is isolated. This last reason, though quite applicable to a building surrounded by a large number of similar structures, becomes debatable where only two or three buildings interact, since several studies have shown quite adverse effects depending on the relative location of these buildings.

For several years now, researchers have strived with limited success to formulate a set of comprehensive and generalized guidelines to define wind load modifications caused by

adjacent buildings. There is a plethora of numbers generated as a result of specific wind tunnel experiments on wind-induced interference effects, but the efforts seem inadequate in light of the countless combinations of parameters involved. The present limited results, therefore, cannot be used to develop empirical relationships or generalized guidelines that may be directly helpful to the structural design practitioner. Since there is little practical utility in these results, it is imperative to tackle the interference problem in a systematic manner in order to come up with a generalized set of guidelines that will be of practical use to building designers and planners.

1.2 Objectives and Scope

With a view of bringing into perspective the significance of the problem as well as past and present research efforts in this area, data collected through literature has been analyzed to identify common points of agreement and areas of concern. However, the analysis has also found large gaps and lack of coherence among the results of various studies. Whilst there is proprietary information on interference effects from specific projects, little of a general nature is available to the designer.

A computer-based approach is therefore undertaken combining systematic experimental results on wind-induced interference effects with artificial intelligence techniques to provide valuable assistance to designers at an early design stage. As shown in Figure 1, a three-stage integration process is proposed to integrate experimental and computerized approaches for a generalized assessment of interference effects. As apparent from Figure 1, the main objectives of the research can be briefly stated as follows:

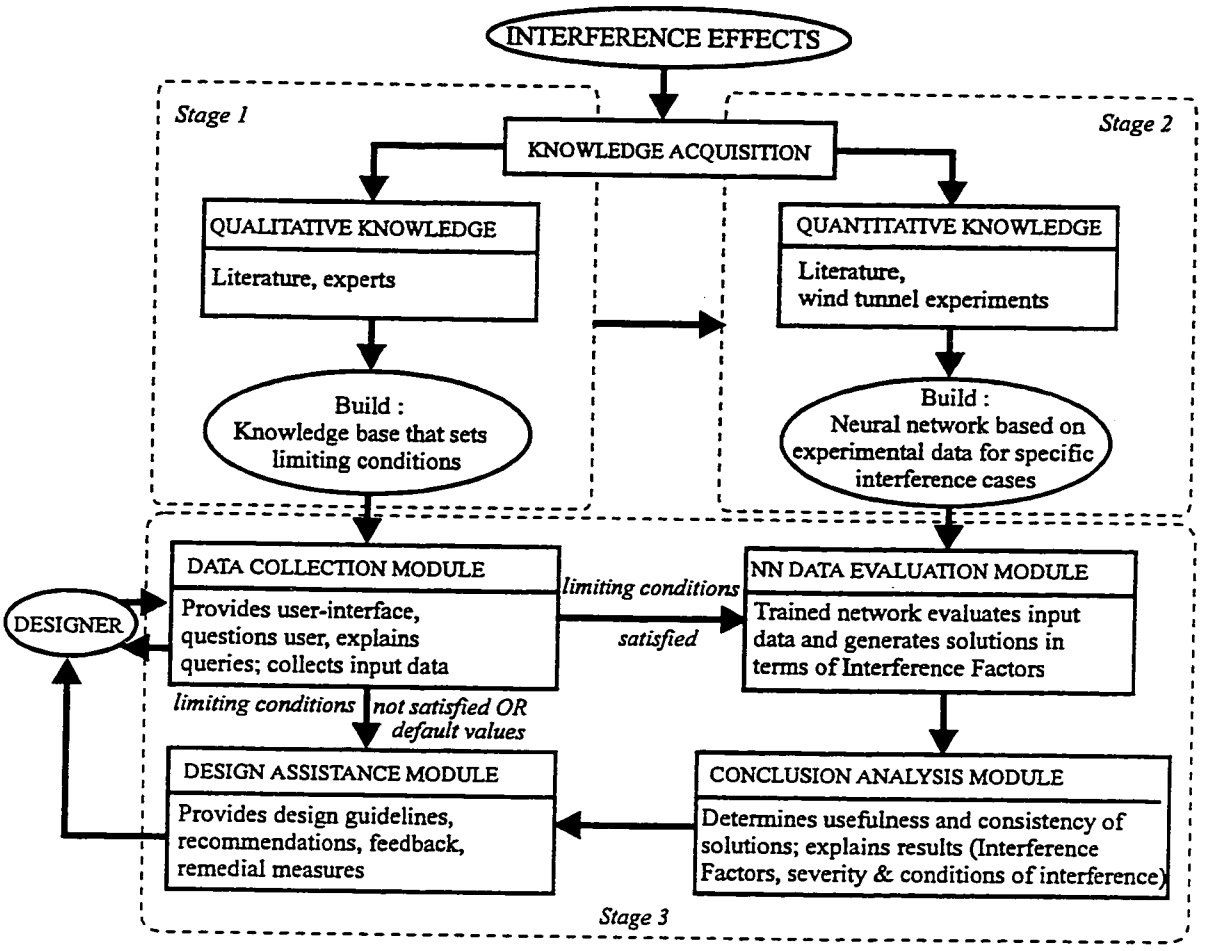

Figure 1. Schematic of the proposed integrated wind design adviser.

- *Knowledge acquisition through literature*: Undertake a detailed and up-to-date review of the existing knowledge on wind-induced interference effects in order to identify the extent of the problem, the past research efforts and to gather the qualitative and quantitative knowledge available.
- *Data acquisition through wind tunnel experiments*: Undertake a detailed and systematic study on interference effects including measurements of aerodynamic forces with the help of extensive wind tunnel experiments on scale building models. Analyze the

database thus generated to develop an empirical model that will provide equations, graphs and contours and general guidelines to evaluate interference effects.

- *Development of a hybrid Knowledge-Based System for design assistance*: Generalization and classification of the relevant knowledge for building design applications and to develop a hybrid knowledge-based adviser for interference effects combining neural networks and knowledge-based systems technology.

The scope of investigation is limited mainly to two adjacent buildings having square plan shape with interfering buildings of various dimensions so as to encompass a general category of relative building sizes. Experiments have also been conducted incorporating the effects of immediate surroundings simulating a "city-centre" situation. Several factors influenced the selection of building geometries and configurations to be tested in the wind tunnel. It is common knowledge that fabricating models for wind tunnel testing and the testing itself can be a time consuming process. Therefore, to derive maximum information from a limited number of wind tunnel experiments, limiting conditions were set up based on an extensive review of prior research and exploratory tests, thus avoiding parameters of little influence.

On the qualitative level, most concepts applied to and conclusions derived from the study of interference effects between two buildings will pave the way for a better overall understanding of the phenomenon of interference. The scope, although focusing on specific configurations, includes the essential characteristics of wind flow around bluff bodies that could be used for other building configurations as well. On the quantitative level, it is expected that the proposed neural network model would help derive the extent of interaction, i.e., generalize the results including cases not tested in the wind tunnel. The use

of knowledge-based approach for organizing and relating the qualitative and quantitative information would prove a useful and practical "design adviser" at preliminary design stages.

1.3 Research Outline

A detailed analysis of previous studies reveals a lack of generality in the results. Eventhough most previous work on wind-induced interference effects deals with specific building configurations and situations, some basic knowledge can be extracted from a thorough analysis of the literature results which will eventually pave the way for further research investigations. An extensive experimental programme is thus developed to study the wind flow mechanisms and to quantify the extent of wind load modification on buildings due to interference effects. Based on these results, general guidelines and limiting conditions are formulated and remedial measures suggested.

On the basis of an analysis of the literature results, a preliminary framework for the experimental programme is set up, basically by excluding cases that the majority of studies have found to be relatively insignificant with regards to interference effects. For example, the effect of a shorter upstream building can be disregarded on a taller downstream building. On the other hand, certain factors like the spacing between adjacent buildings and their relative arrangement constitute the most important parameters influencing interference effects and are considered accordingly. The entire experimental programme is divided into two categories: exploratory or pilot tests and detailed experiments. All measurements are carried out at the Building Aerodynamics Laboratory of the Centre for Building Studies, Concordia University.

Exploratory tests are designed mainly to provide a quick, preliminary estimate of the extent of interference that would eventually form the basis of the detailed experiments. These tests also help verify some of the literature results. A simple three-component strain gauge force balance has been fabricated and carefully calibrated to measure the along-wind drag and across-wind lift forces as well as the torsional moment about the vertical axis of the building. Measured forces on a building due to interference from an adjacent building are compared with those on an isolated building.

Detailed tests may provide an accurate and adequate measure of the interference effects. This is done with the help of a "pressure model" that consists of a plexiglass model fitted with several pressure tappings uniformly distributed on each of its four walls. Pressure measurements are carried out by using pressure transducers. The digitization of pressure signals and analysis of the data is done by a Data 6000 Waveform Analyzer.

To obtain a trend of the variation of interference effects with the size of the upstream building, experiments are conducted with interfering building sizes (width and height) equal to 2/3, 1.5 and 2 times that of the principal building. Some cases are also subjected to further wind tunnel experiments for several wind directions and for simulated suburban and urban upstream approach terrain conditions. In addition, experiments have been conducted to obtain an assessment of the interference effects on a building due to its immediate surroundings, simulating a "city centre" situation.

Finally, a database of experimental cases is constituted in order to provide valuable assistance to building designers at an early design stage. The database is used to model interference effects via a novel technique based on Neural Network representations, capable of developing functional relationships among limited experimental data and documented

cases. The ability of Neural Networks to generalize when presented with limited data makes them an attractive tool for knowledge acquisition on wind-induced interference effects for which there is no acceptable theory or empirical generalization at present.

1.4 Thesis Organization

The remainder of the thesis is divided into eight chapters. Chapter 2 elaborates on some background information and provides a context for discussion and research investigation in the remainder of the thesis. Prior research in the area of wind-induced interference effects and the potential applications of artificial intelligence technology to wind engineering problems are critically examined and avenues for improvement are suggested. These avenues serve as part of the motivation for the proposed research. Chapter 3 presents details on the experimental methodology used in this investigation. It explains the experimental set-up, fabrication of the models and the force balance, as well as details of the wind tunnel and the data acquisition process. Chapter 4 contains the results of the exploratory interference effects tests that provide a basis for detailed experiments. Chapter 5 presents the results of detailed wind tunnel experiments on an isolated building model. Chapters 6 and 7, containing the results of detailed interference effects experiments, form the core of the dissertation. Chapter 6 presents results for interference between two similar buildings and chapter 7 presents the results of the detailed parametric study. The experimental results are analyzed and discussed in detail vis-à-vis the interference mechanism. Chapter 8 rounds up all the data and knowledge gathered in this study to develop a hybrid Knowledge-Based Design Adviser that includes knowledge acquisition and modelling of interference effects through neural networks. The ninth and the final chapter provides concluding remarks and a

summary assessment outlining the task accomplished, important contributions made and future research directions.

May Vāyu (the Wind god), lord of firmament, protect me. In this pursuit for knowledge, in this righteous and duty bound action, in this sacerdotal undertaking, in this honourable and noble cause, in this state of consciousness, in this dedication and determination, in (following) this code of conduct and self control, and in this great assembly of elite scholars; may I receive your blessings.

- Atharv Veda, Book V, Hymn 24(8), 1500B.C.

2

Prologue

This chapter aims at providing a critical review of the research developments on wind-induced interference effects on buildings (Khanduri et al. 1997a). Although several studies have assessed the effects of interference on the velocity distribution around buildings, this research deals primarily with wind load modifications due to interference effects. Most of the previous studies have dealt with a specific configuration and some repetitions, differences of view points and emphasis are inevitable. The objectives of this review are to trace a historical summary of the relevant material, to describe, compare and evaluate the available experimental data in order to identify common points of agreement and areas of concern, to formulate on this basis general guidelines and limiting conditions, and finally to suggest methodologies to strengthen and broaden the scope of research on wind-induced interference effects. Interference mechanisms are discussed in detail vis-à-vis the experimental results of various studies.

2.1 A Historical Perspective

Wind-induced interference effects on buildings are not a recent concern; the earliest quoted work related to interference effects dates back in the thirties. Through extensive wind-tunnel experiments, Harris (1934) found that torque on the Empire State building in New York would be doubled if two building blocks were built across the two streets adjacent to the building. Almost a decade later, Bailey and Vincent (1943) attempted to determine general relationships between wind-speed and the distribution of wind-pressure over sloped, flat and stepped roofed

buildings, both under fully exposed conditions and when in close proximity to other buildings. This indeed was a bold step at that time, considering that research on wind effects in the first half of the twentieth century was just broadening in scope to include most areas now identified as part of wind engineering such as topographic effects on wind velocity distributions, wind forces on buildings and the boundary layer concept. For the following two decades or so, wind engineering research and consequent generalizations and codification of wind effects on buildings were completely focused on the "single building" and Bailey and Vincent's marvellous foresight in generalizing interference effects was put in cold storage.

The resurrection of interference effect studies occurred in the early seventies. This sudden interest could perhaps be traced back to the collapse of three out of the eight natural draft cooling towers at Ferrybridge, England in 1965, which was attributed to interference effects (Armitt 1980). Studies on interference effects began in real earnest with a series of simple, exploratory tests (Kelnhofer 1971, McLaren et al. 1971 and Lee and Fowler 1975). These involved two rigid square or rectangular building models, one serving as the instrumented test model, and the other as the adjacent building model. The models were tested in simulated open-country terrain, in simple tandem or side-by-side arrangement. Only mean pressure measurements were made but this was enough to highlight the seriousness of interference effects. This effort gathered momentum in the second half of the seventies, when researchers began using aeroelastic models for interference tests to measure dynamic moments (Melbourne and Sharp 1976 and Saunders and Melbourne 1979). Perhaps for the first time it was found that one of the most important aspects of the interference problem was the substantial increases in the maximum torsional moment, which could be more than three times that measured on the isolated building model (Blessmann and Riera 1979 and Ruscheweyh 1979). In addition to the open-country exposure, building models were tested in simulated suburban and urban

exposures. As one would expect, open-country exposure gave the most adverse interference effects (Melbourne and Sharp 1976). Another development was the study of interference effects on a large group of buildings (Soliman 1976). This indeed was a daunting task, given the complexity of building arrangements and the complex nature of wind; nevertheless, the findings contributed to our knowledge and understanding of the interference mechanism due to the grouping effects of buildings.

The eighties saw a spate of publications encompassing a wide range of issues on interference effects. It was conclusively proven that interference was indeed a major problem which could reduce or significantly increase wind loads on a structure. Attention was therefore focused on interference effect studies vis-à-vis the existing codal provisions (Stathopoulos 1984a). Attempts were also made to suggest ways to codify these effects (Holmes and Best 1979, Bailey and Kwok 1985 and Kwok 1989), which met with some success when the Australian Standard for Minimum Design Loads on Structures (SAA 1989) incorporated detailed shielding factors and buffeting contour maps as a very general interference effects guideline for designers. English (1985) explored the possibility of deriving a broadly applicable quantitative description of shielding provided by an upstream building based on the results of previous studies. There were detailed studies on the characteristics of fluid forces acting on buildings and the flow pattern around them under conditions of interference (Sakamoto et al. 1987 and Sakamoto and Haniu 1988). Interference effects due to a large group of low-rise buildings received considerable attention (Hussain and Lee 1980). In addition to the usual cuboidal building models, models of various shapes (Thoroddsen et al. 1985) and roof slopes (Wiren 1983 and Stathopoulos 1984a) were tested for interference. The measurements were more detailed, with studies reporting mean and fluctuating pressures, moments, structural response and load spectra as well.

The research momentum of the eighties has been carried well into the nineties. In the initial half of this decade (1990-1995) research on interference effects has developed both in substance and number of applications, and research activity has been phenomenal. Work has continued on previous thrust areas such as shielding effects of upstream buildings (English 1990 and English 1993), aerodynamic interference due to tall buildings (Taniike 1991, Taniike 1992, Yahyai et al. 1992 and Zhang et al. 1994), interference effects due to groups of buildings Tsutsumi et al. 1992, Jozwiak et al. 1993 and Holmes 1994) and flow visualization studies to explain the phenomenon of interference (Gowda and Sitheeq 1993). New and innovative research directions include the study of interference from a statistical point-of-view (Ho et al. 1990), suggestion of factors of safety to cover amplification of member stresses or forces due to interference effects (Sanni et al. 1992), torsional response of eccentric tall buildings under conditions of interference (Zhang et al. 1993), computation of wind flows around tall interfering buildings using a steady-state k-ε model of turbulence (Paterson and Papenfuss 1993), and the modelling of interference effects using artificial neural networks (Khanduri et al. 1995a).

2.2 Interference Mechanism

There are many parameters which effect the manner in which one building modifies the forces on another building in its vicinity. These are: size and shape of the building, wind velocity and direction, type of approach terrain and above all, the location and proximity of neighbouring buildings. To understand the effect of adjacent buildings on wind loads, it would be worthwhile to examine the wind flow mechanism around a single building and then see how it is modified

by bringing an additional building in the vicinity. To keep matters simple, cuboidal shaped buildings with wind approaching normal to a face and the resulting mean pressures are considered.

In the case of wind flow around an isolated building, the windward walls are subjected to positive pressure due to the direct impact of wind; negative pressure (suction) is generated on the other three walls and roof due to separation of flow around the edges of the building. To enable the data obtained from wind tunnel tests on scale models to be applied directly to the prototype, surface pressure values on the building model are reduced to non-dimensional pressure coefficients by referencing them to the mean dynamic velocity pressure $(1/2)\rho U^2$ (where ρ is the density of air and U represents the free-stream mean velocity at the top of the building). Thus, non-dimensional mean pressure coefficient, $\overline{C}_p$ is defined as,

$$\overline{C}_p = \frac{\overline{P} - P_s}{\frac{1}{2}\rho U^2} \tag{2.1}$$

and the root-mean-square pressure coefficient, $\widetilde{C}_p$ is defined as,

$$\widetilde{C}_p = \frac{\widetilde{P}}{\frac{1}{2}\rho U^2} \tag{2.2}$$

where, $\overline{P}$ = local mean surface pressure; P_s = free stream static or atmospheric pressure and $\widetilde{P}$ = root-mean-square of the fluctuating component of surface pressure.

Figure 2.1 shows a sketch of streamlines around a single isolated building and the resulting mean pressure distribution, $\overline{C}_p$ at approximately 3/4 of the building height from the ground (Baines 1963).

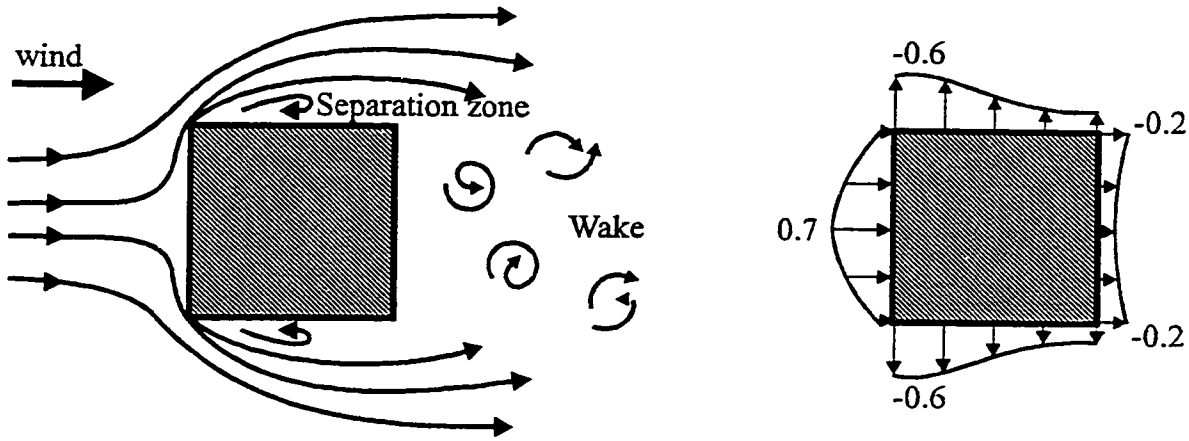

(a) Flow pattern around a building

(b) Mean pressure ($\overline{C}_p$) distribution (Baines 1963)

Figure 2.1 Wind loading on an isolated building.

With the inclusion of another building in the vicinity, the loading pattern becomes quite complex. The buildings may experience increased or reduced wind loads depending upon their geometries, spacing as well as the characteristics of wind flow and upstream terrain. Figure 2.2 shows the modification of the streamlines due to an adjacent building and the resulting pressure distribution at the base around these buildings (Taniike 1991). In this particular case, the wake of the upstream building is considerably disturbed by the downstream building and a part of the shear layer is greatly accelerated around the inner side wall of the downstream building. This results in an increase in the negative pressure (suction) on the inner side wall of the downstream building and the generation of a net inward lift. Sakamoto and Hanıu (1988), Taniike (1992) and Gowda and Sitheeq (1993) have performed flow-visualization around a pair of buildings to study the flow pattern generated due to interaction effects.

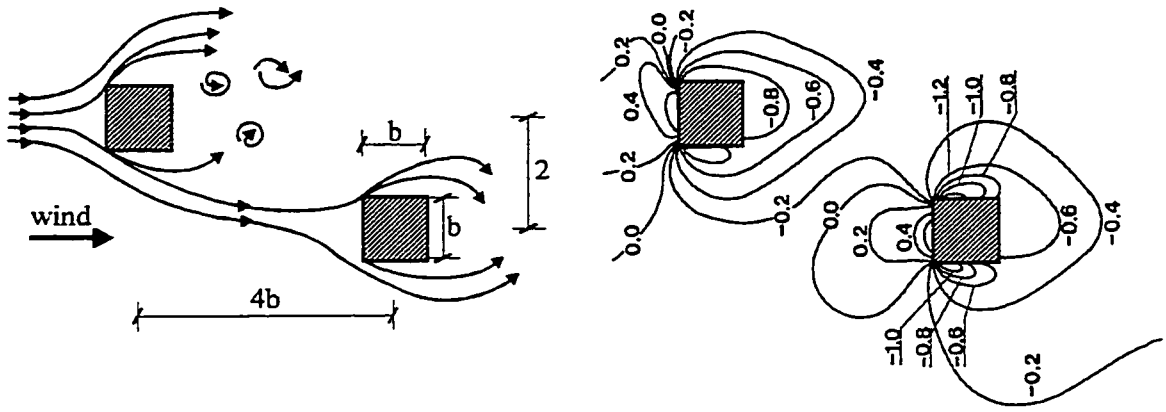

(a) Flow pattern around twin buildings

(b) Mean pressure distribution around the base (Taniike 1991)

Figure 2.2 Wind loading on two adjacent buildings

Figure 2.3 shows flow-visualization results taken from Gowda and Sitheeq (1993) for a single tall building model and for building models in tandem arrangement. It can be seen from Figure 2.3(b) that when the clear spacing between the models is small, the downstream model is completely submerged by the shear layers emanating from the upstream model, thus undergoing high suction on all its exposed faces. With an increase in the spacing between the two models, these shear layers direct towards the front face of the model, resulting in an increase in the pressure distribution on the front face of the downstream model. At a further increase in the clear spacing between the two models, the influence of the wake of the upstream model on the front face of the downstream model tends to diminish and the downstream model approaches the behaviour of an isolated free-standing model as shown in Figure 2.3 (c).

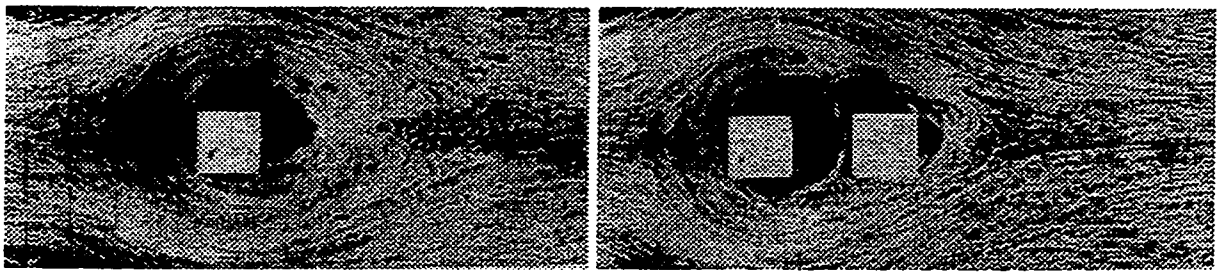

(a) Isolated building model (b) Two building models at a clear spacing of b

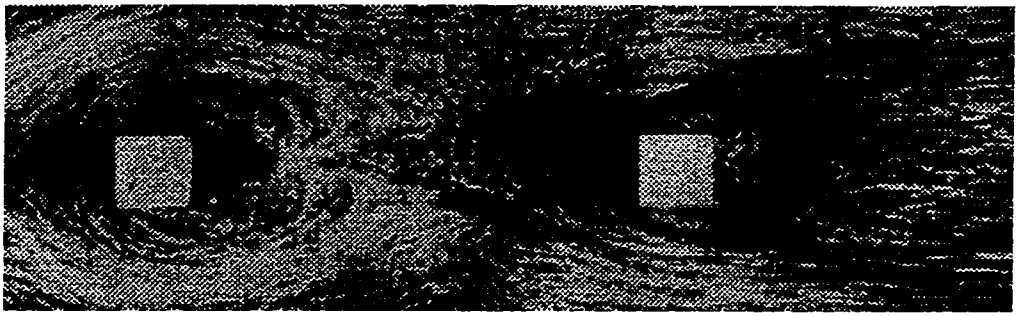

(c) Two building models at a clear spacing of 6b

Figure 2.3 Flow-visualization for square plan building models of width b (=100m) and height 5b (Gowda and Sitheeq 1993).

The arrangement of buildings, their relative size and the direction of wind determine the extent of interaction. However, the following general conditions may be expected when two buildings interact.

When an upstream building blocks another building, it increases or decreases the forces on the downstream building by modifying the structure of wind in its wake. Mean along-wind forces on a downstream building are reduced due to shielding by the upstream building. This shielding clearly decreases as the separation between the buildings increases. Also, it would be expected that increasing the number of nearby structures of significant size would result in less severe wind downstream, thus leading to net shielding effects, for example in the case of a city-centre.

The increased turbulence intensity in the wake of an upstream building tends to increase the dynamic loading on the downstream building. For large separation distances, the vortices get enough time and space to become well-organized before they hit the downstream building, thus increasing the vertical correlation of wind loading which is responsible for higher dynamic loads. For smaller separation distances, the downstream building interferes with the steady vortex shedding and disrupts its frequency, thus destroying the vortex shedding mechanism and resulting in a small increase in dynamic loads. A downstream interfering building has very little effect on the loads and response of an upstream building for most locations. However, for locations of close proximity, a downstream building can significantly alter the wake characteristics of the upstream building thus resulting in high dynamic loads on it.

Due to non-uniformities in the wind flow caused by other buildings or structures, wind pressure may be unevenly distributed on the sides of a building, thus producing, in addition to the overturning moment, a torsional moment about the vertical axis. This effect is expected to increase significantly for close proximity locations, especially when the upstream building blocks a building side or if the separated shear layers impinge on one side more than the other. Such a twisting of the building can impose severe strain on the joints between the elements of the structural bracing system.

Maximum interference effects can be expected for the open-terrain exposure, steadily reducing for the suburban and reaching a minimum for the urban terrain. This is because for the open terrain, a low turbulence intensity promotes an organized wake behind an upstream building with a high energy content. The high energy vortices in the wake of the upstream building excite the downstream building and lead to high interference effects, i.e., increased dynamic loads on the building. An urban approach terrain on the other hand creates turbulence which disturbs the organized vortices and reduces the strength of vortex shedding by

redistributing energy to a wide band of frequencies. This leads to lower levels of excitation for the downstream building, resulting in smaller interference effects as compared to the open terrain.

Tall buildings upstream may produce adverse effects on a downstream building. This phenomenon has been explained by Baines (1963), by considering the boundary layer flow around high-rise buildings. The pressure on the front face of a building decreases downwards due to the decreasing velocity in the boundary layer, consequently, the pressure gradient induces a downward draft of air which can result in substantial velocities (and pressures) at lower levels. Thus, smaller structures in the immediate vicinity of tall buildings would be subjected to higher wind loads. Larger cross-sections upstream are expected to produce higher interference effects on the downstream building because of an increase in the size of the upstream wake, and therefore, higher dynamic wind loads are expected; mean loads, however, would be reduced due to greater shielding.

2.3 Prior Research

There have been very few studies on a large group of buildings as compared to those on a smaller group limited to two or three buildings, probably due to the difficulties caused by the many parameters involved. However, the study of this aspect is a class in its own because of the limitless variation in the arrangement and geometries of buildings, generating a large variability in wind loads. A majority of studies in this area have been done to investigate wind pressure characteristics from the point of view of natural ventilation (Wiren 1983, Wiren 1985, Tsutsumi et al. 1992 and Jozwiak et al. 1993). Other works related to large building groups have been reported by Soliman (1976), Hussain and Lee (1980) and Lee (1989). All these studies highlight the fact that increasing the number of surrounding obstructions generally

reduces the wind loads on a building. A detailed and comprehensive study on interference effects of grouped low-rise buildings was carried out by Holmes and Best (1979). Their results, with those of Hussain and Lee (1980), were incorporated in The Australian Standard for Minimum Design Loads on Structures (SAA 1989) in terms of a shielding multiplier (between 0.7 to 1.0, depending upon the spacing, dimensions and the number of upstream buildings) for the derivation of the gust wind speeds. However, cases involving a few (three or less) upstream buildings, where wind speeds might actually be increased drastically have yet to receive the attention they deserve by the codes, mainly because of the lack of adequate data on which to base codal guidelines and recommendations. This review lays particular emphasis on this class of building interference situations. Because of the heavy demands on time and resources involved in experimenting with large building groups, the experimental approach in the majority of studies has been to minimize building model configurations and keep them simple while searching for limiting conditions.

Interference effects have been quantified in literature in two ways: one is where the pressure values at designated points on a rigid test model are measured and reported in terms of pressure, drag and lift coefficients, or moments; the other involves reporting moments about the base or displacements or accelerations at the top of an aeroelastic model. Interference effects on buildings are commonly expressed in terms of an Interference Factor (IF) (or Buffeting Factor or Shielding Factor) given by,

$$\textit{Interference Factor(IF)} = \frac{\textit{Force on a building with interfering buildings present}}{\textit{Force on an isolated building}} \quad (2.3)$$

The main parameters affecting interaction between adjacent buildings are the type of upstream terrain, shape and size of buildings, the incident wind direction and last but not least, the building arrangement and spacing. The effects of these parameters are discussed in detail in the following subsections.

2.3.1 Effect of upstream terrain

It is well known that wind pressures on buildings are affected by terrain roughness. In the case of an isolated building, with increased surrounding obstructions the mean wind pressures acting on the building decrease while the unsteady pressures increase. Similarly, the magnitude of increase in wind loads due to adjacent buildings is strongly dependent on the upstream terrain. Kwok (1989), Melbourne and Sharp (1976), Blessmann (1985) and Kareem (1987) investigated interference effects in various simulated exposure conditions (open country, suburban and urban) and concluded that interference effects were more pronounced for the open-country exposure. Due to the low degree of turbulence associated with open-country exposure, fluctuations in the wake of an upstream building are well-correlated and, therefore, cause enhanced wind loads on the downstream building. On the other hand, a more turbulent urban exposure works to dampen the strength of such a wake, thereby reducing the overall wind loads on the downstream building. Mc Laren et al. (1971) observed that for a pair of identical square models arranged side-by-side and normal to the mean flow, the mean drag coefficient decreases steadily with the increase on the upstream turbulent intensity. On the basis of extensive wind tunnel tests, Taniike (1991) investigated the mutual interference between neighbouring tall buildings in a highly turbulent flow over

an urban area. Interference effects decreased exponentially with an increase in turbulence, and vanished altogether when turbulence intensities increased up to 17-18%.

An analysis of the results of the above mentioned studies shows that by changing the upstream terrain exposure from open to suburban, the along-wind and across-wind loads on a downstream building due to an upstream building reduce to about 60% to 80% of the open-terrain values, depending on the building geometries and their spacing; and by changing from suburban to urban terrain, a further reduction in these values to about 50% to 70% of the open terrain values may be expected. There may also be a reduction of 50% in the value of torsional moment on moving from an open to an urban exposure. Thus, a small group of buildings located at the waterfront, an open field, or at the edge of a city centre would be more susceptible to interference effects.

2.3.2 Effect of geometrical parameters

Wind loads on buildings increase with increasing height of buildings. Kelnhofer (1971), Melbourne and Sharp (1976), Saunders and Melbourne (1979), English (1990) and Sykes (1983) measured the effect of changing the relative height of upstream building on the wind loads on a downstream building. It was observed that mean along-wind loads were reduced by increasing the height of the upstream building due to shielding, but dynamic loads increased. On the basis of experiments, Melbourne and Sharp (1976) concluded that the interference effect of an upstream building reduces significantly once its height is less than 2/3 of the downstream building. Saunders and Melbourne (1979) reported that an upstream building of the same height as the downstream building increases the along-wind dynamic moments by up to 70% over and above an isolated building value; an increase by 50% in the height of the upstream building increases this value to 90% at a reduced velocity of 2

(ratio of hourly mean wind velocity at the top of building to the natural frequency of the building times its breadth). Similarly, the across-wind dynamic loads also increase with an increase in the height of the upstream building, apparently due to the increasing correlation of vortices from the upstream building with height. Stathopoulos (1984a) studied the interaction effects of adjacent high and low-rise buildings and found significant amplification of roof peak suction coefficients on the low-rise buildings for specific configurations.

A limited number of studies have dealt with mutual interference between buildings of different foot-print (cross-section) areas. The size of the upstream building affects both the mean and fluctuating forces on the downstream building. Taniike (1992) and Taniike and Inaoka (1988) measured the forces on a tall building with a square foot-print caused by proximity effects using upstream interfering buildings of same height but various foot-print sizes in a low turbulence wind environment. The mean forces decreased with an increase in the size of the upstream building due to shielding provided by the large upstream building. It has been suggested (Taniike 1992) that since large buildings upstream shed large vortices which increase the fluctuating velocity of the flow, the along-wind fluctuating forces and response have a tendency to increase with the size of the upstream building. However, in the across-wind direction these forces on the downstream building tend to decrease with increase in size of the upstream building.

While most of the researchers have focused attention on buildings of square or rectangular foot-print, a study by Peterka and Cermak (1976) examined the effect of four octagonal nearby structures on the wind pressure along the circumference of a central circular structure. It was observed that adverse effects can be encountered depending on the

relative placement of structures in the approaching wind. These effects may be decreased by introducing variations in building geometries. Thoroddsen et al. (1985 and 1987) have presented mean and fluctuating moments due to a square upstream building of width D, on downstream buildings having rectangular, parallelogram and triangular cross-sections. Figure 2.4 shows some results taken from Thoroddsen et al. (1985) indicating that there seem to be similar trends in the values of Buffeting Factors, BF (same as Interference Factor, IF) irrespective of cross-sectional shapes of downstream buildings. Root mean square (rms) along-wind loading reaches a maximum for relatively short separation distances of around 1.5D and thereafter shows a decreasing trend with spacing (Figure 2.4(a)). Rms across-wind loading, on the other hand, shows a steep increase with augmenting the along-wind spacing and reaches a maximum at a spacing of around 4.5D (Figure 2.4(b)). Figure 2.4(a) shows that maximum along-wind BF is obtained for the downstream building with parallelogram foot-print. It is also clearly evident from the figure that parallelogram and triangular foot-prints are more susceptible to an increase in rms loading than the traditional rectangular building.

2.3.3 Effect of wind direction and building orientation

Wind effects on buildings depend not only on the magnitude of wind speeds, but on the associated wind directions as well. Since in actual situations the direction of wind is always changing, it is important to study the effect of wind direction on interference effects.

In case of an isolated building with a square cross-section, the maximum drag force is registered when the wind strikes the building normal to one face i.e., at a 0° angle of attack. The maximum mean torque, however, would be for a wind direction at an angle of attack of

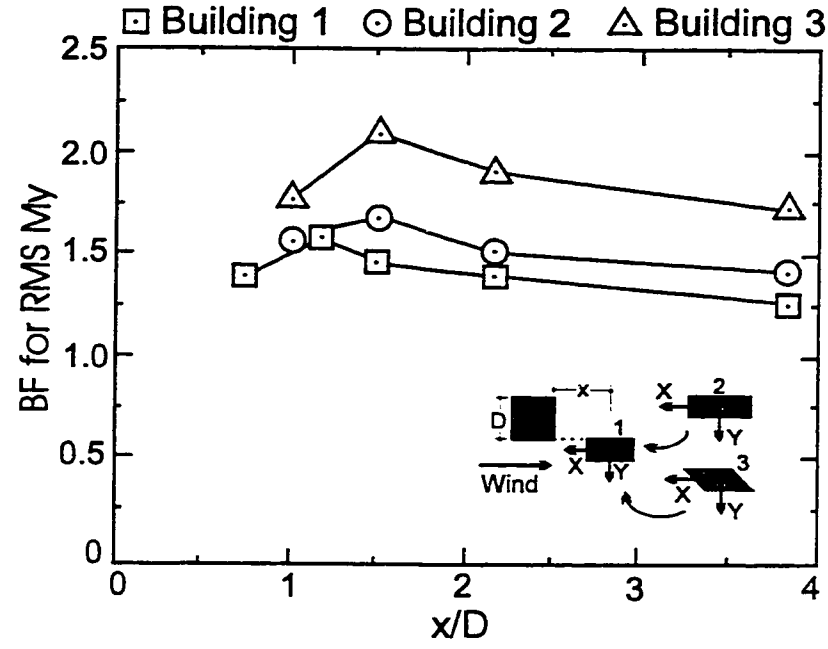

(a) Along-wind loading

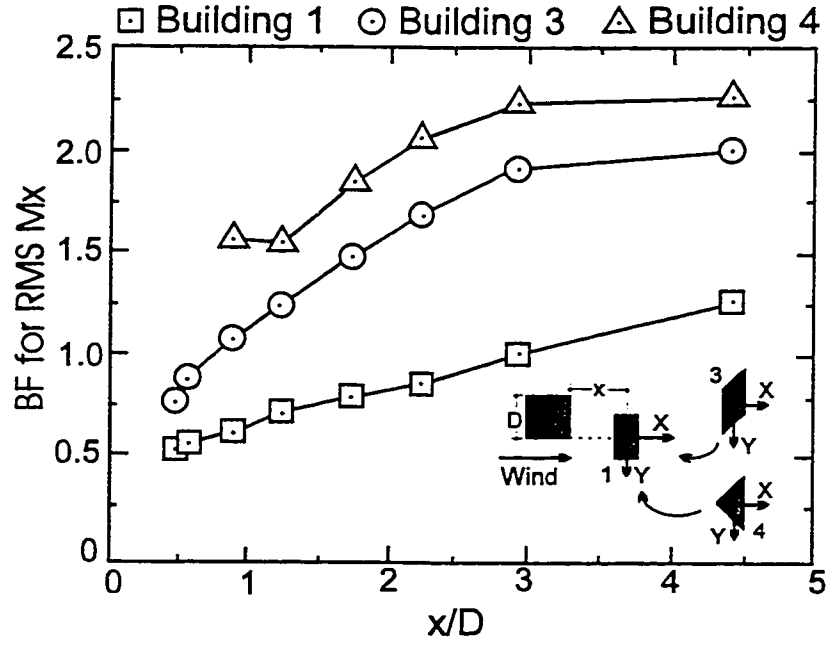

(b) Across-wind loading

Figure 2.4 Rms Buffeting Factors on downstream buildings of various shapes due to a square upstream building (Thoroddsen et al. 1985)

about 75° to a face of the building (Blessmann and Riera 1979 and Isyumov and Poole 1983). With two or more close-by adjacent buildings, this scenario is expected to change.

Quite early on, Harris (1934) suggested that wind pressure on adjacent buildings varies with wind direction. A few previous studies (Saunders and Melbourne 1979 and Sanni et al. 1992) have suggested that interaction effects for two buildings will be the largest for a 0° angle of attack of wind. Saunders and Melbourne (1979) tested two tall building models for interference with the upstream model oriented with one face normal to wind and also at 45° to wind. The results have consistently shown that the model oriented with zero angle of attack has a response greater than that with an angle of attack of 45°. Sykes (1983) found that for two cuboidal building models set at 30° yaw to wind, interference effects were somewhat smaller than those measured in an approximately corresponding situation but with the models set normal to wind direction.

However, detailed measurements on the effect of angle of attack of wind on interaction between adjacent buildings show that the critical wind direction may vary, depending upon the building geometries and their relative arrangement (Kelnhofer 1971, Blessmann and Riera 1979, Wiren 1983 and Wiren 1985). In a detailed study on the effect of adjacent low-rise building blocks on wind pressure distributions and heat loss due to uncontrolled ventilation for a single family house, Wiren (1985) measured the average pressure coefficients for two similar low-rise, roof-sloped buildings in tandem arrangement vis-à-vis a similar isolated building for different angles of attack of wind. It was found that one house located upwind of the test house had a significant effect on the pressures over all building surfaces at small wind angles. This effect decreased and became negligible (compared to isolated building values) at about 30° angle of attack of wind (for all house surfaces except

the windward facade walls) and at about 90° angle of attack of wind for the windward facade walls.

2.3.4 Effect of building arrangement and spacing

The spacing between adjacent buildings and their relative arrangement are the most important factors governing interference effects. Common sense suggests that interference effects between two buildings should decrease by increasing the separation distance, such that beyond a certain spacing, buildings behave as isolated under the action of wind. It is interesting to note, however, that in the case of tall buildings, interference effects in terms of dynamic loads can be significant up to a distance of 1 km downstream (Saunders and Melbourne 1979). In the same study dynamic moments on an aeroelastic model of a 150m tall and 37m wide, square building were measured in the presence of similar single and twin buildings as upstream obstructions. It was concluded that if a medium-sized building near a waterfront or other clear fetch area has similar or taller buildings built upstream at critical locations, the downstream building will suffer significant increases in peak loads and serious dynamic effects. In a detailed interference study on two tall buildings, Bailey and Kwok (1985) examined the increased along-wind and across-wind responses of a 216m tall and 24m wide, square aeroelastic building model due to interference from a similar neighbouring building and found that both upstream and downstream buildings were affected. These effects will be discussed in detail in the following section.

2.4 Analysis And Discussion

To evaluate the influence of building arrangement and separation on interference effects, the results reported previously have been analyzed and compared. English (1990 and 1993) has

also attempted such a comparison but the data used were limited and originated from various sources encompassing a broad range of testing techniques, flow conditions, building geometries and configurations. A regression equation for a two-building configuration (English 1993) to predict mean along-wind Shielding Factors (SF) i.e., ratios of mean overturning moment or drag force for each applicable shielded configuration to the corresponding moment or force for an isolated building (see equation 2.3), is suggested as,

$$SF = -0.05 + 0.65x + 0.29x^2 - 0.24x^3 \qquad (2.4)$$

where, $x = \log\left[\frac{S(h+b)}{hb}\right]$; S = clear spacing between the two buildings; b = width of the buildings and h = height of the buildings.

To estimate the severity of interference effects, wind loading on a building in the presence of an adjacent building is compared with the wind loading on an isolated building. Results taken from studies sufficiently similar in terms of building geometries and flow conditions to merit a comparison, are expressed in terms of the Interference Factor (IF). Eventhough there is discrepancy between individual studies, data seem nevertheless to follow a general trend so that an average IF curve represented by a polynomial can easily be fitted for each case. The majority of studies have measured the effects of interference on aerodynamic drag and lift, overturning moments and torsion.

2.4.1 Drag and lift

For flows about symmetrical shapes, a drag force may be identified acting in the mean wind direction and a lift force at right angles to it. These aerodynamic forces are expressed in terms of non-dimensional drag and lift coefficients; their magnitude depends upon building geometry, upstream terrain and wind direction. These forces are obtained by assigning a

representative area to each pressure tap location on the face of the model and multiplying it by the pressure at that location. The products are then summed up for each instrumented face of the model in the along-wind and across-wind directions to yield the drag force and the lift force respectively. Alternatively, pneumatic averaging (Surry and Stathopoulos 1978) can be used to expedite the measurements. Drag and lift coefficients are defined and discussed in chapter 3.

Figure 2.5 represents data from three studies (Lee and Fowler 1975, Sakamoto and Haniu 1988 and Taniike 1992) on interference effects between two square plan buildings of equal size (Khanduri et al. 1995c). An average curve representing a polynomial of the third order defining the Interference Factor (IF) as a function of building spacing ratio S/b, where S is the spacing between the two buildings and b is the building width, is fitted in each case. Figures 2.5(a), (b) and (c) demonstrate that the effect of the adjacent building is to lower the mean drag force on the principal(instrumented) building, since the Interference Factor in each case is never greater than 1 (isolated building case). The average estimate in Figure 2.5(a) indicates that the mean drag Interference Factor for an upstream building model due to a downstream model in tandem arrangement does not go much below 1. A slight decrease in mean drag is observed around a clear spacing (S) of 3-4 times the model width (b). This is due to the fact that the separated shear layers from the leading edges of both sides of the upstream model start to flow intermittently into the region between the two models at this spacing, thus decreasing the negative pressure on the rear surface of the upstream model. Therefore, the upstream building is not significantly effected.

However, this is not so in the case of a downstream building with an upstream interfering building. Figure 2.5(b) gives an estimate of the extent of shielding provided by

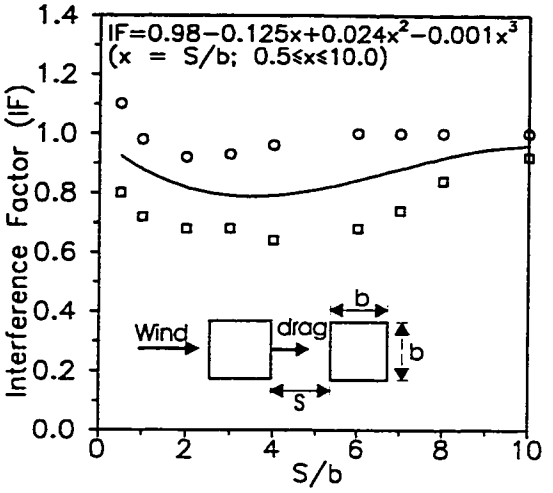

(a) Mean drag IF for upstream building

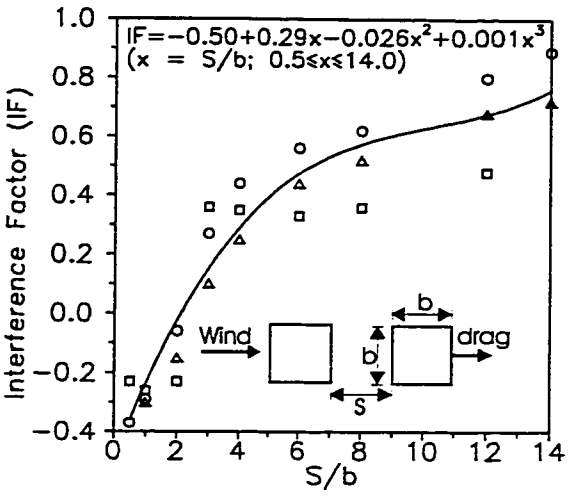

(b) Mean drag IF for downstream building

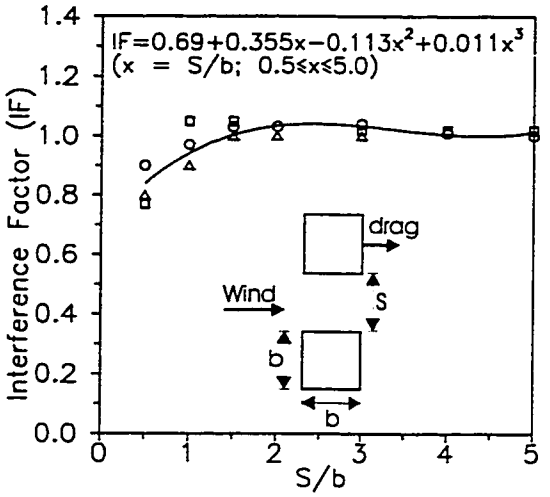

(c) Mean drag IF for side-by-side arrangement

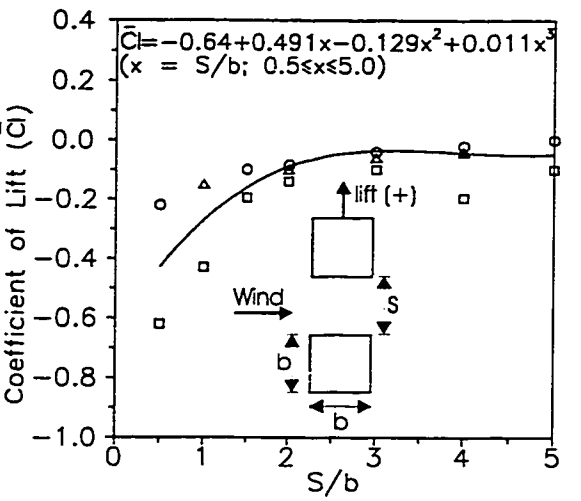

(d) Coefficient of mean lift for side-by-side arrangement

PARAMETERS	□ Lee and Fowler (1975)	○ Sakamoto and Haniu (1988)	△ Taniike (1992)
Building/Model dimensions	25.4mmx25.4mmx460mm (1:1:18)	25mmx25mmx75mm (1:1:3)	70mmx70mmx315mm (1:1:4.5)
Terrain	open	open	open

Figure 2.5 Comparison of mean drag and lift due to interference

the upstream structure to the downstream building. The effect of shielding is to lower the drag force on the downstream building. As expected, the closer the two buildings, the higher is the level of shielding. At a distance of about twice the building width, there is practically no drag force on the building, and at still lower spacings, a negative shielding (suction) is experienced by the downstream building. This is because the negative pressure on the leeward face of the downstream model is small as compared to that on the windward face since the separated shear layers from the upstream model reattach on the sides of the downstream model and become weak by the time they reach the leeward end. It is interesting to note that shielding can be quite significant at a distance as large as 12 times the building width, where an Interference Factor of 0.7 implies a shielding of 30%. It can be seen from Figure 2.5(c) for models arranged side-by-side, that the mean drag interference factor is almost equal to 1 after a clear spacing of around twice the model width, which implies that at this spacing, the models can be considered to be isolated from the point-of-view of mean drag. This finding confirms that of Mc Laren et al. (1971) and Sayers (1991). A similar comment can be made about mean lift for side-by-side arrangement (Figure 2.5(d)), where after a clear spacing of twice the model width the mean lift becomes zero (isolated building case). However, at closer spacings a negative lift is generated because the velocity of flow through the channel between the two models increases, thus generating a larger negative pressure on the inner side wall than on the outer.

2.4.2 Overturning moments

The dead load of a building tends to resist the overturning or toppling effect of wind. Overturning moments may be problematic for the whole building especially in the case of relatively tall and slender structures. Base overturning moments are generally expressed

about axes normal to the building faces; in the wind tunnel they are usually measured with the help of a strain gauge balance that permits rotation about the base of the structure. The base overturning moments (mean or rms) are expressed in terms of non-dimensional moment coefficient, C_{M_y} , in the along-wind direction as,

$$C_{M_y} = \frac{M_y}{\frac{1}{2}U^2 bh^2} \tag{2.5}$$

and C_{M_x} in the across-wind direction as,

$$C_{M_x} = \frac{M_x}{\frac{1}{2}U^2 lh^2} \tag{2.6}$$

where M_y = overturning moment in the along-wind direction; M_x = overturning moment in the across-wind direction; l = length of the building in the along-wind direction; b = breadth of the building in the across-wind direction and h = height of the building.

Figure 2.6 shows the results of Saunders and Melbourne (1979), Bailey and Kwok (1985) and Taniike and Inaoka (1988) for mean and dynamic IF for base overturning moments on a building due to interference effects caused by another building at various upstream locations (Khanduri et al. 1995c). For clarity of presentation, data points shown are for curve Sx = 2b only; the data sources for all three curves, however, are the same. The extent of shielding provided by the upstream building becomes apparent in Figure 2.6(a) which shows the variation of mean along-wind moments with spacing between two buildings. Clearly the maximum shielding occurs when two buildings are in tandem position, i.e. Sy = 0. For along-wind distances as large as 8 times the building width (b),

shielding can be considerable, since according to Figure 2.6(a) the along-wind moment on the downstream building is reduced to almost half of that of an isolated building at this spacing. It can also be seen that at an across-wind spacing (Sy) of 4b the effect of shielding vanishes altogether (isolated building condition) irrespective of the location of the building in the along-wind direction. The average curves shown here are quite similar in trend to those in Figure 2.5(b) which gives the mean drag IF for a downstream building model in tandem arrangement with an upstream model. Tandem arrangement locations in Figure 2.6(a) are, Sx =2b, Sy = 0; Sx = 4b, Sy = 0 and Sx = 8b, Sy = 0. The values of IF at these locations are, -0.24, 0.24 and 0.55 respectively. The corresponding situations in Figure 2.5(b) are, S = b, S = 3b and S = 7b, for which IF are, -0.25, 0.14 and 0.53. Based on the proximity of IF values for the two figures, it can be inferred that the shielding effect is similar for both mean drag (Figure 2.5(b)) and mean along-wind moments (Figure 2.6(a)).

The dynamic wind loads due to interference follow a different trend from that of the mean loads and the effects are much more severe. Figures 2.7(b) and 2.7(c) show curves from the data of Saunders and Melbourne (1979) and Bailey and Kwok (1985) for dynamic along-wind and across-wind IF for moments on a downstream building due to an upstream obstruction at various along-wind and across-wind separations. IF values greater than 1 are measured at most locations. IF as high as 1.55 is measured at Sx = 4b, Sy = 1b (see Figure 2.6(b)), which indicates a 55% increase in along-wind dynamic overturning moments. The results show that dynamic IF for both along and across-wind can be quite high and attain maximum values in the range covered by Sx = 4b to 8b and Sy = 0 to 4b with increases in dynamic IF by up to 60%. Bailey and Kwok (1985) have also investigated the effects of a downstream interfering building on a similar upstream building. In general, the effects were

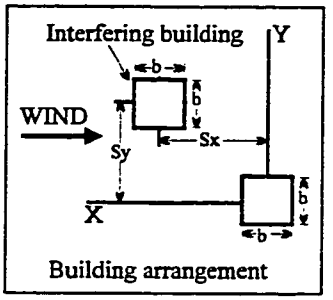

Interference Factor (IF) =

$$\frac{\text{Base moment (with upstream building)}}{\text{Base moment (isolated building)}}$$

Reduced Velocity =

$$\frac{\text{Hourly mean velocity at top of building (U)}}{\text{Natural frequency of building (f) x width (b)}}$$

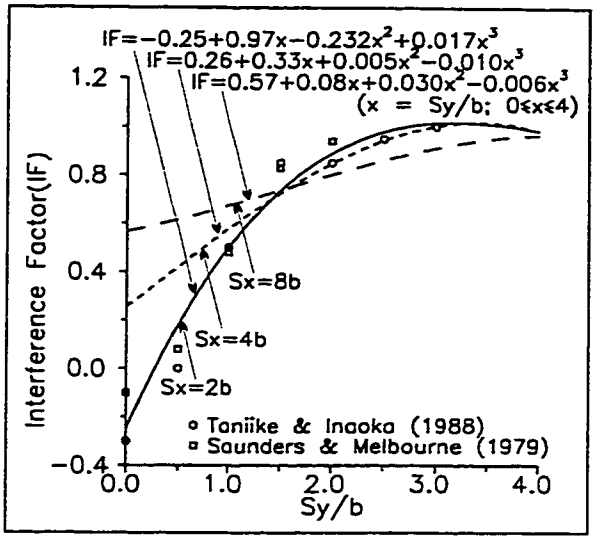

(a) Mean along-wind Interference Factors

Note : Data points shown are for curve Sx = 2b only.

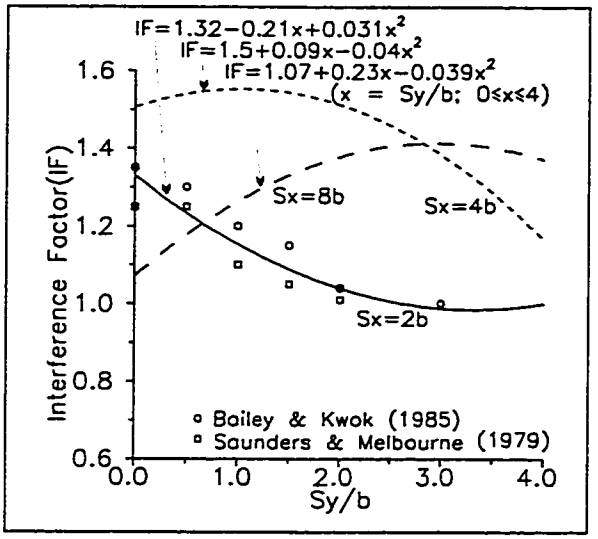

(b) Dynamic along-wind Interference Factors

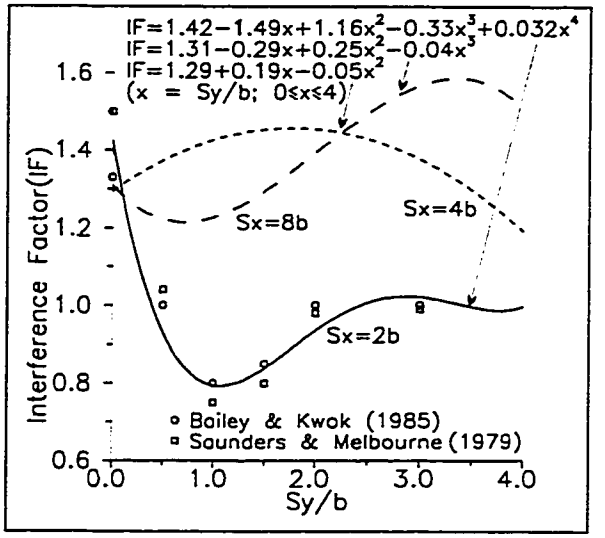

(c) Dynamic across-wind Interference Factors

PARAMETERS	Saunders and Melbourne	Bailey and Kwok	Taniike and Inaoka
Building/Model dimensions	37mx37mx150m (1:1:4)	24mx24mx216m (1:1:9)	70mmx70mmx315mm (1:1:4.5)
Terrain	open	open	open
Reduced Velocity	6	6	5

Figure 2.6 Effect of interference on mean and dynamic Interference factors

insignificant for most relative locations. However, for a small range of locations between Sx = -b to -2b and Sy = 0.75b to 1.5b, the dynamic overturning moments on the upstream building increased by 100% to over 300% of the isolated building value. This was attributed to the alteration of the wake characteristics of the upstream building due to the sharp convergence of the wind flow through the narrow channel between the two buildings.

The regression curves and polynomials based on literature results are only as good as the data they are supposed to represent. Because of limited comparable data, the curves are based only on the building spacing ratio (spacing/building width). Nevertheless, they can give an approximate estimate of the IF within specified limits of spacing between two buildings. For better and reliable results, the regression polynomial should take into account the building geometry, upstream terrain conditions and wind direction in addition to the building spacing. The situation, therefore, becomes rather complex to be handled by a single "all-in-one" regression equation, and a new technique incorporating neural network learning, described later in the paper has been proposed to take care of multiple inputs and it extrapolates the results reasonably well.

2.4.3 Torsion

For two buildings in close proximity, torsion may become a major problem as highlighted by Blessmann and Riera (1979 and 1985), Ruscheweyh (1979), Thoroddsen et al. (1985 and 1987), Zhang et al. (1993) and Reinhold and Sparks (1980). Torsion is due to the eccentricity of the centroid of the wind force distribution in comparison to the centroid of the lateral resistive system (or centre of stiffness). In the case of buildings with symmetric geometries, torsional moments may be caused by non-uniformities in the wind flow due to

adjacent structures. This effect may further be accentuated if a building is not geometrically symmetric or if the lateral resistive system of the building is not symmetric. Torsional response of buildings can be measured in three ways:

a) Pressure measurement on rigid building models (Isyumov and Poole 1983). This involves weighting individual pressure taps by their respective moment arms to provide a direct measure of the component torque for each half face of the building.

b) Force balance technique (Melbourne and Sharp 1976 and Sykes 1983). It utilizes a rigid building model mounted on a strain gauge balance that permits rotation about the base and provides a direct measure of the torsional force; however it does not provide information on building motion-induced effects.

c) Aeroelastic technique (Zhang et al. 1994 and Isyumov 1982) that takes into account the aeroelastic effects and provides information on the aerodynamic damping. However, comparing the results of tests of wind-induced response on a 390m tall building using high frequency force balance and aeroelastic model techniques, Isyumov et al. (1992) concluded that additional motion-induced forces in the case of aeroelastic model were small and satisfactory estimates were obtained with the much simpler high frequency force balance model.

Figure 2.7 taken from Thoroddsen et al. (1987) shows the variation of rms torsional loading with along-wind separation distance for buildings of various cross-sectional shapes, blocked partly by an upstream rectangular building. It can be seen that torsion for a downstream rectangular building increases by 1.8 times the maximum torsional loading on an isolated building (for any wind direction) at an along-wind separation distance of about three times the upstream building width. It has been generally observed that torsional

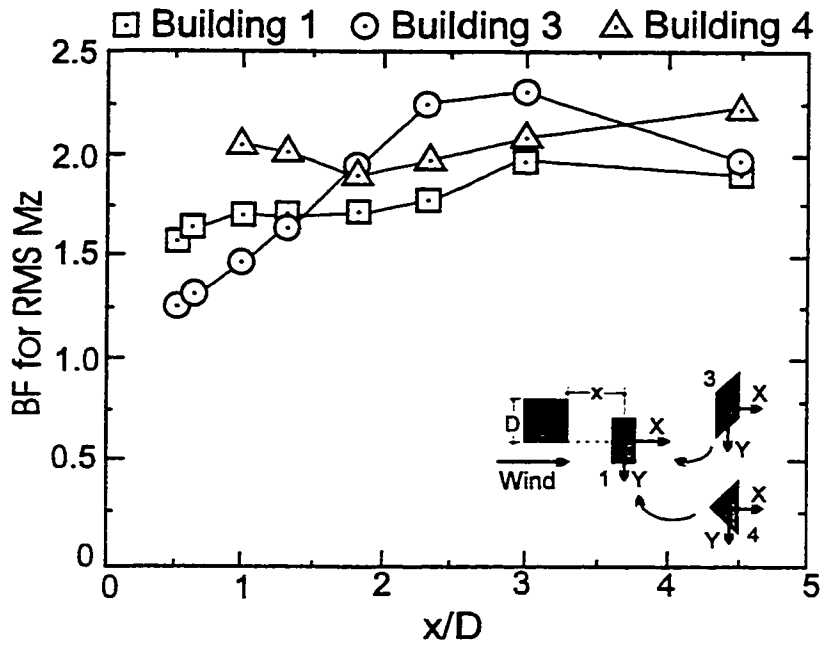

Figure 2.7 Rms torsional moment (M_z) due to interference (Thoroddsen et al. 1987)

loading increases for close building locations in the across-wind direction. In a study on the torsional response of an eccentric square cross-section building by Zhang et al. (1993), it was observed that the maximum mean torsional response of an eccentric building (with elastic centre shifted away from the centre of mass by 10% of the building width) was 20% larger than that of a similar isolated building, while the standard deviation of response increased by up to 70% at a reduced velocity of 6. However, for most locations, mean torsional response of the eccentric building was reduced due to shielding effect from the interfering building. For a smaller interfering building with edge dimensions reduced to 60% of the principal building (building affected by interference), the dynamic torsional effects were much higher and in some cases increased by up to 360% over the isolated building value at locations upstream at Sx = 3b to 6b and Sy = 0 to b, where b is the width of the buildings. This is attributed to the vortex shedding from both sides of the

interfering model alternately impinging the principal building at the same frequency as that of the principal building, causing torsional resonant buffeting of the principal building.

2.5 Hybrid Knowledge-Based Systems - State of the Art

The main source of knowledge on interference effects remains detailed wind tunnel experiments. The complex nature of the problem and the large amount of variables involved make it impossible to test all building interference situations. The experimental approach adopted has been to minimize the number of model configurations and to keep them simple while searching for limiting conditions. The generalization of results thus obtained to various other building configurations and wind conditions still remains elusive. Two off-shoots of research in the field of Artificial Intelligence (AI) offer excellent means for organizing and relating the data generated through wind tunnel tests, Neural Networks (NN) and Knowledge-Based Systems (KBS). The application of Knowledge-Based Systems (KBS) in engineering is quite well established now. KBS technology has been applied to wind engineering problems as well. There has been a lot of excitement recently about neural networks (NN), which in its current state of development, is an attempt to mimic the human thought process to solve complex problems with incomplete or confusing information. KBS and NN technology, both off-shoots of research in AI, have been recently combined to solve broader and more diverse areas of application; such systems are known as *Hybrid Knowledge Based Systems.*

There are few instances of application of KBS in wind engineering. From an overview of about thirty six KBS in structural engineering in 1990, Reed (1990) found that only two were related to wind. Fundamentals and applications of NN in civil engineering have been

provided by Flood and Kartam (1994). Recently, NNs have also been applied in wind engineering for predicting wind-induced damage to buildings (Sandri and Mehta 1995). Khanduri et al. (1995a and 1997b) have demonstrated the suitability of NN for expanding the solution of wind interference problems to more cases than those currently covered by limited wind tunnel data.

A computer-based approach to complement the scarcity of experimental data to provide valuable assistance to designers at an early design stage is suggested by Khanduri et al. (1995b and 1995c). A hybrid KBS is proposed based on the use of Neural Network (NN) representations that are capable of developing functional relationships among experimental data and documented cases. A three-stage integration process between KBS and NN is followed to arrive at a hybrid KBS configuration for the assessment of wind-induced interference effects on design loads for buildings: data collection and knowledge structuring by KBS, data evaluation and generalization by NN and conclusion analysis and design guidelines by KBS. Such a hybrid KBS will constitute a practical tool at early design stages, enabling the evaluation and refinement of close-to-optimum building configurations with respect to wind interference effects.

The following sub-sections provide a brief review of the developments in research applications of KBS and NN in the engineering field in general and wind engineering domain in particular. The benefits derived by combining the two technologies are also discussed.

2.5.1 Knowledge-based systems

One area of AI research which is quite advanced is that of Knowledge Based Systems (also

known as Knowledge Based Expert Systems or Expert Systems). KBS provide the potential of computerizing the knowledge of experts in specific domains such that problem solving behaviour of experts can be simulated. Research in AI was formalized in the 1950s, but a major resurgence and commercialization of AI began in the late 1970s on the basis of the success of a few programs that performed specific tasks almost as well as human experts and thus came to be known as Expert Systems (Parsaye and Chignell 1988). One of the early knowledge based systems was DENDRAL (Buchanan et al. 1978), that was used for determining the molecular structure of organic compounds from mass spectral and nuclear response data. It was followed by several knowledge based systems covering a diverse range of applications. Two of the successful ones were: MYCIN (Shortliffe 1976) which contains judgement rules extracted from physicians and uses them to diagnose various blood and meningitis infections; and PROSPECTOR (Duda et al. 1979) that contains rules gleaned from geologists and performs geological analysis of aerial photographs, aiding a human expert in the evaluation of the mineral potential of exploration sites. An overview of knowledge based systems developed in a wide range of knowledge domains can be found in Waterman (1985). KBS has been applied to a wide array of engineering problems; the discussion herein will be restricted to structural engineering in general and buildings in particular.

One of the early KBS in structural engineering was SACON (Bennett et al. 1978), which provides knowledge in the use of a complex finite element program for structural analysis. This was followed by a spate of KBS in structural engineering as detailed in Allen (1987). Building design process is largely characterized by the contribution of numerous diverse disciplines in a loosely organized manner and KBS are suitable for automating this design

process (Bédard and Gowri 1990). One frequently cited building design system is HI-RISE (Maher 1984), a system that generates and evaluates preliminary structural design for high-rise buildings. Other significant works in the domain of building engineering are: DESTINY (Rehak et al. 1985), a conceptual model of a KBS that performs integrated structural design for arbitrary building types and FLODER (Karakatsanis 1985) that designs floor framing systems. Bédard and Ravi (1992) explain a KBS module that generates space layout alternatives for office buildings taking multidisciplinary criteria, which is a part of an integrated design system for multi-storey buildings to assist at the preliminary design stage. Wind Engineering is but a small problem domain in the larger context of such a building design process. There are very few instances of applications of KBS in the field of wind engineering; two of the early attempts were: WINDLOADER (Sharpe et al. 1990), which is a knowledge based software program developed to assist in the correct interpretation of the Australian Wind Loading Code and WISER (Kareem and Allen 1990) which is a KBS for the design modification of high-rise buildings for serviceability. A recent practical and useful application of KBS to wind engineering is WIND-RITE (Smith et al. 1995), a KBS developed for the insurance industry that grades individual buildings, on a relative scale, for their wind resistance. Other noteworthy applications are in the areas of Pedestrian Level Winds (Wu et al. 1993) and Structural Safety Assessment with emphasis on wind effects (Chen and Reed 1990).

2.5.2 Neural Networks

A Neural Network is composed of many interconnected processing elements that operate in parallel, in a way quite similar to the function of neurons in the human brain to encode

information. The beginning of research in artificial NN training algorithms can be traced back to 1949 when D. O. Hebb proposed the learning law based on models of the human learning process. The first artificial NN were developed in the decade spanning 1950 and 1960, and were initially implemented as electronic circuits. Due to a few failures of the networks in solving certain problems, research in NN lapsed into obscurity for nearly two decades. However, thanks to the dedicated efforts of a few researchers, a new foundation emerged upon which the more powerful multilayer networks of today are developed. In the last few years, theory has been translated into applications and the increase in the amount of research activity has been phenomenal. Today, NN are being used for a variety of commercial applications, including speech, character and text recognition; database management, financial analysis; forecasting, image and signal processing; medical diagnosis; dealing with fuzzy, chaotic or incomplete information and structural control.

Neural networks based on the backpropagation algorithm have been used in a number of engineering applications as described in Garrett (1992) and Flood and Kartam (1994). In structural and construction engineering, several applications of neural networks based on experimental data have recently been reported in the area of concrete material modelling (Wu and Ghaboussi 1992); structural system identification of an instrumented bridge structure (Chen and Shah 1992); prediction of initial cable tensions in a guyed communication tower (Issa 1992); selection of vertical formwork for a bridge site (Kamarthi et al. 1992); hysteretic modelling of steel structures (Yamamoto and Sakai 1993) and construction cost estimation (Moselhi et al. 1991 and Rao et al. 1993). Hajela and Berke (1992) have demonstrated the pattern mapping, classification and optimization capabilities of NN to solve a number of structural analysis and design problems.

2.5.3 Hybrid knowledge based systems

As pointed out above, KBS and NN each have demonstrated capabilities that have been applied to solve a wide array of engineering problems. Each approach has various advantages and disadvantages. Table 2.1 summarizes the strengths and weaknesses of KBS and NN. Integrating the two to exploit the advantages of both approaches would result in a system that is more powerful and broad based, yet quick; with more human-like responses but accompanied with logical explanations. Such knowledge based systems that combine the rule-based approach with neural networks are often referred to as "hybrid" knowledge based systems. (Caudill 1990). Various integration strategies for KBS and NN and their potential applications can be found in Kartam et al. (1993).

Table 2.1 Knowledge Based Systems vis-à-vis Neural Networks

Knowledge-Based Systems	Neural Networks
• Long development time; knowledge acquisition is time consuming	• Short development time for acceptable results and high speed of computing due to parallel processing.
• User-friendly; explain their response due to a logical reasoning process.	• No explanation facility available because a network does not reason its way from problem to solution.
• Brittle failure occurs when problem deviates even slightly from the expected problem domain.	• "Fault tolerant" due to their distributed nature. Degrade gracefully, i.e., provide reasonable response when presented with incomplete or noisy input.
• Good performance for well-defined problems.	• Applicable to poorly defined problems due to their ability to generalize, i.e., provide response for previously unseen input.
• Good for problems where explicit rules can be formulated.	• No rules needed but are generated through training on a comprehensive set of examples.
• Lack learning ability.	• Possess inherent learning capability.

A major impediment in the application of KBS technology into practice is the so-called "knowledge acquisition bottleneck" which makes it difficult to acquire or generate useful knowledge that can support real tasks. This is particularly important in the area of wind engineering where the development of a KBS depends primarily on data generated through wind tunnel experiments. For KBS to be robust, data covering a wide range of conditions expected to be encountered in actual practice is needed. Since generation of large amounts of data in a wind tunnel can be both expensive and time consuming, alternative methods of creating data have to be explored. Reich and Fenves (1989) propose machine learning techniques for generating knowledge for developing a KBS for the preliminary design of cable-stayed bridges. Such NN representations are capable of developing functional relationships from discrete values of input-output quantities obtained from computational approaches or experimental results (Gunaratnam and Gero 1993).

The ability of NN to be trained to generalize when presented with limited data examples makes it an attractive application for knowledge acquisition on interference effects due to adjacent buildings where no currently acceptable theory or generalization exists for describing an input/output response. A combination of knowledge based systems and neural networks have the potential to model and solve complex interference effects problem in wind engineering.

Because of the demonstrated capability of KBS in dealing with ill-structured problems and NN in solving complex multivariate and non-linear problems with incomplete or confusing information, these two tools offer viable complements to detailed wind tunnel testing. It is anticipated that KBS and NN will play a major role in solving and generalizing wind interference problems in the foreseeable future.

2.6 Summing Up

The main objective of the analysis presented in the chapter is to scrutinize trends in experimental data in order to assess the possibility of generalization. Because of the dearth of "comparable" studies, this attempt has achieved to show only approximate trends. It however underscores the need for a systematic, coherent and comprehensive approach to the problem of interference. On the basis of this analysis and comparisons of literature results, the following general guidelines have been formulated:

- The critical locations for an upstream interfering building are at Sx = 4b to 8b and Sy = 0 to 4b, where b is the width of the building, producing an amplification of up to 60% in the dynamic overturning moments on a similar downstream building. Mean loads on a downstream building generally decrease due to shielding effect.
- Interference causes substantial increases (by up to 100%) in the maximum dynamic torsional moment of the downstream building, especially when the upstream building blocks a side of the downstream building. The critical region is around Sx = 3b to 9b and Sy = 0 to 2b upstream. Mean torsion is generally reduced.
- Effect of an upstream taller building on a downstream building is more significant than the reverse case. Mean along-wind loads are reduced, but dynamic loads are increased by more than 70% for taller upstream buildings.
- Mean loads decrease with increase in the foot-print size of the upstream building, but dynamic loads increase by up to 200% on a tall, square downstream building due to a square upstream building of similar height, but 2.5 times wide.

- The critical wind direction for interference depends upon the geometry and arrangement of buildings, but generally a direction of wind normal to the building face may produce significant interaction effects.
- Interference effects are significant in open country exposure, steadily decreasing for suburban exposure and urban exposure. Thus, buildings located along a waterfront, deserts or an open area such as a park are more susceptible to interference effects.
- Effect of downstream interfering building is not as significant as that of an upstream building, but for small proximity locations at Sx = -b to -2.5b and Sy = b to 2b, dynamic overturning moments on a similar upstream building may increase by up to 200% over an isolated building value.
- The wind loading of a building is generally less severe if it is surrounded by a large group of buildings of significant size, thus leading to net shielding effects.
- KBS and NN technology have been applied to very few problems in wind engineering. These two AI technologies hold good promise in automating the knowledge dealing with interference effects.

2.7 Avenues For Improvement

One aspect of the effect of adjacent buildings that causes high ground level wind speeds (not covered in the present review), commonly known as "the pedestrian level discomfort" (Isyumov and Davenport 1975, Lawson and Penwarden 1975 and Wu et al. 1993), has been the subject of a much better-focused research than that on wind load modifications on buildings. Significant efforts have been devoted to codify the ground level wind environment for quite some time. This is perhaps because the effects of wind and adjacent

buildings on pedestrians are immediately apparent as they affect human beings directly, whereas the effects on building loads are not. Therefore, the idea of 'pedestrian level discomfort' is more easily appreciated than the concept of adverse wind loads on buildings due to interference. The above review has nevertheless highlighted the importance of interference effects between adjacent buildings, and the need to view wind-induced interference problem from a practical design standpoint and attempt some kind of codification and generalization of these effects.

2.7.1 Grey areas

Eventhough prior studies have underscored the severity of wind-induced interference effects, they have only managed to touch the tip of the iceberg. Some important aspects have been overlooked. The reason for this appears to be the enormity and complexity of the problem. Nevertheless, a systematic and detailed study of wind-induced interference effects seems to be in order. The major areas requiring further investigation are,

- Effect of relative building sizes
- Effect of incident wind direction
- Effect of immediate surroundings
- Empirical modelling
- Use of effective CAWE (Computer-Aided Wind Engineering) techniques for generalization of experimental results as well as for providing practical design assistance.

This research, while aiming to fill-in the gaps left by previous studies through detailed wind tunnel experiments, strives to find ways to generalize the solution of complex problem of wind-induced interference effects by making use of AI techniques.

2.7.2 Practical design considerations

The studies reviewed provide either the mean or the fluctuating component of the wind loads due to interference. For design of civil engineering structures, peak values of the loads are usually required and these can be obtained using the method suggested by Davenport (1964), wherein the peak load is the sum of the mean load and g times its standard deviation; where g is a statistical peak factor (3.5 to 4.5). A value of $g = 3.8$ is commonly used to predict the hourly peak values in the analysis of force balance model test results (Isyumov et al. 1992).

Regarding local loads and based on experiments on a scale model of the Texas Tech building, Carpenter (1994) found substantial increases in peak wind pressure, especially on roof and wall corners, by positioning two identical blocks adjacent to each other. These are extremely pertinent to design and special efforts must be made to ensure their consideration.

The plethora of numbers (interference factors) generated as a result of the wind tunnel experiments on interference effects and the subsequent lengthy analytical and empirical equations may not be directly useful to the structural design practitioner. Therefore, the formulation of simple and straightforward design guidelines would be helpful, especially in the preliminary design stages, to assess and estimate the effects of adjacent buildings on wind loads. On the basis of wind tunnel experiments involving models of two 216m tall

buildings of square cross-section (width 24m), Kwok (1989) suggests three rules to interpret the results of interference effects:

(a) A potential increase in wind loads of 10% to 30% may be expected to be within the normal safety factor in design.

(b) An increase of 30% to 50% should be of considerable concern, especially in terms of serviceability requirements of the building. A comprehensive wind tunnel model testing is recommended.

(c) An increase of greater than 50% will be well outside the safety margin used in normal design, thus making wind tunnel tests mandatory.

2.7.3 Towards codification and generalization

In a wind-tunnel test to determine design cladding pressures on two adjacent tall buildings, Surry and Mallais (1983) observed high suction regions near the ground for some particular geometries and spacings between the two buildings. This questions code recommendations which suggest design values of local suction increasing with height. Stathopoulos (1984a) has also pointed out gross overestimation or underestimation of the wind loads by codes and standards, as already mentioned. In spite of a few scattered attempts towards generalization and codification of interference effects (Bailey and Vincent 1943, Stathopoulos 1984a, Thoroddsen et al. 1987, Kwok 1989 and English 1993), a well-focused and systematic effort is needed in order to formulate general and simplified guidelines on interference effects for codification purposes.

Whilst there is proprietary information on interference effects from specific projects, little of a general nature is available to the designer. Most of the interference effect studies

reviewed involve two or three buildings with identical, square cross-sections. In actual situations, there will be several adjacent buildings with different sizes and shapes. Adding generality would be an extremely difficult, complex and time-consuming task, because of the many parameters involved. However, several limiting conditions based on the results of previous studies could serve to restrict the number of variables. For example, open country exposure which has been found to give the most critical interference effects; and wind normal to the model face may be taken as starting points for the codification process. The effect of rectangular buildings of various cross-sectional sizes and heights should be studied in detail before any generalization. Representative building sizes could be chosen to cover the various cases of interfering buildings likely to be encountered, for instance, small, medium and large buildings. The critical cases thus obtained could be subjected to more detailed tests involving various wind directions, terrain conditions and building geometries to generate a comprehensive database for purposes of codification. Once the database is completed, advanced computerized avenues could be implemented to provide general design assistance (Khanduri et al. 1995b).

Empirical modelling based on the database generated by wind tunnel tests could provide equations to evaluate wind loads on adjacent buildings. Regression polynomials for interference factors on buildings under proximity effects like those shown in Figures 2.5 and 2.6 could be provided. Such equations can be used for an approximate estimation of wind forces on a building under interference conditions for preliminary design purposes.

2.8 Summary

The chapter summarizes research developments in the area of wind-induced interference on buildings and compares and analyzes the results of various studies. The data available from the literature is of a very diverse nature and most studies cannot be compared directly because of differences in building geometries and wind flow conditions. Although adjacent buildings can drastically modify wind loads on buildings, there is very limited well-focused research in this area. It is imperative, therefore, to study the effects of building interference on wind loads in a more systematic manner through detailed wind tunnel experiments. Empirical modelling and consequent generalizations to account for interference effects will pave the way for simple design guidelines, thus leading eventually to codification. Hybrid Knowledge Based Systems offer a viable alternative to extensive wind tunnel testing and can help generalize and organize limited wind tunnel results.

We will hear the full range of sounds of wind instruments: the frenzied cadenzas of the turbulence section, with bass notes of the energy producing eddies and pizzicata of their dissipation. We will listen to the playful repartee between the exponents of the power law melody, played no doubt by the violins, and the heavenly sounds of the logarithmic theme played on the harp. There will be swing and sway of the long span bridge section; the syncopated rhythms of the chimney section playing the 'Vortex Street Blues'; the electronic music of the transmission lines and the Wagnerian galloping of the prisms. The crystal notes of the cladding section may have the faint suggestion of tinkling glass but no more than that. The final movement will be the brassy, military sounds of the codes and standards.

- Alan Garnett Davenport. The Relationship of Reliability to Wind Loading. Journal of Wind Engineering and Industrial Aerodynamics. 1983.

3

Experimental Methodology

3.1 Overall Approach

On the basis of an analysis of the literature results, a preliminary framework for the experimental programme is set up. The severity of interference effects notwithstanding, these experimental investigations purport to fill in the gaps left by previous studies and augment their findings in a systematic and detailed fashion. The entire experimental programme is divided into two categories: exploratory or pilot tests, and detailed experiments. Exploratory tests are designed mainly to provide a quick, preliminary estimate of the extent of interference that would eventualiy form the basis of the detailed experiments. These tests also help verify some of the literature results. A simple three-component strain gauge force balance was fabricated and calibrated to measure the along-wind drag and across-wind lift forces as well as the torsional moment about the vertical axis of the building. Detailed tests provide an accurate and detailed measure of the interference effects. The principal building consists of a plexiglass model fitted with 12 pressure tappings uniformly distributed on each of its four faces. Pressure measurements are carried out by using pressure transducers. The digitization of pressure signals and analysis of the data is done by Data6000 waveform analyzer. The aerodynamic forces are measured in terms of non-dimensional along-wind drag and across-wind lift coefficients, for various wind directions and approach terrains. All measurements are carried out at the Building Aerodynamics Laboratory of the Centre for Building Studies, Concordia University.

The main aim of this research is to investigate systematically the interaction between two prismatic building models of various relative sizes under the influence of wind. Measurements are carried out to examine the mean and fluctuating aerodynamic forces acting on these models representing typical shapes of small, intermediate and large sized buildings in various arrangements. The database generated is analyzed to create simple and generalized sets of guidelines on interference effects along with the development of empirical models. A knowledge base is finally developed based on the qualitative and quantitative relationships derived from the experiments and observations. This knowledge base constitutes the foundation of a PC-based adviser on interference effects as explained in chapter 8.

3.2 The CBS Wind Tunnel

The boundary layer wind tunnel of the Centre for Building Studies (CBS) at Concordia University, where the experiments are carried out, has a working section about 12m long with a cross-section 1.8m x 1.8m. The roof is of adjustable height to allow for zero longitudinal pressure gradient for various floor roughness characteristics simulating different terrain exposures. The maximum wind speed at the test section is 14m/s. The boundary layer develops naturally over a rough floor. Thus different wind tunnel floor roughnesses will simulate boundary layer conditions representative of different terrain exposures. Specific details can be found in Stathopoulos (1984b).

3.2.1 Wind speed and turbulence intensity profiles

In the CBS wind tunnel, the open country exposure condition represents exposure A as per

the National Building Code of Canada (NBCC 1985) or exposure C of the American Standard (ANSI 1982). This terrain develops in the wind tunnel over the roughness of a carpet. The suburban terrain exposure corresponds to exposure B of NBCC (1985) and ANSI (1982). This is achieved in the CBS wind tunnel by means of corrugated foam pads placed over the carpet all along its length. The urban exposure may correspond to exposure C of the NBCC (1985) or exposure A of ANSI (1982). This terrain condition is simulated by placing egg box panels over the wind tunnel floor. The egg boxes are fixed on the panels in a certain defined pattern so as to create the necessary roughness that simulates the required turbulence at the centre of the turntable where the instrumented model is located.

The vertical distribution of the mean velocity and the longitudinal turbulence intensity for the three simulated flow conditions are shown in Figure 3.1. It is clear that for the same terrain roughness the turbulence intensity decreases with the increase in height above the ground, and for the same height, the turbulence intensity increases with the increase in terrain roughness. The velocity profile exponent in each case is estimated by using the power law equation,

$$\frac{\bar{v}}{v_g} = \left(\frac{z}{z_g}\right)^{\alpha} \tag{3.1}$$

where, $\bar{v}$ = mean wind velocity at a given height; v_g = mean wind velocity at gradient height; z = height above ground; z_g = gradient height and α = power law exponent.

Thus the best fitted velocity profile exponents are 0.15 for the open terrain, 0.25 for the suburban and 0.36 for the urban terrain exposure. The turbulence intensity at the building height (80m) is 7%, 13% and 25% for the open, sub-urban and urban approach terrain respectively.

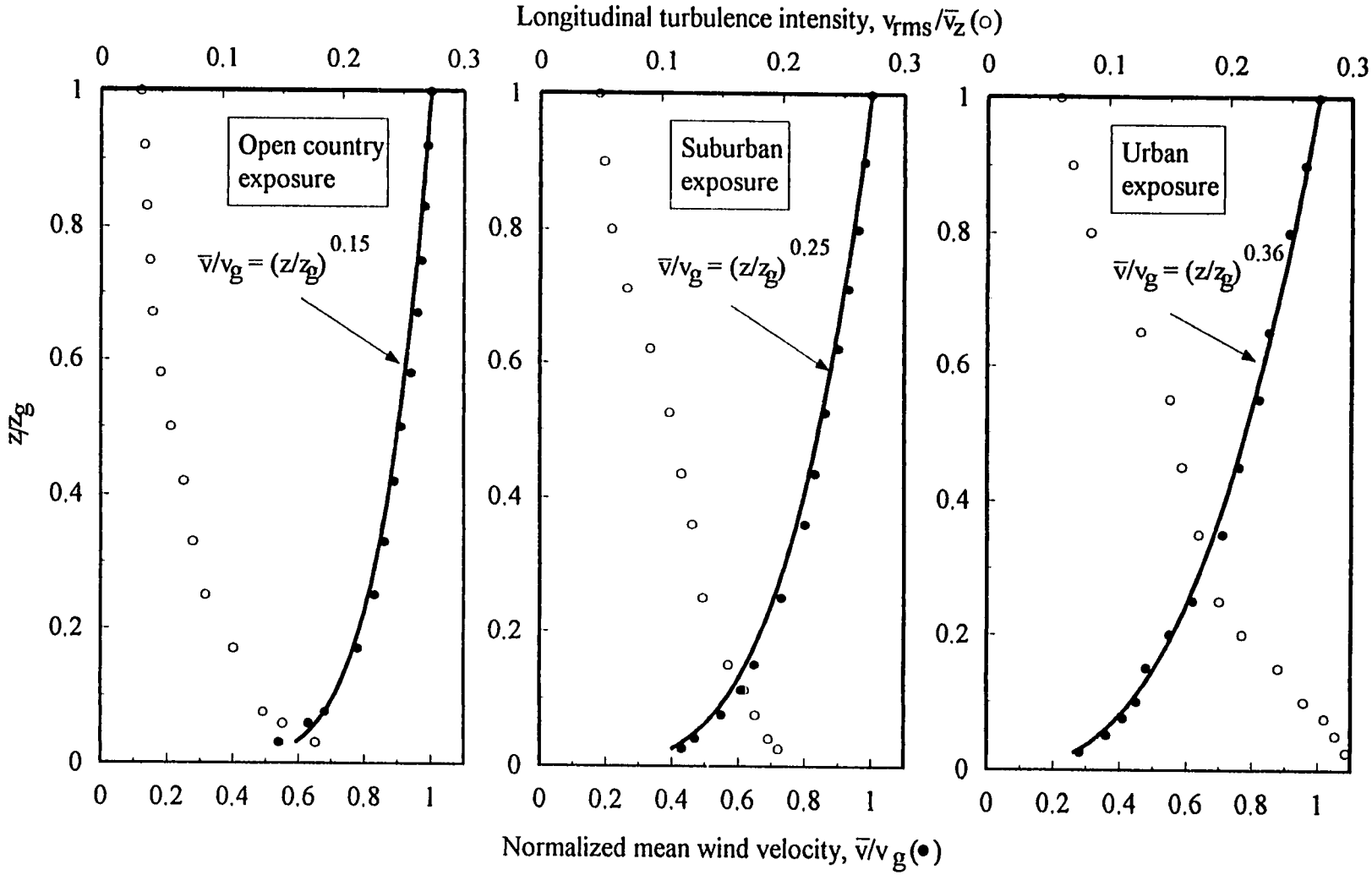

Figure 3.1 Mean wind velocity and turbulence intensity profiles

3.2.2 Spectrum of longitudinal turbulence

In order to fix a geometrical scale for the model, spectra measurements are performed for all the three terrain exposures. The Fast Fourier Transformation (FFT) method was used for the development of spectral estimates. Typical spectra measured at the building height (80 m) are presented for the three exposures in Figure 3.2. These spectra are compared with Davenport's empirical equation for the power spectral density (Davenport, 1961),

$$\frac{nS(n)}{\sigma^2} = \frac{2}{3}\frac{x^2}{(1+x^2)^{4/3}} \tag{3.2}$$

$$x = \frac{n}{\bar{v}_{10}}1200 = \frac{n}{\bar{v}_z}\frac{\bar{v}_z}{\bar{v}_{10}}1200 \tag{3.3}$$

where, n = frequency; $S(n)$ = power spectral density of the longitudinal turbulence component; σ^2 = variance of longitudinal wind velocity; $\bar{v}_{10}$ = mean wind velocity at 10m height and $\bar{v}_z$ = mean wind velocity at height z.

Figure 3.2 shows a good agreement between the curves based on CBS experimental data and Davenport's empirical curve. The length scale of turbulence in the longitudinal direction is obtained as follows:

Time scale $\bar{\tau}$ of a random process, that gives an idea of the average duration of the eddies, i.e. the duration for which the velocity fluctuations will be sustained, is defined as,

$$\bar{\tau} = \int_0^\infty R_v(\tau)d\tau \tag{3.4}$$

where $R_v(\tau)$ is the auto-covariance, given by,

$$R_v(\tau) = \left[\overline{(v(t) - \bar{v})(v(t+\tau) - \bar{v})}\right] \tag{3.5}$$

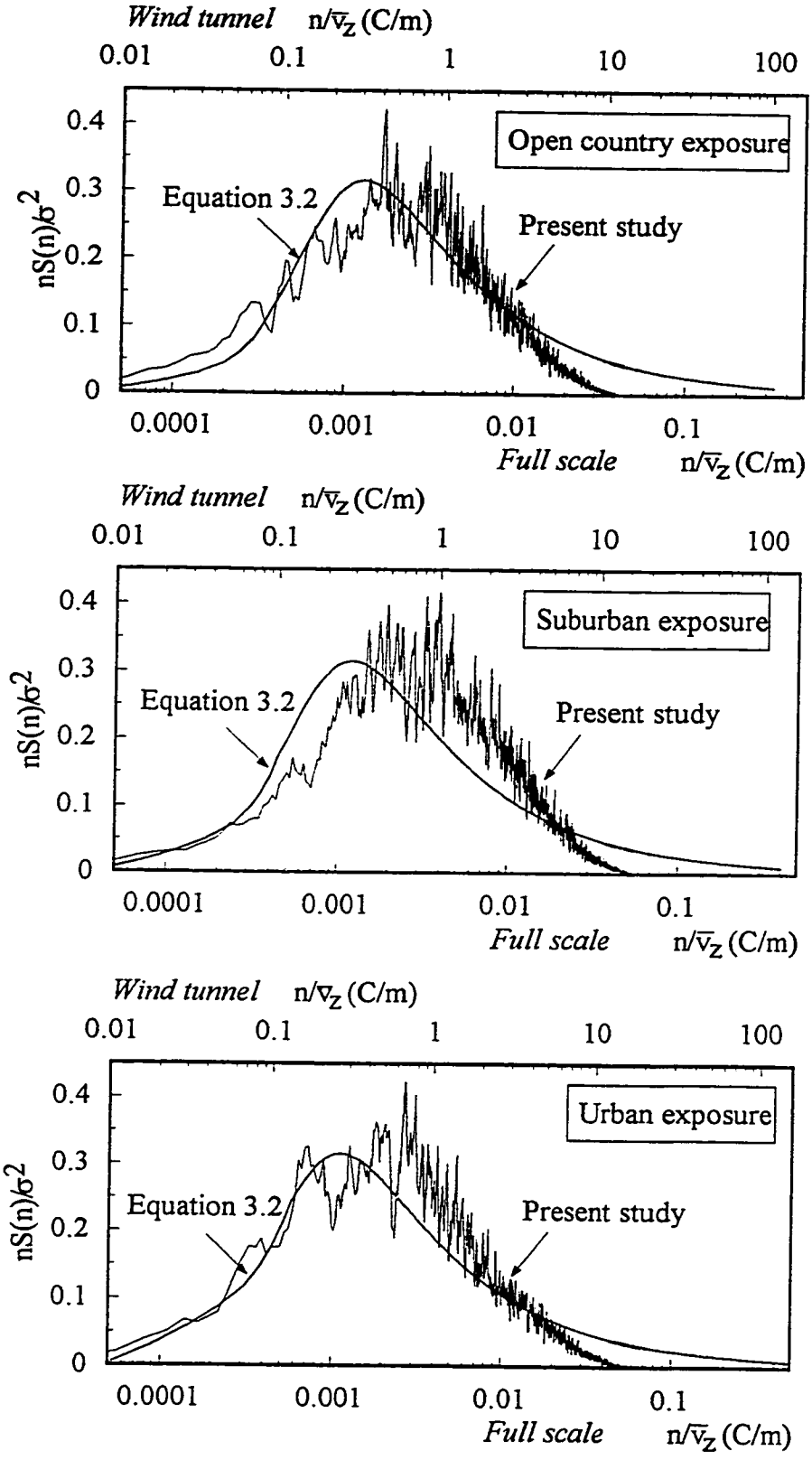

Figure 3.2 Spectra of longitudinal turbulence component at building height (80m)

where, $v(t)$ = velocity in time t; $v(t+\tau)$ = velocity at a time lag of τ and $\bar{v}$ = mean velocity. Thus, length scale of turbulence in the longitudinal direction is given by,

$$L_x = \bar{v}\,\bar{\tau} \tag{3.6}$$

For the present study, $\bar{\tau}$ is estimated by integrating the autocovariance function of the velocity time history at building height (see equation 3.4). Multiplying this by the mean velocity at the building height, a length scale of 0.29m is obtained for the open terrain in the wind tunnel. On using a length scale (L_x) of 112m for full scale as suggested by Stathopoulos (1984), a geometric scale of 112/0.29 = 386 is obtained. Therefore, a geometric scale of 1:400 is used in the present study.

3.3 Experimental Set-Up

The experiments involve two rigid, prismatic building models of various sizes, one serving as the instrumented "principal" test model and the other as the mobile "interfering" building model that is used to provide interference by locating it at specific positions upstream or downstream of the principal building. Force or pressure measurements are made on the instrumented model with the interfering model nearby. These measurements are also made on the principal model in isolated condition to facilitate a direct indication of the effect of the interfering building.

3.3.1 Characteristics of the test models

Typical dimensions of the models have been selected to be representative of real buildings at a geometric scale of 1:400. A total of 10 basic combinations of the interfering building dimensions will cover a significant range of relative building sizes. The principal building is

made of styrofoam for exploratory experiments with the force balance and of plexiglass for pressure measurements. The models providing interference are made of wood. If b and h are the breadth and height respectively of the square plan shaped principal building model, the relative dimensions of the interfering building models are: breadth: b/1.5, b, 1.5b, 2b and height: h, 1.5h, 2h. Additionally, a scale model of Montreal city downtown is used to study the effect of immediate surroundings on the interference between two buildings of equal size arranged in various "critical" configurations within the city centre model. The dimensions of the building models are given in Table 3.1.

Table 3.1 Dimensions of the building models tested in the wind tunnel

Model Number	*Length (mm)*	*Breadth (mm)*	*Height (mm)*
Principal (instrumented) model:			
P_0	50 (b)	50 (b)	200 (h)
Interfering (dummy) models:			
I_1	50 (b)	50 (b)	200 (h)
I_2	33 (b/1.5)	33 (b/1.5)	200 (h)
I_3	75 (1.5b)	75 (1.5b)	200 (h)
I_4	100 (2b)	100 (2b)	200 (h)
I_5	50 (b)	50 (b)	300 (1.5h)
I_6	75 (1.5b)	75 (1.5b)	300 (1.5h)
I_7	100 (2b)	100 (2b)	300 (1.5h)
I_8	50 (b)	50 (b)	400 (2h)
I_9	75 (1.5b)	75 (1.5b)	400 (2h)
I_{10}	100 (2b)	100 (2b)	400 (2h)

3.3.2 Arrangement

The models are arranged in tandem, side-by-side and staggered fashion. Each of the 10 basic cases shown in Table 3.1 are tested by placing the interfering building model at various locations on a grid with the principal building stationed at the origin as shown in

Figure 3.3. For 0° incident wind normal to the building face, only the positive Y-axis quadrants are considered. For other selected wind angles the interfering building is placed in all four quadrants. The distances in the X and Y-axes are designated as Sx and Sy respectively and the interfering building is located around the principal building at distances that are multiples of the principal building width, b; for instance, a location may be designated as Sx = 2b and Sy = 5b. On an average, about 70 locations for each building configuration are tested for 0° wind and double of that for other angles. The locations (Sx, Sy) are based on pilot studies as well as literature results, with closer observations considered around critical locations.

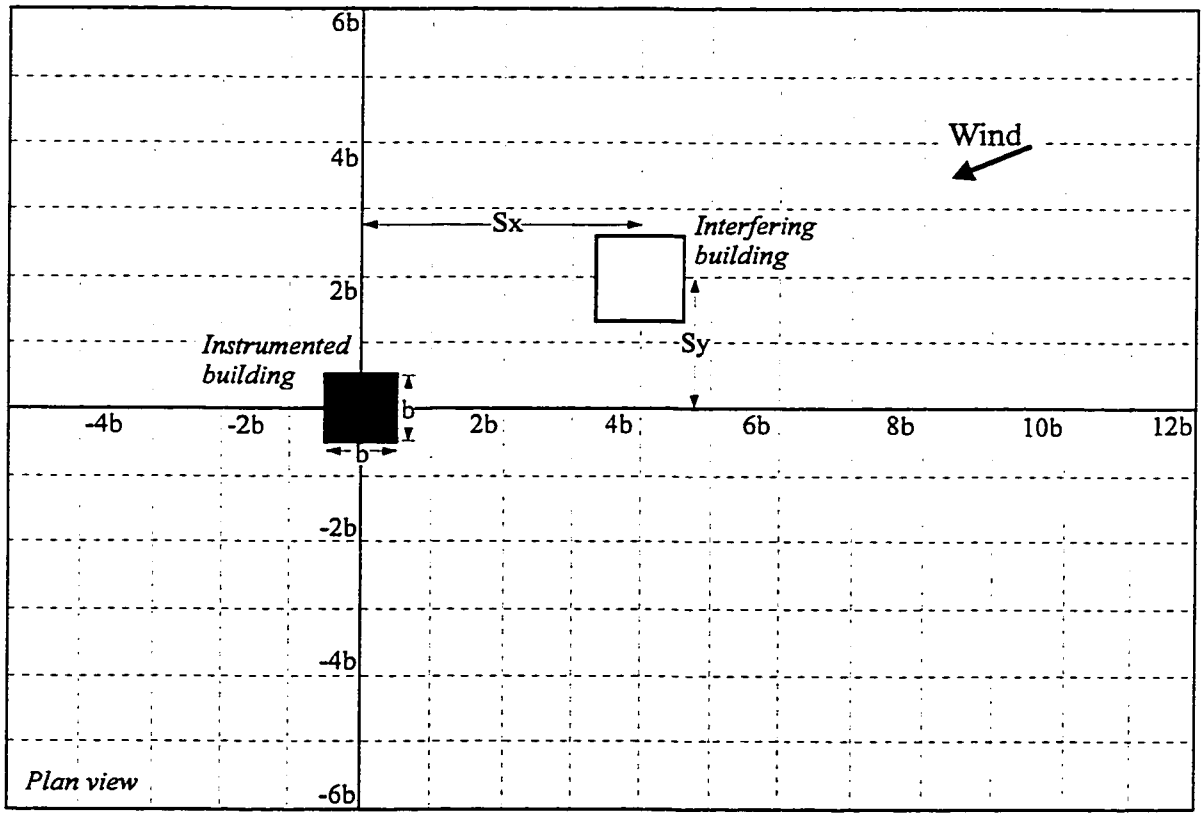

Figure 3.3 Building arrangement

3.3.3 Approach terrain

Since the open approach terrain exposure gives the most adverse interference effects, all model configurations are tested under this terrain category for all the designated wind angles. The two "equal building", P_0-I_1 configuration (see Table 3.1) is also tested for the suburban and urban approach terrains for 0° wind angle. The critical cases thus found are tested within a simulated city centre environment with a suburban approach terrain.

3.3.4 Wind direction and building orientation

All the building configurations shown in Table 3.1 are tested for 7 wind directions: 0°, 15°, 30°, 45°, 60°, 75° and 90° with an open approach terrain. Buildings tested with suburban and urban approach terrains are subjected to a 0° wind, with a premise that similar trends (increase or decrease in interference effects relative to the 0° wind) would be expected for other wind directions as well. The Montreal downtown model is oriented in such a way so that the wind approaches from a south-south-west direction, which is the worst wind direction based on meteorological observations (Wu 1994).

3.4 Exploratory Tests - Fabrication Of A Three-Component Force Balance

Exploratory tests are designed mainly to provide a quick, preliminary estimate of the extent of interference that would eventually form the basis of the detailed tests. These tests also help verify literature results. A simple three-component strain gauge force balance was fabricated to measure the along-wind drag and across-wind lift forces and the torsional moment about the vertical axis of the building. The balance is mounted with a 50mm x 50mm x 200mm styrofoam building model (principal building) and fixed on the floor of the

wind tunnel. The balance assembly is connected to a data acquisition system that provides the mean and fluctuating voltages proportional to the applied forces from three strain gauges under the action of wind. An interfering building model made of wood is placed at various locations around the principal building model. Measured forces are compared with that on an isolated building model.

A two-component force balance with good sensitivity and stiffness was developed by Whitbread (1975). The shear and moment were measured at the base of a 305 mm (12 inch) tall carbon fibre shell of a building model using integrated silicon sensors. Tschanz (1982) developed a high frequency, sensitive but rigid five-component balance-model system to measure the total dynamic wind forces on the base of a building model.

The design of the balance used in this study is based on two main criteria: 1) quick, easy and inexpensive fabrication and 2) reasonably acceptable performance commensurate with the exploratory nature of the tests. Thus the design of the balance is believed to represent the best compromise of desirable attributes for the intended application. Figure 3.4 shows the photograph of the balance-model assembly and Figure 3.5 shows the schematic of the balance. The main components, fabrication and the calibration process of the balance is explained briefly in the following sub-sections.

3.4.1 Base plates

Three interconnected aluminum base plates form the basic components of the force balance. The plates are stacked over each other, separated by frictionless bearings. The bottom plate is fixed over a vertical steel rod that is free to rotate about its longitudinal axis. The top two plates can move in mutually perpendicular directions in a horizontal plane. The smooth

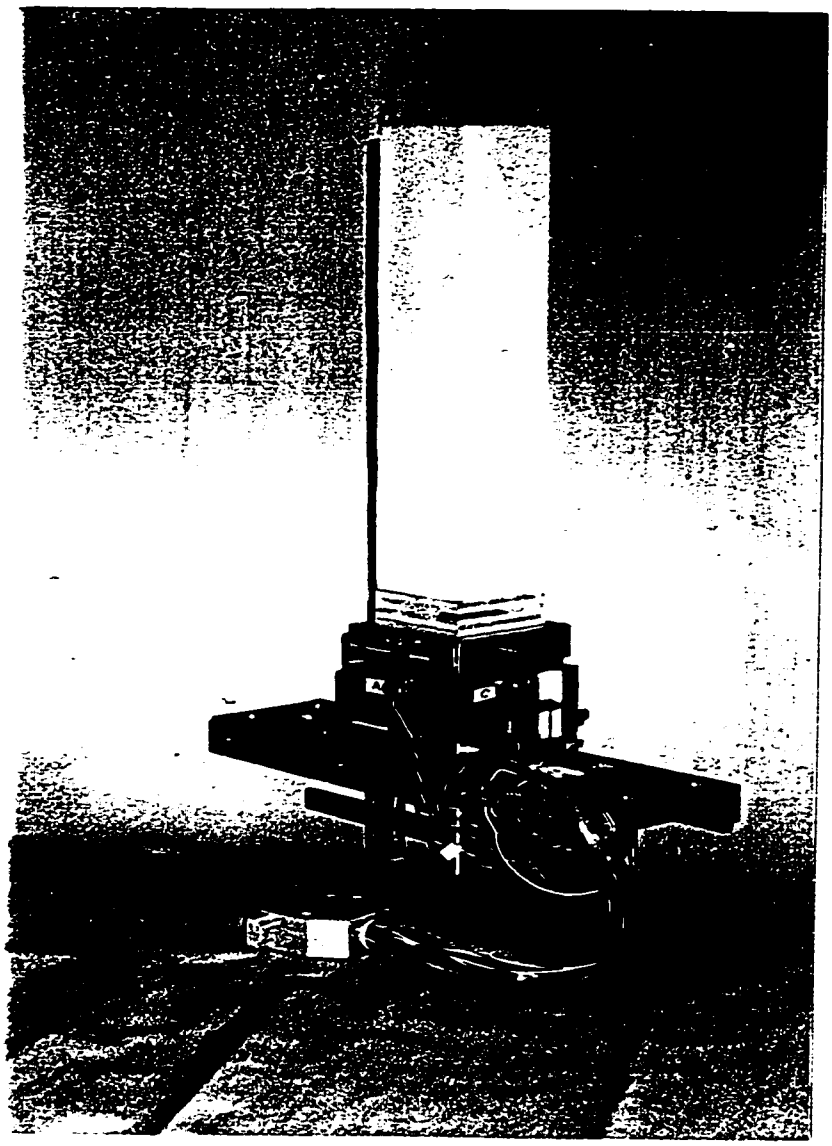

Figure 3.4 The three-component force balance

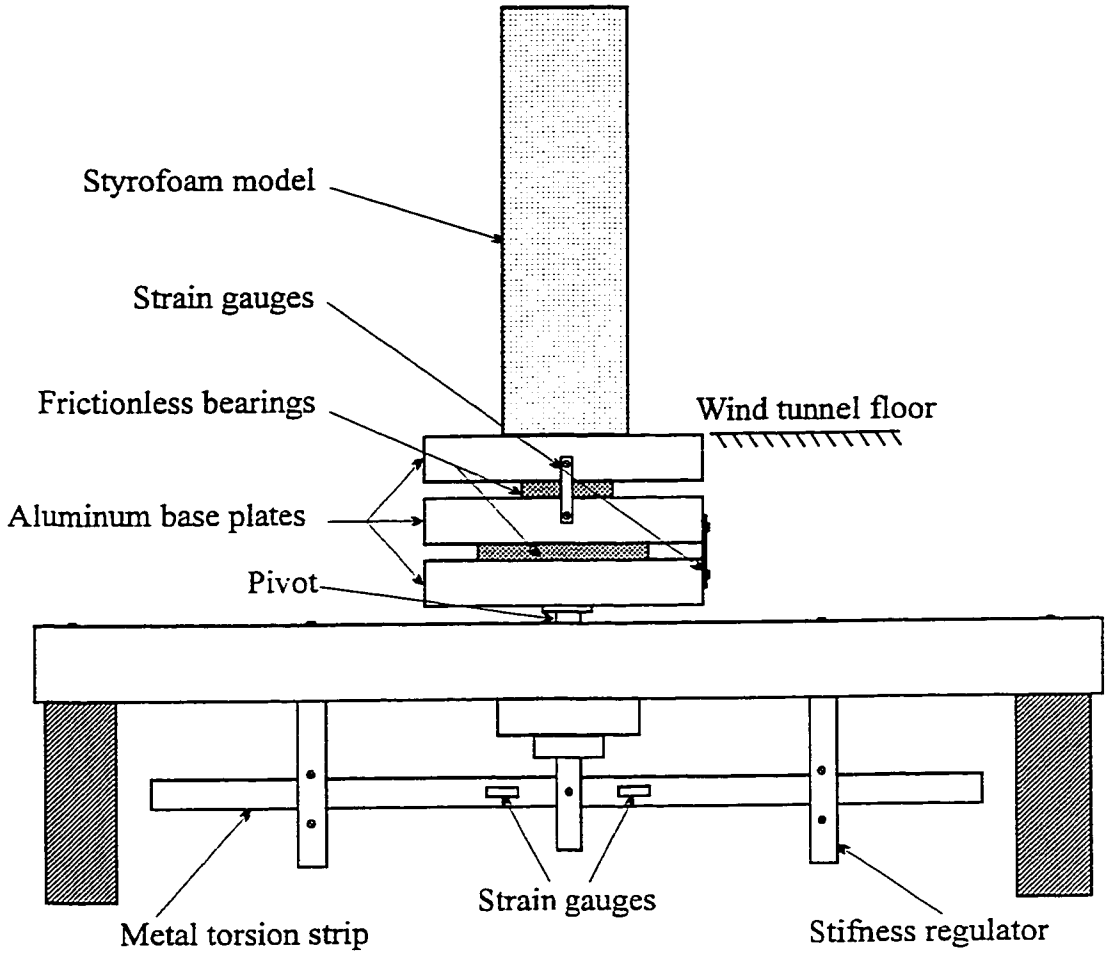

Figure 3.5 Schematic of the three-component force balance

movement is facilitated by two LBSB-5 frictionless bearings having a maximum travel of 12.77 mm (0.5 inch) and a maximum load capacity of 22.25 N (5 lb).

3.4.2 Thin beam load cells

Attached to the base plates are two thin beam load cells each containing a specially integrated strain gauge laminated to the beam. Both the top and middle and the middle and bottom pair of plates are interconnected by each load cell attached to the two mutually perpendicular edges as shown in Figure 3.5. The sliding action of the plates bends the beams and results in a voltage fluctuation that is captured by the data acquisition system. This arrangement measures the shear force on the building in two mutually perpendicular directions. A third set of load cells is fixed to a thin metal strip ("torsion strip") attached to the vertical steel rod that divides the strip in the middle. These load cells measure the torsional moment of the building under the action of a force. The torsional stiffness of the balance can be regulated by two aluminum grips that can slide along the torsion strip and can be fixed at any location thus changing the stiffness of the metal strip.

The range of shear forces expected to be resisted by the balance-model assembly for a 50mm x 50mm x 200mm building model is of the order of about ± 1.1 N (0.25 lb) (using equation 3.7 (page 74) and assuming a drag coefficient of 1.3 (Liu 1991) and wind velocity at building height of 11m/s). As per literature results, this value is increased by about 100% to account for interference effects. Moreover, keeping in view future use of the force balance, possibly for larger building models, a safe expected range of forces of ±4.45 N (1 lb) is assumed. Thus, the thin beam load cell selected is OMEGA LCL-454G with a rated capacity of ±4.45 N (1 lb). Some important specifications of the load cells are as follows:

- Excitation: 5 Vdc, 12 V maximum
- Rated output: 2 mV/V
- Operating temperature: -54°C (-65°F) to 93°C (200°F).

3.4.3 Voltage supply, signal amplification and filtering

The load cells have to be excited by a supply voltage. To obtain a high output voltage per strain, the excitation should be as high as possible so that small strains can be measured without a large error from noise and other unwanted signals. On the other hand, the supply voltage should be kept as low as possible to avoid heating of the load cells. A 10 Volt battery supplies the voltage to the load cells. The small output of the strain gauges is amplified approximately 100 times to interface with the data acquisition system and the signal is filtered using a KROHN-HITE 3342 low-pass filter.

3.4.4 Calibration of the force balance

The three-component force balance is calibrated carefully to determine the calibration slope and cross-talk, if any, due to the misalignment of various components of the force balance. A simple calibration rig is fabricated; it consists of a pulley system through which a known load can be applied to the balance assembly and the resulting voltage changes measured on a voltmeter. To measure cross-talk, loads are applied in one direction (say X) and voltage changes measured for the other two components, i.e. torque and loads at right angles to X. The maximum error due to cross-talk for each of the three component directions is about 3% of the load applied in the main direction. Figure 3.6 shows the calibration plots (load vs.

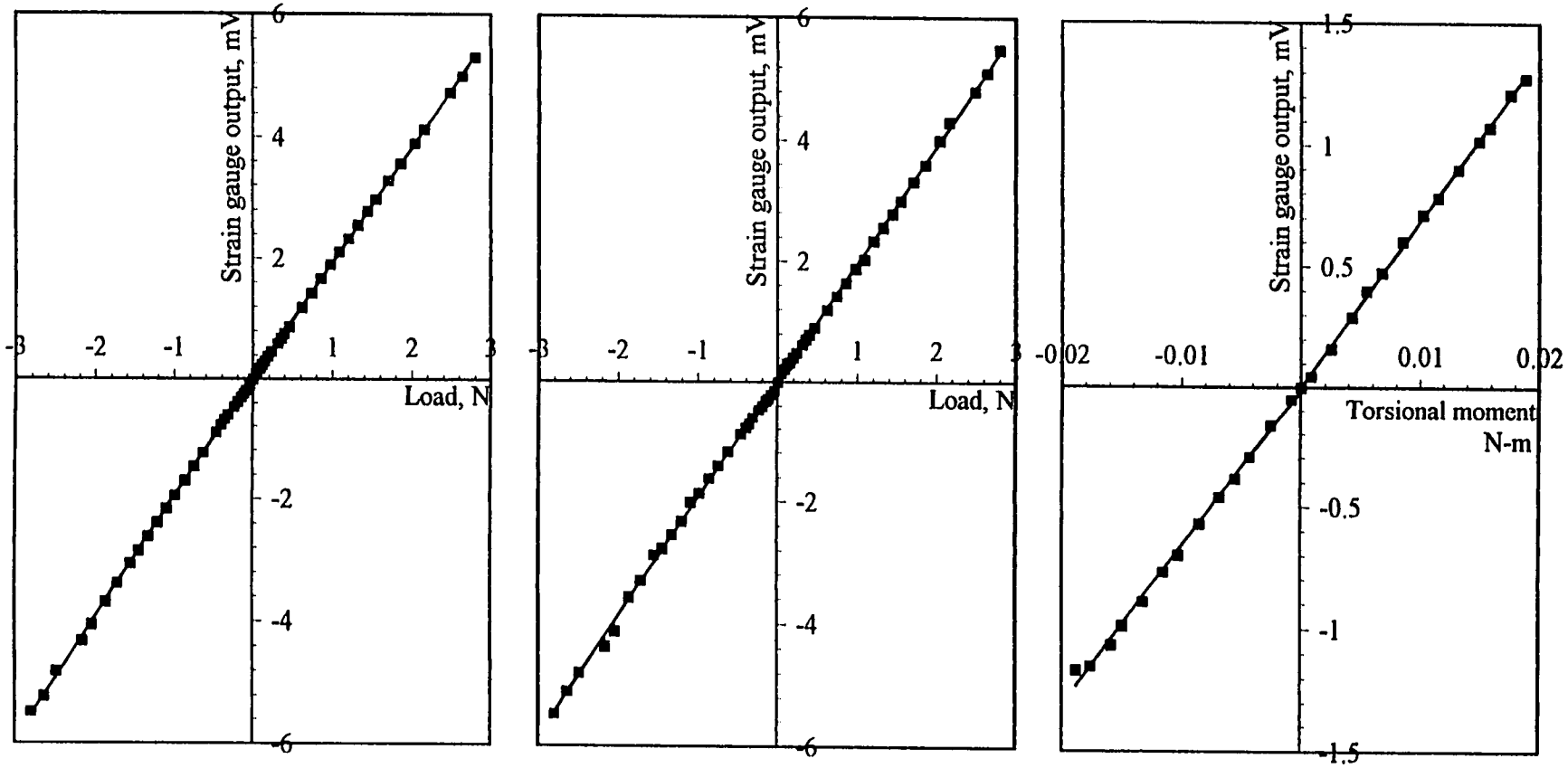

(a) Drag (b) Lift (c) Torsion

Figure 3.6 Force balance calibration curves

voltage) for along-wind loading (drag), across-wind loading (lift) and torsional moment (torsion). These are all linear.

3.4.5 Building model for force balance

The building models should have a small density, otherwise the overall frequency of the balance-model assembly would be significantly reduced due to its high inertial mass. styrofoam, owing to its extremely light weight, was the material of choice for fabricating the principal building model. A 50mm x 50mm x 200mm styrofoam building model with sharp edges and a weight of 13g was fabricated. The model is glued onto a thin, lightweight 50mm x 50mm x 10mm wooden strip to facilitate its fixing onto the force balance.

3.5 Detailed Tests - The Pressure Model

Detailed tests are targeted at specific areas identified by exploratory tests. They are purported to provide an accurate and detailed measure of the interference effects. The principal (instrumented) building consists of a 50mm x 50mm x 200mm plexiglass model fitted with 12 pressure tappings uniformly distributed on each of its four faces (total 48 pressure taps). The model represents, in full scale, a 20m x 20m square plan building with a height of 80m. Figure 3.7 shows the photograph of the principal model made of plexiglass and the interfering models made of wood.

3.5.1 Instrumentation

Pressure measurements are carried out by using multi-input manifolds (Surry and Stathopoulos 1978) connected to Honeywell pressure transducers which accurately transfer

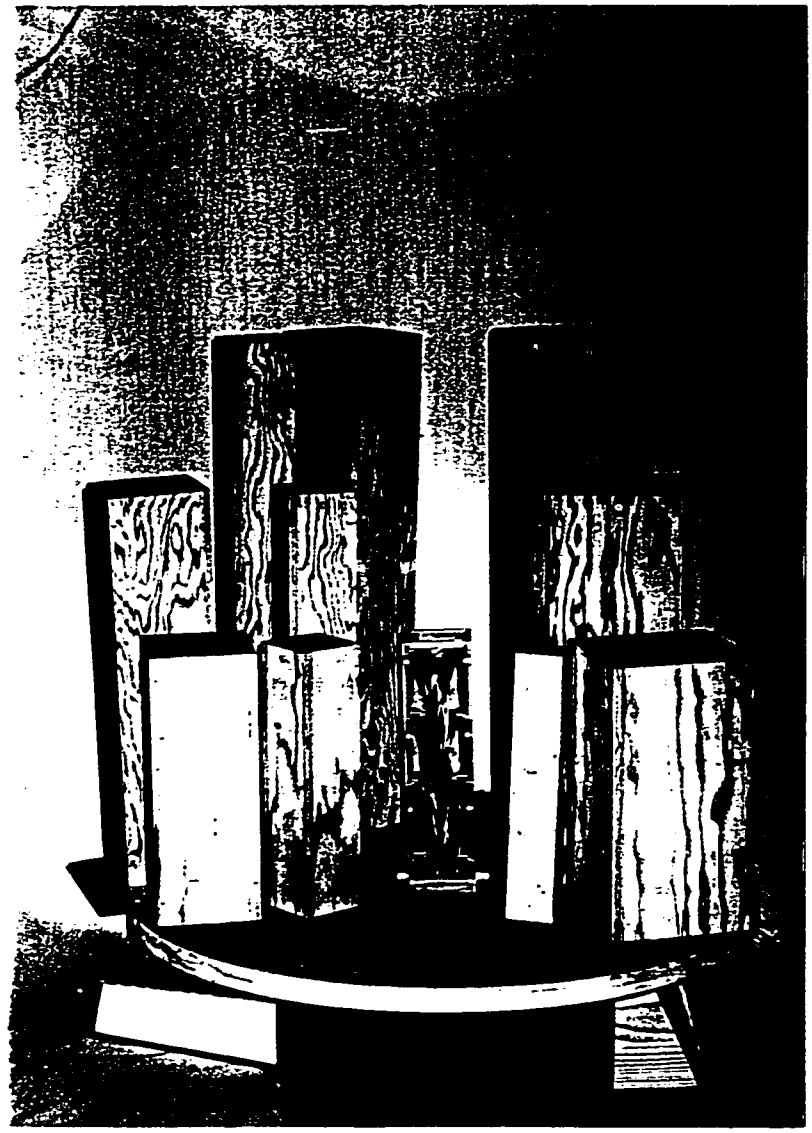

Figure 3.7 The principal (instrumented) building model surrounded by interfering building models made of wood

a pressure difference into an electric voltage. The connection between the model and the manifold is typically 1.6mm internal diameter plastic tubing containing a restricting insert of small bore made of brass tubing. A pitot static-tube located at the gradient height is connected to pressure transducers for determining the total pressure. The digitization of pressure signals and analysis of the data is done by Data6000 Universal Waveform Analyzer. A sampling frequency of 500Hz over a period of 16 seconds was used to evaluate the mean and standard deviation of the pressure data. The pressure spectra comprised an average of 8 such records. The aerodynamic forces are measured in terms of non-dimensional along-wind drag and across-wind lift coefficients as defined in equations 3.7 to 3.10. These forces are obtained by assigning a representative area to each tap location and multiplying it by the pressure at that location. The products are then summed up for each instrumented face of the model to yield the drag force and the lift force respectively. This kind of arrangement is routinely used for measuring mean drag and lift forces but is unsuitable for measuring fluctuating forces as well as for repetitive measurements, like those involving several interfering building configurations, because of high demands on time and resources. For measuring fluctuating drag or lift, instantaneous pressure values at each pressure tap location and their sum for two opposite faces of the building model are required. Therefore, *pneumatic averaging* (Surry and Stathopoulos 1978) is used to measure the fluctuating pressures in addition to mean pressures as well as to expedite the measurements. It also makes an efficient use of the wind tunnel, instrumentation and computer resources.

3.5.2 Area Averaging

Overall wind loads on a structure are due to the integral effect of surface pressures over the structure areas. As an alternative to direct force measurements, it is often preferable to estimate these loads by integrating or averaging the pressures over a surface. Mean pressures can be obtained by integrating pressure values obtained at various points over the surface under consideration. However, for wind engineering studies, mean values alone are not sufficient. It is also necessary to determine the fluctuating or root-mean-square and peak loads, as well as to obtain spectral information. A problem arises when averaging fluctuating pressures obtained from individual measurements. Since individual maxima of pressures do not occur simultaneously at all pressure tappings, peak pressures obtained from the direct summation of peak point pressures will overestimate the fluctuating and peak structural loads. This has been verified experimentally. However, a *pneumatically* averaged signal provides an instantaneous sum of the pressures at a number of tappings on a model surface, thus representing an area-averaged pressure whose statistics can be investigated.

The area averaging technique consists of pneumatically averaging the pressures from a number of taps connected in a carefully controlled fashion through a multi-input manifold to a pressure transducer. The transducer reads the instantaneous spatially-averaged pressure acting on the area associated with the pressure tap locations. Surry and Stathopoulos (1978) have shown that such manifolds can be used to determine both mean and fluctuating pressures accurately. Sockel and Krönke (1992) measured area loads with pneumatic averaging method and found good agreement for mean values when compared with numerically averaged results of transducers flush-mounted on the surface of the model. Gumley (1983), used detailed theoretical analysis backed by experiments, to validate the

area averaging procedure on such systems and to describe the properties of manifold networks. Manifolds of up to 16 inputs have been shown successful for area load measurements (Surry et al. 1983).

Figure 3.8 shows the 12-input manifold used in this study. Four such manifolds are used, one for each face of the model. Each of the 12 pressure taps is connected to an input of the manifold by a 1.6mm internal diameter plastic tubing containing a restricting insert of small bore made of brass tubing to damp the resonance and to keep the frequency response flat.

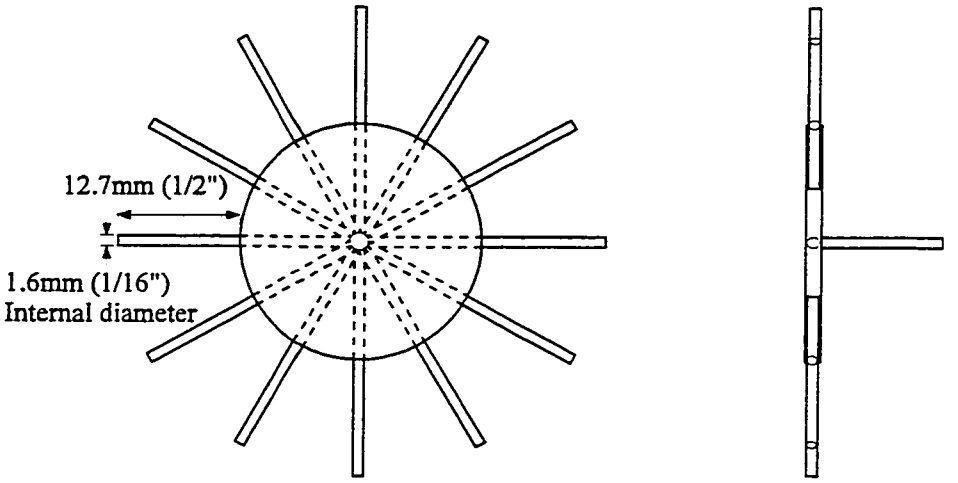

Plan view Side view

Figure 3.8 Pneumatic averager

Restrictors are widely used in wind engineering experiments for the measurement of fluctuating pressures on building models where high frequency response capabilities are desired (Irwin et al. 1979 and Gumley 1983). The total length of the plastic tubing is 600mm, the brass restrictor being inserted at a distance of 355mm from the pressure tap. This tubing system responds adequately to pressure fluctuations on the model up to a

frequency of 100Hz with negligible attenuation or distortion (Stathopoulos et al. 1981). The output of each manifold is connected to a Honeywell transducer. The tubing-restrictor-manifold-transducer system maintains low distortion of the pressure signal while allowing relatively long tube lengths to be used to ease the mounting of instrumentation underneath the building model.

3.5.3 Presentation of Data

Measurements of the surface pressure on the model is reduced to non-dimensional pressure coefficients by referencing them to the mean dynamic velocity pressure $(1/2)\rho U^2$ (where ρ is the density of air and U represents the free-stream mean velocity). The non-dimensional pressure coefficient $\overline{C}_p$, as defined in equation 2.1, enables the application of experimental results on the model directly to the prototype. The term $(1/2)\rho U^2$ is obtained by taking the difference of the total or stagnation pressure measured with the help of a Pitot static tube and the static or ambient pressure.

The manifolds enable the building to be considered as a whole rather than its individual instrumented points and provide the total mean and standard deviation of the wind forces acting on each of the four walls of the building. A data acquisition program was written to capture 16s of simultaneous force data as well as the force spectra. The forces on two opposite walls are subtracted to give overall forces in two mutually perpendicular - the along-wind (drag) and across-wind (lift) direction. The forces are measured with respect to the building axis system as shown in Figure 3.9. The mean and fluctuating forces are eventually converted into non-dimensional force coefficients given by the following equations:

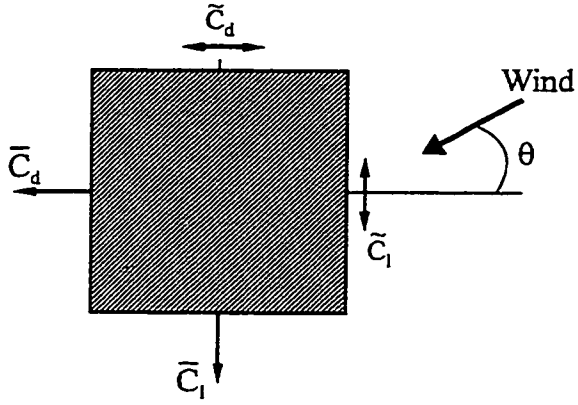

Figure 3.9 Representation of force coefficients on the building axis system

$$\bar{C}_d = \frac{\bar{F}_d}{\frac{1}{2}\rho U^2 A} \tag{3.7}$$

$$\bar{C}_l = \frac{\bar{F}_l}{\frac{1}{2}\rho U^2 A} \tag{3.8}$$

$$\tilde{C}_d = \frac{\tilde{F}_d}{\frac{1}{2}\rho U^2 A} \tag{3.9}$$

$$\tilde{C}_l = \frac{\tilde{F}_l}{\frac{1}{2}\rho U^2 A} \tag{3.10}$$

where $\bar{C}_d$ and $\bar{C}_l$ are the mean drag and mean lift coefficients, respectively; $\bar{F}_d$ and $\bar{F}_l$ are the mean drag and mean lift forces, respectively; $\tilde{C}_d$ and $\tilde{C}_l$ are the fluctuating drag and fluctuating lift coefficients, respectively; $\tilde{F}_d$ and $\tilde{F}_l$ are the fluctuating drag and fluctuating lift forces, respectively; ρ is the density of air; U is the free-stream mean velocity at the top of the building and A is the projected area of building face normal to

the direction of wind. The results of interference tests are presented in terms of an Interference Factor (*IF*) given by:

$$IF = \frac{\textit{Force coefficient on principal building (interfering building present)}}{\textit{Force coefficient on principal building (isolated condition)}} \qquad (3.11)$$

The Interference Factors are presented in terms of contours, graphs and simple recommendations. These sets of contour maps are eventually used for providing simplified and general guidelines on interference effects. Empirical modelling based on the database generated by wind tunnel tests provide curve fitting equations for the evaluation of wind loads on a building affected by interference caused by an adjacent building.

Theorists conduct experiments with their brains. Experimenters have to use their hands, too. Theorists are thinkers, experimenters are craftsmen. The theorist operates in a prismatic place free of noise, of vibration, of dirt. The experimenter develops an intimacy with matter as a sculptor does with clay, battling it, shaping it, and engaging it.

-James Gleick, Chaos: Making of New Science (1987)

4

Experimental Results - Exploratory tests

On the basis of an analysis of the literature results, a preliminary framework for the experimental programme is set up and, as explained previously, the entire experimental programme is divided into two categories: exploratory or pilot tests and detailed experiments. The main aim of the exploratory tests is to provide a quick, preliminary estimate of the extent of interference that would eventually form the basis of the detailed experiments. These tests also help verify some of the literature results. A three-component strain gauge force balance is used to measure the along-wind drag and across-wind lift forces on the principal building due to a similar adjacent building. The fabrication details and the working of the force balance have been discussed in chapter 3. Measured forces on a building due to interference from an adjacent building are compared with those on an isolated building and some of the results are validated by comparison with available literature data. The results are presented in terms of drag and lift Interference Factors, IF (see equation 3.11). The extent of interference is defined on a grid similar to that shown in Figure 3.3 with areas of special significance highlighted on it. The main target of investigation in the pilot study is the two equal building configuration (P_0 - I_1) because some literature results for comparison and validation are available for this configuration only. This limited exercise has helped gauge, to a reasonable degree of confidence, the overall scenario and trends, and prepare legitimate cases for a detailed analysis. Sections 4.1 and 4.2 validate the available literature results as well as demonstrate the effectiveness of the

force balance. To reiterate once again, the main purpose of this exercise is to garner trends rather than absolute values. These trends are presented in the form of *Interference Influence Grids* in section 4.3. The knowledge of such trends helps understand the influence of the interfering building and reduce drastically the number of configurations to be tested during detailed experiments.

4.1 Mean Loads

The effect of interference on mean loads is shown, for four typical cases, in Figure 4.1, wherein the present force balance results are compared with literature data. All cases are tested with wind normal to a face of the principal or instrumented building. The agreement between the two seems to be quite good in general except for the results of Lee and Fowler (1975). This can be explained by the fact that while the buildings tested by Sakamoto and Haniu (1988) and Taniike (1991) had more or less similar relative dimensions as in the present study (width:depth:height = 1:1:4), Lee and Fowler's 25.4mm x 25.4 x 460mm (1:1:18) building model represents a tall and slender building.

As expected, mean loads are reduced due to the effects of interference. In Figure 4.1(a) this translates to a beneficial *shielding* when two buildings are arranged in tandem. However, for close separation (less than 2b, where b is the width of the principal building), the principal building may experience severe suction (IF < -0.10), i.e., a pull directed towards the interfering building. In case of close tandem locations, both buildings are completely submerged in the wake of the upstream building, the pressure on the windward face of the principal building is reduced drastically due to the almost complete shielding provided by the upstream building. The reduction is so high that the usual pressure on this

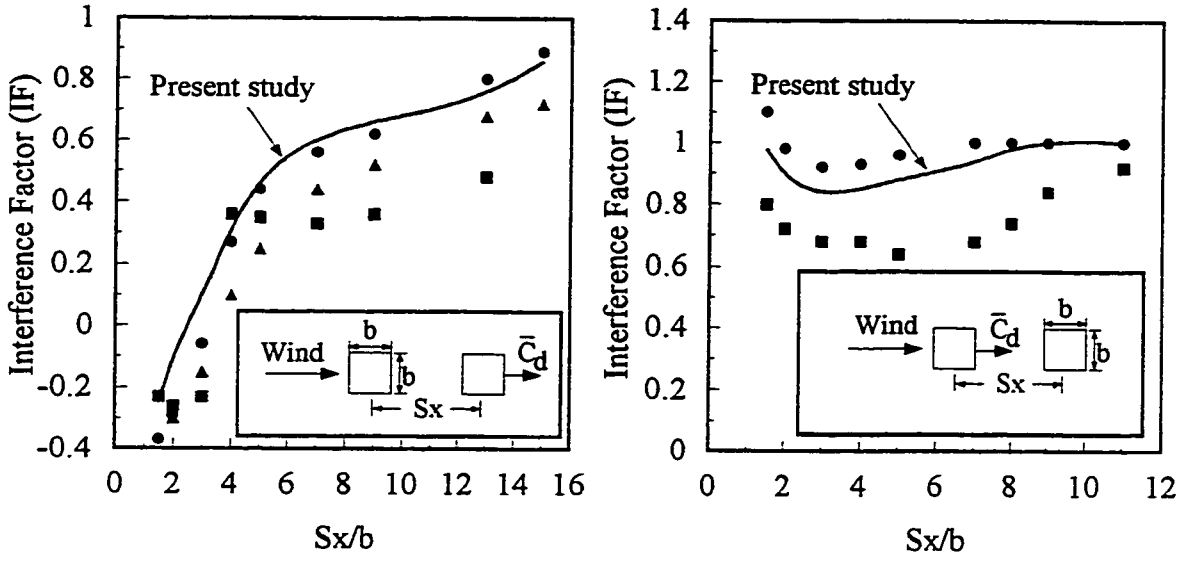

(a) Mean-drag IF for downstream building (b) Mean-drag IF for upstream building

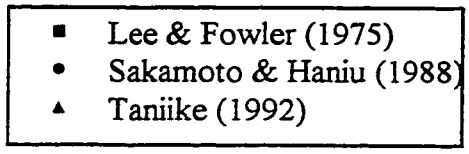

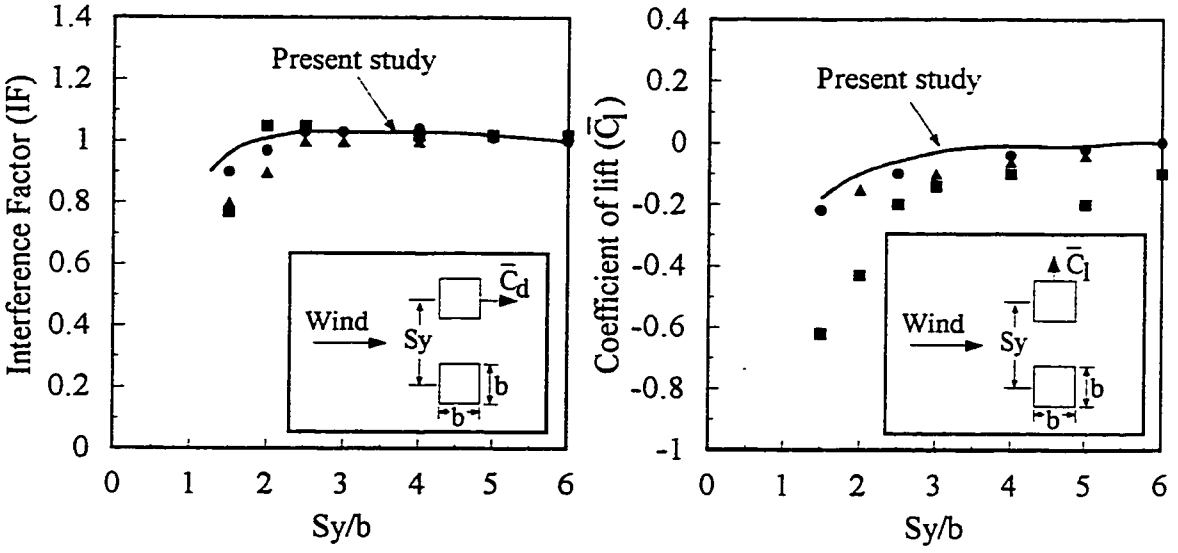

(c) Mean-drag IF (d) Coefficient of lift

Figure 4.1 Effect of interference on mean wind forces

face changes into suction on account of the high velocity eddies forming in between the small gap between the two buildings. Moreover, the two close-spaced buildings almost replicate a rectangular building with a larger along-wind length so that the velocity of the flow reduces considerably on reaching the leeward end of the principal building, reducing the suction on its leeward face and hence the principal building experiences a reduction in overall drag. The shielding effect of the interfering building is felt from as far as 12 times the building width, reducing the mean drag on the principal building by 30%. When the principal building is located upstream of the interfering building (see Figure 4.1(b), the effect is not as spectacular barring a minor dip in the IF curve around a spacing of 2b. For most of the part, the IF value hovers around 1.0, an isolated building condition.

Figures 4.1(c) and 4.1(d) compare the values of mean drag and lift when two buildings are arranged side-by-side. Mean drag remains virtually unaffected. However, in case of mean lift, high suctions ($\overline{C}_l < -0.10$) are registered again, for close spacings of less than 2b ($\overline{C}_l$ for isolated building is 0). This is due to the so-called "channelling effect" created by the speeding-up of wind through the narrow channel between the two buildings. This reduces the force on the inside wall of the principal building, thus causing a pull or suction directed towards the adjacent building. A complete scenario including the effects of interference for staggered locations is presented in Interference Influence Grids in section 4.3.

4.2 Dynamic Loads

Dynamic loads are expressed in terms of the standard deviation of fluctuating drag in the along-wind direction and fluctuating lift in the across-wind direction. Both quantities

register considerable increase on account of interference. Figures 4.2 and 4.3 compare Interference Factors (IF) for representative locations with literature results. The agreement seems to be quite satisfactory in general, except in case of Figure 4.2(c) and Figure 4.3(c) where one of the literature results does not seem to follow the general trends of the other two data sets. A reason for this disagreement is not available at this time, however, a clearer picture is expected to emerge after detailed experiments. Figure 4.2 shows IF for dynamic drag, registering high values around an along-wind spacing (Sx) of 4b. The maximum value of IF reached (not shown here) was 1.74 around Sx = 3b and Sy = 1.5b, i.e. an increase of 74% in dynamic drag. Figure 4.3 shows IF for dynamic lift. The values are, in general, higher than dynamic drag and the area around the principal building where interference effects are prevalent is also wider than the case of dynamic drag. The largest value of dynamic lift IF observed (not shown here) was 1.84 around Sx = 5b and Sy = 2.25b. A comprehensive scenario is presented in Interference Influence Grids in the following section.

4.3 Interference Influence Grids

The results of the exploratory tests are presented in terms of Interference Influence Grids (IIG). These grids represent, at this stage, the extent of interference on a buildings by an adjacent building of equal size subjected to wind blowing normal to a face of the building. The IIGs, in a sense, present the summary of the exploratory tests and serve as the preliminary knowledge source for the detailed interference effects experiments. They are refined after carrying out the detailed experiments, to incorporate in addition to accurate IFs, the effect of building geometry, wind direction and upstream terrain conditions.

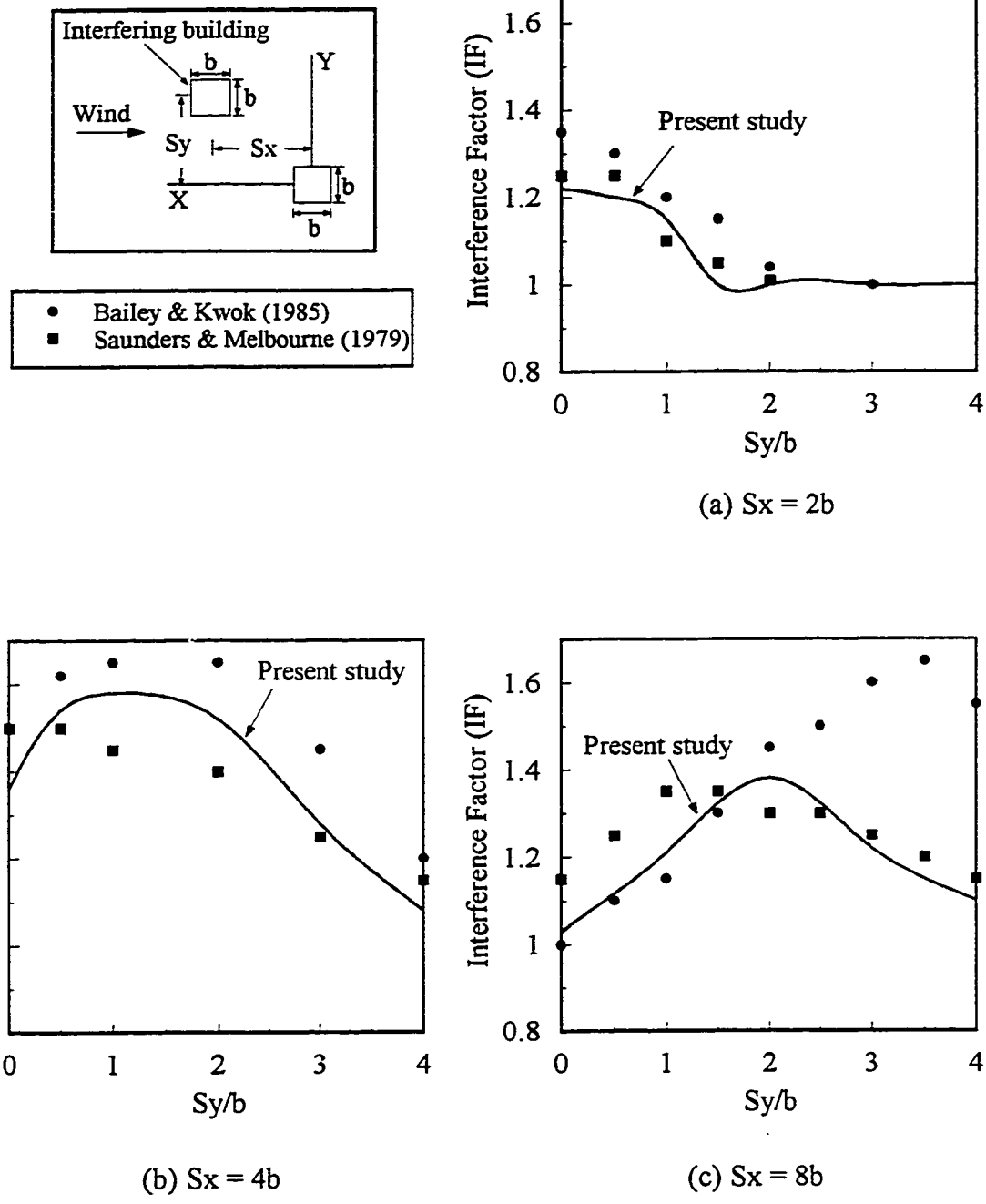

Figure 4.2 Comparison of dynamic drag

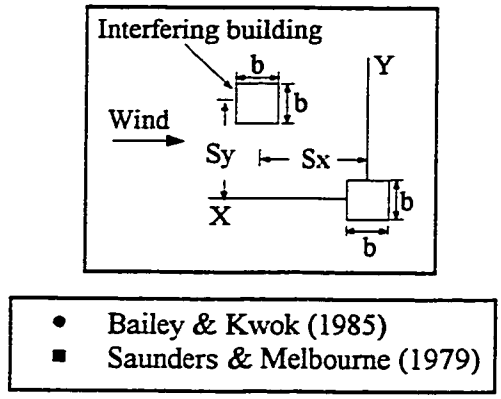

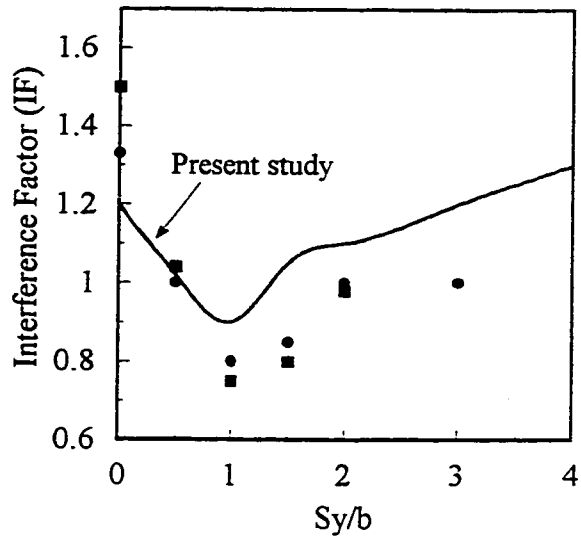

(a) Sx = 2b

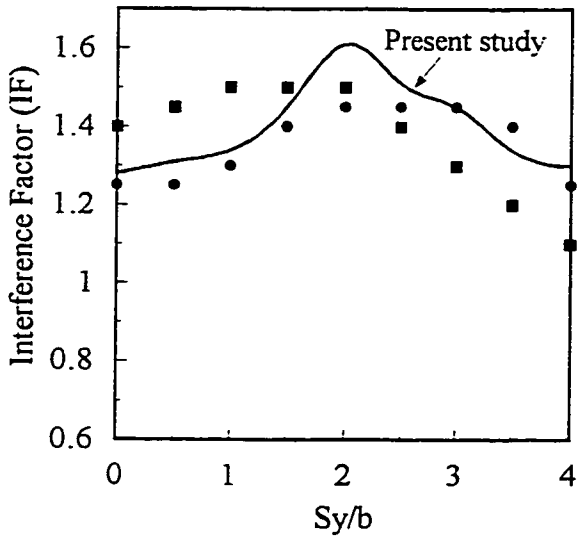

(b) Sx = 4b

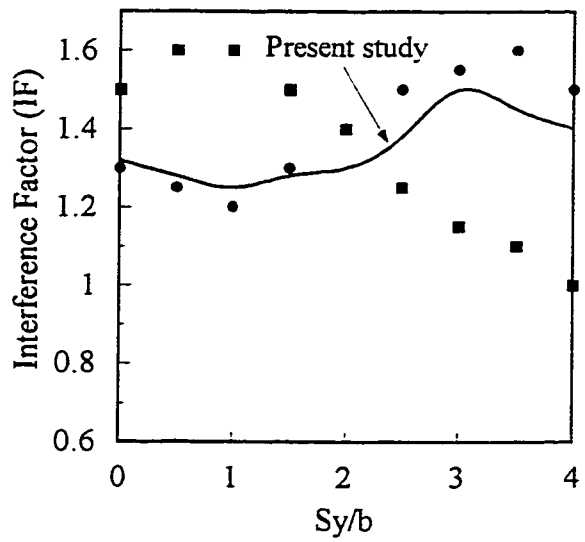

(c) Sx = 8b

Figure 4.3 Comparison of dynamic lift

Figure 4.4 shows IIGs for mean interference effects. The large area (white) unaffected by interference effects is conspicuous in Figure 4.4, as are the areas of high shielding shown in Figure 4.4 (a). As discussed previously, high suction location in case of mean drag (Figure 4.4 (a)) is immediately in front of the principal building, whereas for mean lift, this area lies to the side of the principal building. The critical locations for mean drag are the ones where excessive shielding or high suctions are produced. The high suction region is at Sx < 2b reducing the overall coefficient of mean drag ($\overline{C}_d$) on the principal building to about -0.30 ($\overline{C}_d$ for isolated building is 1.30). High shielding is observed up to an along-wind separation of 10b. Coefficient of mean lift ($\overline{C}_l$) increases considerably (up to 0.30) for Sx = 1.5b to 5b and Sy = b to 2.5b upstream and, for Sx = -1.5b to -2.5b and Sy = b to 2b downstream. However, $\overline{C}_l$ reduces (up to -0.25) for sideways locations spanning Sx = -b to b and Sy = b to 3b ($\overline{C}_l$ for isolated building = 0). Close locations at less than 2b distance around the principal building are a cause for special concern from the point of view of mean forces.

Figure 4.5 presents IIGs for dynamic or fluctuating interference effects. It is clear that the influence zone for dynamic lift (Figure 4.5 (b)) is larger than that of the dynamic drag (Figure 4.5 (a)). The area of high dynamic drag ($\widetilde{C}_d$) is closer to the principal building whereas the location of high dynamic lift ($\widetilde{C}_l$) is farther upstream and to the side of the principal building. The largest increase in fluctuating drag forces occurs when the principal building is located near the edge of the wake of the upstream building rather than within the wake region. There is no significant increase in forces when the buildings are positioned

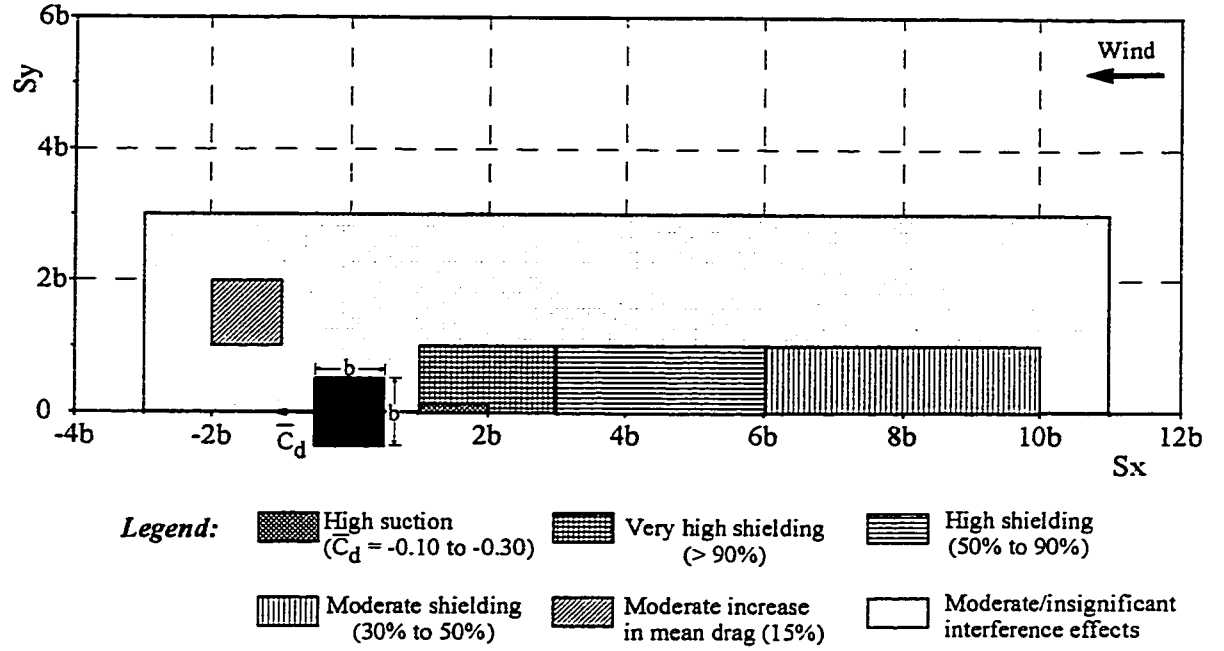

(a) Mean drag

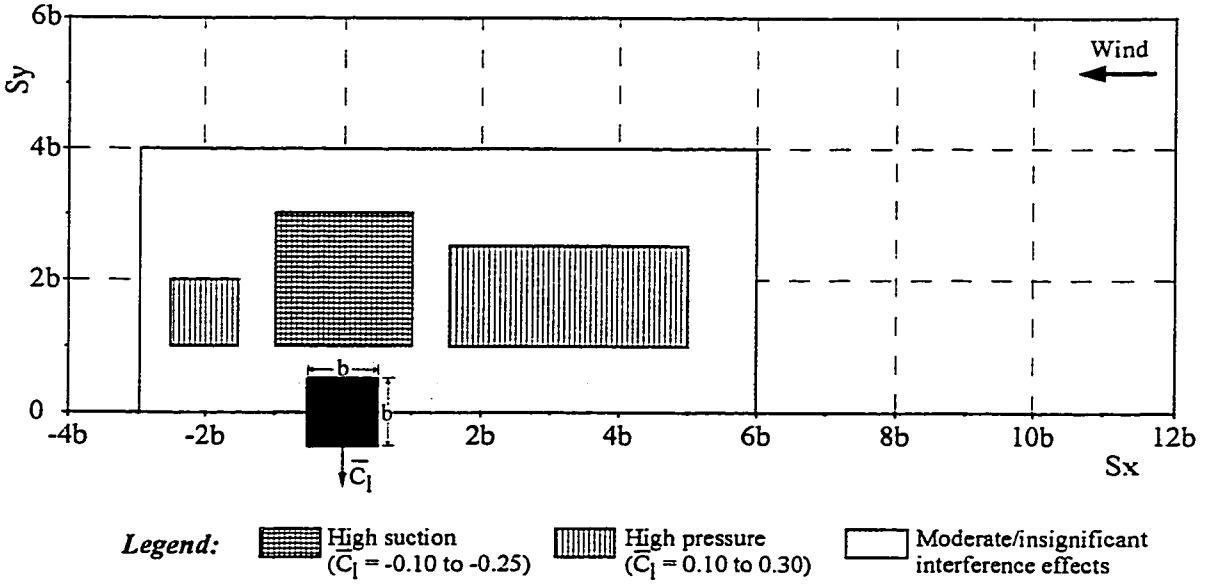

(b) Mean lift

Figure 4.4 Pilot study results - areas of influence for mean interference effects

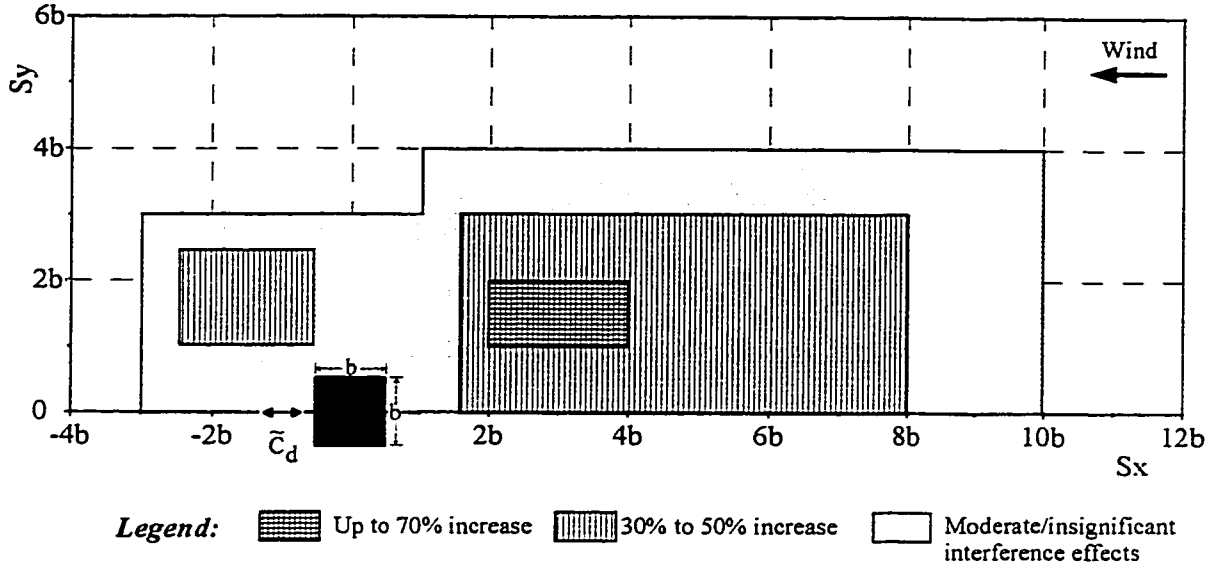

(a) Dynamic drag

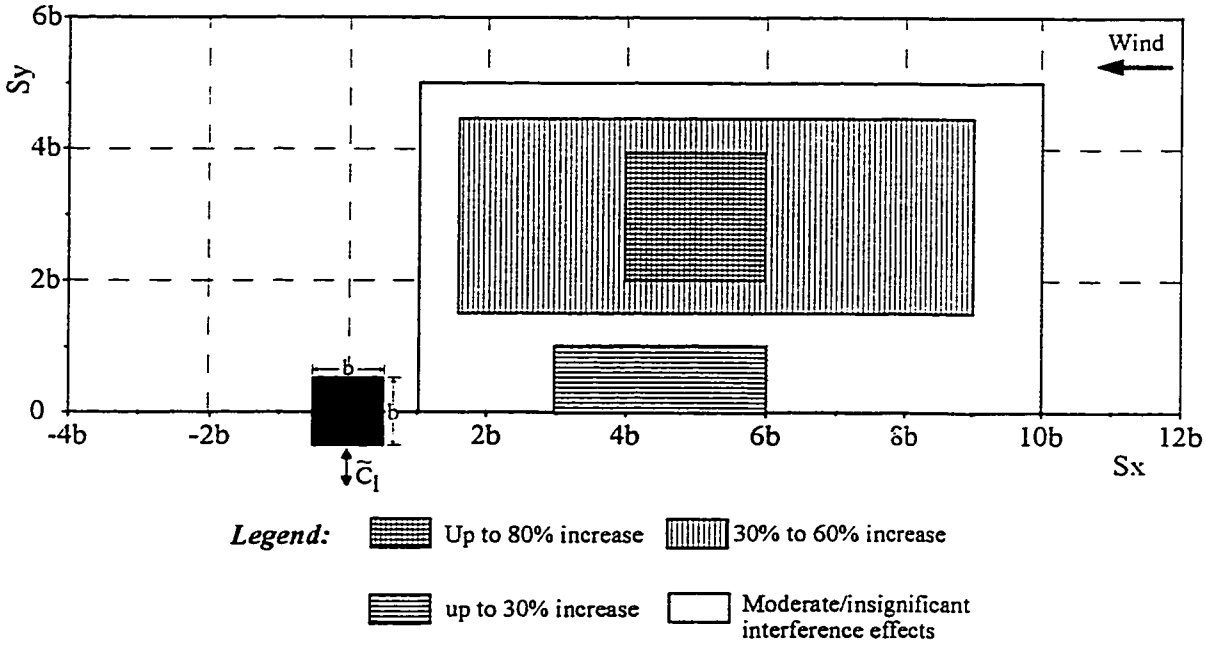

(b) Dynamic lift

Figure 4.5 Pilot study results - areas of influence for dynamic interference effects

in a side-by-side arrangement, the maximum increases occur along a diagonal line making an angle of about 30° to 45° with the normal to the windward face of the building. The sensitive locations upstream for fluctuating drag are Sx = 1.5b to 8b and Sy = 0 to 3b causing an increase of up to 70%, and Sx = 1.5b to 9b and Sy = 1.5b to 4.5b for fluctuating lift, increasing it by up to 80%. Interfering buildings located within a small sensitive spot downstream at Sx = -0.5b to -2.5b and Sy = b to 2.5b cause a 30% to 50% increase in fluctuating drag.

Figures 4.4 and 4.5 will help formulate the strategy for detailed interference effects experiments. They will also help reduce the number of configurations to be tested in the wind tunnel.

4.4 Summary

Preliminary results based on exploratory tests show a considerable change in wind loads on a building due to the presence of a similar adjacent building. Mean loads are generally reduced, causing beneficial shielding for most tandem locations, but also creating high suction for some close locations. Fluctuating loads register a considerable increase over a wide region around the principal building. The available literature results are validated and show similar trends as in the present study. The Interference Influence Grids provide a consolidated picture of the effect of interference and will provide the stepping stone for further detailed experiments.

Everything should be as simple as it is, but not simpler

-Albert Einstein (1879-1955)

5

Detailed Experiments - Isolated Building

Since interference effects are defined relative to an isolated, free-standing building, the coefficient of drag and lift for a single building are measured carefully and validated with literature results. The term isolated free-standing (or isolated) building is applied to a building without any adjacent buildings. Surprisingly, comprehensive studies on tall isolated buildings in boundary layer flow that take into account the building size, turbulence intensity of approach flow and wind direction are relatively few and general trends are difficult to postulate. Although an in-depth study of wind forces on isolated buildings is not the mandate of the present study, certain clear trends in the data have been established and generalized empirical equations defining wind loads on isolated buildings of square foot-print have been suggested. The experimental set-up has been discussed in chapter 3. In this chapter, general flow mechanisms with respect to isolated buildings are discussed and experimental results are presented, compared and analyzed. Data from measurements carried out on a static "pressure" model representing a 20m x 20m x 80m building are presented in terms of drag and lift coefficients. The forces are measured with respect to the building axis system as shown in Figure 3.9. The effect of turbulence and wind direction on building wind loads is discussed and general trends are established.

5.1 General Flow Mechanism

The general wind flow pattern and related mechanism for an isolated building under the

action of wind normal to a face has been discussed in chapter 2, section 2.2. To recapitulate (see Figure 2.1), when wind strikes a building normal to one of its faces, it is slowed down against the front face and generates a pressure on that face, decreasing towards the edges. The pressure cushion drives the flow ahead so that it passes round the sides and over the roof of the building. There is also a down-flow on the lower part of the windward face, forming eddies that direct the wind flow away from the building opposing the general direction of the wind. The flow in the windward eddy spirals along the face of the building and escapes round the sides with increased speed reducing the pressure on the side walls. Suctions are thus developed on the sides of the building parallel to the wind direction as well as on the leeward surfaces and the roof.

The wind does not always blow normal to a face of the building and the flow pattern when the wind strikes a building obliquely should be considered. Figure 5.1 shows the general flow pattern around a building and the resulting mean pressure distribution for oblique winds. The conditions shown may change depending upon the direction of wind.

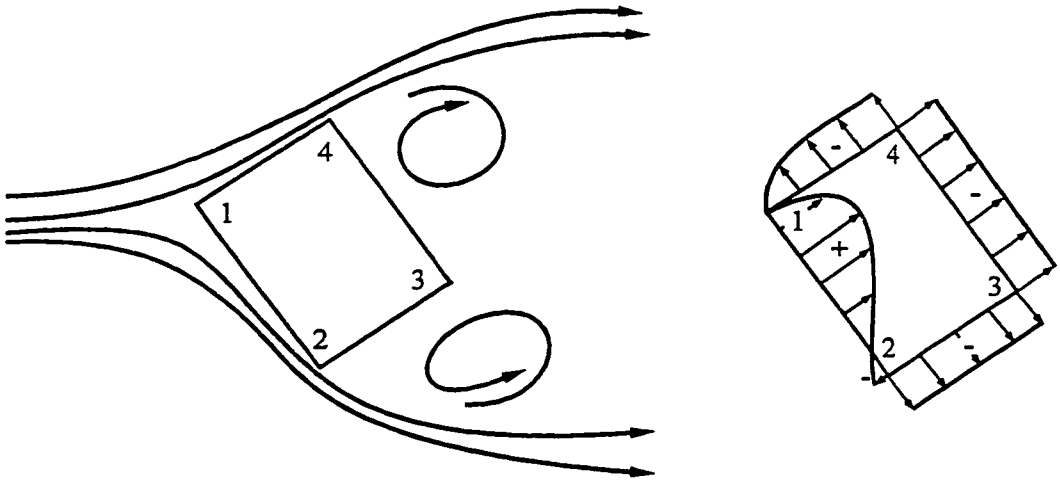

(a) Flow pattern (b) Mean pressure distribution

Figure 5.1 Wind flow and pressure distribution on a building for oblique winds

As shown in Figure 5.1 (a), the flow divides at the leading corner, the wind striking face 1-2 at a large angle is slowed down and pressure is thus developed on the face. As the flow accelerates down face 1-2, it creates suction at edge 2. The face 1-4 which is only glanced by the wind may cause no retardation of the flow, and the acceleration which is necessary for the wind to pass around the building will generally lead to suction on such a face. Suction will also be experienced by the leeward faces 2-3 and 3-4 which are under the influence of the separation bubble in the wake. The magnitude of the wind load on a building is also affected by the turbulence intensity in the approach flow.

In the present study, wind loads on the principal building are expressed in terms of non-dimensional mean and fluctuating (standard deviation) drag and lift coefficients. All coefficients are measured with respect to the building axis system.

5.2 Mean drag and lift

Figure 5.2 shows the variation of mean drag ($\overline{C}_d$) and lift ($\overline{C}_l$) with the angle of attack of wind for open, suburban and urban exposures. It is clear from Figure 5.2(a) that the maximum $\overline{C}_d$ is registered for wind striking the building at an angle (θ) of 0°, normal its face. Also evident is the fact that the drag coefficient reduces with increasing turbulence intensity of wind or, in other words, on changing the upstream exposure from open to urban. Recall from Figure 3.1 that the turbulence intensities associated with the three exposures are: 7% for the open, 13% for the suburban and 25% for the urban exposure, measured at the building height (80m). From Figure 5.2(a), the maximum values of $\overline{C}_d$ (at θ = 0°) are, 1.30, 1.15 and 1.02 for open, suburban and urban exposure respectively. The incident turbulence affects the development of the separated shear layers, the entrainment

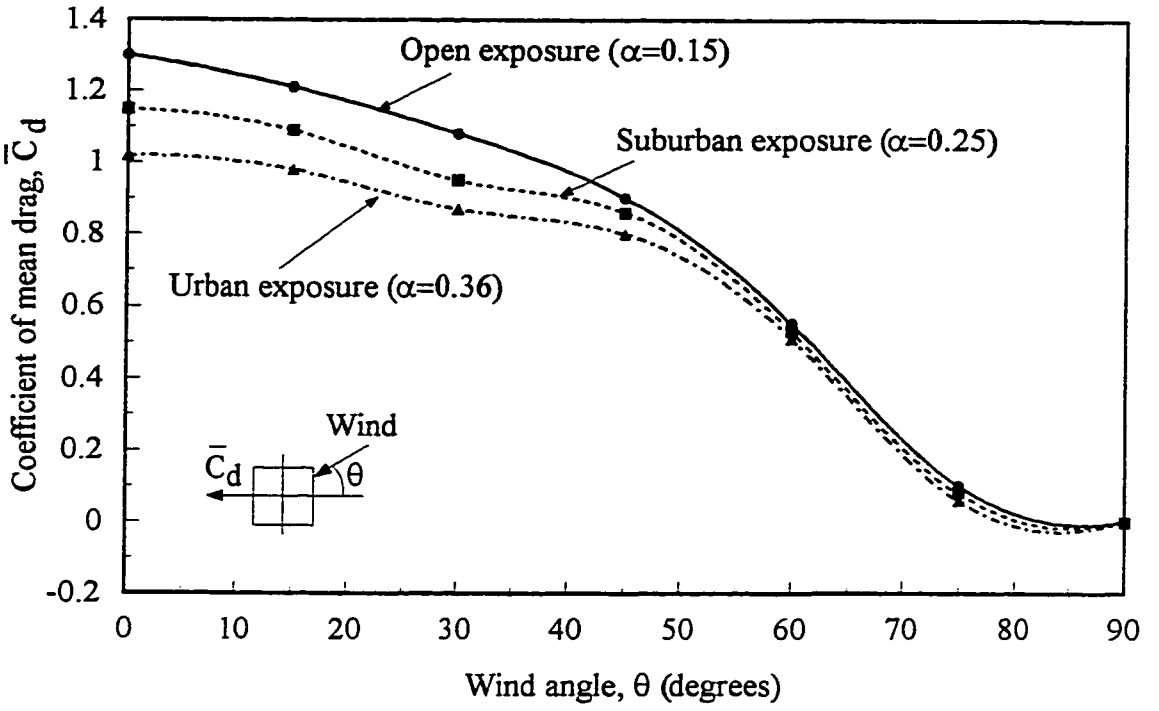

(a) Mean drag

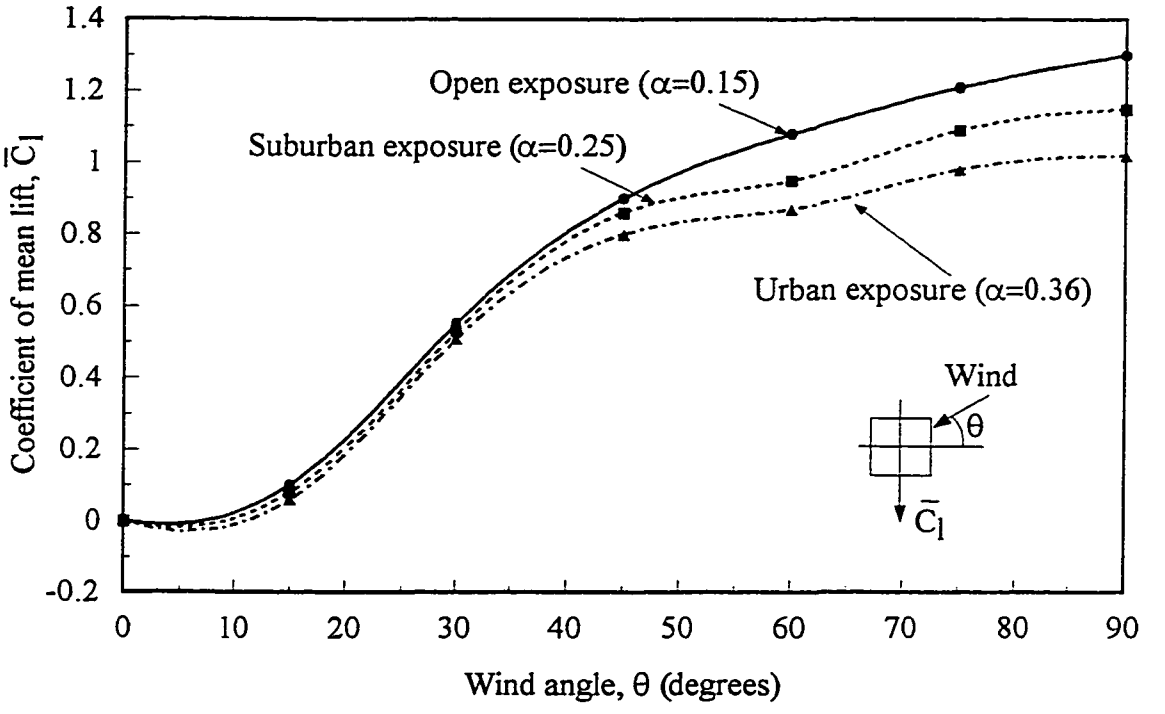

(b) Mean lift

Figure 5.2 Variation of mean drag and mean lift on a building with wind angle

of fluid into these layers, and consequently the reattachment of the shear layers (Laneville et al. 1975). The reattachment of the shear layers separating from the front corners of the building to its sides leads to a pressure recovery that decreases the suction behind the building and hence reduces the drag. Lee (1975) and Akins (1992) found a decrease in the value of mean force coefficients with increasing incident turbulence for a series of rectangular prisms. Bearman (1978), found the base pressure, which effects the drag, relatively insensitive to the scale of turbulence but highly dependent on its intensity, a fact also corroborated by Courchesne and Laneville (1980) and Saathoff and Melbourne (1987). Since $\overline{C}_d$ and $\overline{C}_l$ are represented in building axes (see Figure 3.9), $\overline{C}_l$ values show similar magnitude, but a trend that is opposite to $\overline{C}_d$, with zero value for $\theta = 0°$, a maximum at $\theta = 90°$ but similar values at $\theta = 45°$ (Figure 5.2(b)).

The effect of changing the angle of attack of wind is to alter the path of the shear layers and correspondingly change the forces on the building faces. Figure 5.2(a) shows that for all the three approach terrains, mean drag steadily decreases to zero at $\theta = 90°$. The maximum difference in the value of $\overline{C}_d$ among the three approach terrains is at $\theta = 0°$. With increasing angle of attack of wind θ, this difference decreases and becomes insignificant after $\theta \approx 40°$. Vickery (1966) attributed the decrease in mean and fluctuating forces with increasing turbulence intensity to an increase in the base pressure at small angles of attack. For larger angles of attack where there would be no possibility of reattachment, the changes in the base pressure would be insignificant. Thus, it seems that the appreciable decrease in drag with increasing turbulence intensity continues up to the angle at which steady reattachment to the side face occurs.

Figure 5.3 compares the results of mean drag from the present study with those of Akins (1992), ESDU (1979) and Taniike (1992). Agreement is good with Akins (1992) (power law exponent, $\alpha = 0.12$ and turbulence intensity $I_v = 7.2$ %). ESDU (1979) displays a similar trend, although appreciably higher values. A plausible explanation may be that ESDU (1979) values are culled from various sources and corrected for the effects of varying turbulence intensities in approach flow. The highest value of $\overline{C}_d$ for $\theta = 0°$ is 1.37 by Taniike (1992) owing to a low value of turbulence intensity of less than 2%.

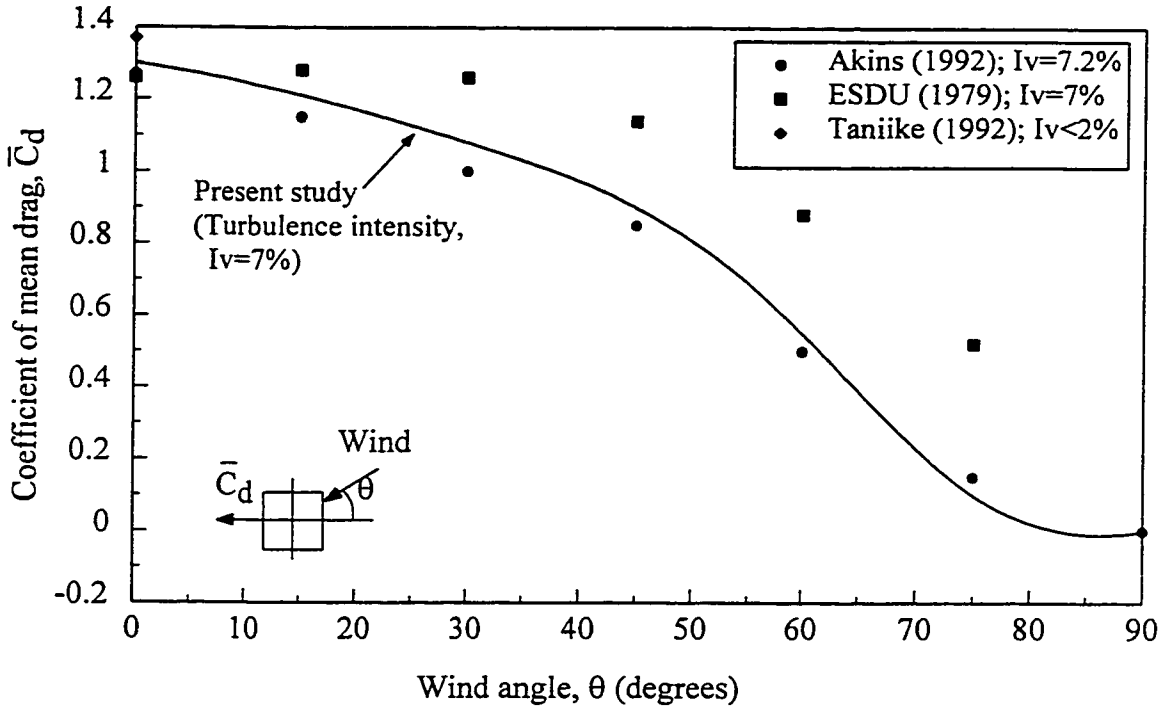

Figure 5.3 Comparison of mean drag for open approach terrain

Based on a thorough analysis of the experimental data, generalized empirical equations defining coefficients of mean drag and lift for buildings of square footprint, taking into account the effects of incident wind direction and turbulence intensity are suggested. The

coefficient of mean drag, $\overline{C}_d$ is given by,

$$\overline{C}_d = A - B\left(\frac{\theta}{100}\right) - \left(\frac{\theta}{100}\right)^2 \tag{5.1}$$

where, θ is the angle in degrees, of incident wind with the normal to the building face (see Figure 3.9) and A and B represent the effects of the incident turbulence intensity I_v (%), and are given by,

$$A = 1.9(I_v)^{-0.19} \tag{5.2}$$

$$B = 3.0(I_v)^{-0.80} \tag{5.3}$$

For calculating the values of mean lift, $\overline{C}_l$, θ is replaced by 90° - θ in equation 5.1.

Table 5.1 shows the comparison of the above equations with experimental results. The mean of the sum squared errors (MSE) over all measured wind directions are 0.006, 0.008 and 0.009 for the open, suburban and urban exposures, respectively. Except for θ = 75°, where the errors in the predictions are rather large, the empirical equations predict the values of coefficient of mean drag reasonably well for an upstream turbulence range of 7% to 25%.

Table 5.1 Comparison between observed (experimental) and predicted (regression) values for mean drag coefficient

Wind angle (°)	*Upstream exposure*					
	Open		Suburban		Urban	
	Observed	Predicted	Observed	Predicted	Observed	predicted
0	1.30	1.31	1.15	1.17	1.02	1.03
15	1.21	1.19	1.09	1.09	0.98	0.97
30	1.08	1.03	0.95	0.96	0.87	0.87
45	0.90	0.82	0.86	0.79	0.80	0.72
60	0.55	0.57	0.53	0.57	0.51	0.53
75	0.10	0.27	0.08	0.31	0.06	0.30
90	0.00	-0.07	0.00	0.01	0.00	0.01
MSE	*0.006*		*0.008*		*0.009*	

5.3 Fluctuating drag and lift

Figure 5.4 shows the variation of standard deviation of fluctuating drag ($\widetilde{C}_d$) and fluctuating lift ($\widetilde{C}_l$) with the angle of attack of wind for open, suburban and urban exposures. The fluctuating force coefficients decrease with increasing turbulence intensity, which once again emphasizes the influence of turbulence on the flow around a building and the consequent reduction in the fluctuating drag and lift forces. Unlike the mean forces, the effect of turbulence does not diminish at larger wind angles. The periodic vortex shedding is destroyed by high turbulence intensity in the approach flow, resulting in a redistribution of the energy associated with pressure fluctuations over a wide frequency range and hence lower fluctuating forces are registered for higher turbulence intensities. For $\theta = 0°$, $\widetilde{C}_d$ is 0.25 which compares well with a similar value found by Reinhold et al. (1977), but for a very tall building model (aspect ratio 1:17.5) and at a turbulence intensity of 12%; and, a value of 0.22 found by Vickery (1968) for a building of similar proportions as used in this study and at a turbulence intensity of 10.5%. On the basis of experiments on a tall, square building, Kareem (1982) and Kareem and Cermak (1984) found the value of fluctuating lift ($\widetilde{C}_l$) to be 0.34 for the open terrain ($\alpha = 0.12$) and 0.27 for the urban terrain ($\alpha = 0.34$). The corresponding values for the present study are 0.35 and 0.25 respectively. No other comparable data is available for other incident wind angles.

Figure 5.5 shows the drag and lift time histories measured simultaneously for the windward, leeward and side faces of the building with an open approach terrain and a 0° wind azimuth, normal to the windward face. From Figure 5.5(a), the pressure on the windward face and suction on the leeward face are clearly evident. The nature of

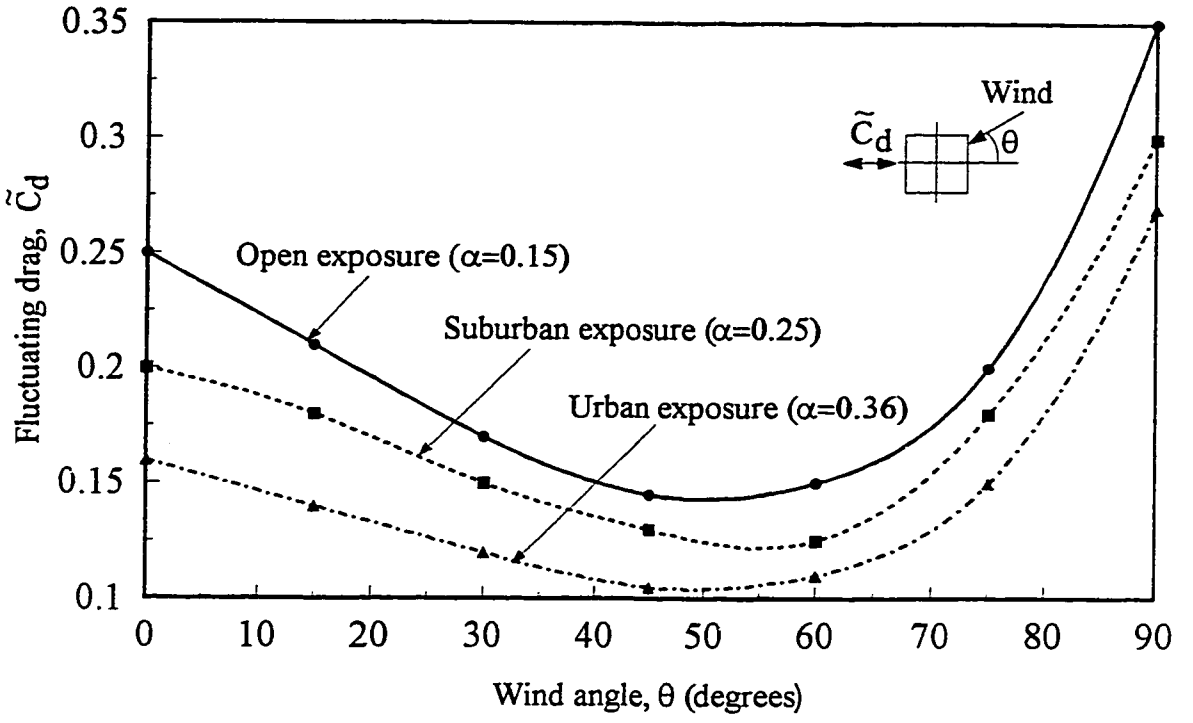

(a) Fluctuating drag

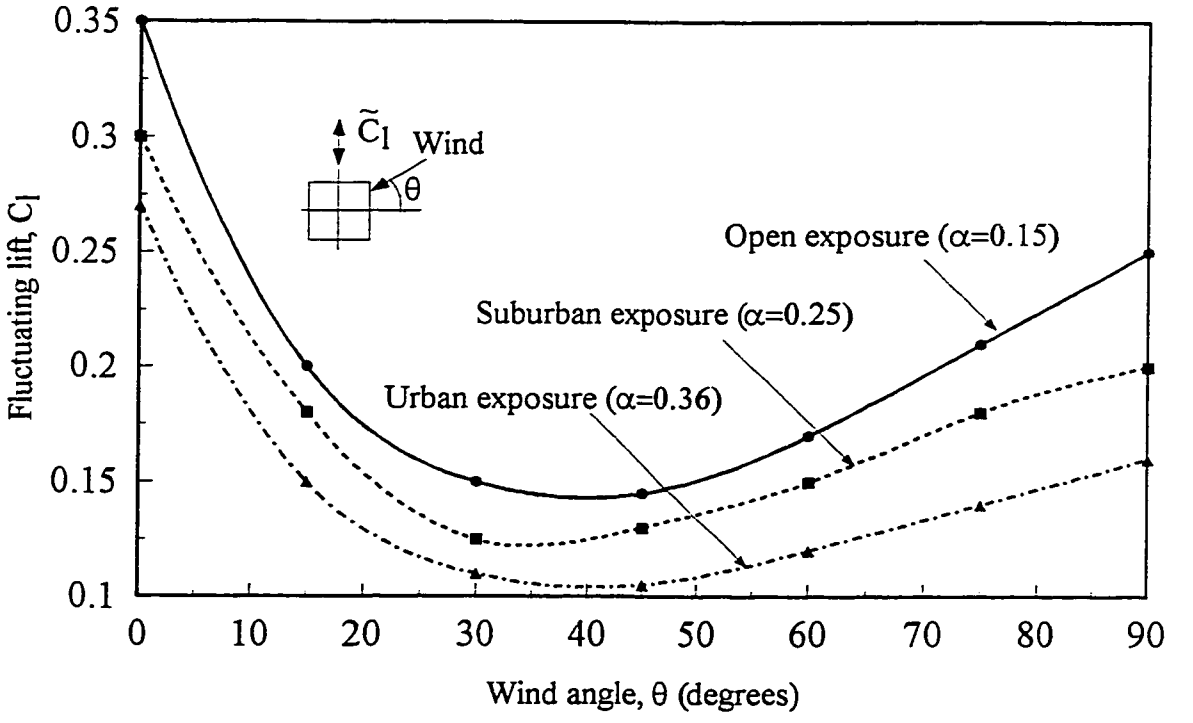

(b) Fluctuating lift

Figure 5.4 Variation of fluctuating drag and fluctuating lift on a building with wind angle

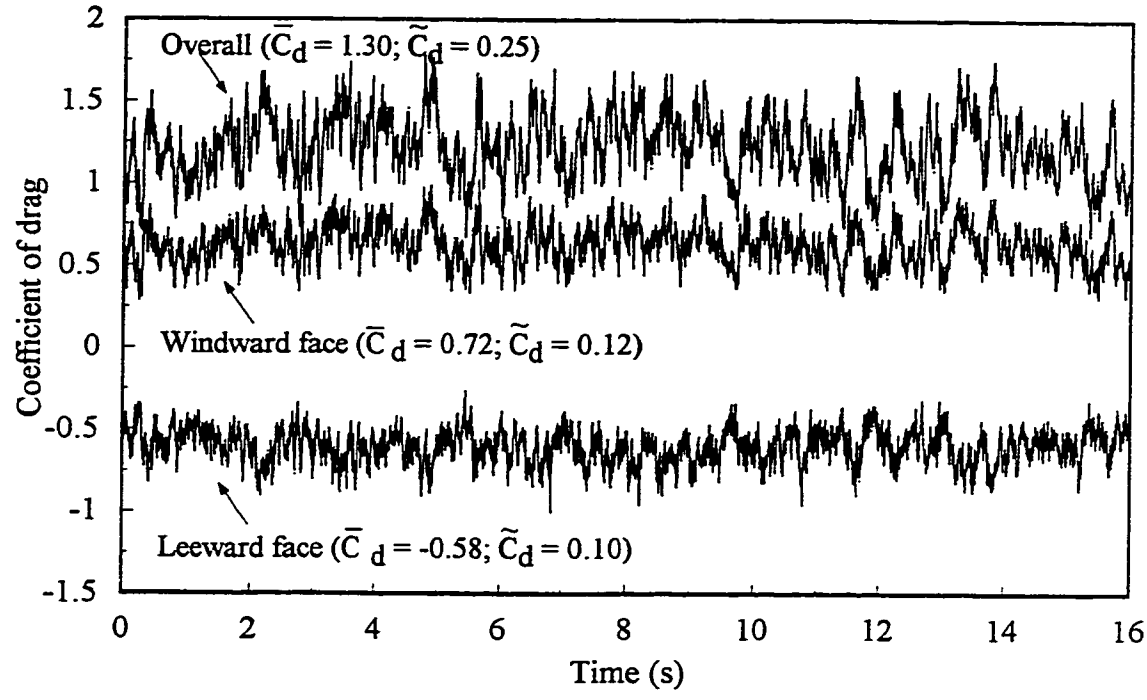

(a) Drag

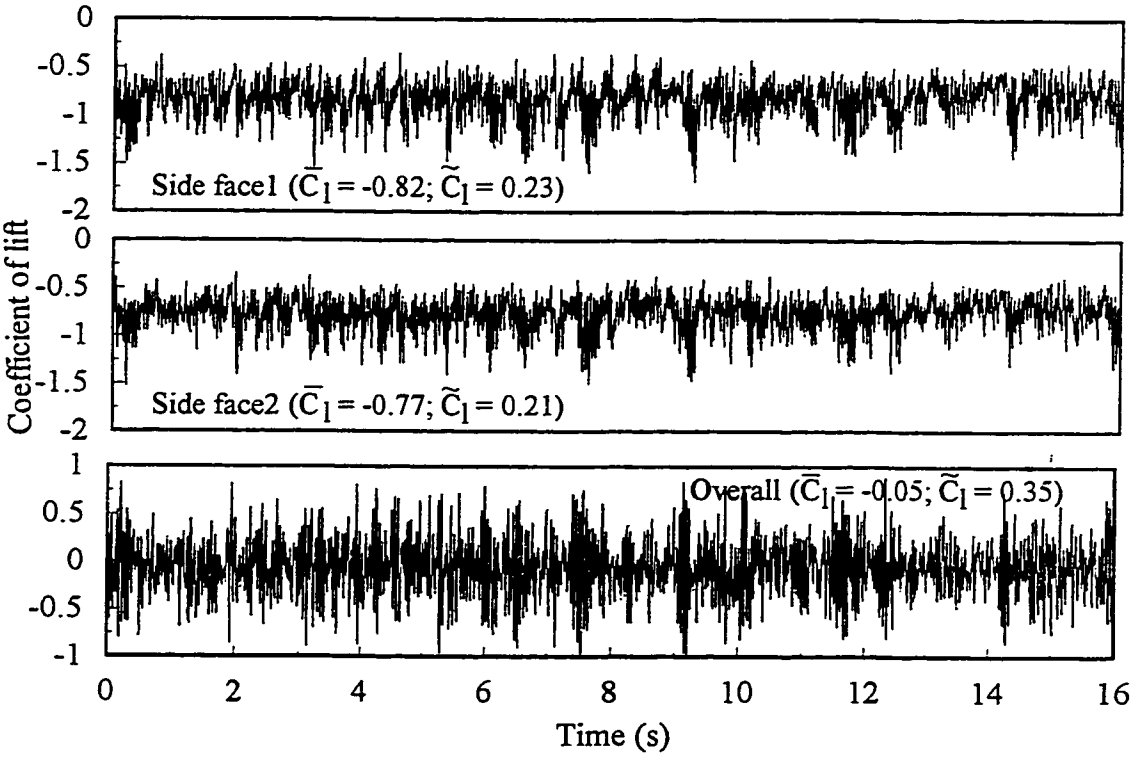

(b) Lift

Figure 5.5 Time histories of drag and lift fluctuations for isolated building in open exposure

fluctuations, or the time histories, on the windward and the leeward faces are almost identical. As expected, lift fluctuations (Figure 5.5(b)) generate suction on both side faces of the building. Sharp fluctuations on both walls give rise to a high overall $\widetilde{C}_l$ of 0.35. Since the mean forces on both the faces are almost the same, the overall mean lift is near zero. This is clearly discernible in the overall lift fluctuations plot where fluctuations about the zero line are almost similar in magnitude but in opposite direction. Note the clear difference in the time histories of overall drag (Figure 5.5(a)) and overall lift (Figure 5.5(b)). While the drag time history appears to be broad-banded, the lift fluctuations seem to be on the narrow-band side.

Figure 5.6 shows the spectrum of drag and lift fluctuations on the instrumented building. Comparisons with the estimates of Kareem (1982) and Tschanz (1982) show a general agreement in the trends. The slight disagreement in the values could be due to the differences in the approach flow characteristics. No spectral peak is encountered for fluctuating drag in Figure 5.6 which shows that the energy is distributed over a wide range of frequencies. The spectra of fluctuating lift is remarkably different. It exhibits a spike in a narrow band centred at the Strouhal frequency ($nb/\bar{v}_z \approx 0.10$), where the bulk of the energy is concentrated and indicates the occurrence of vortex shedding. This typical characteristic of the measured spectra is quite similar to that reported by Vickery (1966), Kareem (1982) and Kareem and Cermak (1984).

As done for the mean forces, an analysis of the experimental measurement results on fluctuating forces have yielded generalized empirical equations defining coefficients of fluctuating drag and lift for buildings of square footprint, taking into account the effects of incident wind direction and turbulence intensity. The coefficient of fluctuating drag, $\widetilde{C}_d$ is

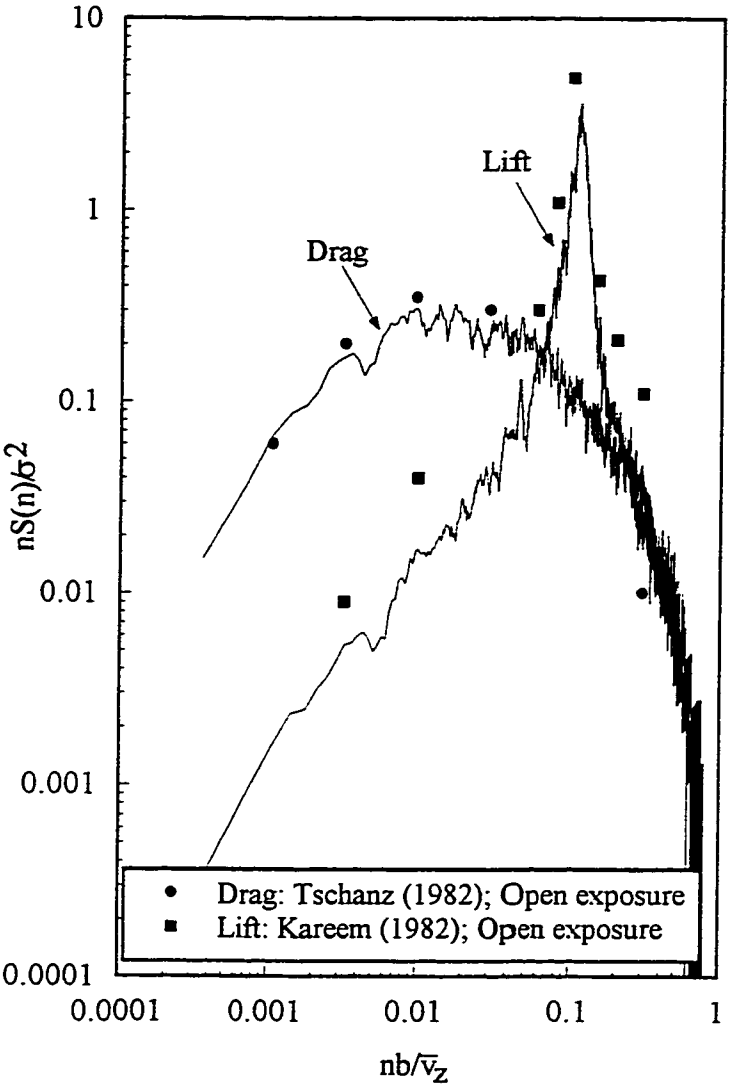

Figure 5.6 Spectrum of drag and lift fluctuations on isolated building in open exposure

given by,

$$\tilde{C}_d = C - D\left(\frac{\theta}{100}\right) + E\left(\frac{\theta}{100}\right)^2 \tag{5.4}$$

in which C, D and E defining the effects of turbulence intensity, are given by,

$$C = 0.52(I_v)^{-0.34} \tag{5.5}$$

$$D = 1.18(I_v)^{-0.33} \tag{5.6}$$

$$E = 1.26(I_v)^{-0.26} \tag{5.7}$$

Fluctuating lift, $\tilde{C}_l$ can be obtained by replacing θ by 90° - θ in equation 5.4.

Table 5.2 shows the comparison of the above equations with experimental results. The maximum error between calculated (regression) and observed (experimental) values for all the three exposures is -0.03, insignificant from a practical standpoint. The mean of the sum squared errors (MSE) over all measured wind directions are 0.0004, 0.0003 and 0.0003 for the open, suburban and urban exposures, respectively. Thus, the empirical equations predict the values of coefficient of fluctuating drag reasonably well for an upstream turbulence intensity range of 7% to 25%.

Table 5.2 Comparison between observed (experimental) and predicted (regression) values for fluctuating drag coefficient

Wind angle (°)	*Upstream exposure*					
	Open		Suburban		Urban	
	Observed	Predicted	Observed	Predicted	Observed	predicted
0	0.25	0.27	0.20	0.22	0.16	0.18
15	0.21	0.19	0.18	0.16	0.14	0.13
30	0.17	0.15	0.15	0.13	0.12	0.10
45	0.14	0.14	0.13	0.12	0.11	0.10
60	0.15	0.17	0.13	0.15	0.11	0.13
75	0.20	0.23	0.18	0.20	0.15	0.17
90	0.35	0.32	0.30	0.28	0.27	0.25
MSE	*0.0004*		*0.0003*		*0.0003*	

It can thus be suggested that the nature of fluctuating forces on a square building, quite like the mean forces, depend upon the degree of turbulence in the incident flow and its angle of attack. These two parameters influence the modifications taking place in the structure of the separated shear layers, thus effecting the boundaries of the flow reattachment region on the sides of the building and hence the overall fluctuating forces.

5.4 Summary

A thorough investigation of mean and fluctuating forces on a single, free-standing building with a square foot-print is undertaken to provide a reference for the study of interference effects due to adjacent buildings. The experimental results compare well with available literature data. The effect of incident turbulence in reducing the mean drag on a building is prevalent for wind angles of less than about 40° and becomes insignificant at larger angles. Turbulence also reduces fluctuating forces for all wind angles. At a wind angle of 0°, the value of fluctuating lift is appreciably higher than that of fluctuating drag. The empirical equations suggested will help provide quick estimates of mean and fluctuating force coefficients on buildings with square foot-print.

If we take in our hand any volume, of divinity or school metaphysics, for instance, let us ask: "Does it contain any abstract reasoning concerning quantity or number ? No. Does it contain any experimental reasoning, concerning matter of fact or existence ? No." Commit it then to flames: for it can contain nothing but sophistry and illusion.

- David Hume, An Inquiry Concerning Human Understanding (1748)

6

Interference Effects - The Datum Case

Based on the results of exploratory tests detailed in chapter 4, Interference Influence Grids (IIG) were set-up. These grids present broad and general guidelines by defining areas around a building sensitive to interference effects, and also by establishing limiting conditions for detailed experiments. This is important, especially in light of the complex nature of interference effects and the overwhelming number of possible building configurations and flow conditions.

The *"datum"* or basic case is typical of most previous studies dealing with wind-induced interference effects. This comprises two identical interfering buildings of square cross-section in an open exposure and a zero degree wind azimuth, normal to the building face (henceforth called the "normal wind"). Since the effect of the relative building sizes, the incident wind directions and the upstream exposures will be compared to and discussed vis-à-vis the datum case, it is therefore important to treat and discuss this benchmark case separately.

Mean and fluctuating drag and lift force measurements are carried out on a static "pressure" model. The details of the model, the pressure measurement system used and the experimental methodology are outlined in chapter 3. In this chapter, experimental results for the datum case are presented, compared, analyzed and discussed. Interference effects are measured in terms of area-averaged loads as explained in chapter 3. Drag and lift spectra are used to explain the interference mechanisms and typical spectral shapes for various

interfering building locations are presented by means of simple Interference Spectral Diagrams. Finally, the entire sets of results are presented as IIGs, refined in light of the detailed experimental results. The IIGs embody the essence of wind-induced interference effects for the datum case.

6.1 Overall Approach

Having identified and defined, in chapter 4, the areas around the principal building sensitive to wind-induced interference effects by means of IIGs, the stage is now set for studying interference effects in detail. Although the exploratory tests, described in chapter 4, greatly help reduce the number of configurations to be subjected to detailed tests in the wind tunnel, carrying out detailed experiments requires considerable time, effort and planning. As explained in chapter 3, the effect of interference is studied by measuring the mean and fluctuating forces on the principal building model (P_0) due an interfering building model (I_0) of identical size at different positions around the principal building. The drag and lift forces are measured with respect to the building axis system shown in Figure 3.9.

Figure 6.1, based on the results of the exploratory tests and the IIGs (see Figures 4.4 and 4.5), shows the detailed experimental plan, with the principal building at the origin and the locations of the interfering building shown by black dots. These dots are denser for critical regions and are sparse for locations of lesser significance from the point-of-view of interference. The separation between the two buildings is designated by the centre-to-centre distance, Sx in the horizontal axis (along-wind direction) and, Sy in the vertical axis (across-wind direction), measured in terms of b, the width of the square principal building.

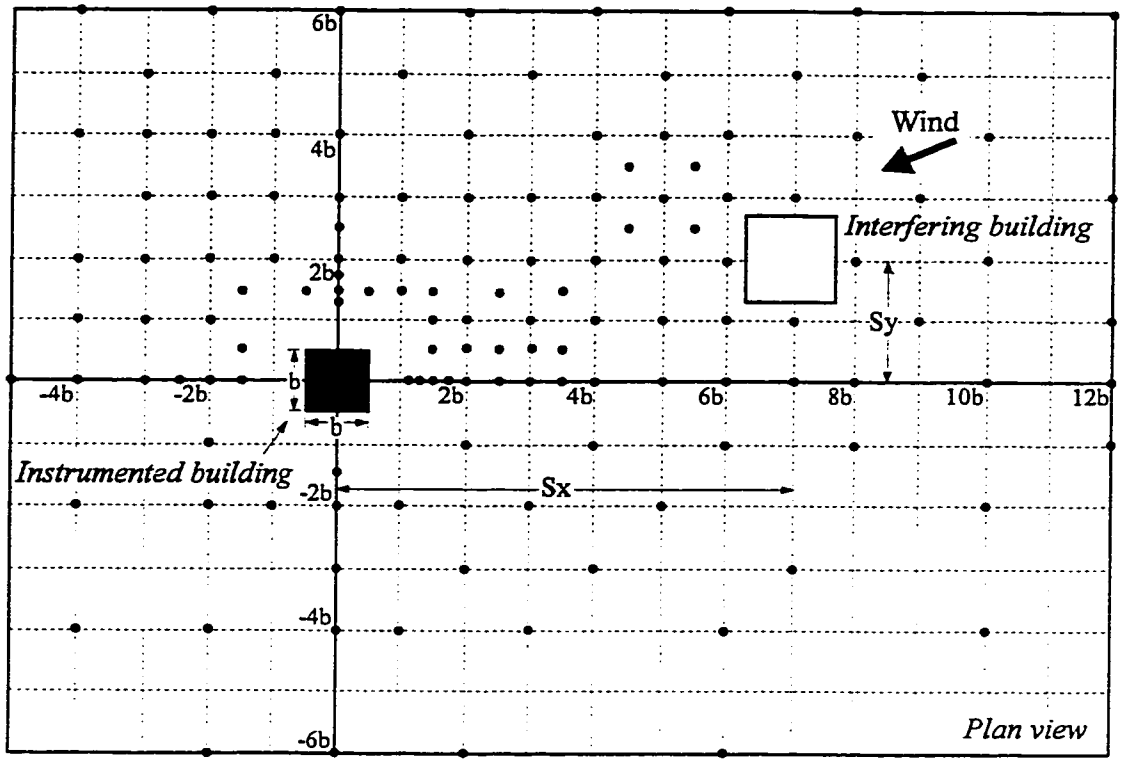

Figure 6.1 Detailed experimental plan - locations of interfering building tested in the wind tunnel

As explained in chapter 3, seventeen different interference cases can be classified as: ten interfering building sizes, five extra wind angles (in addition to the normal wind, already accounted for in the building sizes) and two extra upstream exposures (suburban and urban) in addition to the open exposure. The various interfering building situations tested in the wind tunnel are shown in Table 6.1.

Table 6.1 Interfering building situations tested in the wind tunnel

Number of interfering building sizes	*Wind angles*	*Exposure*	*Number of cases tested (approximate)*
10 (I_1^* to I_{10})	0°	Open	1000
1 (I_1)	0°	Suburban	100
1 (I_1)	0°	Urban	100
1 (I_1)	15°, 30°, 45°, 60°, 75°	Open	625

* same size as the principal building.

The ten building sizes and two extra upstream exposure cases were tested for 0° wind and taking advantage of the symmetry about the horizontal axis, the interfering building was placed only in the two positive Y quadrants (see Figure 6.1). About a hundred such locations for each of these twelve interference cases were selected, bringing the total number of testing situations to 12x100 = 1200. For the five extra angles, the interfering building was placed in all four quadrants. This increased the number of locations to about 125 and the total number of interference situations is 5x125 = 625. Thus, the overall testing situations are 1825. Figure 6.1 and the above numbers are meant to provide an approximate idea of the experimental effort involved. The locations of the interfering buildings did not follow a rigid pattern: in fact they were altered during the experiments to reflect the actual interference situation prevailing for a particular configuration. The advantage of symmetry was taken to avoid unnecessary, repetitive testing, especially, for situations involving oblique winds. For instance, coefficient of lift for 15° wind angle at Sx = 2b and Sy = 4b is similar to coefficient of drag for Sx = 4b and Sy = 2b for a wind angle of 75° (see Figure 3.9 for the definition of various force coefficients). In this chapter, results of the normal wind (0° wind angle) case, involving two identical buildings, in an open exposure are discussed.

Area-averaged loads are obtained for each of the four walls of the principal (instrumented) building model. For each location (Sx, Sy) of the interfering building model, data was collected instantaneously at all four walls of the instrumented model, over a 16 second sampling period, with a frequency of 512 Hz. The statistics were thus computed for a total of 8192 data samples for each face of the building model. Spectra measurements were done for several locations and the data was collected similarly, but was averaged over eight records, each containing 8192 data samples.

Results are presented as interference effects contour diagrams, showing the drag or lift force on the principal building due to the combined action of wind and interference effects due to an adjacent building at Sx and Sy. The contours show force coefficients for mean loads and the Interference Factor (IF) for fluctuating loads, given by equation 3.11.

6.2 Detailed Experimental Results - Mean Loads

The detailed experimental results regarding the effects of interference on mean wind loads will be presented in this section. These results will be analyzed and discussed in a subsequent section. For the datum case, the mean loads comprise the mean drag on a building, in the along-wind direction, and the mean lift, perpendicular to it.

6.2.1 Mean drag

Mean drag coefficient ($\overline{C}_d$) is given by equation 3.7. Figure 6.2 shows the contours for mean drag coefficient on the principal building due to an identical adjacent building at various locations around it. Comparisons with literature results (Sakamoto and Haniu 1988) are also shown and the agreement seems to be satisfactory. The extent of shielding is immediately apparent from the figure. The value of $\overline{C}_d$ for the principal building when the interfering building is located at Sx $\approx$ 11b is 0.90. Comparison with a $\overline{C}_d$ of 1.30 for isolated building indicates a 30% decrease in mean drag. This means that a downstream building experiences considerable shielding due to an upstream building located as far away as 11 times the building width or 220m (about one quarter of a kilometre), in full scale, in this case. Shielding would increase further for larger interfering buildings as will be seen in

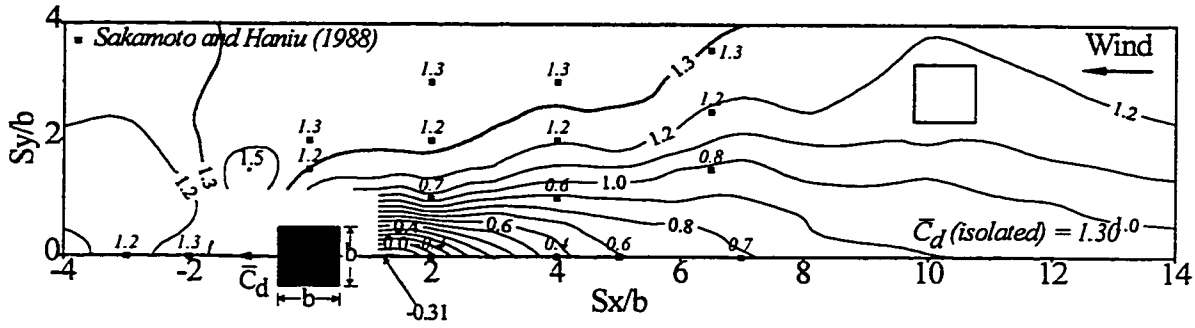

Figure 6.2 Effect of interference on mean drag coefficient

chapter 7. The shielding increases to 50% at Sx ≈ 5b. At Sx ≈ 2b, $\overline{C}_d$ becomes zero suggesting an absence of drag force on the principal building or, in other words, a complete shielding of the principal building by the upstream building.

Shielding is beneficial for a building since it reduces the drag force on the building, thus sparing its structural system and the cladding of high wind loads. However, for close proximity locations (less than 2b) of the upstream building, $\overline{C}_d$ becomes negative due to high suction created on the windward face of the principal building. The overall mean drag coefficient can decrease to as low as -0.31 for Sx = 1.25b. Compared to the isolated building value of 1.30, this amounts to a decrease of 123% in the mean drag coefficient. There is a small patch downstream around Sx = -b and Sy = 1.5b, where $\overline{C}_d$ actually increases to about 1.50, an increase of 15%, rather insignificant from a practical standpoint.

Overall, a narrow strip, or a *"shielding belt"*, of width b, extending up to a distance of about 10b directly upstream of the principal building can be identified as the region of significant interference effects. The design for wind loads should account for this shielding region, decrease the mean loads on the principal building accordingly and thus take advantage of the beneficial effects of interference. However, for two buildings in tandem at

very close quarters (Sx < 2b), suctions generated on the windward face of the downstream building can be a cause of concern from the point-of-view of building energy management and structural support of cladding. High suctions may result in heat loss from a building, imposing considerable strain on the heating, ventilation and air-conditioning system and, consequently, on the overall building operation and maintenance costs.

6.2.2 Mean lift

The coefficient of mean lift ($\overline{C_l}$) is given by equation 3.8. Figure 6.3 shows the contours for coefficient of mean lift on the principal building due to an identical adjacent building at various locations around it. Comparisons with literature results (Sakamoto and Haniu 1988) are quite satisfactory. As opposed to the contours for mean drag coefficient discussed in the previous section, the tandem arrangement is not at all a significant parameter in this case. In fact, mean lift coefficient for tandem arrangement is zero. This is to be expected for a 0° wind that creates a symmetric flow around the buildings, resulting in forces of equal magnitude on both side faces of the principal building, therefore a zero net lift. Similarly, the net $\overline{C_l}$ for an isolated building is also zero.

In general, mean lift does not seem to be greatly affected by interference for most locations of the interfering building. However, when the interfering building is situated to a side of the principal building (Sx = 0), creating a channel between the two buildings, high suction is generated on the inner side face of the principal building adjacent to the channel. The overall lift on the principal building is directed towards the interfering building, akin to a force of attraction between the two buildings. At a sideways spacing of Sy = 1.5b, $\overline{C_l}$ is -0.22. The high suction region extends up to Sy ≈ 4b where $\overline{C_l}$ is still -0.10.

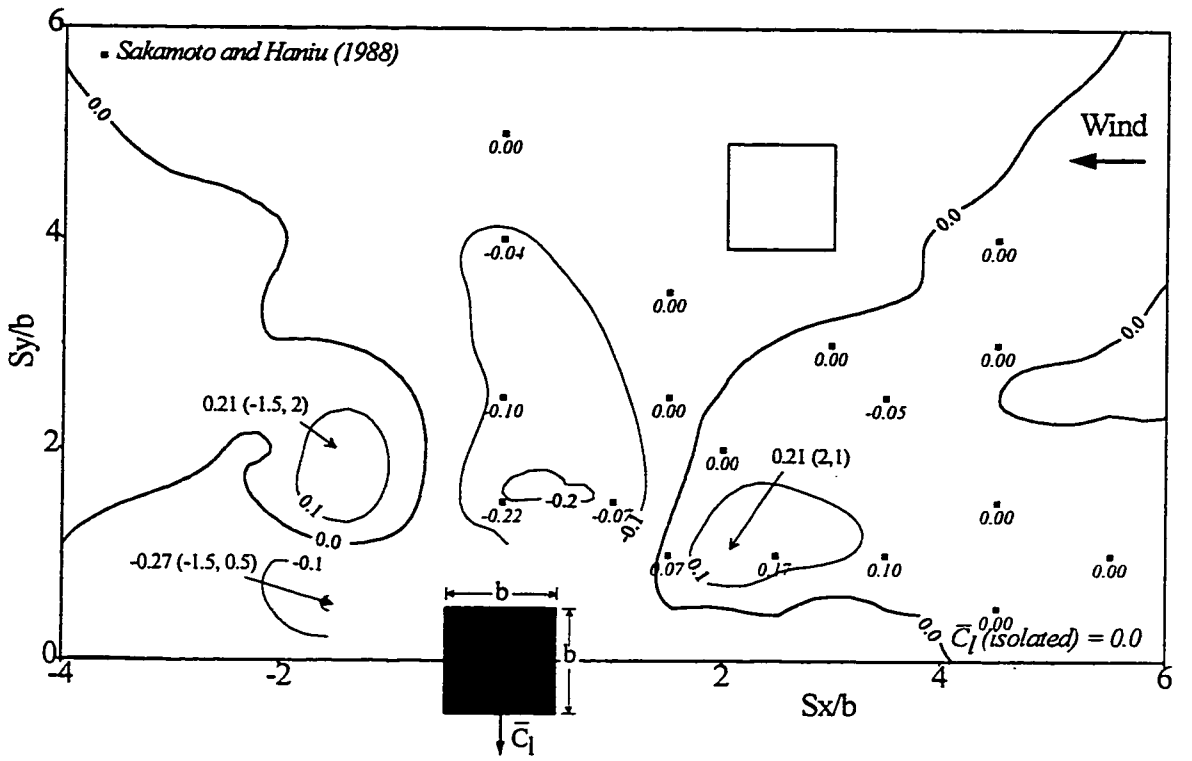

Figure 6.3 Effect of interference on mean lift coefficient

It is interesting to note the diagonal pattern of the $\overline{C}_l$ = 0.0 contours to the downstream and upstream on the side of the principal building. Thus, a *"suction sector"* can be identified on the side of the principal building, stretching diagonally up to a distance of 5b to its side responsible, predominantly, for the negative lift or suction on the principal building. However, the critical region from the point-of-view of negative lift is not as large; it is a small narrow strip extending up to Sy = 2b to the side of the principal building and having a width spanning Sx = 0 to Sx = b, where $\overline{C}_l$ falls below -0.15. The minimum value of $\overline{C}_l$ of -0.27 is registered when the interfering building is located downstream at Sx = -1.5b and Sy = 0.5b. There are few noteworthy locations for positive lift; small patches exist on the upstream and downstream of the principal building, where the mean lift

coefficient is greater than 0.10. The maximum $\overline{C_l}$ of 0.21 is registered at the interfering building locations of Sx = 2b and Sy = b upstream, and Sx = -1.5b and Sy = 2b downstream.

6.2.3 Mean loads - analysis and discussion

The most striking characteristic regarding the effects of interference on mean loads is the high degree of shielding (reduction in mean drag) offered to the principal building by an upstream interfering building. However, high suctions created due to close proximity locations of the interfering building in front and to the side of the principal building should be a cause for concern. The following sub-sections discuss the results of the detailed experiments.

6.2.3.1 Mean drag

The shielding as well as suction for tandem arrangements, quite clearly, has to do with the obstruction of wind by the interfering building. Basically, this interference lowers the pressure on the windward face of the principal building and the overall drag, which is the difference between the total pressure on the windward face and the leeward face, is reduced. For close tandem locations (Sx $\leq$ 2b), the separated shear layers from the upstream building reattach to the sides of the principal building, eventually rolling down weakly behind it. For example, for an interfering building at Sx = 1.5b, the suction ($\overline{C_d}$) on the rear face of the principal building is reduced to -0.29 from -0.58 in the isolated building case. Some shear layers also escape into the narrow gap between the two buildings, bending sharply and speeding into the channel from both leeward corners of the upstream building. This high

velocity flow from both ends of the channel never strikes the front surface of the principal building, it just skims over the surface, colliding in the middle to form a high velocity backward flow. This skimming backward flow is responsible for high suction on the front face of the principal building. Thus, the windward face of the principal building which in an isolated condition would register an overall positive $\overline{C}_d$ of 0.72, is instead subjected to a suction of -0.50. Hence, the net $\overline{C}_d$ on the principal building is -0.50 -(-0.29) = -0.21. Table 6.2 gives the $\overline{C}_d$ values on the windward and leeward faces of the principal building for various close tandem locations of the principal building. Since the windward face is subjected to far more turbulent shear layers inducing a backward flow, it is more sensitive to building spacing than the leeward face which exposed to a flow rendered mild by reattachment to the side faces of the principal building.

Table 6.2 $\overline{C}_d$ values for close tandem arrangement (Sy = 0)

Sx/b	*Windward*	*Leeward*	*Overall*
(1)	*(2)*	*(3)*	*(2) - (3)*
Isolated	*0.72*	*-0.58*	*1.30*
1.25	-0.57	-0.26	-0.31
1.50	-0.50	-0.29	-0.21
1.75	-0.44	-0.31	-0.13
2.00	-0.37	-0.32	-0.05
2.50	-0.16	-0.34	0.18

As the spacing between the two buildings becomes larger, $\overline{C}_d$ increases, but remains far below the isolated building value even at an along-wind spacing of 14b ($\overline{C}_d$ = 0.97). This highlights the extent of shielding provided by the upstream building. Shielding is further discussed with respect to other parameters in chapter 7.

6.2.3.2 Mean lift

The most notable effects of interference on mean lift are the suction on the principal building for side-by-side arrangement and pressure for close staggered arrangements. Two buildings positioned side-by-side create a channel between them. For narrow widths of the channel, the velocity of flow through the channel increases, thus creating high suction on the inner sides of the two buildings. For example, for a side-by-side spacing of Sy = 1.5b, the suction ($\overline{C_l}$) on the inner face (the channel side) of the principal building is increased to -0.93 from -0.82 in the isolated building case, and reduced to -0.71 from -0.77 in the isolated building case on the outer face. Thus, for Sy = 1.5b, an overall $\overline{C_l}$ of -0.93 minus (-0.71) = -0.22 is created.

For some close staggered locations, positive lift is encountered. For example, an upstream interfering building at Sx = 2b and Sy = b creates a $\overline{C_l}$ of 0.21 on the principal building. This is because the separated shear layers from both sides of the upstream building get just enough space to develop and reattach on the inner side of the principal building, reducing the suction on that side to -0.60 from an isolated building value of -0.82. The $\overline{C_l}$ of -0.81, on the opposite side, is not very different from the isolated building value of -0.77. Thus, the overall $\overline{C_l}$ of -0.60 - (-0.81) = 0.21 is obtained. Table 6.3 gives the $\overline{C_l}$ values on the two sides of the principal building for various close locations of the principal building. Note the interesting situation that arises for close downstream locations at Sx = -1.5b and Sy = 0.5b and Sx = -1.5b and Sy = 2b. The $\overline{C_l}$ value of -0.27 for the first location changes to a positive $\overline{C_l}$ of 0.21 when the interfering building is moved sideways to the second

Table 6.3 $\overline{C_l}$ values for various interfering building locations

Sx/b (1)	*Sy/b* (2)	*Inner side* (3)	*Outer side* (4)	*Overall* (3) - (4)
Isolated		*-0.82*	*-0.77*	*-0.05 (≈0)*
0.0	1.5	-0.93	-0.71	-0.22
0.0	2.0	-0.95	-0.78	-0.17
0.0	3.0	-0.96	-0.83	-0.13
-1.5	0.5	-0.81	-0.54	-0.27
-1.5	2.0	-0.62	-0.83	0.21
2.0	1.0	-0.60	-0.81	0.21

location. In the first case, the suction on the outer face of the principal building is greatly reduced. It is believed that at such an arrangement, the flow passing into the narrow channel glides strongly along the rear face of the principal building towards its outer side. This flow obstructs the regular suction-creating flow at the outer face of the building, reducing its velocity considerably. Hence, the suction at the outer face of the principal building is reduced. On moving the downstream building to a side, to the second location, this backward flow can no longer reach to the outer side, but is strong enough to interfere with the flow passing along the inner face. This reduces the suction on the inner face of the principal building, and the overall lift is increased.

6.3 Detailed Experimental Results - Fluctuating Loads

As already explained in chapter 5 dealing with isolated buildings, the nature of unsteady or fluctuating forces is quite different from the mean forces. Similarly, the changes in fluctuating loads due to interference are also remarkably different from those on the mean loads. Results show that while the effect of interference on mean loads is generally beneficial (shielding), it is exactly the reverse in case of fluctuating loads which generally

increase due to interference. The fluctuations in drag are almost entirely due to the action of the incident turbulence of the longitudinal component of the wind velocity. However, the unsteady lift results from the alternate vortex shedding from the two sides of the building which may cause the building to vibrate laterally. Interference due to an adjacent building causes significant changes in the incident turbulence as well as the vortex shedding and therefore alters the fluctuating forces on a building.

6.3.1 Fluctuating drag

Fluctuating drag coefficient ($\widetilde{C}_d$) is defined by equation 3.9. Figure 6.4 shows the Interference Factor or IF (see equation 3.11) contours for fluctuating drag coefficient for the principal building due to an identical adjacent building at various locations around it. IF represents the increase (IF > 1) or decrease (IF < 1) in fluctuating drag on the principal building due to interference. An IF of 1 suggests no effect due to interference as in an isolated building condition. Comparisons with available literature results (Saunders and Melbourne 1979) show a reasonable agreement.

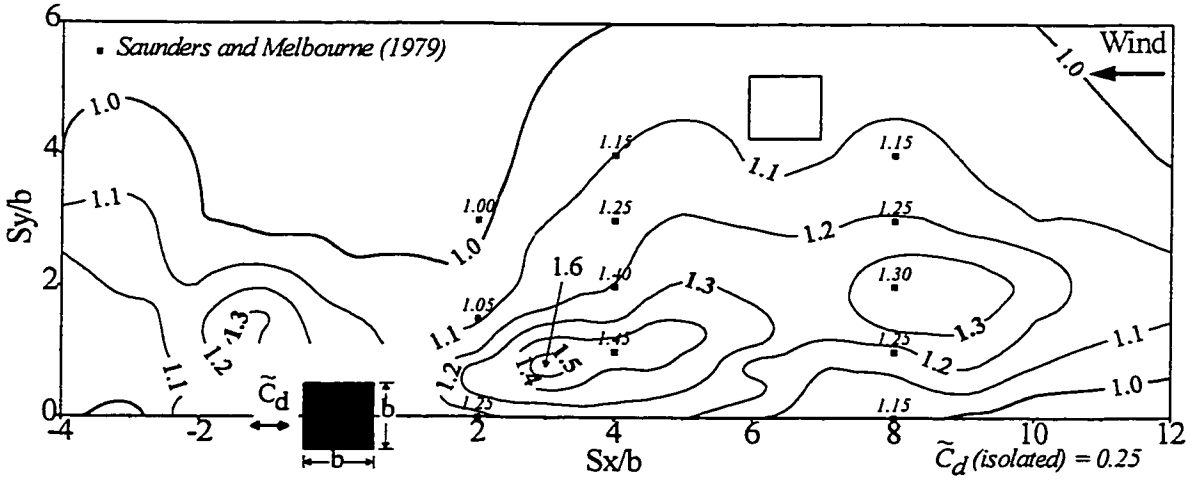

Figure 6.4 Interference Factor (IF) contours for fluctuating drag

The increase in fluctuating drag is immediately apparent. The largest IF of 1.6 is obtained upstream at Sx = 3b and Sy = 0.75b, which indicates an increase of 60% over the isolated building fluctuating drag coefficient of 0.25. Applying the yardsticks established in chapter 2, viz., an increase in wind loads of over 30% to be of significant concern, especially in terms of serviceability requirements, and above 50% well outside the safety margin used in normal design, several locations can be identified on Figure 6.4 where interference effects appear to be significant. A 30% to 60% increase is registered upstream, for the area bounded approximately by Sx = 2b to 6b and Sy = 0.25b to 1.5b. It is noteworthy that IF decreases below 1.3 for a small distance upstream, beyond Sx = 6b, but increases again by 30% to 40% further upstream from Sx = 7.5b to 9.5b and Sy = 1.5b to 2.5b. There is a small patch downstream where IF increases up to 1.37 at Sx = -1.25b and Sy = 1.25b. For upstream tandem locations (Sy = 0), fluctuating drag increases by about 20% between 2b to 5b, with a 25% increase at Sx = 4b.

6.3.2 Fluctuating lift

Fluctuating lift coefficient ($\tilde{C}_l$) is defined by equation 3.10. Figure 6.5 shows the Interference Factor (IF) contours for fluctuating lift coefficient for the principal building. Comparisons with force balance results of Bailey and Kwok (1985) show a reasonable agreement for Sx = 2b and Sx = 4b, but a poor agreement for Sx = 8b, although a similar trend. The reasons for disagreement could be attributed to the differences in the flow conditions and the sizes of the models.

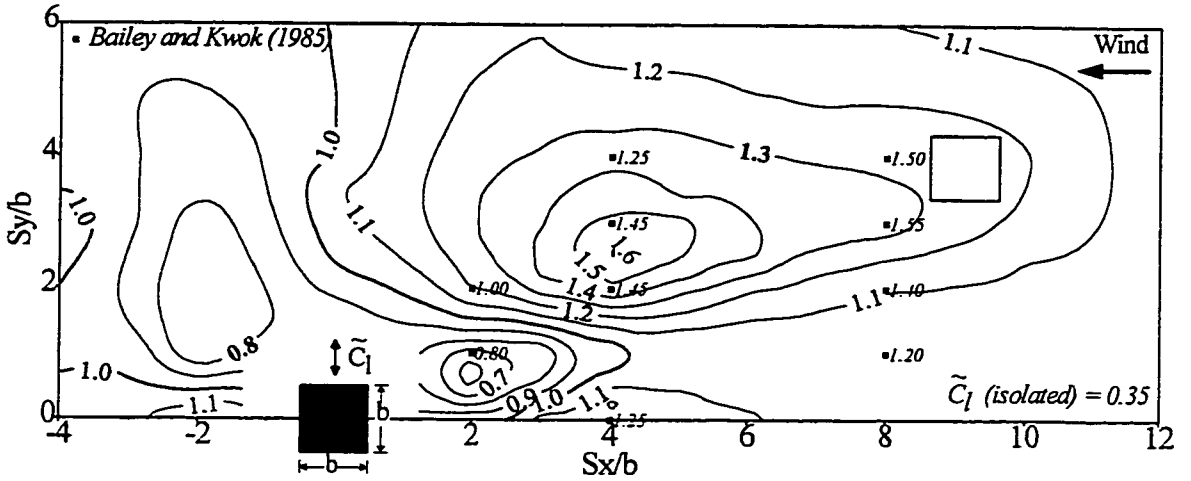

Figure 6.5 Interference factor (IF) contours for fluctuating lift

The increases in fluctuating lift are similar in magnitude to fluctuating drag, but the region of significant increase is shifted away from the horizontal axis, at an angle of about 45° with the horizontal. The maximum IF is 1.61 at Sx = 4b and Sy = 2.5b, indicating a 61% increase over the isolated building $\tilde{C}_l$ value of 0.35. This increase suggests that at this location, the velocity of the separated shear layers from the upstream interfering building is the highest, as well as the rolling up of the shear layers from the principal building may be synchronized with those from the upstream building. The region of 30% to 60% increase in fluctuating lift is large and spans approximately from Sx = 2.5b to 7.5b and Sy = 2b to 4b. In this region, the downstream (principal) building is greatly influenced by the wake of the upstream building and is subjected to high fluctuating lift. Increases for tandem arrangements (Sy = 0) are less than 20%, both for upstream and downstream locations. There is a small close proximity location upstream, for which the fluctuating lift actually decreases by up to 50%. Interestingly, the smallest fluctuating lift on the downstream building is generated around the same upstream location where the fluctuating drag on the

downstream building is the largest, approximately around Sx = 2.5b to 3.5b and Sy = 0.5b to 1.5b.

6.3.3 Interference excitation spectra

The interference mechanism causing drag and lift excitation was studied by examining the changes in the principal building spectra from which the frequency composition of the drag and lift excitation was identified. The spectra were calculated for several important configurations and have been used to identify the flow mechanisms and can be used to calculate the building response. The spectra of the principal building under interference were determined using the Data6000 Waveform Analyzer that performs a Fast Fourier analysis of the recorded pressure signals.

The load spectra of the principal building were altered significantly due to interference caused by a building positioned at specific locations. The dominant frequencies in the approach flow caused by vortex shedding from the upstream building were registered in the load spectra in the form of peaks, the magnitude of which depends on the strength of the vortices. In the subsequent sub-sections, some typical spectra are presented and discussed. The principal building load spectra due to interference are compared with its spectra in isolated condition. The spectra are normalized by the corresponding variance for ease of comparison.

6.3.3.1 Drag spectra

Figure 6.6 shows the normalized drag interference spectra of the principal building for various locations of the interfering building of identical size along with the drag spectra of

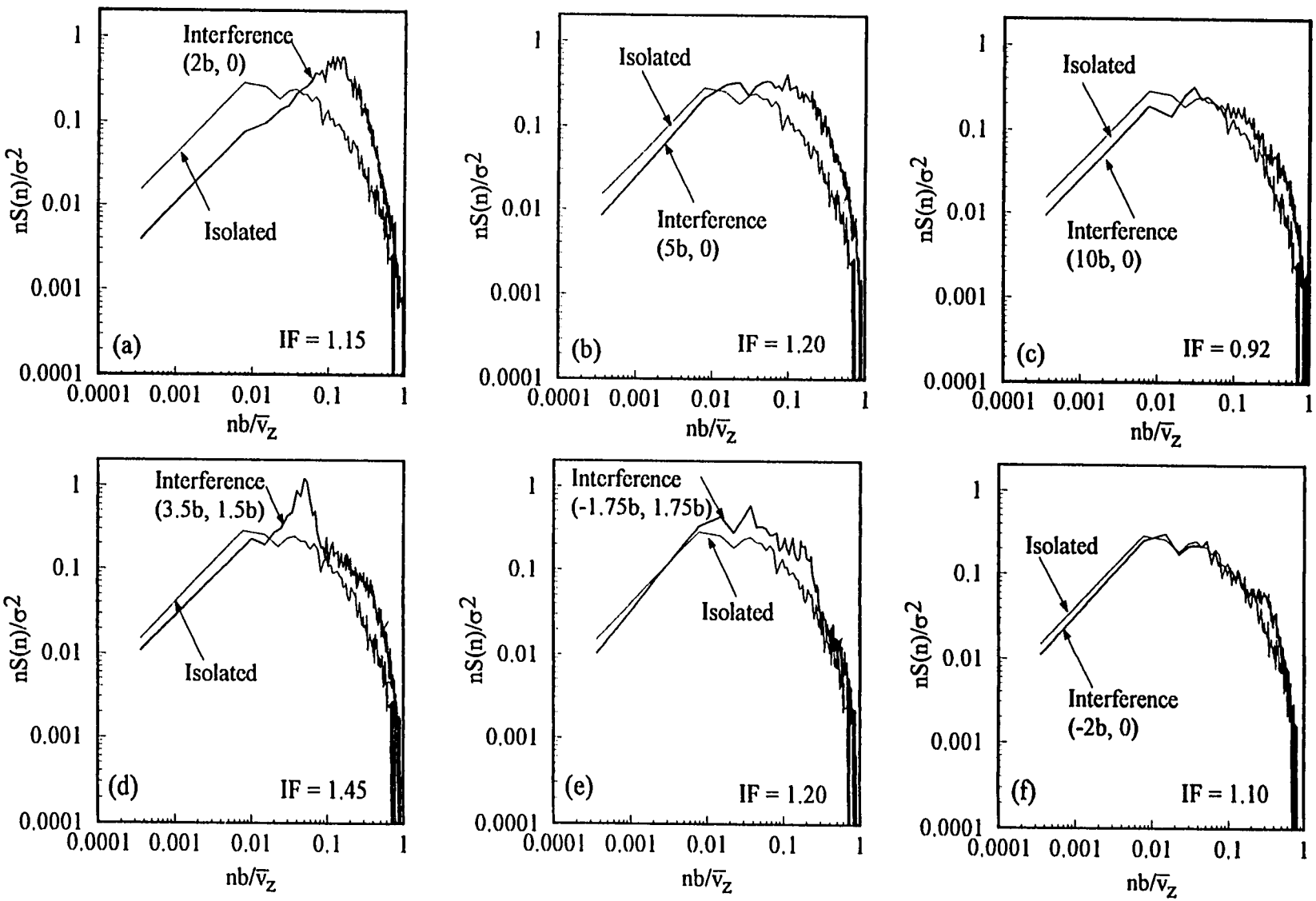

Figure 6.6 Spectrum of drag fluctuations on a building with and without interference due to an identical building.

the isolated building. Figure 6.6(a) to 6.6(c) show the drag spectra for tandem locations (Sx = 2b, 5b and 10b) of the upstream building. The principal building drag force spectrum is modified to some extent by an interfering building at a close tandem spacing of Sx = 2b (Figure 6.6(a)), which continues till Sx = 6b and remains unchanged thereafter. Note the similarity between the spectra of the principal building in isolated condition and with an interfering building at Sx = 10b (Figure 6.6(c)). Figure 6.6(a) shows a mild peak at a reduced frequency of 0.1, which corresponds to the frequency of vortex shedding from the interfering building. The mildness of the peak shows that the vortex shedding is not severe and hence, a small increase of about 15% (IF = 1.15) in fluctuating drag.

The drag spectrum shows a significant change for staggered locations of the interfering building. For distance at Sx = 3.5b and Sy = b an interfering building creates a sharp peak in the drag spectra as shown in Figure 6.6(d). The peak is centred around the Strouhal frequency of the interfering building, which is at a reduced frequency of 0.06. The sharp peak is indicative of the high energy content of the wake from the interfering building which is responsible for high fluctuating drag (IF = 1.45) (see Figure 6.4). This spectral shape is typical of interfering building locations between Sx = 2b to 6b and Sy = 0.5b to 1.5b. In general, no appreciable peaks are registered for downstream locations of the interfering building. However, for a close downstream location of Sx = -1.75b and Sy = 1.75b, mild peaks are registered which indicate a modification in the wake characteristics of the upstream building, and a small increase in fluctuating drag.

6.3.3.2 Lift spectra

The lift spectrum of the principal building is altered and generally "mollified" by an interfering building. Figure 6.7 shows the normalized spectra of lift fluctuations on the principal building with and without interference due to an identical building, at various locations. Figure 6.7(a) and 6.7(b) show the lift spectra for two typical locations of the interfering building which cause a significant increase in the fluctuating lift of the principal building. The most striking observation is the similarity in the spectral shapes, for the isolated building and the interfering building case, in the two figures. Such a spectral shape is typical of interfering building locations within Sx = 3b to 7.5b and Sy = 2b to 4b. Eventhough the magnitude of the variance σ^2 of lift is higher for interference than the isolated case, the two curves seem, almost, to overlap because each is normalized with the corresponding variance. The interfering building spectra in both cases are characterized by strong vortex shedding, centred at a reduced frequency of 0.1, and as a result, high IFs of 1.48 and 1.40 are registered in case of Figures 6.7(a) and 6.7(b), respectively.

Figure 6.7(c) compares the lift spectra for close proximity locations of the upstream interfering building, at Sx = 2b and Sy = b, with the isolated building spectra. The disruption of the vortex shedding mechanism of the upstream building by the closely located downstream building is clearly discernible, since the sharp peak at a reduced frequency of 0.1 now is dampened and the energy is distributed over a wider range of frequencies, which results in a lowering of the fluctuating lift by 36% (IF = 0.64). This typical behaviour is prevalent within Sx = 1.5b to 4b and Sy = 0 to 1.5b. Figure 6.7 (d) shows the reduction in the peak of the interfering building spectra for close side-by-side arrangement. Figures 6.7(e) and 6.7(f) show spectra for downstream locations of the

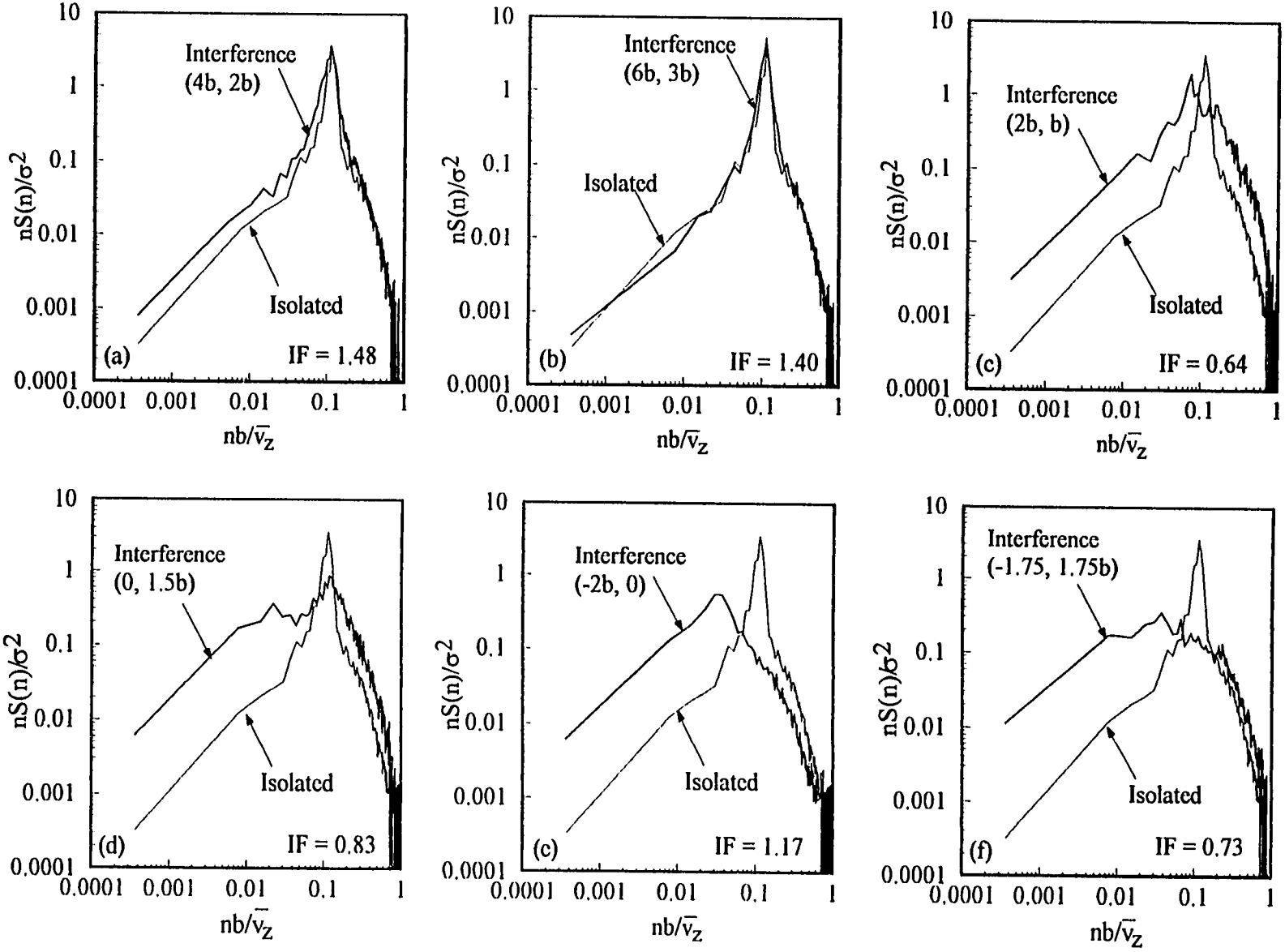

Figure 6.7 Spectrum of lift fluctuations on a building with and without interference due to an identical building.

interfering building. For downstream tandem location of Sx = -2b, the peak is not only lowered considerably, but also shifted to a reduced frequency of 0.03, indicating that the downstream building interferes with the vortex shedding of the upstream building.

6.3.4 Fluctuating loads - analysis and discussion

The organized vortex shedding from the upstream interfering building is the major cause of the increase in fluctuating loads on the principal building. This phenomenon is known as *"vortex buffeting"*. A downstream interfering building, in general, has insignificant effect on the fluctuating loads of the principal building for most locations. However, at a small region downstream, close to the principal building, the interfering building can create an instability in the principal building, altering its wake characteristics. The fluctuating drag is increased by up to 40%, but fluctuating lift remains generally unaltered.

Based on an analysis of the detailed experimental results, three main zones can be identified, depending on the manner in which the interfering building affects the fluctuating loads on the principal building.

(a) *Proximity zone*: In this region, the principal building is close enough to the upstream interfering building to destroy its vortex shedding mechanism, resulting in a decrease in fluctuating loads (up to 40% from isolated building values), especially for fluctuating lift. This area lies within $Sx \leq 1.5b$ and $Sy \leq 2b$ for fluctuating drag and $Sx \leq 3b$ and $Sy \leq 2b$ for fluctuating lift. Such a *"proximity"* region has also been identified by Thoroddsen at al. (1987) and Sakamoto and Haniu (1988). In this small zone, the two buildings interact strongly with each other, suppressing the rolling up of the separated shear layers from the

downstream (principal) building. This has a disruptive effect on the clear vortex shedding mechanism and results in a low fluctuating lift.

(b) *Interaction zone*: As the distance between the two interfering buildings is increased, the vortex street becomes well-organized before it hits the downstream building. The vortices shed from the upstream building may also interact and synchronize with those from the downstream building, increasing the fluctuating loads on it. This region, where the wake from the upstream building interacts with the downstream building, lies between Sx = 2b to 6b and Sy = 0.25b to 1.5b for fluctuating drag and Sx = 2.5b to 7.5b and Sy = 2b to 4b for fluctuating lift. When the interfering building is located in this zone, the principal building is greatly influenced by its wake, generating high fluctuating loads on the principal building (30% to 60% increase from isolated building values).

(c) *Passive zone*: In the remaining areas, the interfering building has little or no effect on the principal building (less than 15% change from isolated building values). In this region, vortices from the two buildings are shed independently of each other and the principal building is safely removed from the wake of the interfering building. It can also be termed the isolated building condition.

6.4 Design Considerations

A detailed experimental program, while tackling complex issues, also generates large amounts of data, which sometimes can be difficult to interpret. The building designer needs, primarily, a quick idea of the extent and the severity of the problem at hand. In the case of wind design, a preliminary, simplified "tour" of the interference effects problem can help the designer differentiate between critical and unimportant cases. It will also help one judge,

to a good approximation, the severity of interference effects. Based on the prevalent conditions, the designer can then exercise judgement whether to ignore the case, go for a scrutinized analysis or carry out detailed wind tunnel experiments. The need, therefore, is to simplify the problem, while retaining its basic, intrinsic nature.

Having presented, analyzed and discussed the results of detailed experiments on wind-induced interference effects for the datum case, the results will now be provided from the point-of-view of design and codification. The data pertaining to wind-induced interference effects have been presented, in this chapter, by way of contour diagrams in Figures 6.2 to 6.5. These contour diagrams are simplified further by highlighting the most important aspects and neglecting others that appear less critical. Some approximations have been made to render results viable for practical use. For instance, the areas of significant interference effects have been approximated by rectangles rather than curves and the spectral shapes have been smoothed. However, utmost care has been taken to ensure that these approximations retain the essential characteristics of actual cases.

The resulting Interference Influence Grids (IIGs), first described in chapter 4, present an overall, simplified yet comprehensive view of wind-induced interference effects. General spectral shapes are presented for interfering building locations around the principal building. Finally, a simple yet effective strategy for dynamic analysis, incorporating the effects of adjacent buildings, is presented.

6.4.1 Interference Influence Grids

Interference Influence Grids (IIG) were introduced in chapter 4, based on the results of exploratory tests. In light of the results of detailed experiments and their analysis, those

preliminary IIGs can now be refined. The IIGs present an overall picture of wind-induced interference effects in a simplified, yet comprehensive manner. Figure 6.8 presents IIGs for mean and fluctuating loads which can be used as simplified guidelines for preliminary design as well as for codification purposes. The figure shows locations around the principal building where an identical interfering building would create significant interference effects on the principal building.

Figure 6.8(a) shows IIG for mean loads, i.e. mean drag and mean lift. The *shielding belt* shows reductions in mean drag. Locating the interfering building within this belt produces beneficial shielding on the principal building. On the other hand, if the interfering building is located to a side, in the suction region, the principal building is subjected to a negative lift. Figure 6.8(b) shows IIG for fluctuating drag and lift. All the shaded regions represent, in general, increases in fluctuating loads due to interference. The unshaded areas are the locations of insignificant interference effects.

6.4.2 General spectral shapes

It would be useful for the designer to have general spectral shapes for various locations of the interfering building, so that dynamic analysis could be performed considering the effects of interference. The principal building force spectra for various interfering building locations, discussed in the previous sub-sections, have been analyzed, sorted and simplified to obtain general spectral trends for regions around the principal building. Figures 6.9 and 6.10 show the general Interference Spectral Diagrams (ISD) for drag and lift for two identical interfering buildings, with a 0° wind angle, for an open exposure. The ISD for drag is divided into five regions and that for lift into six, based on the characteristics of spectra

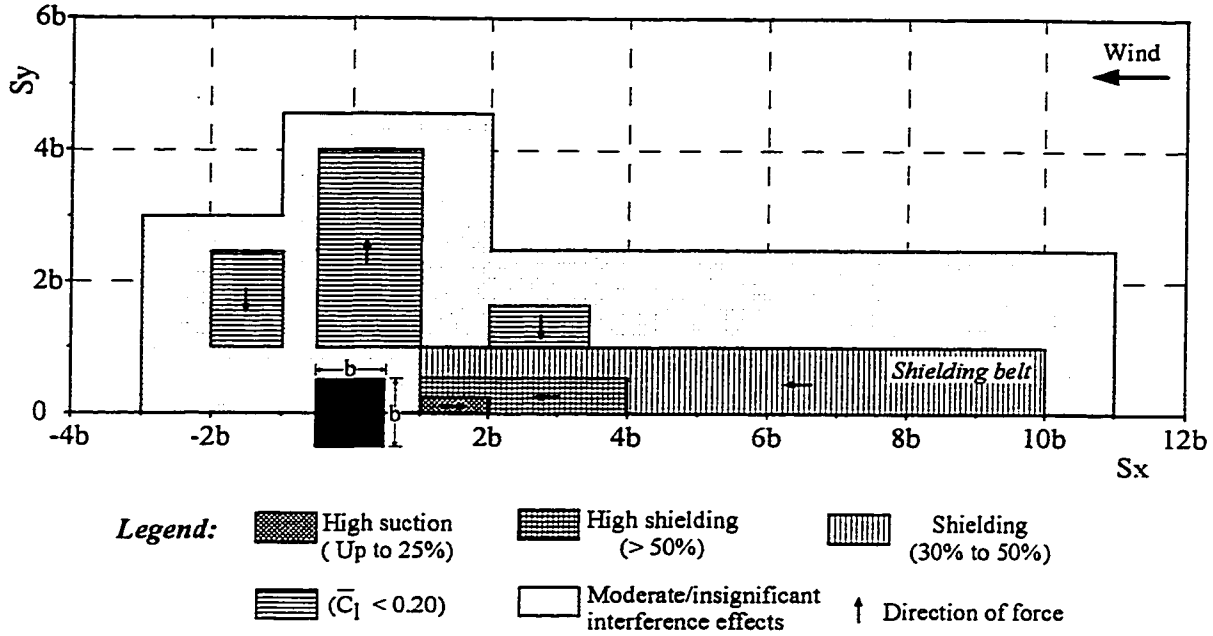

Legend: High suction (Up to 25%); High shielding (> 50%); Shielding (30% to 50%); ($\bar{C}_l$ < 0.20); Moderate/insignificant interference effects; Direction of force

Note: Percentages are with respect to isolated building loads ($\bar{C}_d$ = 1.3; $\bar{C}_l$ = 0.0)

(a) Mean loads

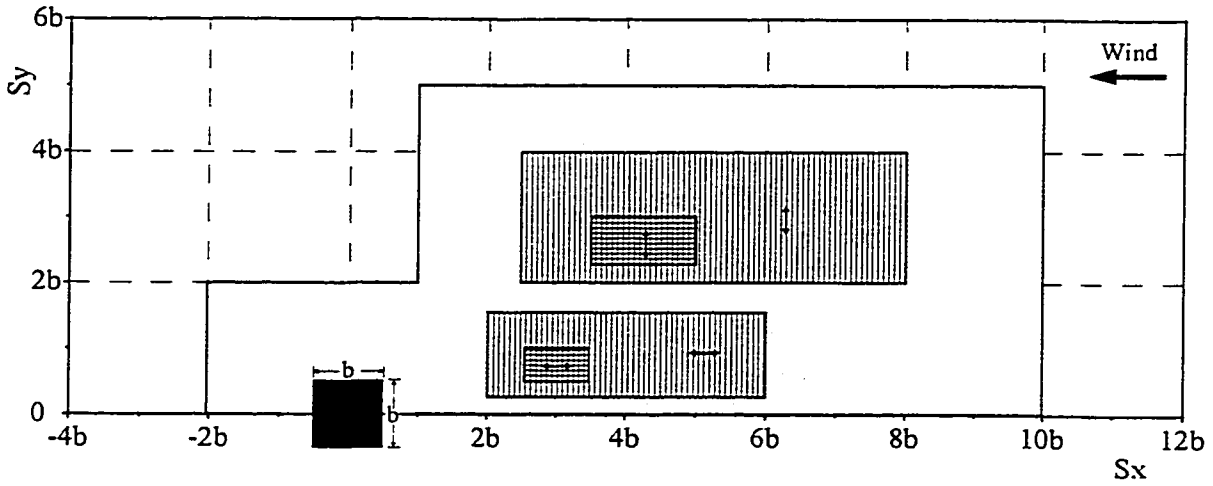

Legend: Up to 60% increase; 30% to 50% increase; Moderate/insignificant interference effects; Direction of force

Note: Percentages are with respect to isolated building loads ($\tilde{C}_d$ = 0.25; $\tilde{C}_l$ = 0.35)

(b) Fluctuating loads

Figure 6.8 Interference Influence Grids

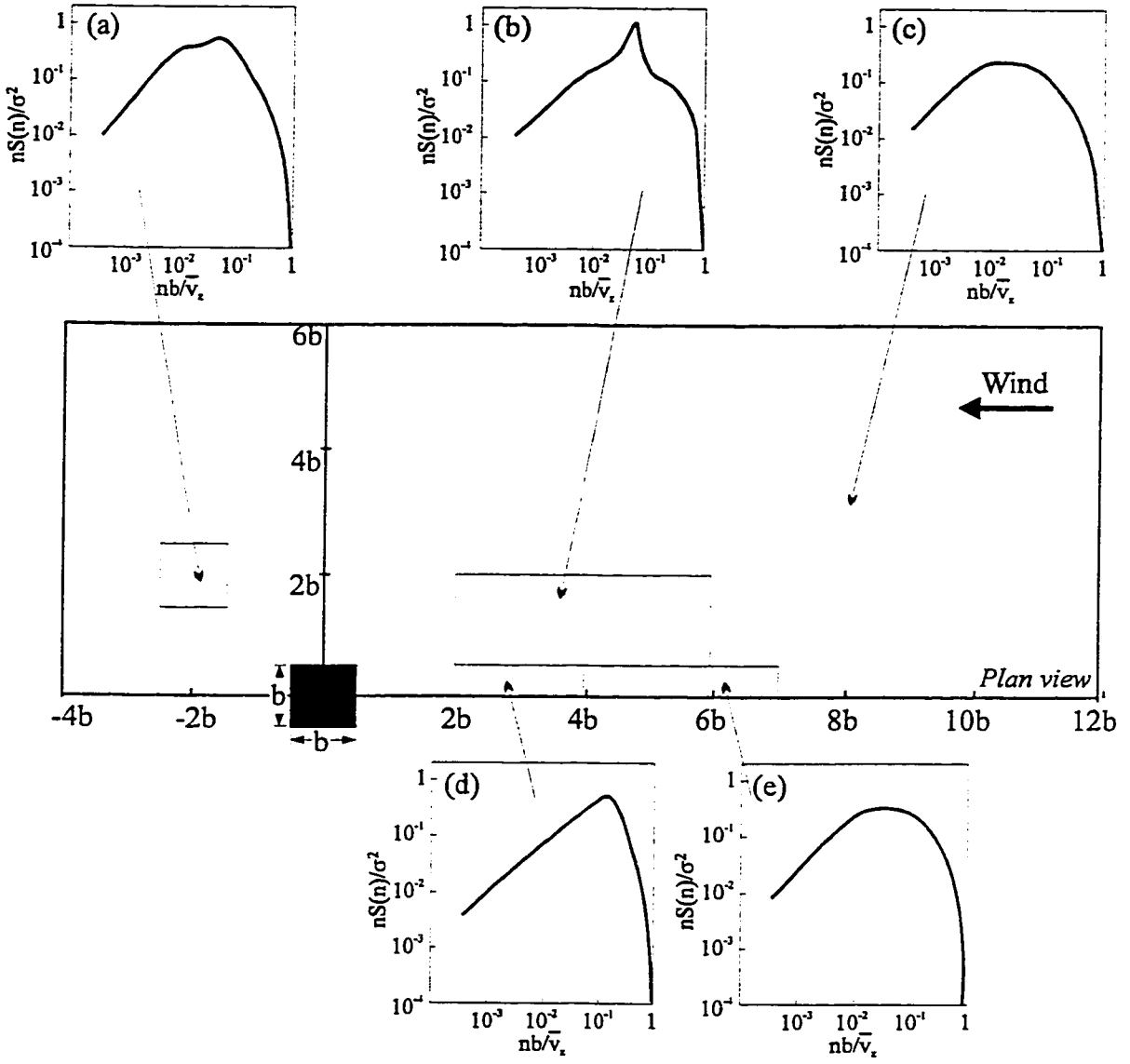

Figure 6.9 Typical drag spectra at various interfering building locations

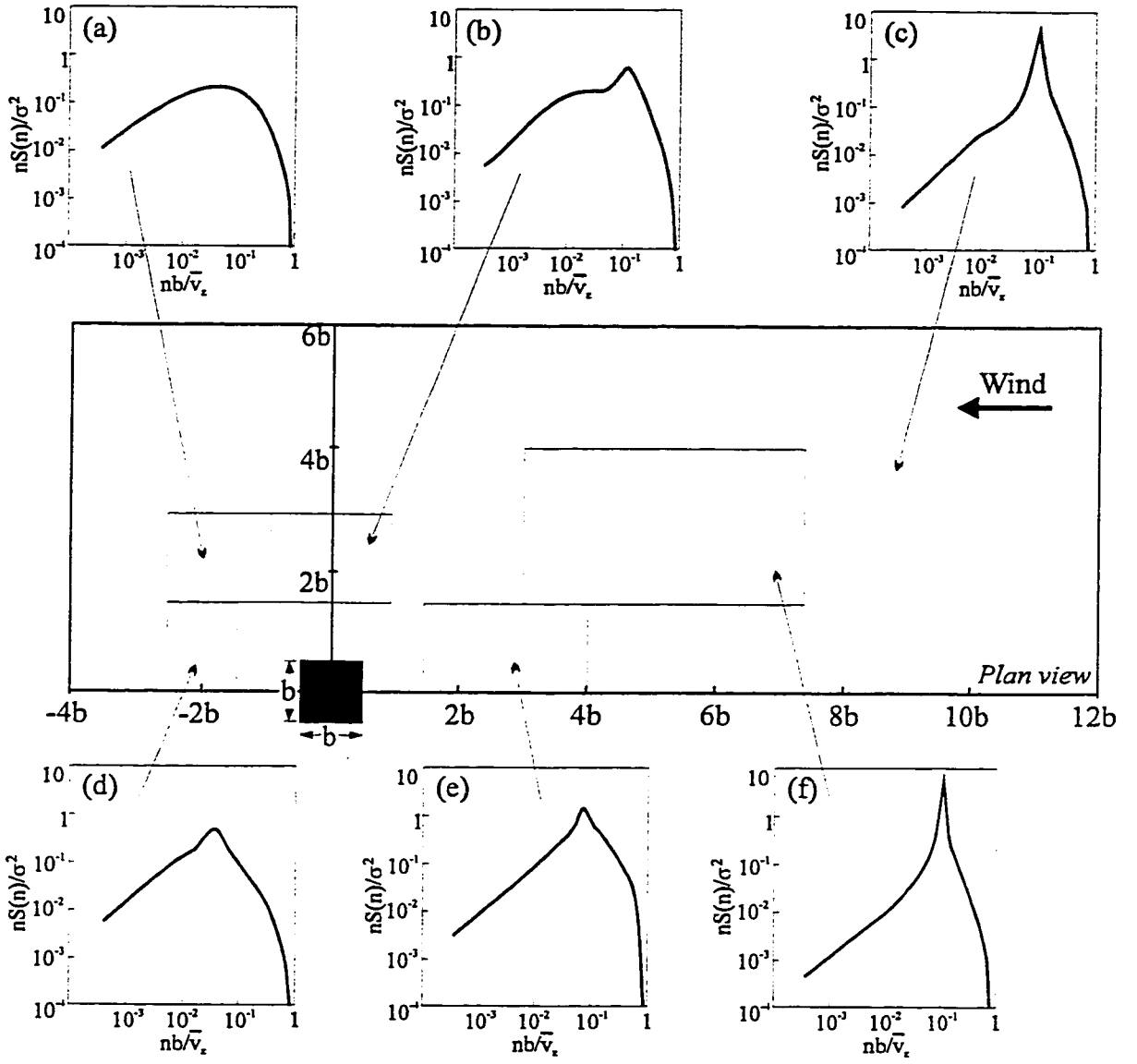

Figure 6.10 Typical lift spectra for various interfering building locations

and vortex shedding of the principal building. Three principal zones, described before, are also corroborated by the spectra:

(a) the *proximity zone*, close to the principal building, where the vortex shedding from the principal building is suppressed by interference from the nearby building. Hence the principal building spectra in this region are distorted or dampened; this can be seen in spectra (a) and (d) in Figure 6.9 and spectra (a), (b), (d) and (e) in Figure 6.10.

(b) the *interaction zone*, where vortex shedding from the principal building is synchronized with that of the interfering building, resulting in a sharp peak in the spectral curve. This is shown by spectra (b) in Figure 6.9 and spectra (f) in Figure 6.10.

(c) the *passive zone*, where the vortex shedding from each building is independent of each other. Thus, the spectra is similar to the isolated building spectra, shown by spectra (c) in Figure 6.9 and Figure 6.10.

The actual spectral curve can be derived, for each location, by multiplying the normalized spectra at that location by the variance of the corresponding fluctuating force. Thus, in order to obtain the correct spectral curve for drag, for a particular location, Figure 6.9 should be used in conjunction with Figure 6.4, from where the values of fluctuating drag ($\widetilde{C}_d$) can be picked up and its variance, $\widetilde{C}_d{}^2$ multiplied with the ordinate of the normalized spectral curve (from Figure 6.9) at that location. Similarly, to obtain the lift spectra, the values of fluctuating lift ($\widetilde{C}_l$) can be taken from Figure 6.5, and used with Figure 6.10.

To obtain the spectrum of response, or in other words the variance of the amplitude of deflection, the procedure suggested by Davenport (1967) can be used, in which the force spectrum is multiplied by a transfer function known as the *mechanical admittance*, to obtain the spectrum of the response. The mechanical admittance depends upon the structural

properties of a building, like its mass, stiffness and damping. The method for evaluating structural response due to time-dependent loads is described, briefly, in Appendix A.

Davenport's schematic representation of the process is modified by the introduction of normalized spectra and interference contour diagrams for fluctuating forces. The entire process is shown schematically, in a simplified form, in Figure 6.11. The area under the spectral curve of a function is equal to the variance of that function. The variance of the response is therefore found from the area under the response spectrum, given by equation A.10 in Appendix A.

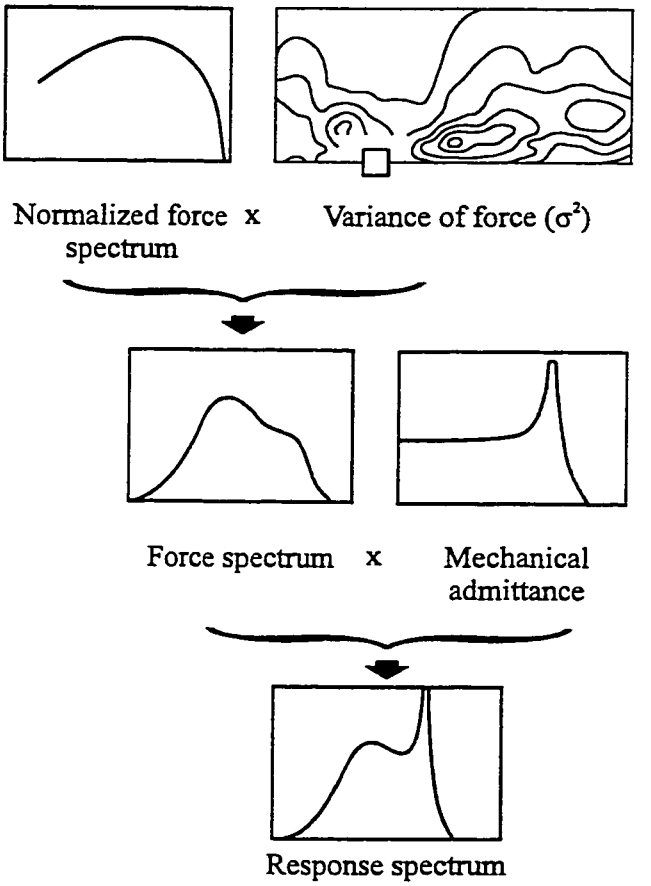

Figure 6.11 Evolution of the response spectrum from the normalized force spectrum - A schematic representation

6.5 Summary

Detailed experimental results on interference effects for the datum case have been presented, compared and analyzed. The data is presented by way of interference effects contours. From a practical, design standpoint, the entire bulk of data is collapsed and rounded-up in the form of two simple, easy-to-understand Interference Influence Grids (IIG). Interference Spectral Diagrams (ISD) are drawn up for dynamic analysis. These simple templates can be used for a quick, preliminary analysis and estimate of wind-induced interference effects and also for codification purposes.

Who has seen the wind ? Neither you nor I:
But when the trees bow down their heads,
The wind is passing by.

- Christina Georgina Rossetti. Who Has Seen The Wind ? (1872)

Some people say wind is a current of air: Some produce the ludicrous views that all winds are the same wind blowing in different directions. We must investigate the nature and origin of wind.

-Aristotle. Meteorologica. 340 B.C. (Translated by H. D. P. Lee)

7

Interference Effects - Parametric Study

The effect of wind-induced interference for the datum case was discussed in detail in the previous chapter. The datum case was a simplified situation, in which the interfering buildings were identical, the wind normal to the building face and the exposure open. In reality, these three parameters might vary. However, the datum case not only serves as a benchmark against which the effects of the different parameters can be contrasted and compared, it also provides a very useful, basic insight into the phenomenon of interference.

In this chapter, the effects of various parameters on interference, like the incident wind direction, building geometry and the upstream exposure as well as the effect of immediate surroundings will be studied in detail. The experimental methodology is similar to that followed for the datum case. The results of the wind tunnel experiments will be presented, compared, analyzed and discussed. General guidelines defining the effects of various parameters will be established in terms of simplified figures and regression equations.

7.1 Effects of Incident Wind Direction

Most previous studies have concentrated on a single incident wind direction - a 0° wind, normal to the building face. A probable reason for this is the premise that since the 0° wind gives the largest forces on a single building, it would also cause the most severe interference effects. Another less apparent reason is the excessive number of test cases involved; for example, five additional wind directions would increase the experimental efforts five-folds.

However, in absence of experimental results that account for directional effects of wind, it is difficult to verify the first reason, let alone attempt any generalization of wind-induced interference effects.

The effect of the angle of attack of wind on interference is studied by measuring the mean and fluctuating forces on the principal building model (P_0), due to an interfering building model (I_0) of the same size, located at different positions around the principal building. The disc on which the two models are mounted in the wind tunnel, is rotated with respect to the wind direction in increments of 15°, up to an angle of 75°. The 90° wind angle case is similar to the 0° case rotated by 90°. For wind azimuths greater than 45°, the building faces that represent windward and leeward walls for smaller angles are now actually side walls and, in strict sense, drag should now be lift. However, for the sake of simplicity in this text, the force along the horizontal axis is termed as drag and the force perpendicular to it as lift, as shown in Figure 3.9. The following sub-sections present the experimental results and analyze critically the effects of incident wind direction on interference. Overall extreme effects of wind direction are also evaluated and discussed vis-à-vis the meteorological climate model.

7.1.1 Mean drag

Figure 7.1 shows the effect of angle of attack on mean drag coefficient ($\overline{C}_d$) due to interference. All six templates in the figure show a striking resemblance in the fact that the ridge of the contours are oriented in the direction of the incident wind and the contours exhibit a great degree of symmetry about this ridge. Comparing this feature with Figure 5.1, depicting the wind flow and pressure distribution on a building for oblique winds and the

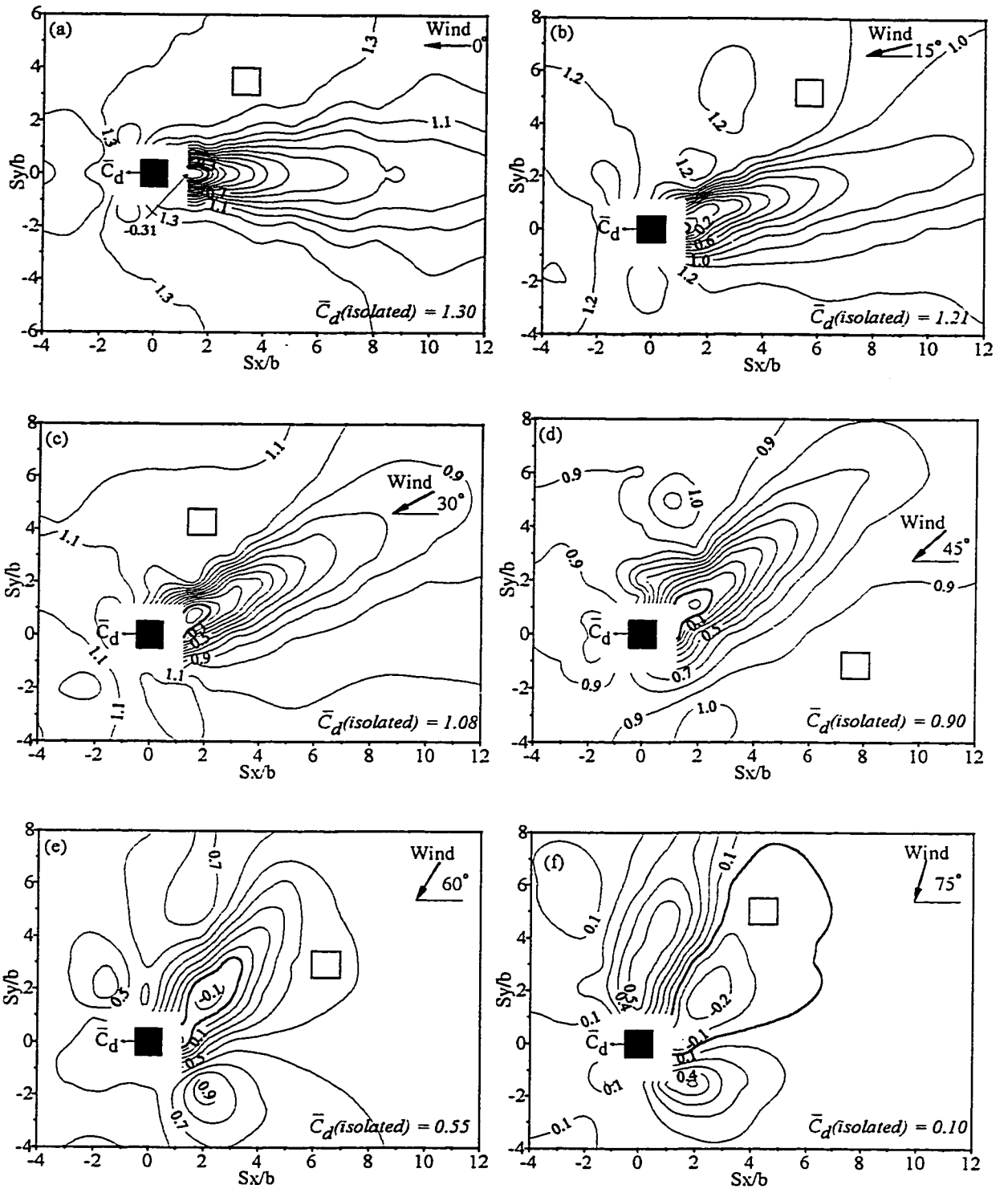

Figure 7.1 Interference effects - Effect of angle of attack of wind on mean drag coefficient.

accompanying explanation, can help realize the reason for this typical flow mechanism. The ridges of the contours shown in Figure 7.1 lie within the wake of the upstream interfering building, around which the flow separates and moves forward, engulfing the downstream building within it. Note the greater distance between the contours along the ridge as compared to the narrow spacing towards the sides. This implies that when the interfering building is positioned along the ridge, the downstream building lies within the wake of the upstream building and is thus subjected to high shielding. Predictably, shielding diminishes quickly when the interfering building is located to a side of the ridge, for now the principal building is partly exposed to the incident flow which increases the drag on it. This is evident by the values of the contours which tend towards the isolated building drag coefficient. For example, in the 30° incident wind case (Figure 7.1(c)), $\overline{C}_d$ is 1.1 for an interfering building location of Sx = 2b and Sy = -2b which is close to the isolated building $\overline{C}_d$ for the same wind angle.

The thick contour line demarcates the boundary of the zero $\overline{C}_d$ contour; in other words, it separates the negative drag (suction) from the positive (pressure). It is clear that the extent of the suction bubble, which always lies to the right of the principal building, tends to increase with wind angle. This is because, for larger wind azimuths, say 75°, the upstream interfering building (located to the right of the principal building in Figure 7.1(f)) forms a channel with the principal building to its side. The wind gushes through this channel, reducing the force on the inside (right) face of the principal building as compared to the opposite side, thus reducing the overall $\overline{C}_d$. This *"channelling"* effect is greater for larger wind angles which results in larger suction bubbles, i.e., a larger extent of suction. However, the largest magnitude of suction (-0.31) on the principal building is registered for

the 0° wind angle due to an interfering building immediately upstream at Sx = 1.25b. The minimum $\overline{C}_d$ (or maximum suction) values for various wind angles and interfering building locations are given in Table 7.1.

Table 7.1 Minimum $\overline{C}_d$ values for various incident wind angles

Wind angle	*Sx*	*Sy*	$\overline{C}_d$	$\overline{C}_d$ *(isolated)*
0°	1.25b	0	-0.31	*1.30*
15°	1.25b	0	-0.14	*1.21*
30°	1.5b	0.5b	-0.15	*1.08*
45°	2b	b	-0.15	*0.90*
60°	2b	2b	-0.19	*0.55*
75°	2b	1.5b	-0.28	*0.10*

In general, the 75° wind angle is responsible for high suctions spread over a larger area, and the 15° wind angle for the lowest.

High positive drag (pressure) is registered when the interfering building is located downstream of the principal building. Table 7.2 gives the wind angles and locations of largest $\overline{C}_d$:

Table 7.2 Maximum $\overline{C}_d$ values for various incident wind angles

Wind angle	*Sx*	*Sy*	$\overline{C}_d$	$\overline{C}_d$ *(isolated)*
0°	-b	1.5b	1.50	*1.30*
15°	-1.5b	0	1.37	*1.21*
30°	-1.5b	b	1.27	*1.08*
45°	-1.5b	0	1.12	*0.90*
60°	2b	-1.5b	1.00	*0.55*
75°	2b	-1.5b	0.55	*0.10*

On evaluating the $\overline{C}_d$ values relative to the isolated building $\overline{C}_d$ for a particular wind angle, overall, the 75° wind angle produces the most dramatic changes owing to the low

value of the isolated building $\overline{C}_d$ of 0.10. However, in absolute terms, the worst values are for the 0° wind angle.

7.1.2 Mean lift

Figure 7.2 shows the effect of angle of attack on mean lift coefficient ($\overline{C}_l$) due to interference. As in Figure 7.1, the ridges of the contours are oriented in the direction of the incident wind and the contours are symmetrical about this ridge. However, unlike the case for mean drag, the size of the suction bubble decreases with the increase in the incident wind angle; the reason though is similar. Two buildings arranged side-by-side are more susceptible to the *"channelling effect"* phenomenon at smaller wind angles than at larger ones and hence experience larger negative lift (suction). The minimum and maximum $\overline{C}_l$ values for various wind angles can be obtained from previous Tables 7.1 and 7.2 because $\overline{C}_l$ for a given angle θ and spacings Sx and Sy is equivalent to $\overline{C}_d$ for 90° - θ at Sy and Sx.

7.1.3 Fluctuating drag

Figure 7.3 shows the contours for fluctuating drag ($\widetilde{C}_d$) Interference Factors (IF) for various incident wind directions. To recapitulate, IF represents the ratio of force coefficient on the principal building with interfering building present to the force on the isolated building. The thick contour line with IF = 1.0 represents the "no interference case" or, in other words, the isolated building situation. Patches of strong interference effects are clearly discernible. Largest increases are obtained when the interfering building is located upstream, however, there are relatively small patches of strong interference for sideways locations as well, especially for the 45°, 60° and 75° wind angles. The largest IFs are

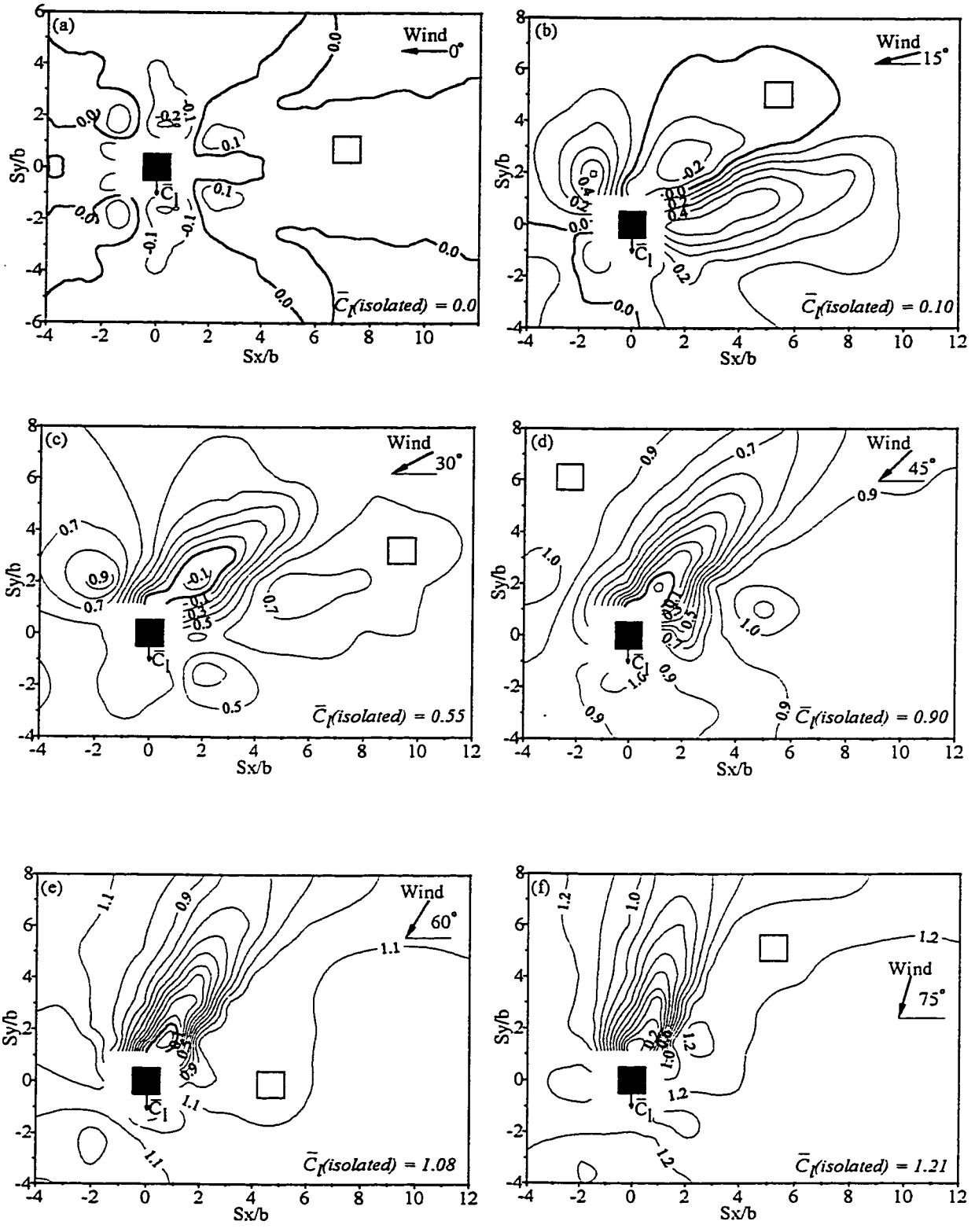

Figure 7.2 Interference effects - Effect of angle of attack of wind on mean lift coefficient.

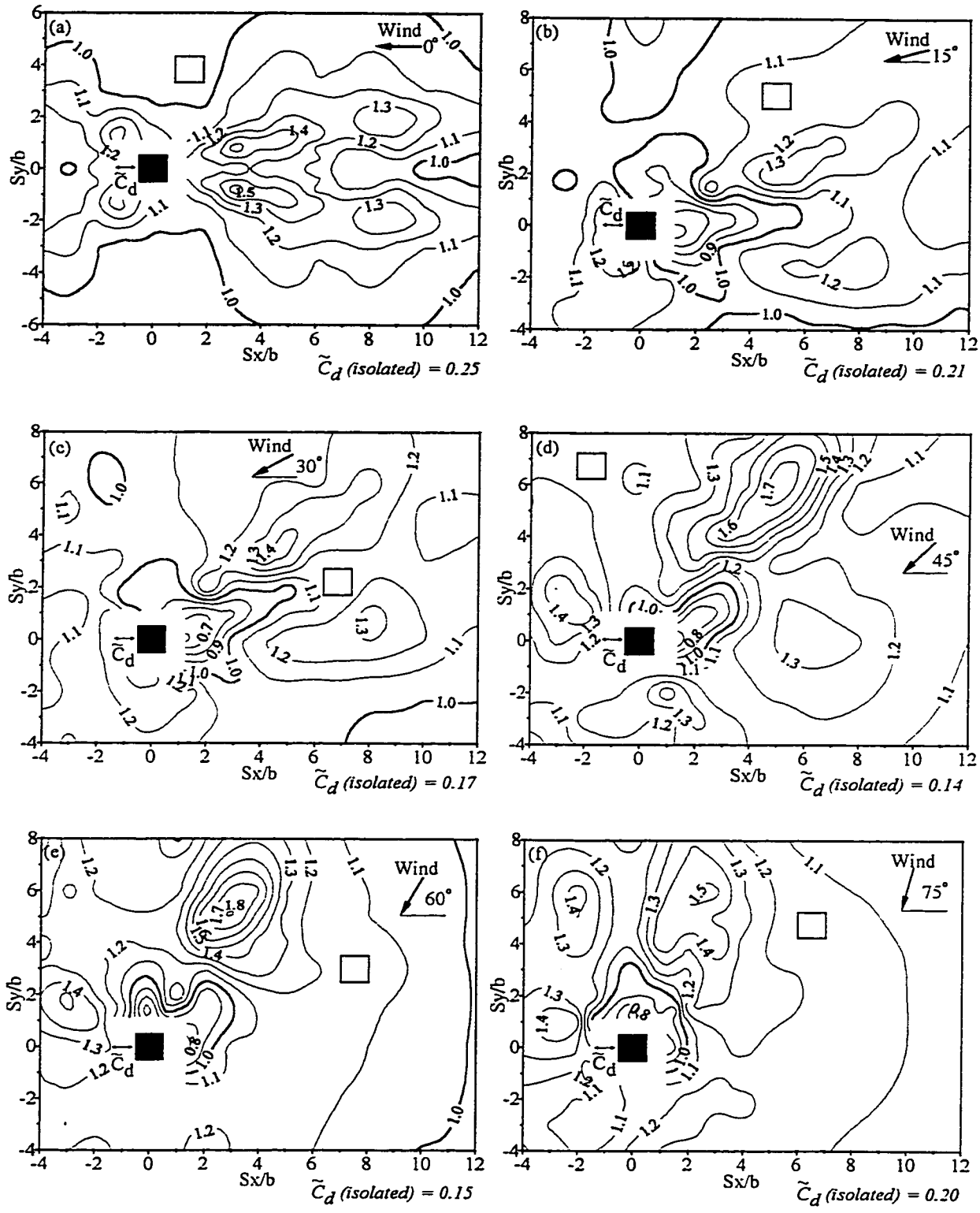

Figure 7.3 Interference effects - Effect of angle of attack of wind on fluctuating drag IF.

registered for the 45° and 60° wind angles, the 45° angle showing a larger extent of increases that is spread in patches around the principal building. An important and interesting observation is that for smaller wind angles (0° and 15°), highest IFs are obtained when the principal building lies near the edge of the wake of the interfering building rather than within the wake itself, however for larger wind angles, high IFs are obtained within the wake region. This has to do with the orientation of the buildings with respect to the flow. For smaller wind angles, only the windward face of the principal building is under the direct onslaught of wind and positioning the interfering building directly upstream does not change this scenario much. However, shifting the upstream interfering building to a side of the principal building creates an imbalance in the wind loads on all the faces of the principal building. The windward face which lies near the boundary of the wake of the interfering building is, in particular, subjected to the more turbulent fluctuating forces, thus increasing the overall fluctuating drag on the principal building. For larger incident wind angles, two of the building faces are exposed to wind and even when the principal building is within the wake of the upstream interfering building, those two faces are impinged upon by high velocity wake fluctuations, thus causing high fluctuating forces. Table 7.3 gives the wind angles and locations of largest Interference Factors (IF) for $\widetilde{C}_d$:

Table 7.3 Maximum IF values for $\widetilde{C}_d$ for various incident wind angles

Wind angle	*Sx*	*Sy*	$\widetilde{C}_d$	*IF*
0°	3b	0.75b	0.40	*1.60*
15°	5b	2b	0.29	*1.40*
30°	5b	4b	0.24	*1.44*
45°	5b	6b	0.25	*1.79*
60°	3b	5b	0.27	*1.82*
75°	3b	4b	0.31	*1.53*

The above table shows that the maximum increase in fluctuating drag is 82% for wind angle of 60° and at an interfering building location of Sx = 3b and Sy = 5b. In absolute terms, however, the maximum fluctuating drag coefficient ($\widetilde{C}_d$) of 0.40 is registered for the 0° wind angle.

7.1.4 Fluctuating lift

Figure 7.4 shows the contours for fluctuating lift ($\widetilde{C}_l$) Interference Factors (IF) for various incident wind directions. Once again, the largest increases are obtained when the interfering building is located upstream, with small patches of strong interference for sideways locations as well, especially for the 15°, 30° and 45° wind angles. The largest IFs are registered for the 30° and 45° wind angles, the 45° angle showing a larger extent of increases that is spread in patches around the principal building. The maximum IF and $\widetilde{C}_l$ values for various wind angles can be obtained from Table 7.3 because $\widetilde{C}_l$ for a given angle θ and spacings Sx and Sy is equivalent to $\widetilde{C}_l$ for 90° - θ at Sy and Sx.

7.1.5 Wind directionality - overall effects

Experimental results presented and discussed above clearly indicate that interference effects vary with wind direction. The interference effect contours already presented are for specific wind directions. Since in general the wind direction keeps on changing, the results for interference effects should incorporate the possibility of wind blowing from any direction. More rational estimates of interference effects must take into account the probability distribution of wind speed and direction. Keeping this in view and from a practical standpoint, the overall effect of wind direction is analyzed in this sub-section from two

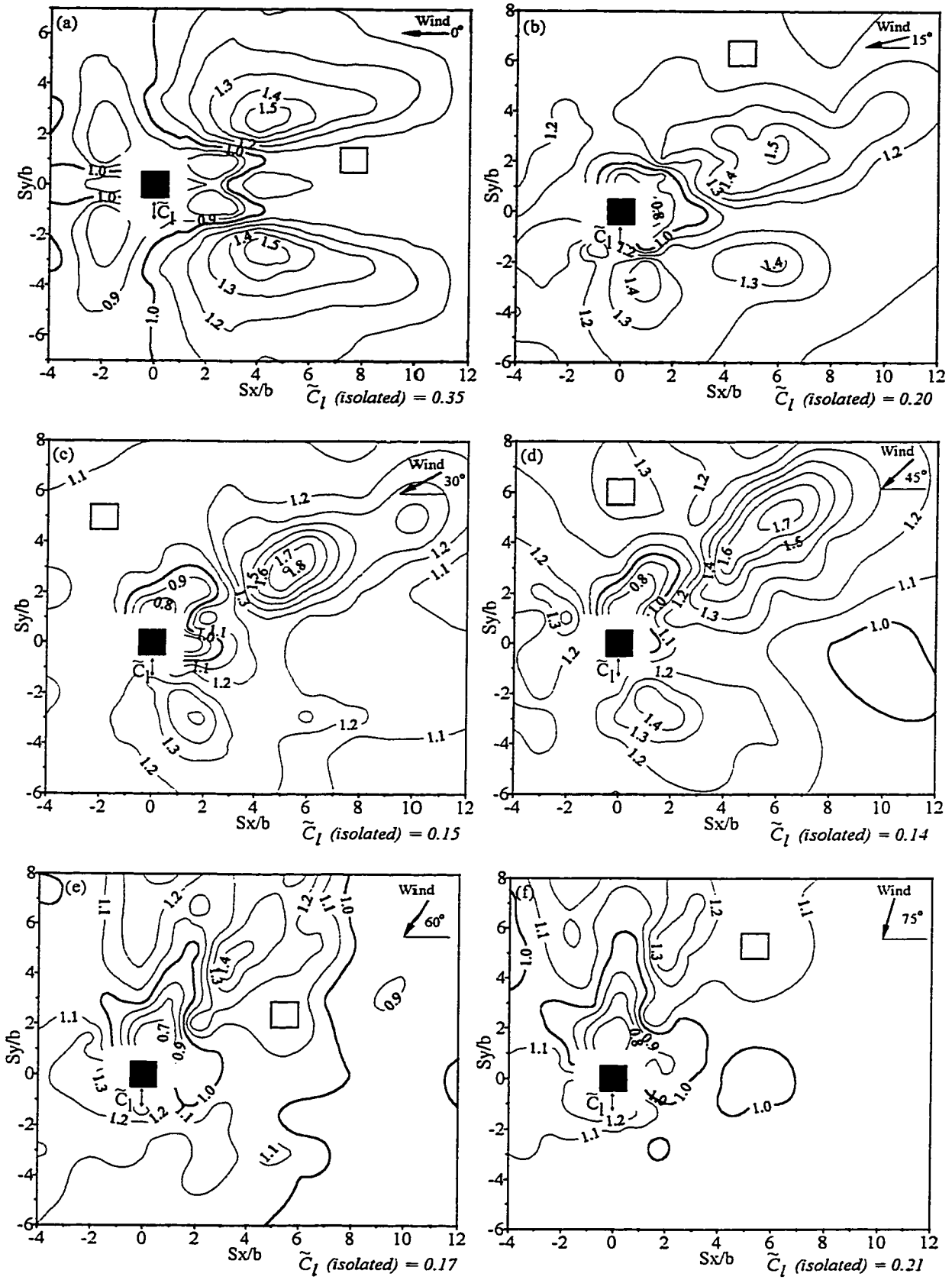

Figure 7.4 Interference effects - Effect of angle of attack of wind on fluctuating lift IF.

perspectives. The first is a simplified approach, where the extreme or worst effects for a particular interfering building location are identified irrespective of the wind direction. In the second approach, interference effects are evaluated with respect to a circular climate model, taking directional probabilities into account. Such an analysis will provide an overall view of interference effects with respect to wind direction and may be helpful in the codification of these effects.

7.1.5.1 Extreme interference effects for all wind directions

The effect of wind direction on interference was shown in Figures 7.1 to 7.4. The extreme interference effects, for each interfering building location, are the maximum and minimum force coefficients for mean loads and the maximum Interference Factors for fluctuating forces. For example, in case of mean drag, the drag coefficients ($\overline{C}_d$) for the interfering building location Sx = 2b and Sy = 0 are, -0.05, 0.38, 0.49, 0.47, 0.95, 1.14 and 1.34 for incident wind angles of 0°, 15°, 30°, 45°, 60°, 75° and 90°. Hence, maximum and minimum $\overline{C}_d$ are 1.34 and -0.05, respectively. It should be noted that unlike the individual wind direction case, where the drag was based upon Figure 3.9 and was always parallel to the horizontal axis (pointing left) the direction of forces now follows the direction of wind. Thus, the drag for wind directions between 0° and 45° (anti-clockwise sense) pushes the building towards left along the horizontal axis and, for wind angles between 45° to 90° pushes the building down, along the vertical axis. Similarly, in case of lift, the force on the principal building acts down, along the vertical axis for the first half quadrant, and towards left for the latter half. The entire data is analyzed and presented from the above perspective.

Figure 7.5 shows contours for maximum mean drag coefficient ($\overline{C}_d$) due to interference, for wind directions lying between 0° and 90°. Eventhough only one quadrant (0° to 90°) is sufficient to describe the entire polar region (0° to 360°), interference contour plots can be drawn for other wind directions around the principal building, by a reflection of the basic plot (0° to 90°) about the horizontal and vertical axes. Thus, the contour plot for 90° to 180° is essentially a reflection about the vertical axis, of the 0° to 90° plot (Figure 7.5) and the plots for 180° to 270° and 270° to 360° are reflections about the horizontal axis, of the 90° to 180° and the 0° to 90° plots, respectively. Also note that 0° to 45° wind angles are sufficient for the analysis presented in this sub-section.

Comparing the $\overline{C}_d$ values in Figure 7.5 with the maximum $\overline{C}_d$ of 1.30 for the isolated building (see last column of Table 7.1), the figure does not show any regions of high interference effects. Thus, designing a building for a $\overline{C}_d$ of 1.30 should be a safe proposition.

Figure 7.6 shows contours for minimum drag coefficient for all wind directions. The minimum $\overline{C}_d$ for an isolated building for all wind directions (between 0° and 45°) is 0.90 (see table 7.1). The hatched regions show areas of high shielding, greater than about 30% ($\overline{C}_d < 0.70$). Shielding is greater than about 50% ($\overline{C}_d < 0.50$) for the cross-hatched regions. Suctions ($\overline{C}_d < 0.0$) are generated for the dark shaded regions close to the principal building. Overall, the shielding region is large, and roughly spans a square area bounded by Sx = -0.5b to 6b and Sy = -0.5b to 6b. The suction region lies within Sx = 0 to 2b and Sy = 0 to 2b.

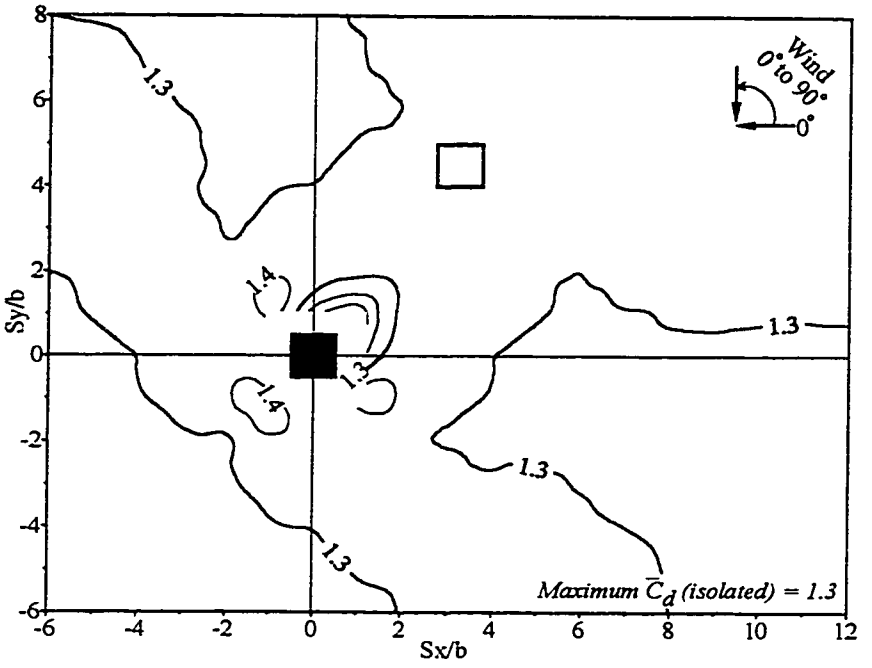

Figure 7.5 Contours for maximum mean drag coefficient for all wind directions.

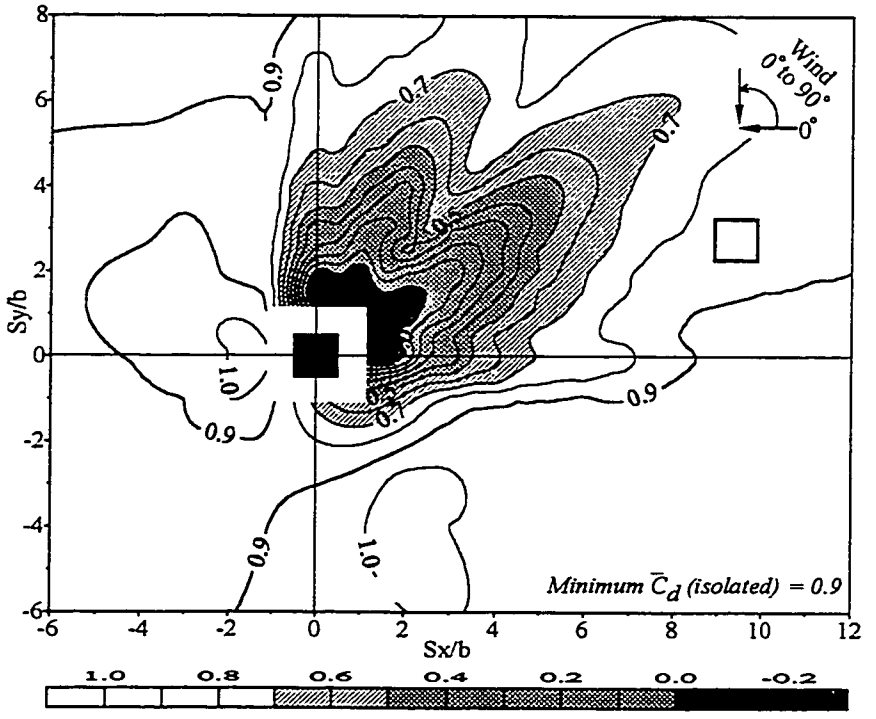

Figure 7.6 Contours for minimum mean drag coefficient for all wind directions.

Figure 7.7 shows the maximum mean lift coefficient ($\overline{C}_l$) for all wind directions. Since the maximum $\overline{C}_l$ for an isolated building is 0.90 (from table 7.1, and $\overline{C}_l(\theta) = \overline{C}_d$ (90° - θ)), and the maximum $\overline{C}_l$ in case of interference remains below 1.10, the increases in mean lift are not significant. Thus a design $\overline{C}_l$ of 0.90, though a bit on the non-conservative side, is still safe.

Figure 7.8 shows the minimum lift coefficient contours. The minimum $\overline{C}_l$ goes below -0.20 for a fairly large patch within Sx = b to 3b and Sy = b to 3b, upstream, and a couple of tiny patches downstream near the principal building. The minimum $\overline{C}_l$ for isolated building is 0.0. Thus, increase in suction is significant in case of lift.

Figure 7.9 shows the Interference Factor (IF) contours for fluctuating drag($\widetilde{C}_d$). It is clear from the figure that $\widetilde{C}_d$ increases by more than 30% over a large area around the principal building. Large increases of greater than 50% are registered when the interfering building is located within Sx = 3b to 6b and Sy = 4b to 8b.

Increases in fluctuating lift ($\widetilde{C}_l$) for all wind directions are large and are shown in Figure 7.10. In fact, for most regions around the principal building within Sx = -5b to 10b and Sy = -5b to 8b, $\widetilde{C}_l$ increases by about 20% to 80%, except for close proximity locations (Sx, Sy < 2b), where $\widetilde{C}_l$ decreases.

7.1.5.2 Meteorological climate model

The wind climate at a location changes with wind direction due to the basic circulation patterns of wind as well as the surrounding topography. Historical meteorological data for

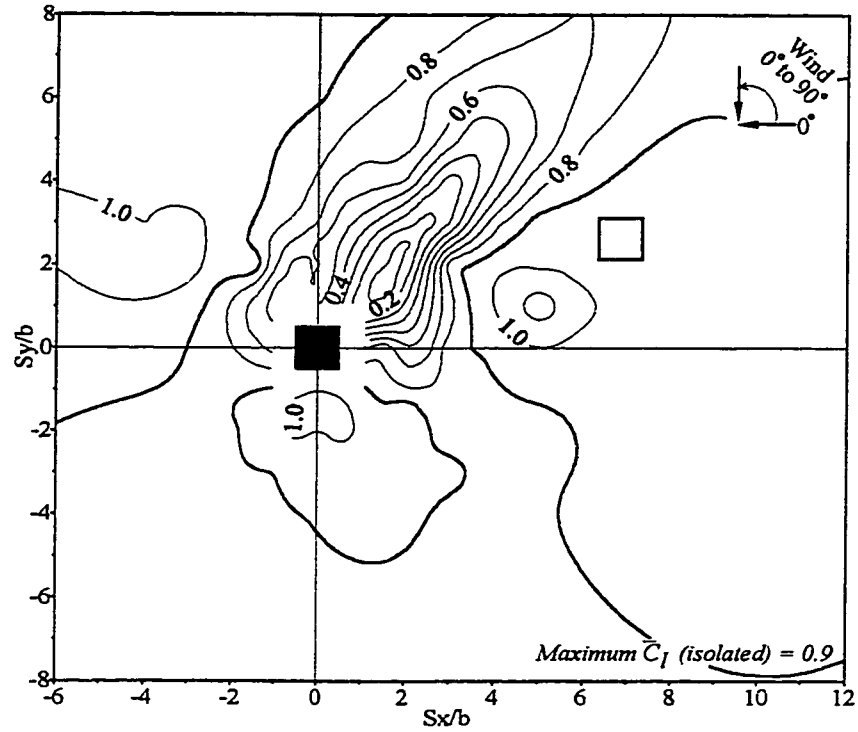

Figure 7.7 Contours for maximum mean lift coefficient for all wind directions.

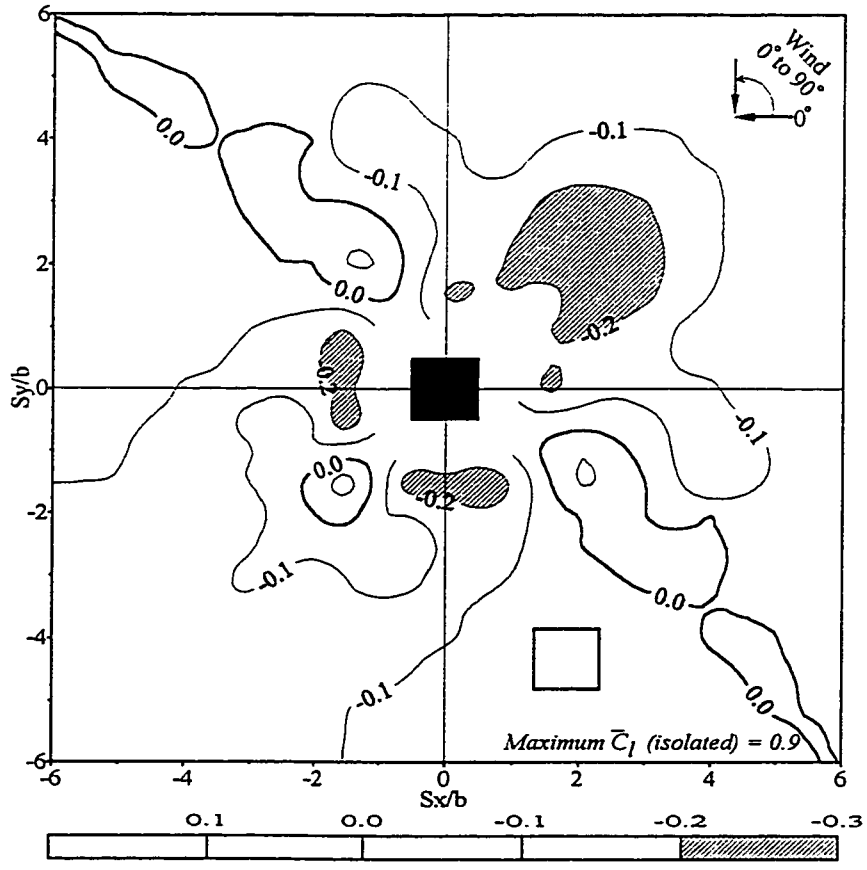

Figure 7.8 Contours for minimum mean lift coefficient for all wind directions.

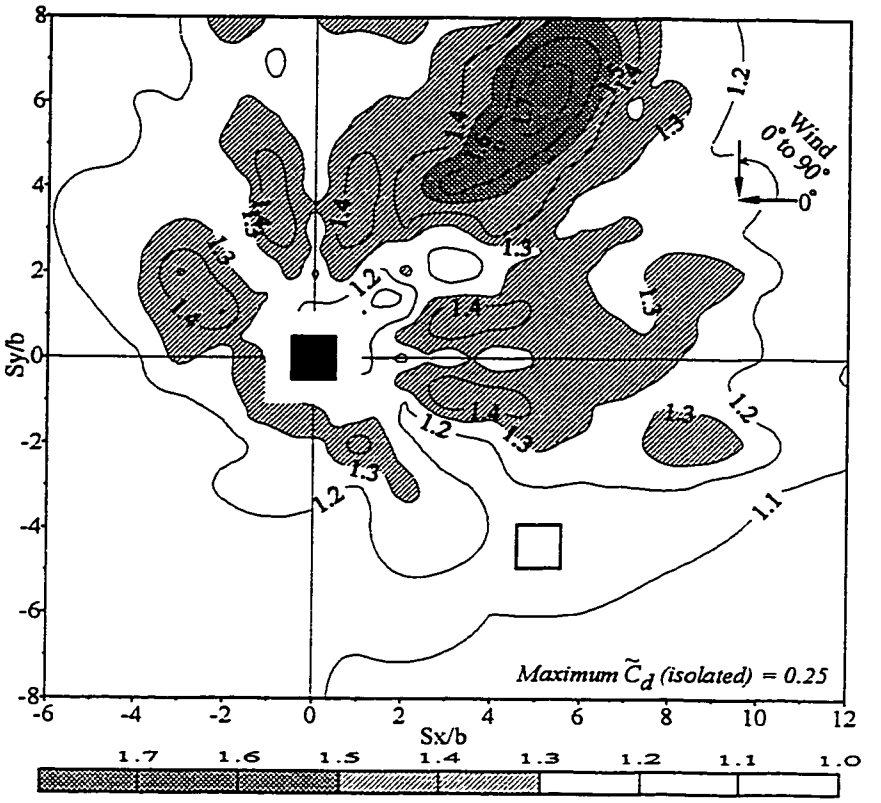

Figure 7.9 Maximum IF contours for fluctuating drag for all wind directions.

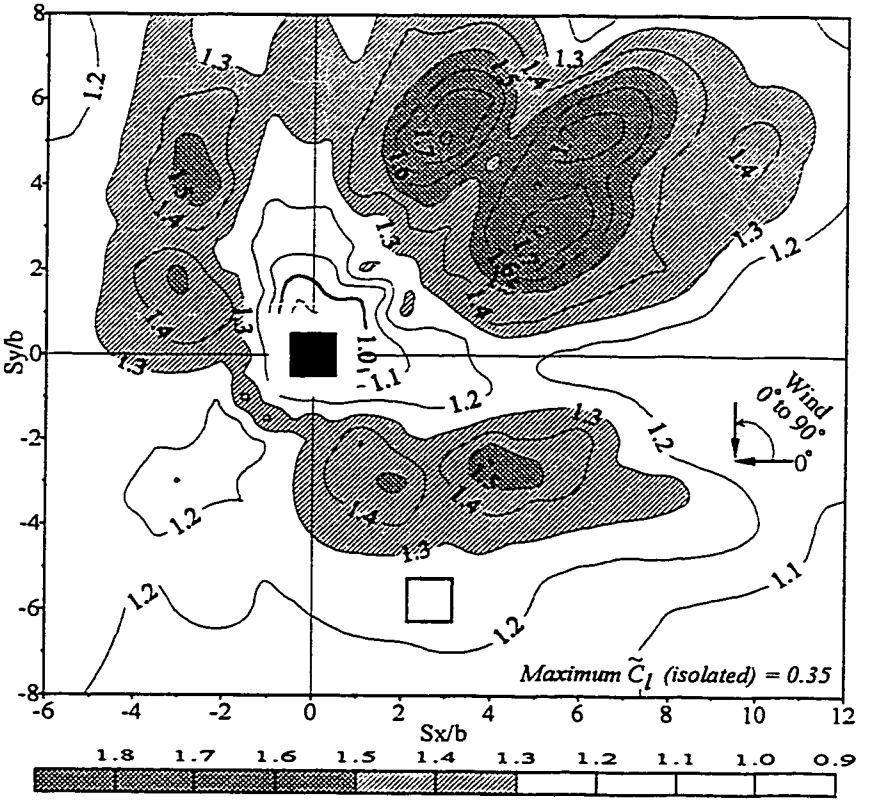

Figure 7.10 Maximum IF contours for fluctuating lift for all wind directions.

a particular site, generally a city or town, can be obtained from a weather station. This comprises wind speeds averaged over a certain period of time at a height of 10 m above the ground. Table 7.4 shows a typical meteorological record for Montreal with hourly wind speed records for 31 years (Wu 1994). The relative frequencies of wind speed exceedance for a particular sector (or wind direction) can be calculated, from Table 7.4, as the ratio of the number of occurrences of wind speeds higher than a particular velocity and the total number of observations for all directions.

Table 7.4 Number of observations of classified wind speeds in 16 compass directions for Montreal (Wu 1994).

		Wind Speed Class (km/h)									
i	Sector	1-10	11-20	21-30	31-40	41-50	51-60	61-70	71-80	81-90	Total
1	N	6182	3864	934	144	17	1	1	0	0	11143
2	NNE	6934	10296	3618	923	178	31	14	9	0	22003
3	NE	4614	9083	4749	1421	308	83	19	4	0	20281
4	ENE	2363	3362	1142	210	30	5	0	0	0	7112
5	E	3051	2499	398	43	2	0	0	0	0	5993
6	ESE	3386	2511	614	68	2	0	0	0	0	6581
7	SE	4962	4904	1837	359	31	2	0	1	0	12096
8	SSE	5057	6117	2109	438	38	6	0	0	0	13765
9	S	4890	3666	591	71	2	0	0	0	0	9220
10	SSW	5670	6976	1678	281	42	0	0	0	0	14647
11	SW	8634	13640	6937	2196	386	69	24	6	1	31893
12	WSW	9018	14715	9706	3744	816	177	39	9	0	38224
13	W	7732	12265	8249	3172	570	89	18	4	0	32099
14	WNW	4826	6271	3317	986	139	18	3	0	0	15560
15	NW	4528	3732	1233	234	19	3	0	0	0	9749
16	NNW	4538	2427	655	73	1	3	0	0	0	7697
										Calm	13689
										Total for all directions	271752

Note: Data are derived from hourly records during the period of January 1, 1960 to December 31, 1990 at Dorval Airport, Montreal.

The directional probabilities from the above data can be used to find the overall effect of wind direction on interference effects. To calculate the cumulative effect of probability of

wind speed exceedance for each location of the interfering building, the value of force coefficient at that location is multiplied by the probability of exceedance for each sector and the products summed-up for all the sectors. Thus, the cumulative force coefficient, $[C]_v$ for a wind velocity of v can be expressed as,

$$[C]_v = \sum_{i=1}^{n} p_i \; C \tag{7.1}$$

where, C = force coefficient for a particular interfering building location, (Sx, Sy); v = wind speed; p_i = probability of wind speed exceedance for sector i and n = total number of sectors or compass directions.

The above methodology is applied to the interference effects data shown in Figures 7.1 to 7.4, by solving one particular case involving all wind speeds. The observations for all wind speeds are taken from the last column of Table 7.4. However, a problem arises, because Table 7.4 uses a wind sector of 22.5°, whereas a wind sector of 15° is used in the interference effects experiments in this study. Therefore, the data of Table 7.4 is modified by narrowing the sector to 15° and recalculating the probabilities of exceedance, now for 24 compass directions, by using a linear interpolation. The modified probabilities of exceedance for all wind directions (last column of Table 7.4) are given in Table 7.5. The table, in a way, represents the probability of wind coming from a particular direction. For example, the probability of wind coming at an angle of 225° is 0.123 or 12.3% i.e. it is the highest.

In this case study, the angles are measured anti-clockwise and the 0° wind angle is assumed aligned towards East. The interference effects data (Sx, Sy and force coefficient) is available for wind angles from 0° to 90°, in the first quadrant. Data for other quadrants, up

Table 7.5 Directional probabilities for all wind speed classes up to 90 km/h for Montreal.

Wind angle (°)	*Probability*	*Wind angle* (°)	*Probability*	*Wind angle* (°)	*Probability*
0	0.0153	120	0.0213	240	0.0490
15	0.0173	135	0.0380	255	0.0345
30	0.0435	150	0.0363	270	0.0240
45	0.0780	165	0.0507	285	0.0325
60	0.0550	180	0.0827	300	0.0343
75	0.0497	195	0.0947	315	0.0470
90	0.0153	210	0.0945	330	0.0203
105	0.0150	225	0.1230	345	0.0163

to a wind angle of 360°, is obtained by mirroring about the appropriate axis, the data in the first quadrant. For instance, interference effects data for the wind angle of 120° is the mirror image, on the vertical axis, of the data for the 60° wind angle. Thus a data base of interference effects for incident wind angles from 0° to 360° at an increment of 15° is created for mean and fluctuating drag and lift.

Equation 7.1 is applied to this data, along with the probability values from Table 7.5, to obtain the weighted sum of the force coefficients at each interfering building location. For comparison, weighted force coefficients for the isolated building are also obtained similarly. The new force coefficient thus represents the expected value of the force on a building, taking into consideration the wind direction and the associated directional probabilities, for Montreal.

Figure 7.11 shows the average mean and fluctuating drag due to interference, weighted by directional probabilities, for Montreal. Figure 7.11(a) shows the mean drag coefficient. Figure 7.11(b) shows the same data in terms of Interference Factors, i.e., normalized by the isolated building average weighted drag coefficient (1.11). By comparing this figure with Figure 7.1 for individual wind directions, it becomes clear that the effects of interference are

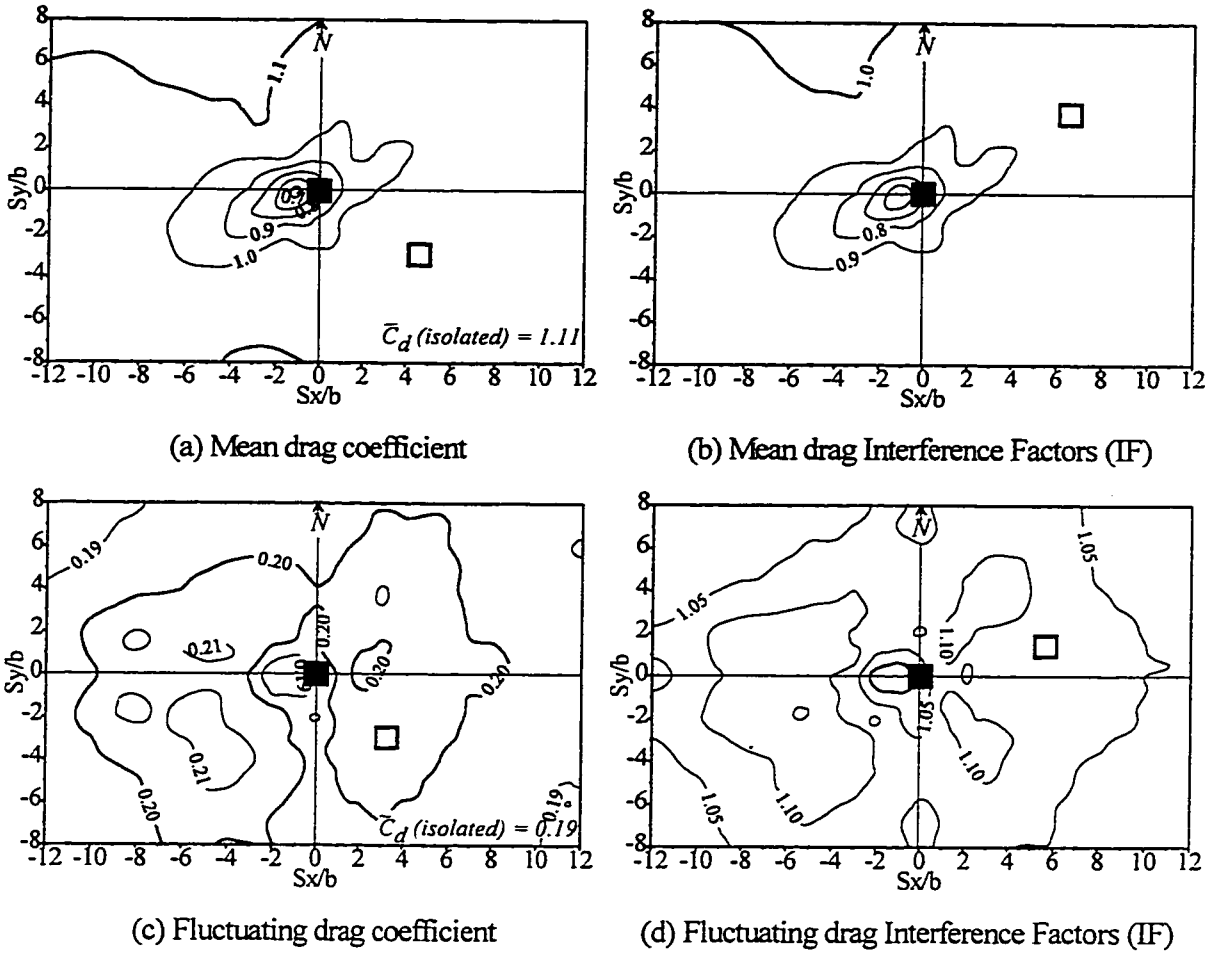

(a) Mean drag coefficient

(b) Mean drag Interference Factors (IF)

(c) Fluctuating drag coefficient

(d) Fluctuating drag Interference Factors (IF)

Figure 7.11 Average mean and fluctuating drag due to interference weighted by directional probabilities (24 wind directions) for Montreal

averaged out and are thus lowered, as expected. Understandably, contours stretch approximately towards West-South-West, the dominant wind direction (225°). Figure 7.11(c) and 7.11(d) show the fluctuating drag coefficient and the corresponding Interference Factors, respectively. Once again, the interference effects are lowered and do not seem to be as critical as the individual effects of wind direction in Figure 7.3.

Figure 7.12 shows the weighted mean and fluctuating lift due to interference. The reduction in mean lift is more apparent than the increase, especially in the south-west

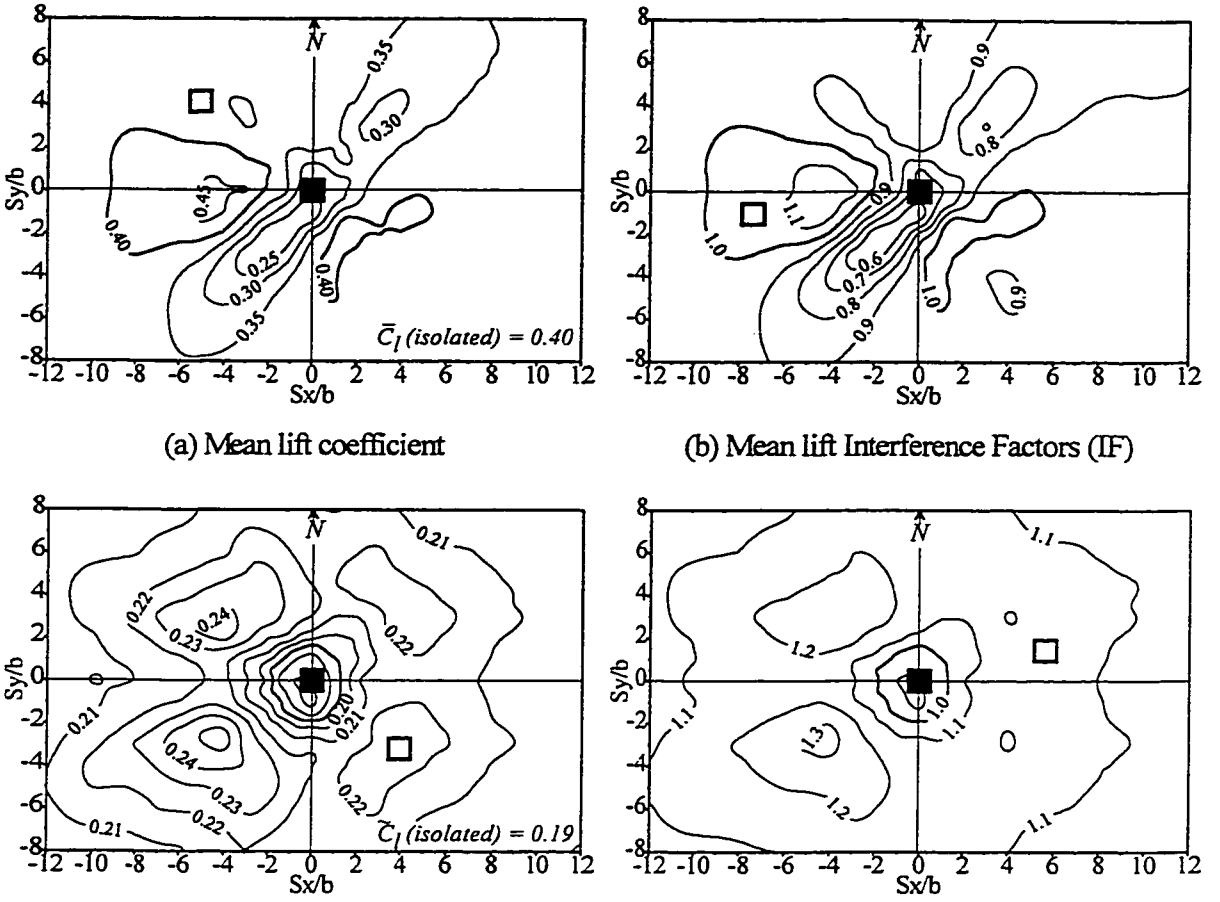

(a) Mean lift coefficient

(b) Mean lift Interference Factors (IF)

(c) Fluctuating lift coefficient

(d) Fluctuating lift Interference Factors (IF)

Figure 7.12 Average mean and fluctuating lift due to interference weighted by directional probabilities (24 wind directions) for Montreal

quadrant (see Figure 7.12(b)). Small increases, of 20% to 30%, in fluctuating lift can be seen in the same quadrant (Figures 7.12(c) and 7.12(d)).

Thus, it is clear from the above analysis, that including the meteorological climate model might actually decrease the effects of interference, since a weighted average of the interference effect values is considered. Moreover, for Montreal, winds blowing from the south-west sector give the most significant interference effects for critical building locations.

7.2 Effects of Interfering Building Size

Previous studies on wind interference effects concentrate mainly on the interference between two identical sized buildings. A few proprietary studies (see chapter 2) do caution against the adverse effects of large interfering buildings, but with little experimental data to suggest a concrete trend. A comprehensive study is thus undertaken to examine, in detail, the effects of interfering building sizes on wind interference. The result of this experimental effort will help establish general guidelines for building design.

As explained in chapter 3, ten interfering building models of various sizes (see Table 3.1) are used to study the effect of the interfering building size on the mean and fluctuating forces on the instrumented (principal) building with 0° wind direction, normal to a face of the building and an open exposure. The range of building sizes covered buildings that were smaller than, equal to or larger than the principal building. The interfering building sizes are divided, relative to the principal building, in three categories: a) increase or decrease in width, heights equal, b) increase in height, widths equal and c) increase in both width and height. The effects of interfering building size on mean and fluctuating forces on a building are presented and discussed, relative to the datum case, in the following sub-sections. These effects are summarized as general design guidelines, presented in the form of simple *Size Influence Grids*.

7.2.1 Mean drag

Figure 7.13 shows the effect of interfering building size on mean drag IF. The contours represent the increase or decrease in the mean drag coefficient with respect to the isolated building mean drag coefficient of 1.30. The datum case is represented by Figure 7.13(b).

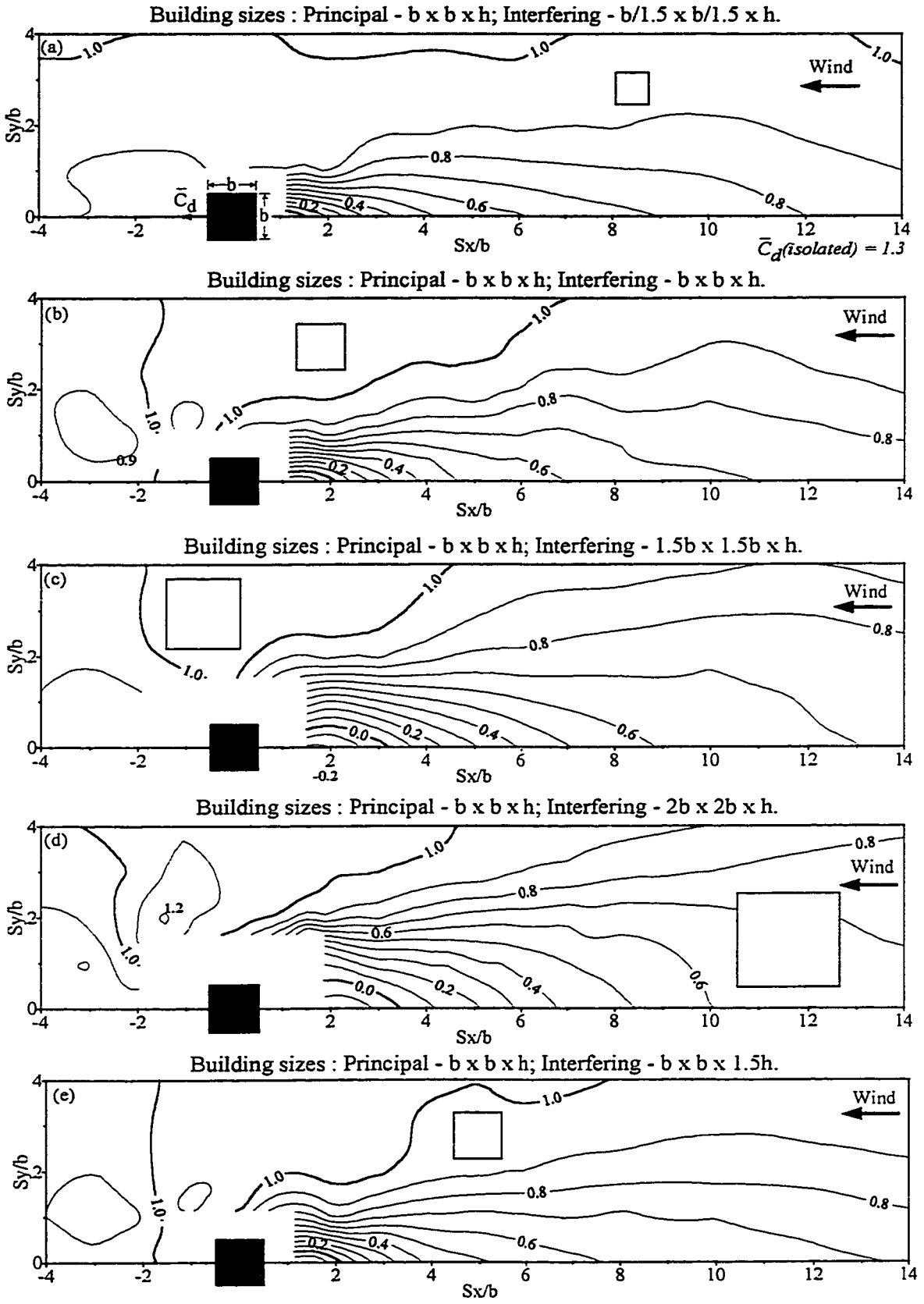

Figure 7.13 Effect of interfering building size on mean drag IF *(Continued...)*

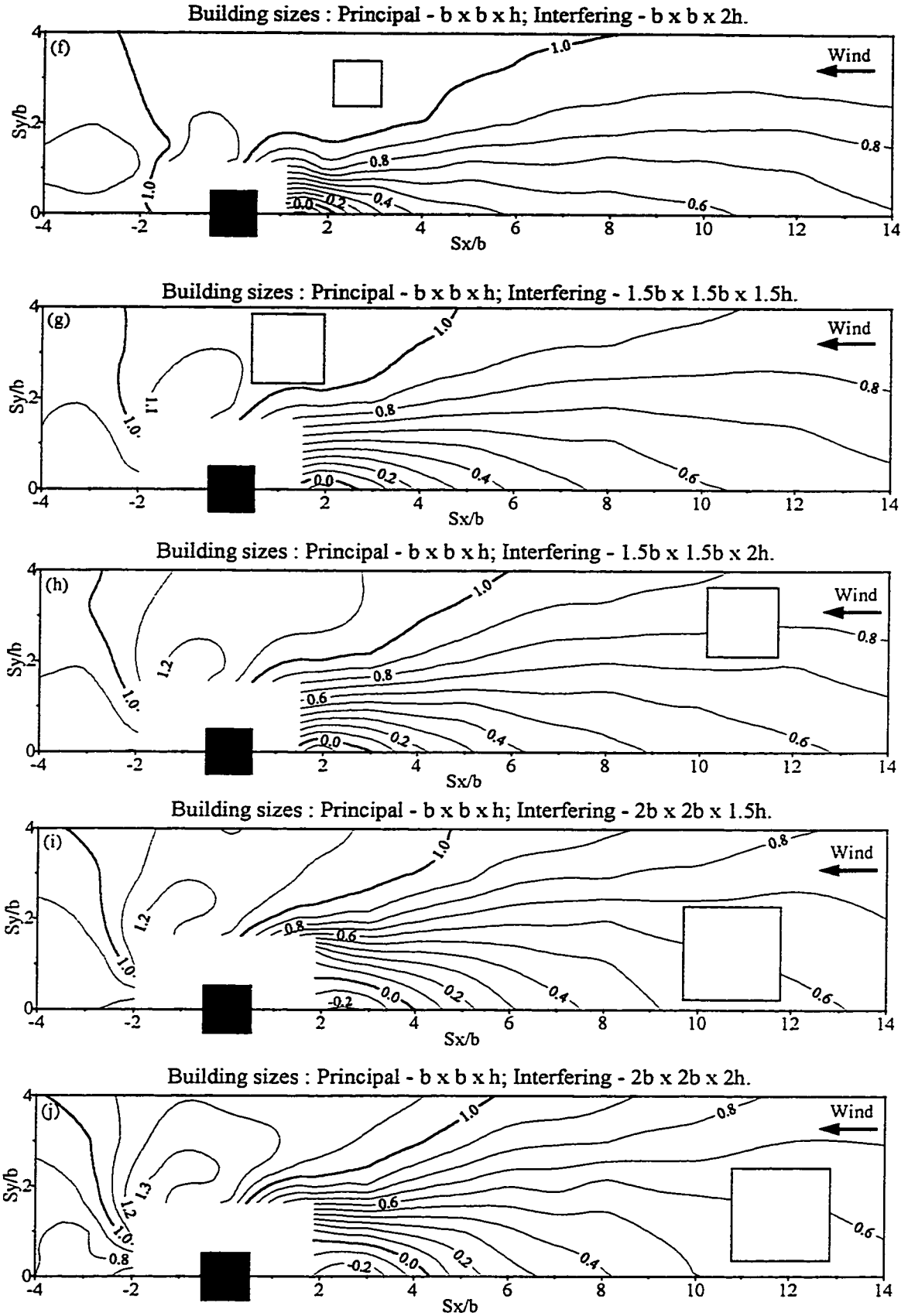

Figure 7.13 *(Continued...)* Effect of interfering building size on mean drag IF.

The "no interference" (IF = 1.0) as well as the "complete shielding" (IF = 0.0) contours are shown by thick lines.

Figures 7.13(a) to 7.13(d) show the effect of gradually increasing the interfering building plan dimensions (height equal to that of the principal building) on the principal building mean drag. It is clear that shielding increases with increasing interfering building size. This is evident from the low IF values for larger interfering building sizes upstream. For instance, at an upstream tandem location of Sx = 6b and Sy = 0, IF = 0.59, 0.57, 0.41 and 0.32 for interfering building width of b/1.5, b, 1.5b and 2b respectively, where b = 20m. With the largest building positioned at Sx = 14b (Figure 7.13(d)), an IF of about 0.7 is registered for the principal building, indicating a 30% decrease in mean drag. This implies that a downstream building experiences considerable shielding due to an upstream building of twice its width located as far away as 14 times the principal building width, or 280m (more than one quarter of a kilometre) in full scale in this case. However, suctions developed (negative IF) for close tandem locations do not follow this trend. Maximum suction (lowest IF of -0.24) is obtained at Sx = 1.25b (clear spacing of 0.25b) when both the principal and interfering buildings are of the same size and gradually decreases (to an IF value of -0.16) at Sx = 2b (clear spacing of 0.5b) for the largest (width) interfering building (Figure 7.13(d)). This is because with increasing upstream building size, the downstream principal building is completely shielded in its wake and the large width of the upstream building does not allow the flow to converge and speedup into the gap between the two buildings. Thus, the pressure within the gap and on the upstream face of the principal building does not go down as much as when shielded by a smaller building and the overall suction (upstream face drag minus the downstream face drag) is reduced.

Interference also causes considerable increase in mean drag, which increases with increasing downstream interfering building size. For both buildings of same size, maximum increase is about 15% at Sx = -b and Sy = 1.5b, increasing to 23% for an interfering building double the plan dimensions of the principal building at Sx = -1.5b and Sy = 2b (see Figure 7.13(d)). This can be explained as follows. As the wind strikes the large downstream building, it is deflected sharply into the gap between the two buildings, at the rear of the principal building. The high velocity flow in the gap increases the suction on the rear face of the principal building, hence the overall mean drag increases too.

Figures 7.13(b), 7.13(e) and 7.13(f) show the effect of increasing the interfering building height (plan dimensions equal to the principal building) on mean drag IF. The interfering building height is varied by 1.5 and 2 times the principal building height. The effects are, in general, similar to the ones discussed above, though a bit subdued. Thus shielding increases with increasing height of the upstream building. However, increasing the building height does not seem to change the suction on the principal building from that due to an equal height case (Figure 7.13(b)) for tandem locations of the interfering building.

Figures 7.13(g) to 7.13(j) show the effect of changing both the width (b) and height (h) of the interfering building on mean drag of the principal building. All the contours are characterized by a high *shielding belt* that in general extends up to a distance of 14b directly upstream and is about 2b wide. An interfering building 1.5 to 2 times the size of the principal building located at the outer periphery of this region offers a shielding of 25% to 30% to the principal building. Shielding is much higher for inner and tandem regions, for instance with the largest building used in this study (see Figure 7.13(j)) located as far away

as 13b (260m) upstream in a tandem position, a high shielding of about 45% is obtained. An interesting observation for Figures 7.13(i) and 7.13(j), involving the two of the larger buildings, is that suction is low at very close tandem locations, gradually increasing farther upstream and decreasing again. For example, for Figure 7.13(j), IFs of -0.18, -0.23, -0.29 and -0.08 are obtained for tandem locations of 1.75b, 2b, 3b and 4b respectively. A previously given argument that has to do with the large size of the interfering building can once again be forwarded as the reason for this behaviour, i.e. with increasing upstream building size, the downstream principal building is completely shielded in its wake and the large across-wind width of the upstream building does not allow the flow to converge and speed-up into the gap between the two buildings. The smaller the gap between the two buildings, the more complete the shielding, resulting in a lower suction within the gap. When the gap is increased, high velocity flow begins to enter into the gap from the sides as well as from the top of the upstream building, increasing the suction on the windward face of the principal building and the overall negative drag on it. Also noteworthy is the increase in the extent of suction with increasing building size. For the largest interfering building (Figure 7.13(j)), suction is predominant upstream in tandem position up to a clear spacing of 2.75b between the two buildings.

As already discussed, large interfering building to the downstream of the principal building causes a considerable increase in mean drag as evident from the steadily increasing values of IF contours at downstream locations in Figures 7.13(g) to 7.13(j). When a building double the size of the principal building is situated downstream at Sx = -1.75 and Sy = 1.75, it increases the mean drag on the principal building by as much as 36% (Figure 7.13(j)).

7.2.2 Mean lift

Figure 7.14 shows the effect of interfering building size on mean lift coefficient. The mean lift coefficient for an isolated building is zero. The thick $\overline{C_l} = 0.0$ contour line represents locations where the interfering building has no effect on the $\overline{C_l}$ of the principal building. The contours show a concentration of high negative lift (suction) locations to the side and high positive lift (pressure) behind the principal building. Both negative and positive $\overline{C_l}$ show a clear increase with increasing width of the upstream building (Figures 7.14(a) to 7.14(d)). However, it is interesting to note that suction actually decreases with increasing interfering building height (Figures 7.14(e) and 7.14(f)). This may be due to the gradual change in the flow around the interfering building to two-dimensional because of its increased height. A detailed explanation is unavailable at this time; a clearer picture may emerge with flow-visualization experiments.

On increasing both the width and the height of the interfering building, both suction and pressure tend to increase. The maximum suction ($\overline{C_l}$ = -0.35) is registered due to an interfering building of double the size of the principal building at a close sideways location of 1.75b. The maximum positive $\overline{C_l}$ due to the same building is a phenomenal 1.6 at a close downstream location of Sx = -1.75b and Sy = 1.75b. This is a significant increase when compared with the mean lift of 0.21 at an almost similar location for the datum case (Figure 7.14(b)).

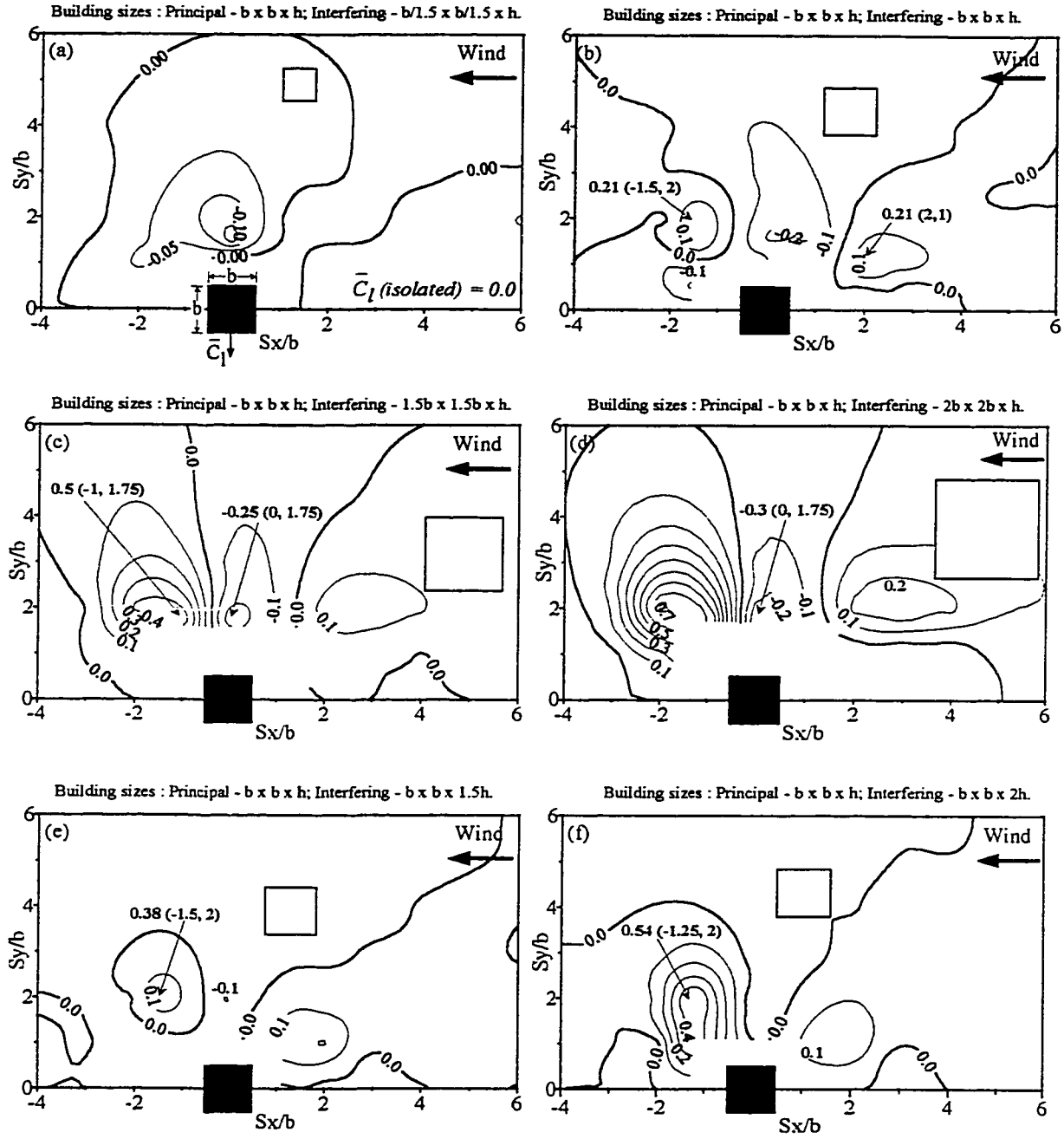

Figure 7.14 Effect of interfering building size on mean lift coefficient *(Continued...)*

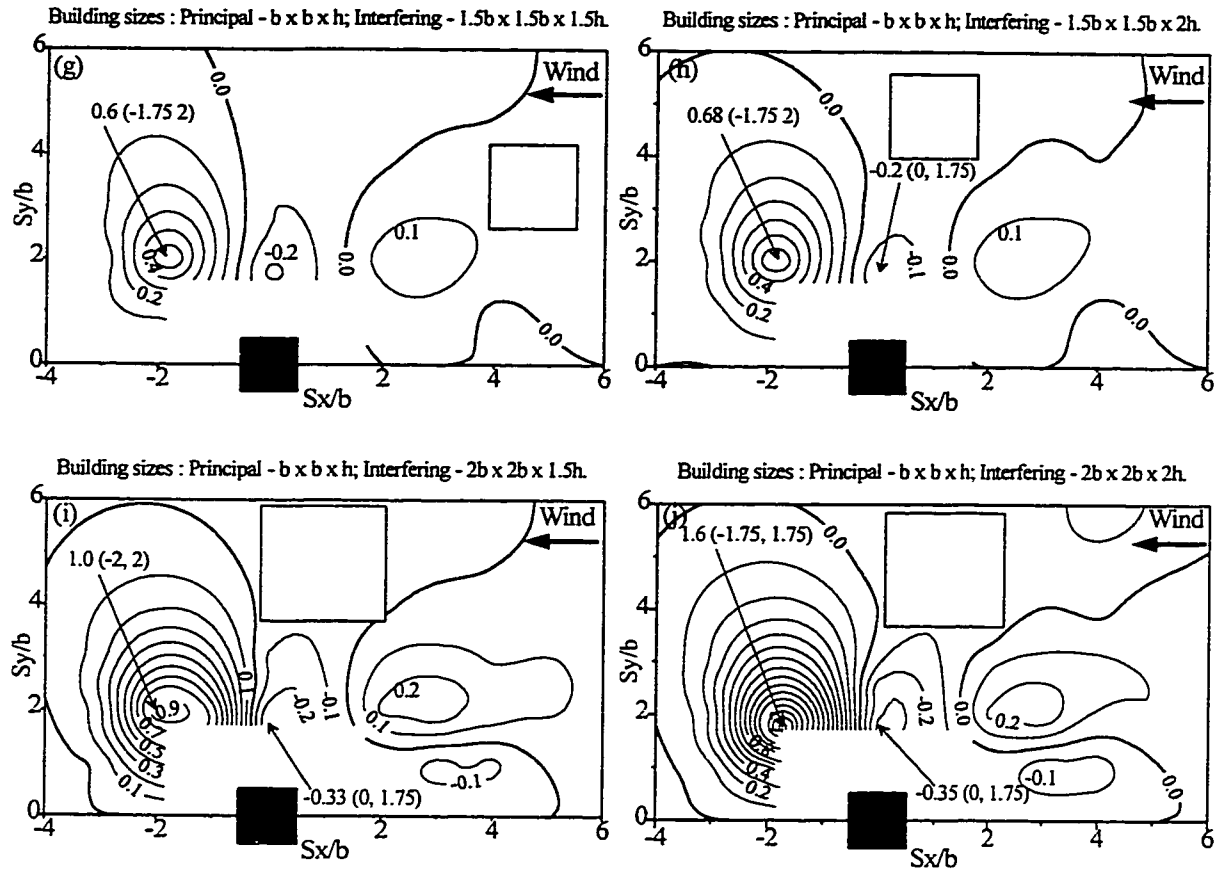

Figure 7.14 *(...Continued)* Effect of interfering building size on mean lift coefficient.

7.2.3 Fluctuating drag

Fluctuating drag increases with the size of the interfering building. Figure 7.15 shows the effect of interfering building size on fluctuating drag ($\widetilde{C}_d$) Interference Factors. The thick contour line with IF = 1.0 represents the "no interference case" or, in other words, the isolated building situation. Fluctuating drag for an isolated building is 0.25.

Figures 7.15(a) to 7.15(d) show the effect of increasing the foot-print size of the interfering building on the $\widetilde{C}_d$ of the principal building. Clearly, $\widetilde{C}_d$ increases with the foot-print size of the interfering building since the size of the vortices shed from the

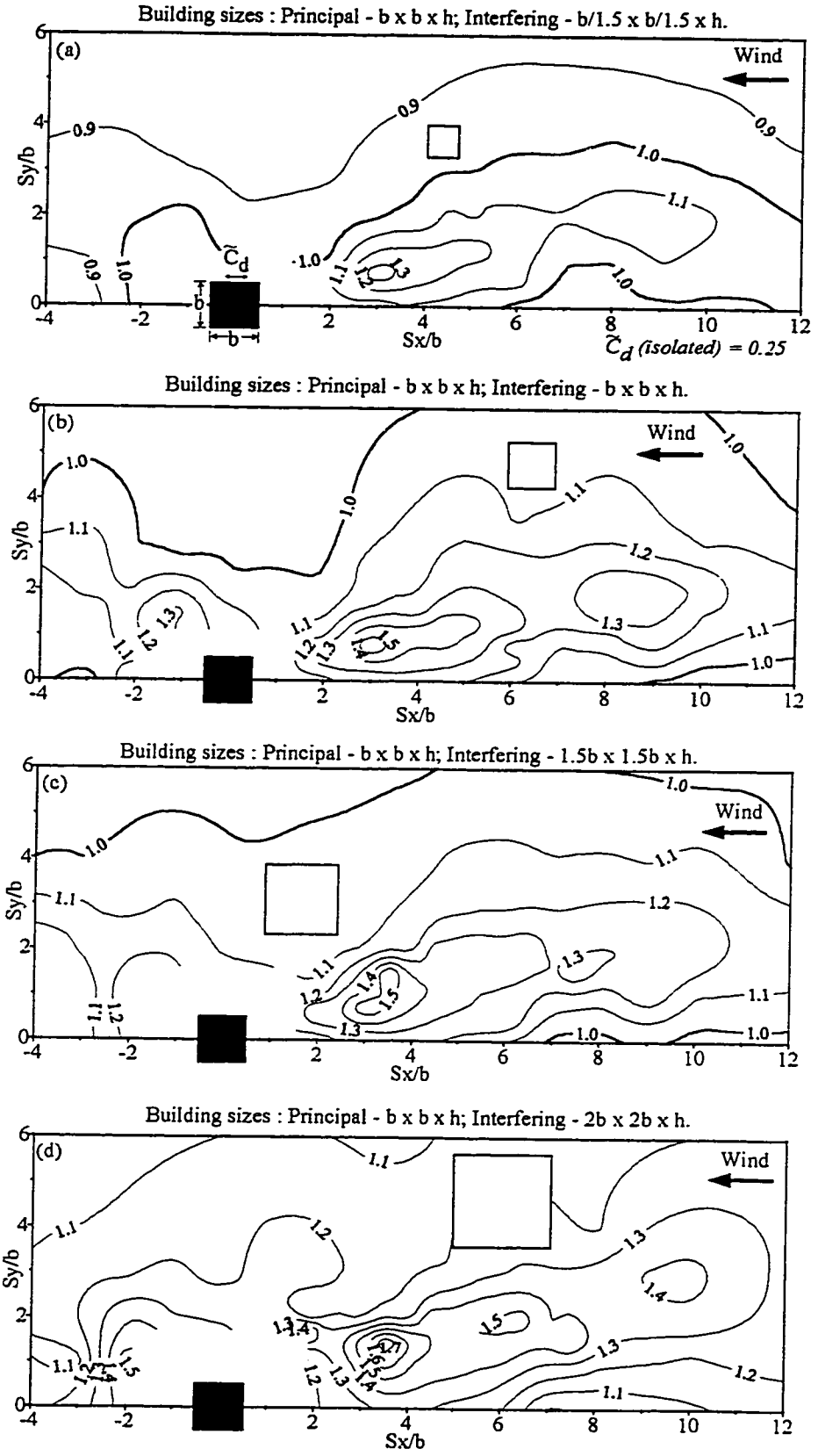

Figure 7.15 Effect of interfering building size on fluctuating drag IF *(Continued...)*

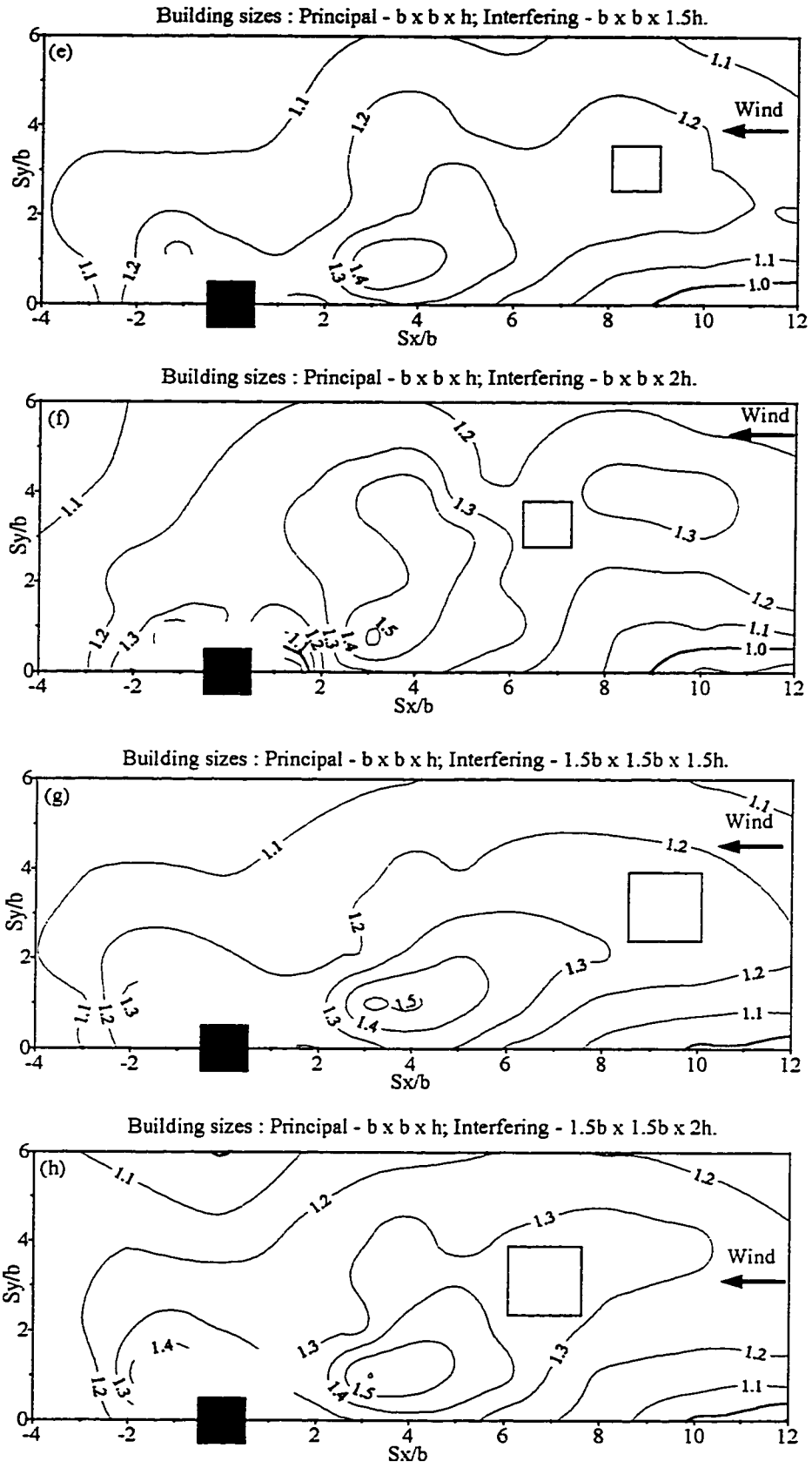

Figure 7.15 *(...Continued)* Effect of interfering building size on fluctuating drag IF.

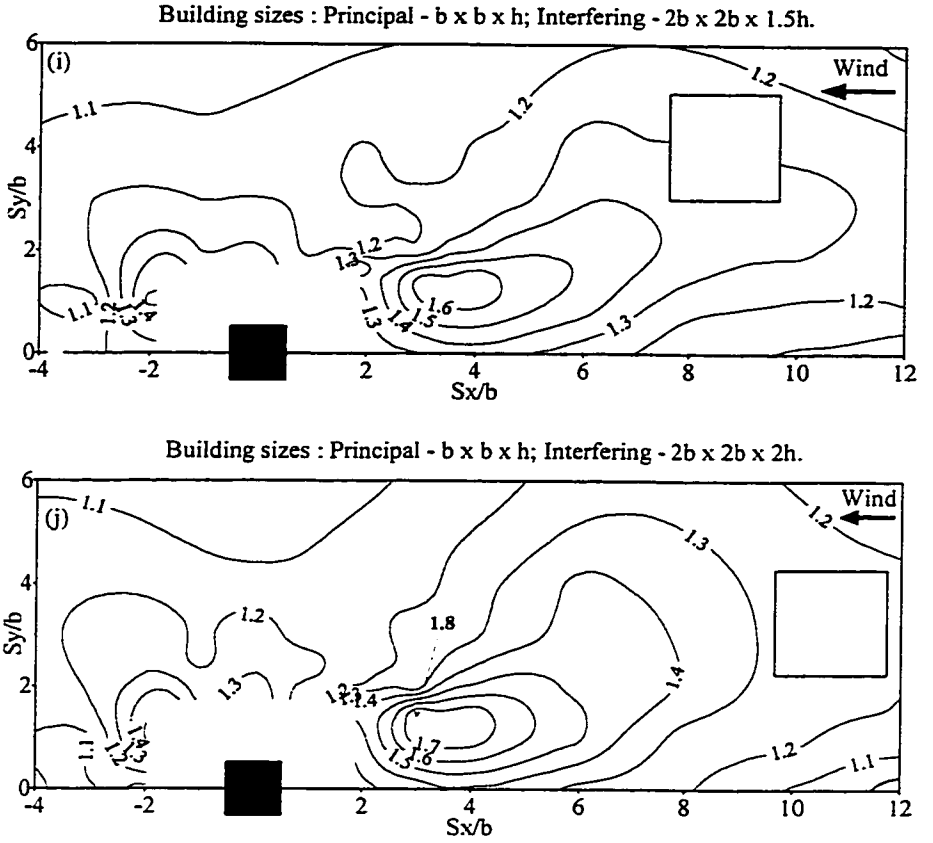

Figure 7.15 *(...Continued)* Effect of interfering building size on fluctuating drag IF.

interfering building increase with its width. Large size vortices generate higher fluctuating velocity in the wake, responsible for high fluctuating drag. Figure 7.15(a) shows that a smaller interfering building does not have any appreciable effect on the principal building, since the maximum increase in the fluctuating drag is 30% (IF = 1.3) over a small region upstream. Considering an increase over 30% to be significant, a high *fluctuating drag belt* can be identified upstream, having a thickness equal to the width of the interfering building, extending up to 10b upstream and inclined at an angle of about 30° to the wind direction, where $\widetilde{C}_d$ increases from 30% to 80%. The inclination is in keeping with the earlier observation that high $\widetilde{C}_d$ is registered when the downstream building is near the edge of the

wake of the upstream interfering building, rather than within the wake itself. From Figures 7.15(a) to 7.15(d), it can be concluded that increases in $\widetilde{C}_d$ of greater than 50% are registered when the interfering building is located upstream between Sx = 3b to 4.5b and Sy = 0.5b to 1.5b. An increase in $\widetilde{C}_d$ of 70% is obtained when a building double the width of the downstream building is located at Sx = 3.5b and Sy = 1.5b. Small patches of increase in $\widetilde{C}_d$ are also visible at close spacings downstream within an area bounded by Sx = -b to -2.5b and Sy = 0 to 2b resulting in increases in $\widetilde{C}_d$ of 30% to 50% (see Figures 7.15(b) and 7.15(d).

Figures 7.15(b), 7.15(e) and 7.15(f) show the effect of increasing the interfering building height on the fluctuating drag of the principal building. The IF magnitude remains more or less unaffected, however, a noteworthy observation is the increase in the size of the high IF contour bubbles in the lateral direction with increasing height of the interfering building. A probable reason for this is the two-dimensionality of the flow. With increasing height of the interfering building, its behaviour tends to that of a two-dimensional, line-like structure. The contribution to the wake due to the down-wash from the top of the interfering building reduces with increasing height and hence, for taller buildings, the wake is not disturbed much by the down-flow. Thus, the wake of a taller building is better organized than a smaller building and hence the larger extent of high fluctuating drag. There is a small increase (up to 30%) in $\widetilde{C}_d$ for close downstream locations of the interfering building (see Figures 7.15(e) and 7.15(f)), not very different from Figure 7.15(b), the two identical buildings case.

The effect of increasing both the plan area and height of the interfering building is to increase the fluctuating drag on the principal building as shown in Figures 7.15(g) to

7.15(j). On doubling the size of the interfering building, the fluctuating drag on the principal building increases by 80% at Sx = 3b and Sy = 1.5b (see Figure 7.15(j)). There is a significant increase in $\widetilde{C}_d$ for close downstream (Sx ≤ 2.5b) as well as close side-ways (Sy ≤ 2b) locations with increases of up to 40% in $\widetilde{C}_d$, as shown in Figures 7.15(h) to 7.15(j).

7.2.4 Fluctuating lift

Figure 7.16 shows the effect of interfering building size on fluctuating lift ($\widetilde{C}_l$) Interference Factors. The thick contour line with IF = 1.0 represents the isolated building situation. Fluctuating lift coefficient for an isolated building is 0.35.

Figures 7.16(a) to 7.16(d) show the effect of increasing the foot-print size of the interfering building on $\widetilde{C}_l$ of the principal building. Unlike $\widetilde{C}_d$ which increases steadily with the foot-print size of the interfering building, $\widetilde{C}_l$ actually decreases. The decrease in fluctuating lift with increasing size of the interfering building has also been reported by Taniike (1992). The smallest increase in $\widetilde{C}_l$ is for the interfering building smaller than the principal building (Figure 7.16(a)), maximum increase is registered when both the buildings are similar in size. The increase then tapers down as the width of the interfering building increases and falls to the small building levels (Figure 7.16(a)) when the width of the interfering building is doubled (Figure 7.16(d)).

Figures 7.16(b), 7.16(e) and 7.16(f) show the effect of increasing the interfering building height on the fluctuating lift of the principal building. IF decreases a bit for the two taller interfering buildings (Figures 7.16(e) and 7.16(f)), but the trend and extent of interference remains more or less unaltered.

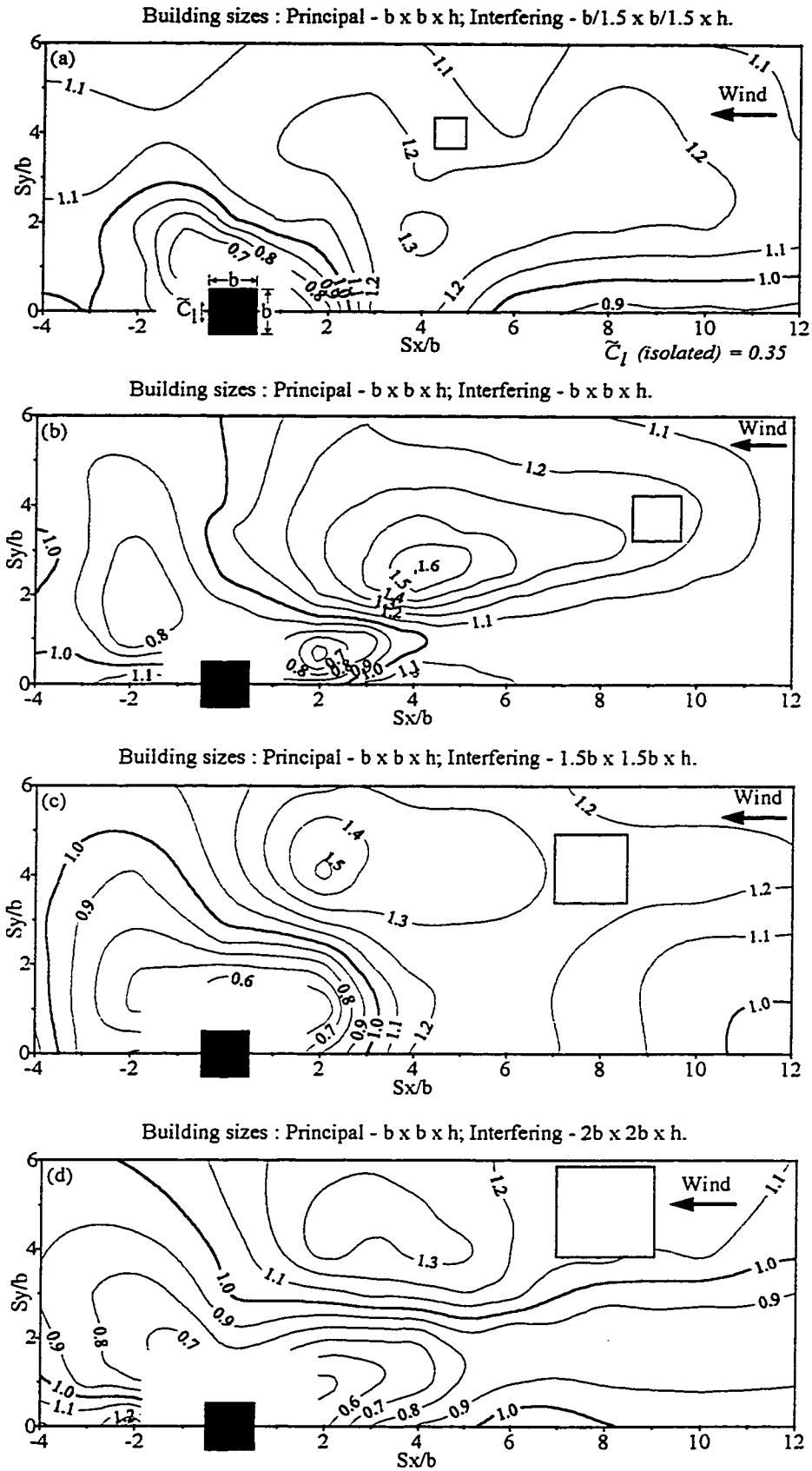

Figure 7.16 Effect of interfering building size on fluctuating lift IF *(Continued...)*

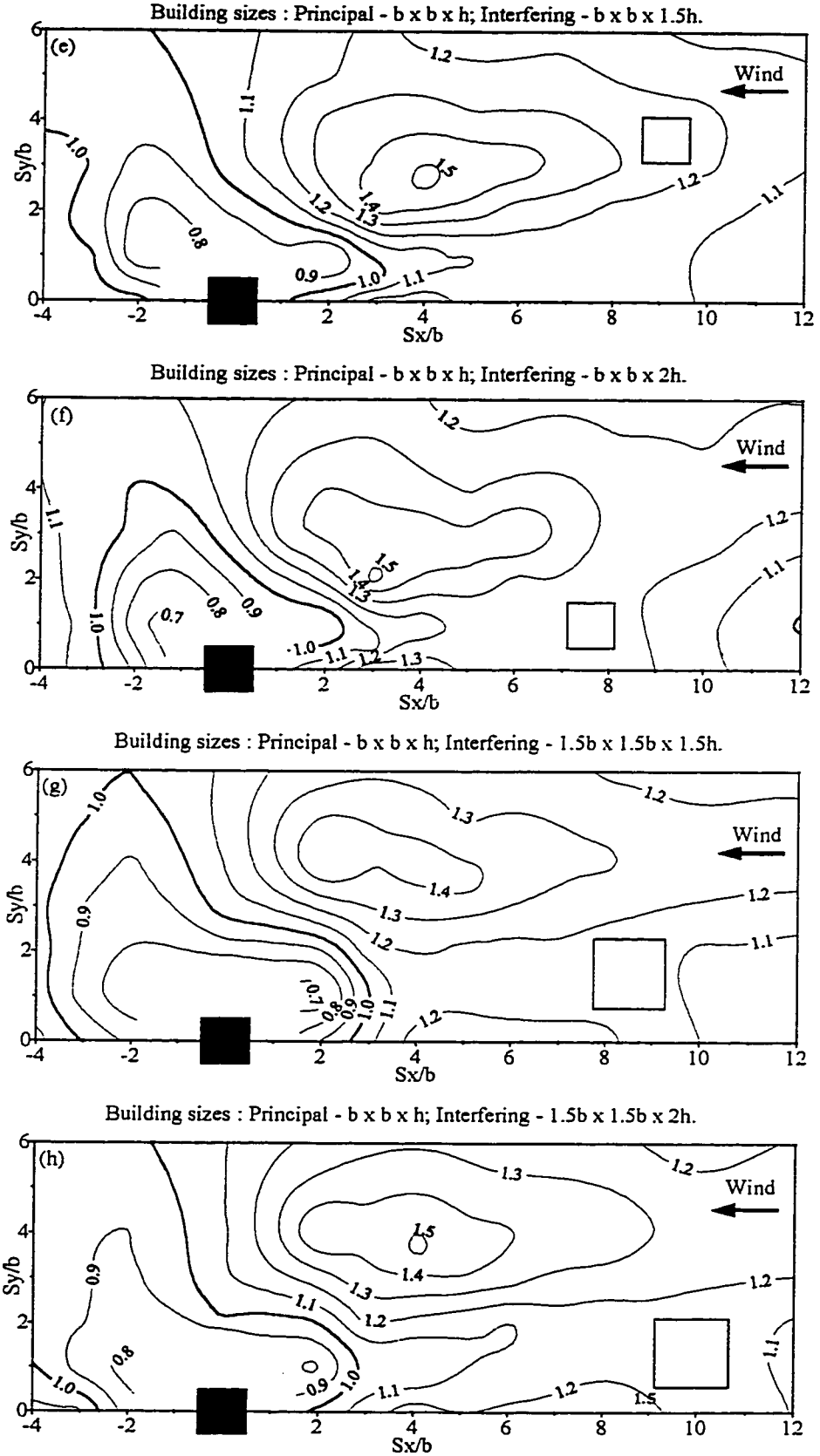

Figure 7.16 *(Continued...)* Effect of interfering building size on fluctuating lift IF.

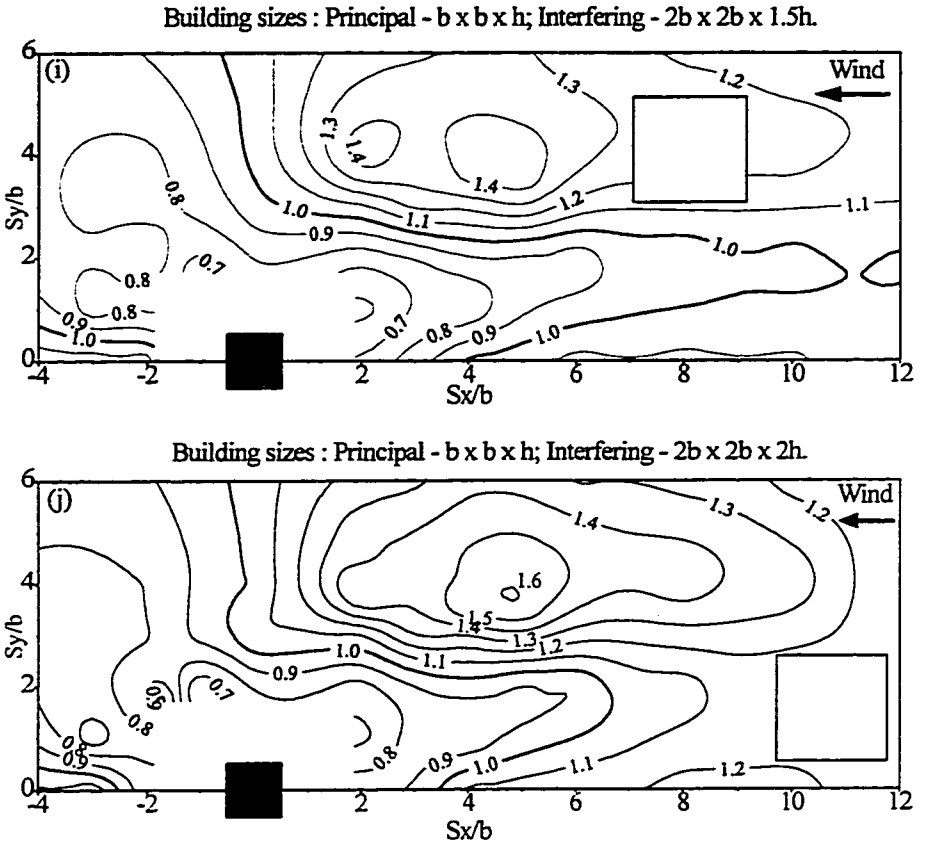

Figure 7.16 *(Continued...)* Effect of interfering building size on fluctuating lift IF.

On increasing both the width and height of the interfering building (Figures 7.16(g) to 7.16(j)), IF remains generally lower than the "datum case" (Figure 7.16(b)), except for the interfering building double the size of the principal building (Figure 7.16(j)), where the increases in $\widetilde{C}_l$ are similar to the "datum case". However, a shift in the extent of interference in the lateral direction, up to Sy = 6b, is clearly discernible.

From the above discussion and an analysis of the data, three zones of interference can be identified:

(a) *Proximity zone* close to the principal building, where $\widetilde{C}_l$ decreases significantly. In this region, the principal building is close enough to the interfering building to destroy its vortex shedding mechanism, resulting in low fluctuating lift on the principal building. This

zone extends between Sx = -2b to 1.75b and Sy = 0 to 2b, where $\tilde{C}_l$ decreases by 30% to 50%, depending on the size of the interfering building.

(b) *Interaction zone* : This is the upstream region between Sx = 1.5b to 9b and Sy = 2b to 6b. When the interfering building is located in this region, the principal building is greatly influenced by its wake, increasing the fluctuating lift on the principal building by 30% to 60%, depending upon the size of the interfering building.

(c) *Passive zone* : This is the remaining region where the interfering building has little or no effect on the principal building. In this region, the principal building is safely removed from the wake of the interfering building. It can also be termed as the isolated building condition.

7.2.5 Effects of interfering building size - overall situation

The effects of interfering building size were presented and discussed in detail in this chapter. From a design perspective, an overall scenario presenting the effects of interfering building sizes on wind interference is desired. Therefore, the individual results for the ten interfering building sizes are integrated and presented as general guidelines. Figures 7.17 and 7.18 present the overall effect of interfering building size on mean and fluctuating loads due to interference. These effects are compared with the interference effects for the datum case (two similar buildings in open exposure with a 0° wind direction) as percentage increase or decrease in the forces relative to the datum case (see Figure 6.8). Three scenarios are presented, viz., the effect of increasing the interfering building i) width, b, ii) height, h and iii) both width and height. Judicious approximations have been made in order to keep the figures simple while retaining the basic, critical information. In Figure 7.18

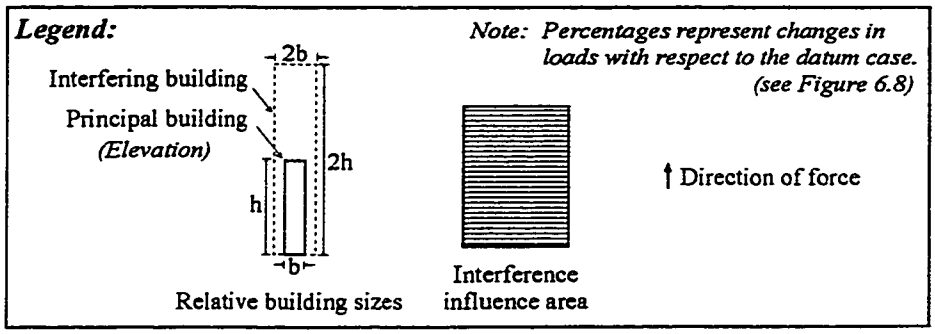

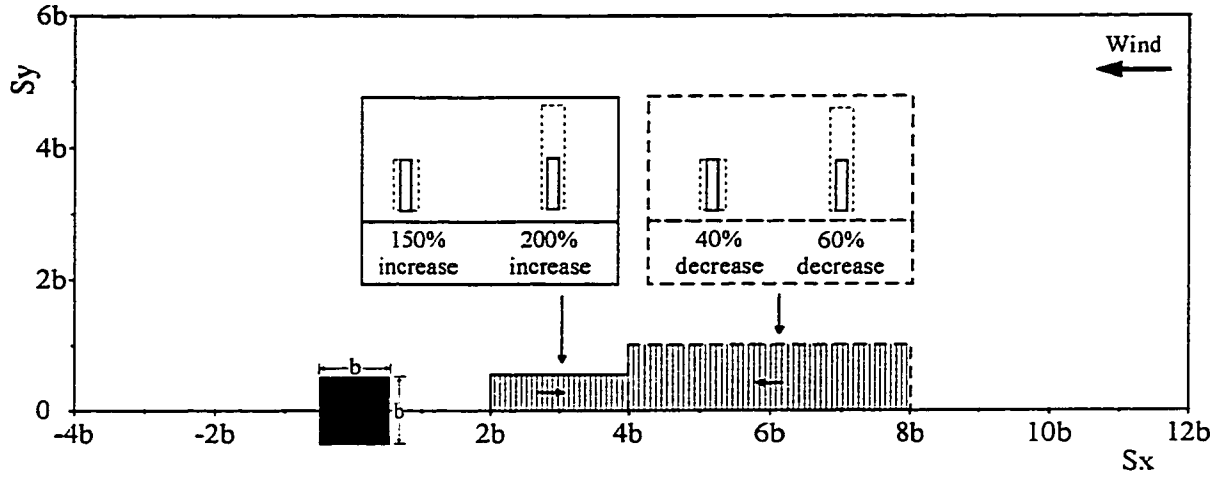

(a) Mean drag

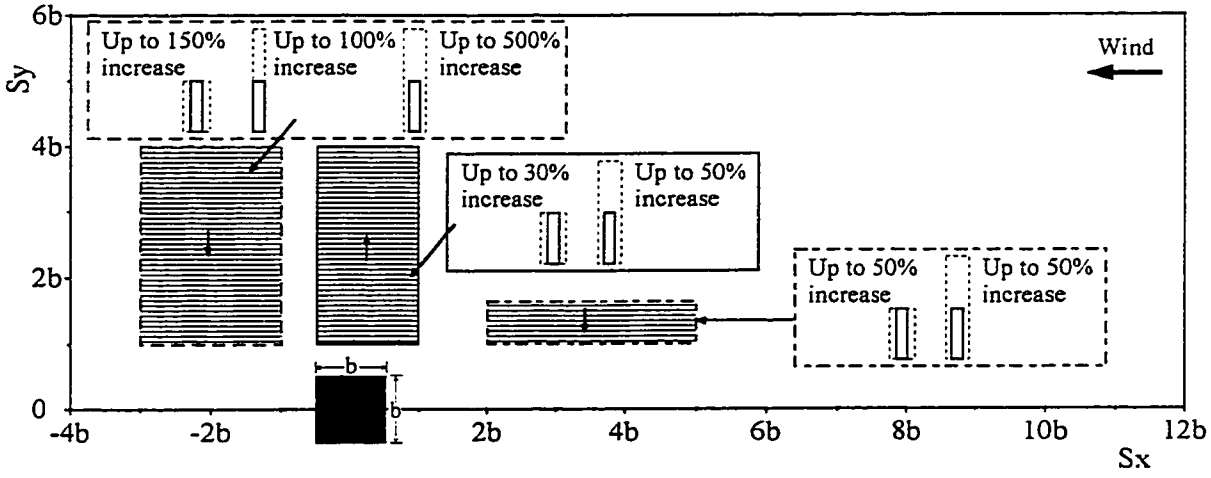

(b) Mean lift

Figure 7.17 Size Influence Grids - Effect of interfering building size on mean loads

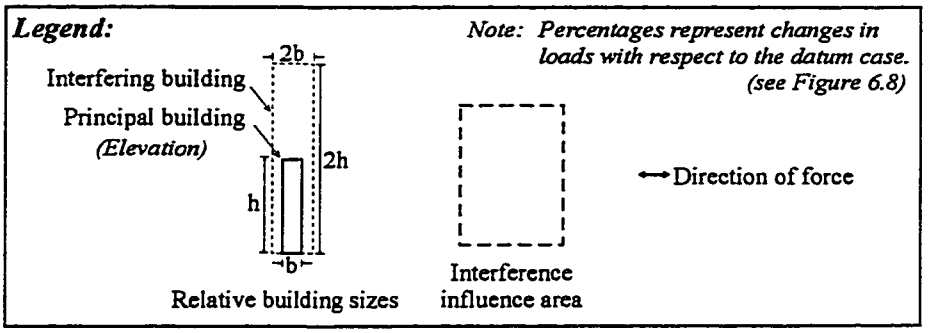

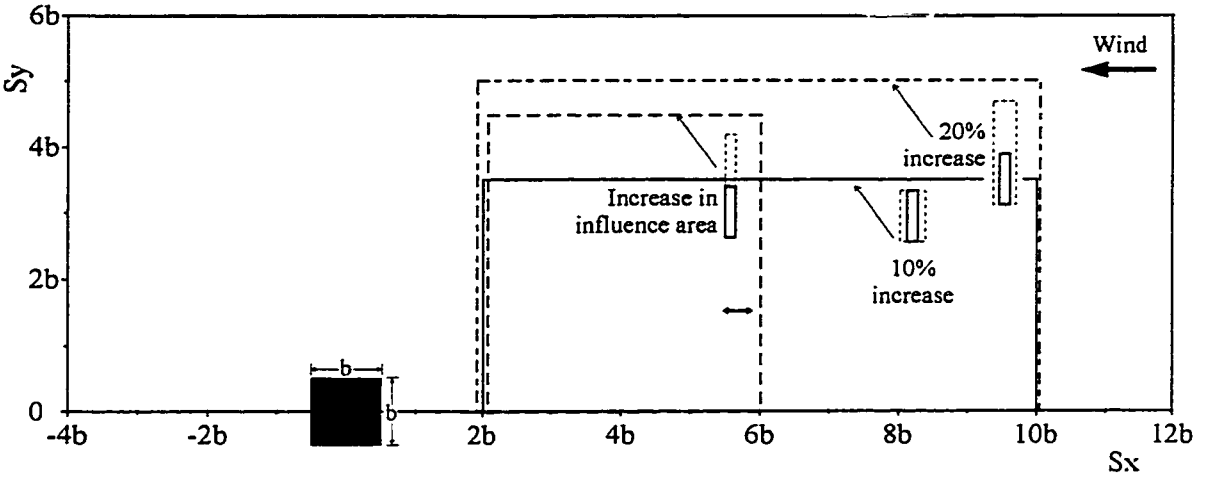

(a) Fluctuating drag

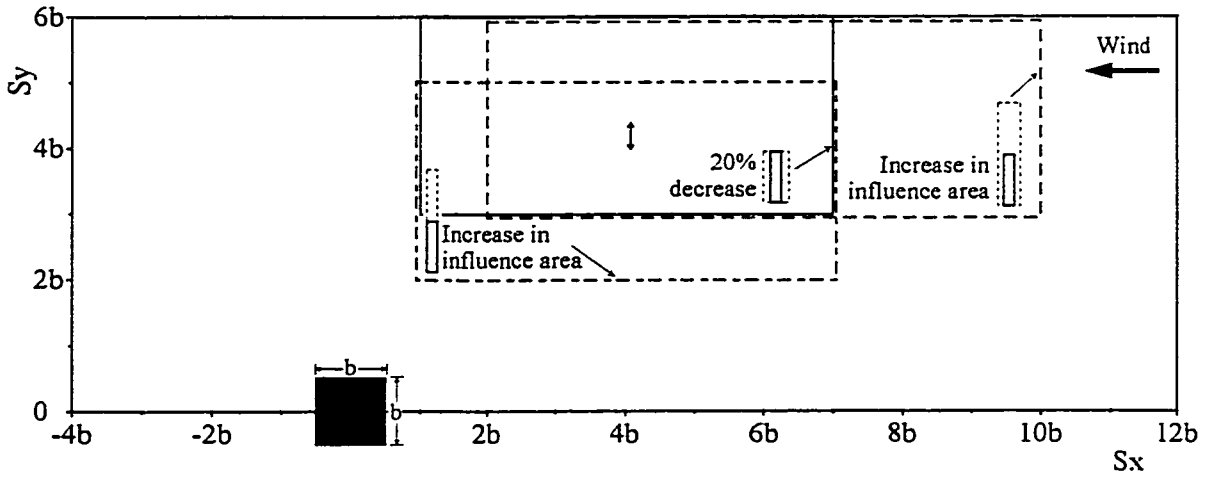

(a) Fluctuating lift

Figure 7.18 Size Influence Grids - Effect of interfering building size on fluctuating loads

the term "increase in influence area" implies an increase in the extent of interference with no increase in loads. A cursory glance at all the figures reveals that a larger interfering building width has more significant effects, both in terms of magnitude and extent of interference, than a larger height. These figures can be used for obtaining a quick and reasonable estimate of the effect of interfering building size on wind loads on a building.

7.3 Effects Of Upstream Exposure

There has been no comprehensive study on the effect of upstream exposure or turbulence intensity on wind-induced interference effects. Most previous studies have concentrated on the open exposure, with the legitimate premise that the worst interference effects would be for the open exposure, owing mainly to a low turbulence intensity in the approach flow. However, in absence of results that take into account a wider range of upstream exposures, general and concrete trends cannot be established. Incorporating additional exposures would indeed increase the experimental effort, but the wealth of information and data generated would be of immense assistance in explaining, with a greater degree of confidence, the effect of turbulence in approach flow on interference effects.

As explained in chapter 3, three upstream exposures are used. Based on Figure 3.1, their properties are listed in Table 7.6. These experiments are conducted for two similar interfering buildings and a 0° incident wind direction, normal to a face of the building. It is believed that results for these basic arrangements will provide a good idea for other configurations involving interfering buildings of different sizes and various wind directions.

Table 7.6 Properties of the three upstream exposures

Exposure	*Power law exponent, α*	*Turbulence intensity, I_v* (%)*
Open	0.15	7
Suburban	0.25	13
Urban	0.36	25

* *At building height*

7.3.1 Mean drag

Figure 7.19 shows the effect of upstream exposure on mean drag ($\overline{C}_d$) Interference Factors (IF). The values of $\overline{C}_d$ for isolated building are 1.30, 1.15 and 1.02 for open, suburban and urban exposure, respectively. The open exposure shows the most severe interference effects, especially with regards to shielding. For example, when a building is placed in front of the principal building at a centre-to centre distance of 11b upstream, $\overline{C}_d$ on the principal building is reduced by 28% (IF = 0.72), 22% (IF = 0.78) and 12% (IF = 0.88) for open, suburban and urban exposure, respectively. Figure 7.19(c) shows that IF remains near 1.0 over a large region, indicating the minimal effect of the interfering building on $\overline{C}_d$ of the principal building for an urban exposure. On a closer analysis, the IF = 0.9 contour for open terrain (Figure 7.19(a)), that represents a $\overline{C}_d$ value of 0.9 x 1.30 = 1.17, is close to an isolated building $\overline{C}_d$ of 1.15 in suburban terrain, and the IF = 0.8 (or $\overline{C}_d$ = 1.04) contour in the open exposure is similar to that of an isolated building $\overline{C}_d$ of 1.02 in an urban exposure. It can thus be inferred that, in general, the responses with interference excitation in a low turbulence flow are almost similar to those of an isolated building in a turbulent flow.

Based on a thorough analysis of Figure 7.19, *Exposure Influence Grids* for mean drag have been drawn up, showing the change in IF due to suburban and urban exposures

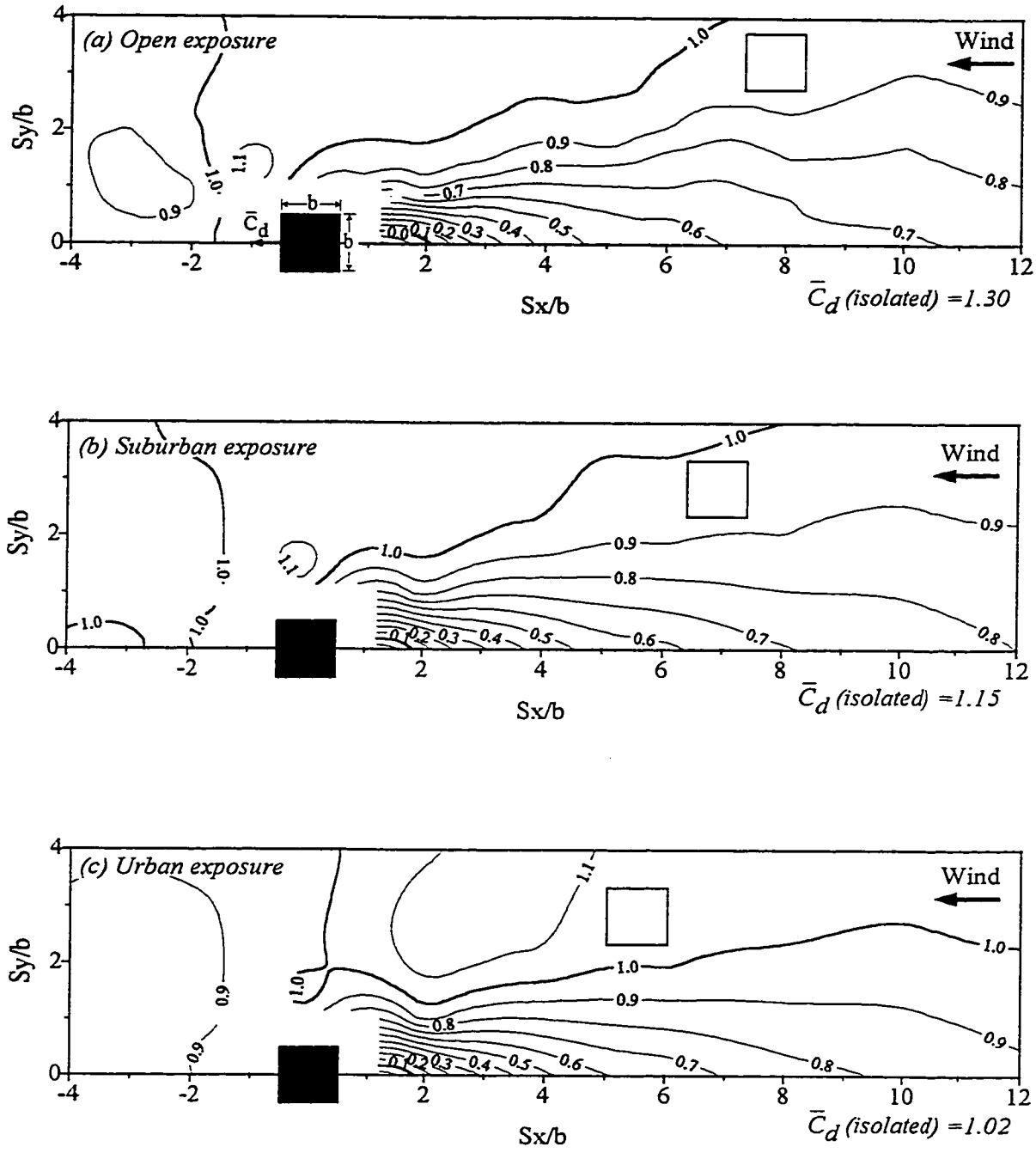

Figure 7.19 Effect of upstream exposure on mean drag IF.

relative to the open exposure (the datum case). Figure 7.20 shows these exposure influence grids for mean drag IF. Figure 7.20(a) shows the IF contours for open exposure and Figures 7.20(b) and 7.20(c) show the approximate percentage change in IF for suburban and urban terrain, respectively. For upstream locations of the interfering building, an increase in IF implies reduction in shielding relative to shielding in the open exposure. Thus, an interfering building in urban exposure offers minimum shielding to the principal building. The most dramatic increases are for close upstream locations (Sx < 2.5b) where increases in IF of up to 50% for suburban exposure and up to 70% for the urban exposure are registered. This increase is welcome, since it signifies a reduction in suction that is rather high for close spacings in the open exposure. Thus it can be concluded that on increasing the turbulence intensity in the approach flow, both shielding and suction due to interference are reduced by various degrees, depending upon the location of the interfering building.

7.3.2 Mean lift

Figure 7.21 shows the effect of upstream exposure on mean lift coefficient ($\overline{C_l}$). Interference effects on mean lift are generally characterized by high suctions due to an interfering building located to a side of the principal building as also by vast areas around the principal buildings where the interfering building has no effect on it. As in the case of mean drag, adding turbulence to the approach flow works to reduce the mean lift due to interference. Suctions are reduced by half on moving from open to suburban and urban exposures, and the extent of both positive and negative $\overline{C_l}$ is reduced, with large areas of zero $\overline{C_l}$ (isolated building case) around the principal building. It is clear from Figure 7.21 that from the point of view of $\overline{C_l}$, interference effects are almost insignificant for suburban

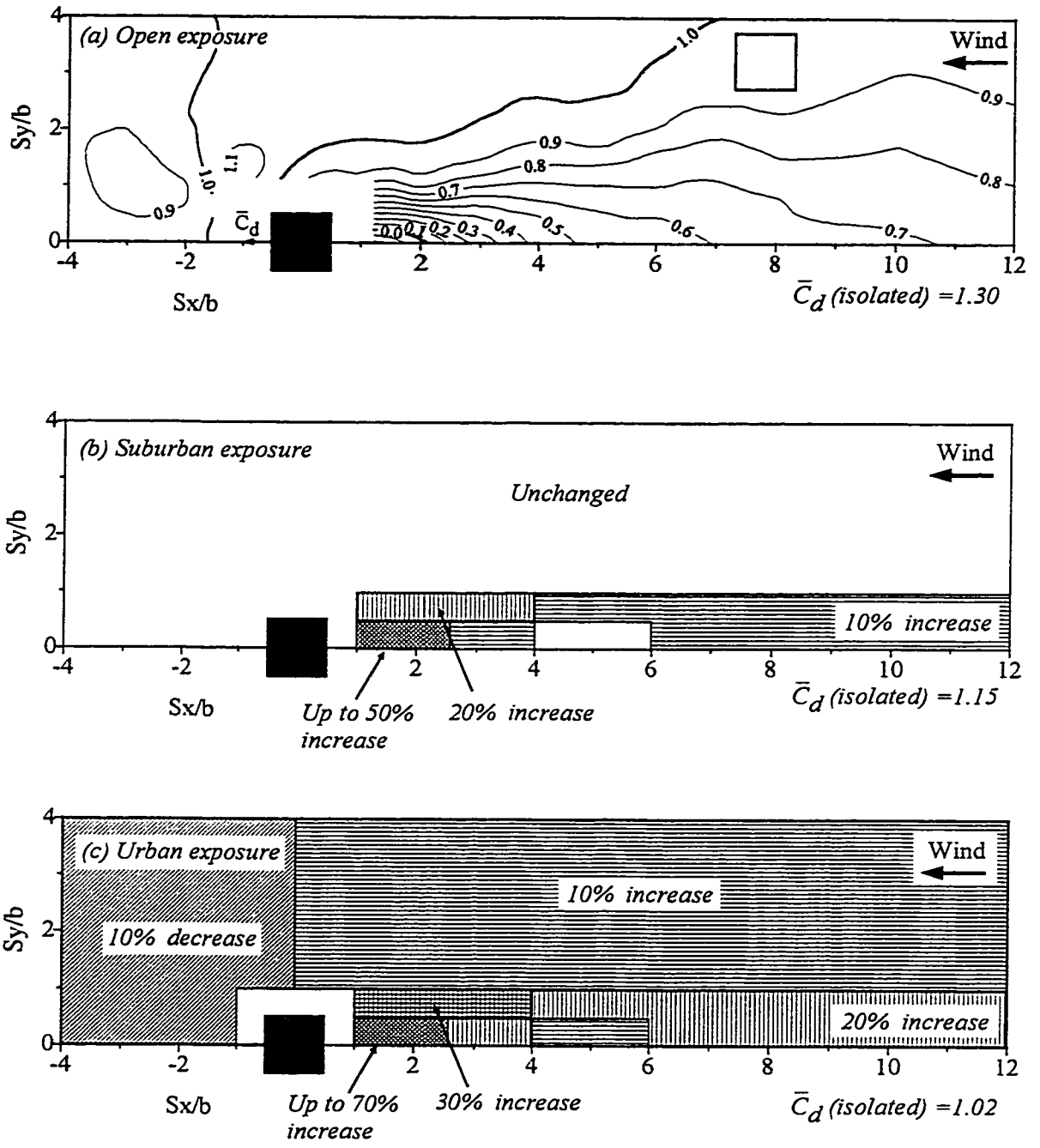

Figure 7.20 Exposure Influence Grids - Changes in mean drag IF in suburban and urban exposures vis-a-vis the open exposure.

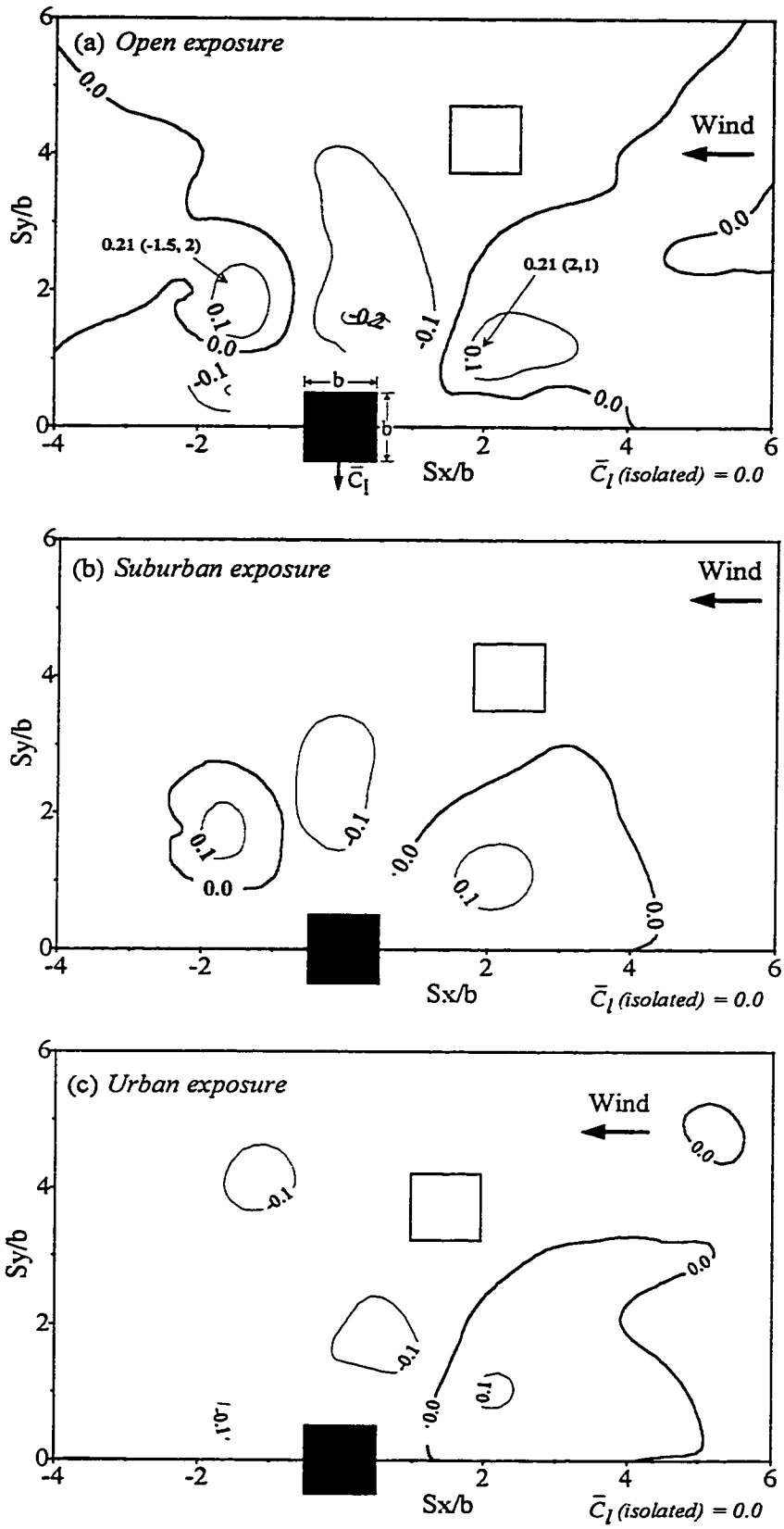

Figure 7.21 Effect of upstream exposure on mean lift coefficient.

and urban exposures and can safely be neglected for a turbulence intensity greater than 13% (see Table 7.6).

7.3.3 Fluctuating drag

Figure 7.22 shows the effect of upstream exposure on fluctuating drag ($\widetilde{C}_d$) Interference Factors (IF). The values of $\widetilde{C}_d$ for isolated building are 0.25, 0.20 and 0.16 for open, suburban and urban exposure, respectively. The maximum IFs are obtained for the open exposure and the minimum for the urban exposure, however, the trend of the contours remains similar for all three exposures. The fluctuating drag is not significantly altered in the urban exposure with a highly turbulent flow (turbulence intensity at building height = 25%), even when the principal building is positioned near the edge of the wake of the upstream building. This is clearly evident from the values of IF which are near unity over a wide region, representing the isolated building situation (see Figure 7.22(c)). Such a behaviour has also been reported by Taniike (1991) with turbulence intensity of about 18% at two-thirds of the building height, suggesting that the dynamic response of the principal building under a highly turbulent flow is independent of the mutual interference effect between twin tall buildings.

An analysis of the results reveals a uniform decrease in IF of about 10% and 20% for suburban and urban exposures respectively, as compared to the open exposure IF values.

7.3.4 Fluctuating lift

The effect of turbulence in approach flow on fluctuating lift ($\widetilde{C}_l$) Interference Factors (IF) follows a pattern similar to that of fluctuating drag, except that the reductions in IF for $\widetilde{C}_l$

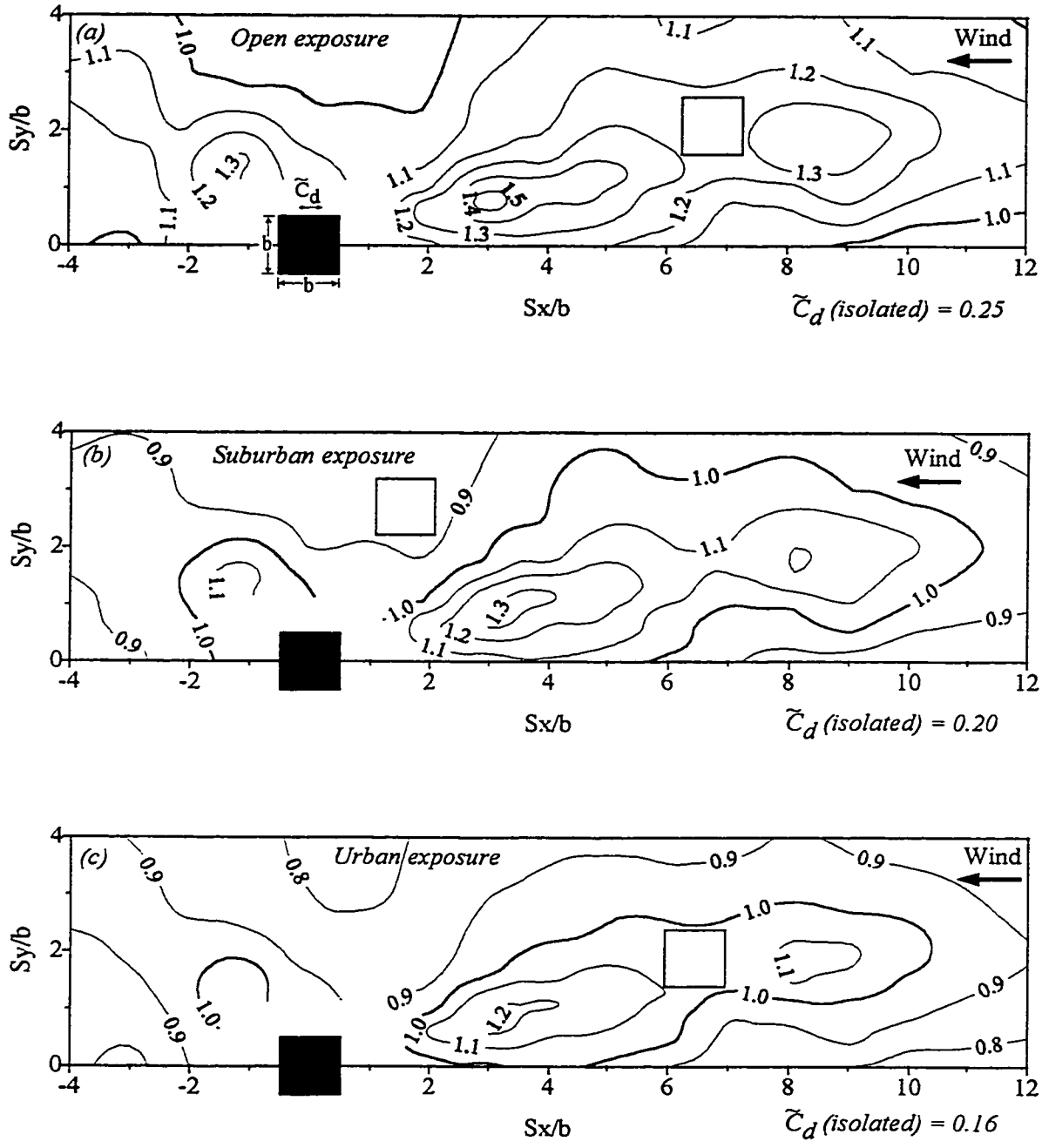

Figure 7.22 Effect of upstream exposure on fluctuating drag IF.

with increase in flow turbulence are slightly higher. Figure 7.23 shows the effect of upstream exposure on fluctuating lift IF. The values of $\widetilde{C}_l$ for isolated building are 0.35, 0.30 and 0.27 for open, suburban and urban exposure, respectively. As in the case of fluctuating drag, the maximum IFs are obtained for the open exposure and the minimum for the urban exposure. Moreover, the fluctuating lift is not significantly altered in the urban exposure, even when the principal building is positioned near the edge of the wake of the upstream building.

Based on an analysis of the results for fluctuating lift IFs, it can be concluded that in general, fluctuating lift IFs decrease by about 10% and 20% for suburban and urban exposures respectively, as compared to the open exposure IF values. There are small patches, especially around the wake region and at close locations downstream, where the decreases are significantly higher. These are: for suburban exposure, areas bounded by Sx = 2.5b to 5.5b and Sy = 2b to 3b upstream (wake region), with a reduction of about 20% in open exposure IFs and downstream areas within Sx = -3b to -b and Sy = 0 to 2b, with decreases of about 30%; for urban exposure, the upstream wake region enclosed by Sx = 2.5b to 4b and Sy = 2b to 3b and a small downstream patch bounded by Sx = -3b to -b and Sy = 0 to b, reducing the open exposure IFs by about 30%.

7.3.5 Discussion

Reduction of mean and fluctuating IFs with increasing turbulence intensity of approach flow points to the disruptive effect of background turbulence on the coherent structure of the wake of the interfering building. Increased turbulence reduces the potential of the wake to cause interference excitation because of a weakening in vortex formation.

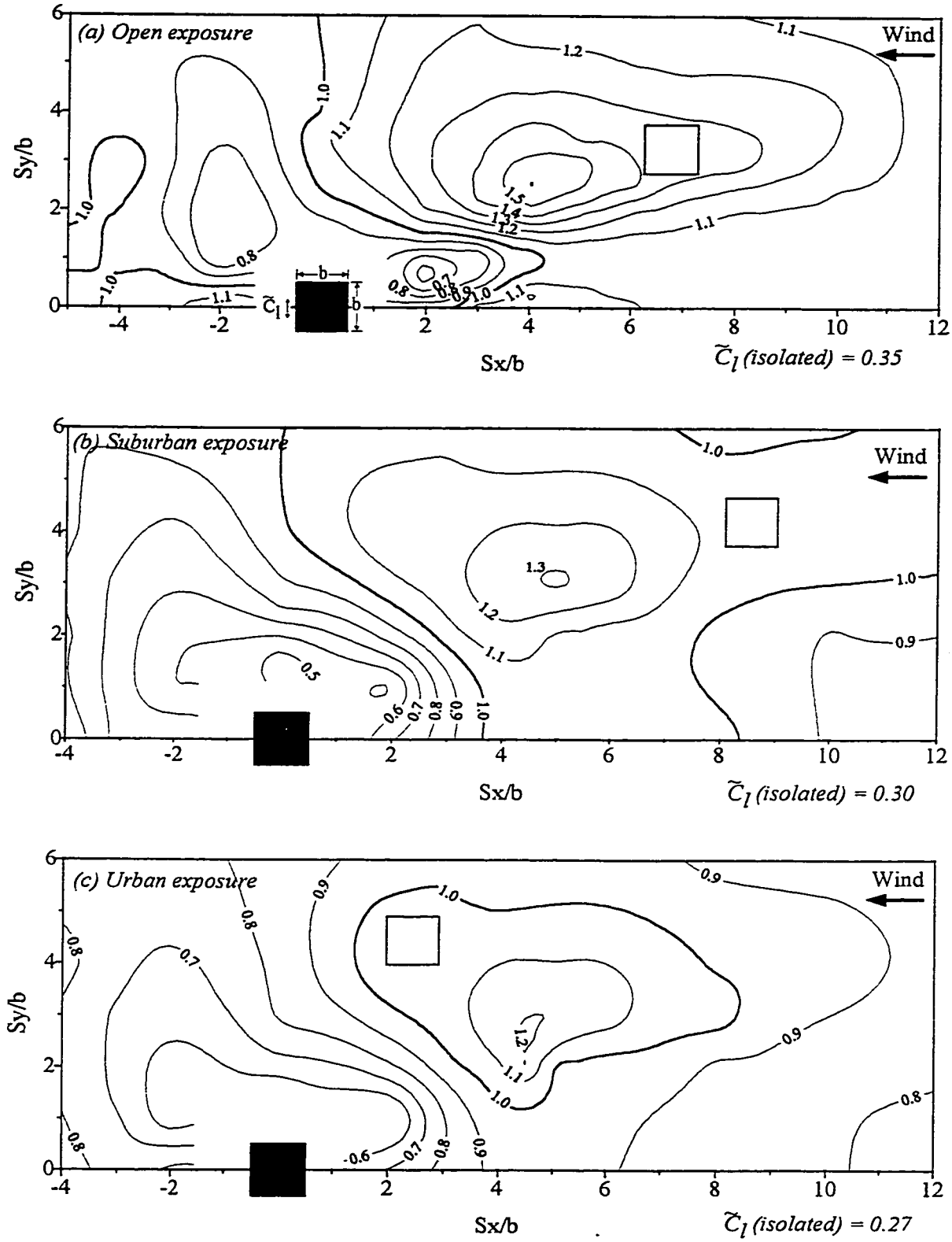

Figure 7.23 Effect of upstream exposure on fluctuating lift IF.

A low turbulence promotes a wake behind an interfering building with a high energy content. The high energy velocity fluctuations in the wake of an upstream interfering building excite the principal building, leading to high fluctuating loads on it. With higher turbulence in the approach flow, shear layers separating from the upstream interfering building grow, entraining the surrounding fluid, resulting in intermittent reattachment of the separated shear layers on to the sides of the principal building and a disruption of the periodic fluctuating velocity near the separation zone. This destroys the energy of the separated flow and leads to weaker vortices around the principal building, resulting in lower level of excitation of the principal building and lower fluctuating loads on it. Kareem (1987) describes the fluctuating flow field in the wake by means of a wake-oscillator model, whereby addition of turbulence in the approach flow is analogous to the addition of damping in the wake-oscillator model, thereby dampening the wake fluctuations which are responsible for exciting the downstream building.

The additional turbulence in the wake, generated by the introduction of the interfering building in a turbulent flow, is unlikely because of the sufficiently high turbulence in the approach flow, as also pointed out by Bailey and Kwok (1985) and Taniike (1991). Thus it can be concluded that in a low turbulence flow, interference effects increase due to the increased turbulence created by the upstream building.

7.4 Effects of Immediate Surroundings

The previous section analyzed, in detail, the effect of upstream exposures on wind interference. One of the main observations was the decrease in interference effects with increasing turbulence intensity in approach flow. Thus, maximum interference effects are

registered for flows developing over a low turbulence open exposure; minimum interference is found highly turbulent urban exposure. The set-up has considered interference between two buildings, devoid of nearby structures, a somewhat idealized situation, though not altogether impossible. For, in a cityscape, several examples exist of twin buildings, removed from the central, multi-building downtown core of the city, like hotel towers near the airport, buildings adjoining the seaport or facing a park. Yet other cases involve the reduction in the number of interacting buildings due to demolition of one or more surrounding buildings. Such situations would be directly amenable to the recommendations of the present study. This is not to suggest the usefulness of the results to only a few, special cases, particularly in view of the recommendations of codes and standards world-wide based, generally, on a "single building" situation, hardly the real situation. Thus, the present study moves a step closer to reality, adding to the knowledge on wind effects on buildings and thereby paving the way for further research in this area.

Based on results presented previously, it is prudent to assume that increasing nearby buildings would not only increase shielding, i.e. decrease mean loads on a building, but would also decrease fluctuating loads. Thus, overall effects, to say the least, would be beneficial. To verify this assumption, further experiments are carried out to study the effects of immediate surroundings on wind-induced interference.

7.4.1 The city-centre model

Figure 7.24 shows the plan of a scale model of Montreal downtown used for evaluating the effects of immediate surroundings on interference between two buildings. The experimental set-up is similar to the one used in the datum case (chapter 6), except that

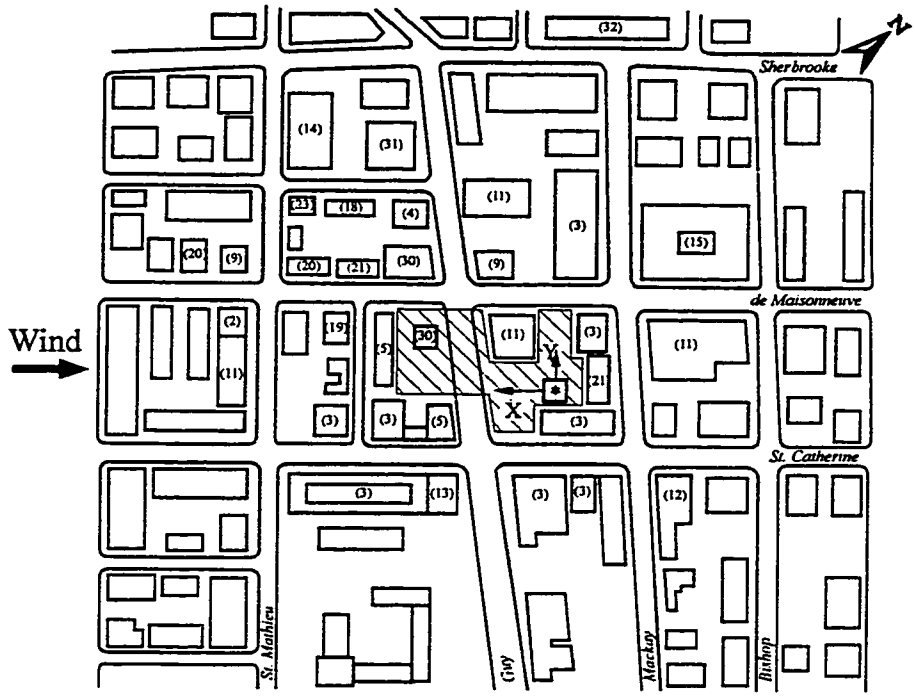

(a) City-centre1 scenario - interfering buildings in the middle.

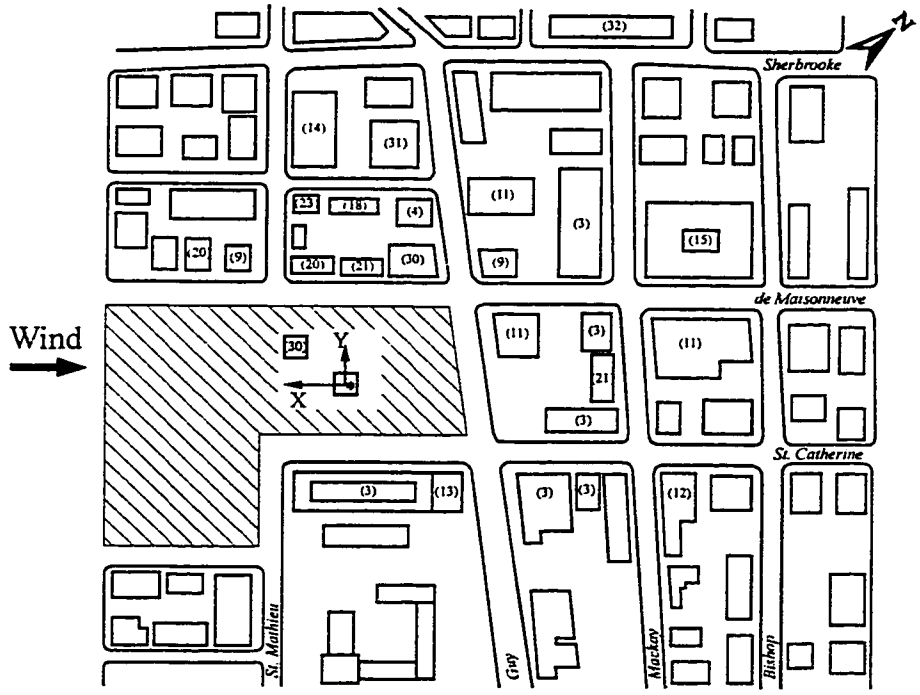

Legend: ▨ *Interference effects testing region.*
* *Origin at the centre of the principal building.*
(5) Number of storeys.

(b) City-centre2 scenario - interfering buildings in an open area.

Figure 7.24 Effects of immediate surroundings on interference - downtown Montreal.

the two interfering buildings now are situated within a city-centre and the flow develops over a suburban upstream exposure. Two scenarios are studied: i) City-centre1 involves the two buildings situated in the middle of the city-centre as shown by the hatched region in Figure 7.24(a) and, ii) City-centre2 includes three blocks of buildings that are cleared away to simulate an open area, like a park or a port as shown in Figure 7.24(b), with the two identical interfering buildings about 30 storeys tall, located within this hatched area. The heights of the surrounding buildings range, on an average, from 3 to 30 storeys, and are shown in parentheses in the figure.

The city-centre model is oriented in such a way that the wind approaches approximately from the south-west direction, the predominant wind direction for Montreal (see Table 7.4). The interfering buildings are arranged to account for the important and critical locations, mainly from the point-of-view of shielding, suction and increase in fluctuating loads. These locations have been identified from previous experimental results of this study. Thus, the two interfering buildings are arranged in tandem for mean drag, side-by-side for mean lift and in critical staggered locations that generate high fluctuating forces. The choice of locations was also limited by constraints imposed by the city-centre model arrangement.

7.4.2 Results

The experimental results shown in Table 7.7 compare the mean and fluctuating forces in the two city-centre situations with those in different upstream exposures, but without immediate surroundings. Interference effects, in general, reduce in the city-centre environment, but increase for a few and these values are italicized in the table. The force

coefficients for the principal building within the city centre, termed as the *isolated* building case, are also shown.

Table 7.7 Interference effects for two identical buildings within two city centre scenarios - comparisons with other exposures without immediate surroundings.

Location		*Mean drag IF*					*Mean lift coefficient*				
Sx/b	Sy/b	City[1]	City[2]	Urban	Sub-urban	Open	City[1]	City[2]	Urban	Sub-urban	Open
1.25	0.0	-0.09	-	-0.16	-0.18	-0.24					
1.5	0.0	-0.06	-0.15	-0.12	-0.13	-0.16			all		
4.0	0.0	0.38	0.41	0.47	0.43	0.44			near 0.0		
5.0	0.0	0.43	0.50	0.59	0.54	0.54					
0.0	1.5	***1.21***	1.12	1.04	1.14	1.00	0.00	-0.10	-0.10	-0.10	-0.20
0.0	2.0	1.10	1.08	0.98	1.08	1.03	0.00	-0.07	-0.10	-0.10	-0.20
1.5	1.5	***1.18***	0.90	0.98	0.94	0.95	0.00	0.12	0.00	0.10	0.00
2.0	1.0	0.90	0.81	0.95	0.86	0.84	0.00	0.16	0.10	0.20	0.20
-2.0	2.0	1.00	1.00	0.85	0.94	0.98	***0.10***	***0.10***	0.00	0.00	0.00
Isolated				$\overline{C}_d$					$\overline{C}_l$		
		0.80	*1.10*	*1.02*	*1.15*	*1.30*	*0.0*	*0.0*	*0.0*	*0.0*	*0.0*
		Fluctuating drag IF					*Fluctuating lift IF*				
1.5	0.0	0.85	0.90	0.95	1.01	1.17	0.84	0.60	0.64	0.57	0.95
4.0	0.0	1.05	1.00	1.02	1.09	1.25	0.91	1.00	0.92	1.06	1.15
0.0	1.5	1.05	1.08	0.92	0.98	1.13	0.94	***1.08***	0.53	0.45	0.83
0.0	2.0	***1.10***	0.92	0.83	0.89	1.02	***1.17***	0.92	0.65	0.61	0.94
1.5	1.5	***1.20***	0.88	0.87	0.93	1.07	***1.10***	0.81	0.59	0.61	0.94
2.0	1.0	1.00	1.00	0.93	1.00	1.15	0.91	0.80	0.44	0.48	0.64
3.5	1.0	***1.30***	***1.30***	1.20	1.31	1.45	-	0.93	0.89	0.98	0.91
4.0	2.0	0.88	0.91	1.04	1.05	1.20	1.00	***1.25***	1.06	1.17	1.48
-2.0	2.0	1.00	-	0.93	0.96	1.10	1.06	-	0.72	0.62	0.72
Isolated				$\widetilde{C}_d$					$\widetilde{C}_l$		
		0.14	*0.22*	*0.16*	*0.20*	*0.25*	*0.16*	*0.25*	*0.27*	*0.30*	*0.35*

[1] Suburban exposure, interfering buildings in the middle of the city centre (Figure 7.24(a))
[2] Suburban exposure, interfering buildings in an open area within the city centre (Figure 7.24(b))

The isolated building force coefficients reduce significantly. Note the sharp decrease in the isolated building mean drag coefficient (0.80) in the city-centre1 situation - a 20% and 40% decrease, respectively, compared with the urban and open exposure values. Isolated building values in the city-centre2 case replicate closely the suburban exposure

values. Based on the results of these experiments, the following general conclusions can be drawn:

- In general, interference effects for two buildings situated within a city-centre are minimal to none. However, for some close spacings between the interfering buildings interference effects increase by up to 30%.
- City-centre2 scenario produces interference effects that are similar to the suburban exposure.
- For close tandem locations, suctions reduce and shielding increases: both are beneficial effects.
- For close side-by-side locations, mean drag increases in both city centre scenarios.
- Mean lift remains close to zero (isolated building value) for city-centre1 but is similar to the suburban case for city-centre2.
- Fluctuating drag reduces in general, except for some close locations where the values are even higher than the open exposure values.

Thus overall, changing the immediate surroundings from open to city-centre is beneficial from the point-of-view of interference. However, an important observation is the close resemblance of the interference effects in the case of city-centre2 environment, that replicates an open park or a sea port, to the case of suburban exposure without immediate surroundings, which may be problematic in some cases from the point of view of fluctuating loads. It therefore follows, from the above observation, that if the interfering buildings are located on the edge of an open exposure like a low turbulence seascape, high interference effects should be expected even when the interfering buildings are surrounded by a dense array of buildings on three sides.

7.5 Shielding Effects - Modelling and Generalization

A proper evaluation of wind loads on sheltered buildings is of utmost importance not only for a correct estimation of wind loads, but also for accounting accurately air infiltration and ventilation rate estimates. Such a goal can only be realized by modelling carefully the effects of various parameters like building geometry, upstream exposure and building spacing on shielding. The results of such a parametric study can be used for developing wind load as well as infiltration estimates during preliminary design and planning stages (Farell and Sitheeq 1993). One of the main observations of the present detailed parametric study is the considerable shielding provided by an upstream interfering building to the downstream (principal) building. This shielding manifests itself in significant reductions in mean drag on the principal building placed in tandem to the upstream building, especially for normal (0°) winds.

Figure 6.8(a) in chapter 6 identifies the so-called *shielding belt* of thickness b, where b is the width of the principal building, extending 10b upstream of the interfering building, with shielding of 30% to 100%. Shielding increases with increasing size of the upstream building. This is shown in Figure 7.17(a) in terms of further reductions of 40% to 60% in the mean drag coefficient, depending on the size of the upstream building. The effect of upstream exposure or the turbulence intensity in the approach flow on mean drag is shown by means of Exposure Influence Grids in Figure 7.20. An increase in mean drag signifies a decrease in shielding. Thus, mean drag increases by 10% to 50% in the suburban exposure and 20% to 70% in the urban exposure, depending on the location of the upstream building.

In this study, the shielding effects data is modelled, empirically, taking into consideration the building geometry, building spacing and upstream exposure. Simple and

easy-to-use empirical equations are suggested for an accurate evaluation of the shielding effects of upstream buildings. Since shielding is a particular property of interference, the Interference Factors are now designated as Shielding Factors (SF). SF therefore represents the ratio of mean drag coefficient of the principal building when shielded by an upstream building to the mean drag coefficient of the principal building in unshielded condition.

English (1993) has suggested a third-order regression polynomial (see equation 2.3), based on data culled from various sources, to predict SF. The equation, while not indicating the limits of along-wind separation (Sx) and building sizes, seems to apply to a narrow range of Sx and only to two similar buildings. On applying the equation to a random sampling of literature data on which it is based, the results are far from persuasive. For example, for two 25mm x 25mm x 75mm building models spaced at clear separation of 6b, Sakamoto and Haniu (1988) suggest a SF of 0.56 based on experiments, as compared to a value of 0.40 calculated by the polynomial - an error of 40%. The polynomial fails completely in the suction zone, i.e. for narrow separations. At a separation of b, the calculated value of SF is 0.15, as compared to a value of -0.29 observed by Sakamoto and Haniu (1988). The main reason for the erroneous behaviour of the above polynomial, as pointed out in chapter 2, is its basis on literature results that span a broad range of testing techniques, flow conditions, building geometries and configuration.

Since the results of the present study are based on wind tunnel experiments, conducted in a uniform and systematic manner, under carefully controlled conditions, it is therefore expected that empirical modelling based on these results will yield better and more rational estimates of Shielding Factors.

7.5.1 Modelling of shielding effects

Shielding effects are modelled for a 0° incident wind angle since it gives the absolute maximum shielding for buildings in tandem (see Figure 7.1). The mean drag data for various interfering building geometries is taken from Figure 7.13 for open exposure. This comprises Interference Factor (IF) (same as SF) values for a range of tandem locations of the interfering building, i.e. for Sx = 1.25b to 14b and Sy = 0. Figure 7.25 shows the variation of SF with normalized along-wind spacing (Sx/b) between two interfering buildings, for ten interfering building sizes.

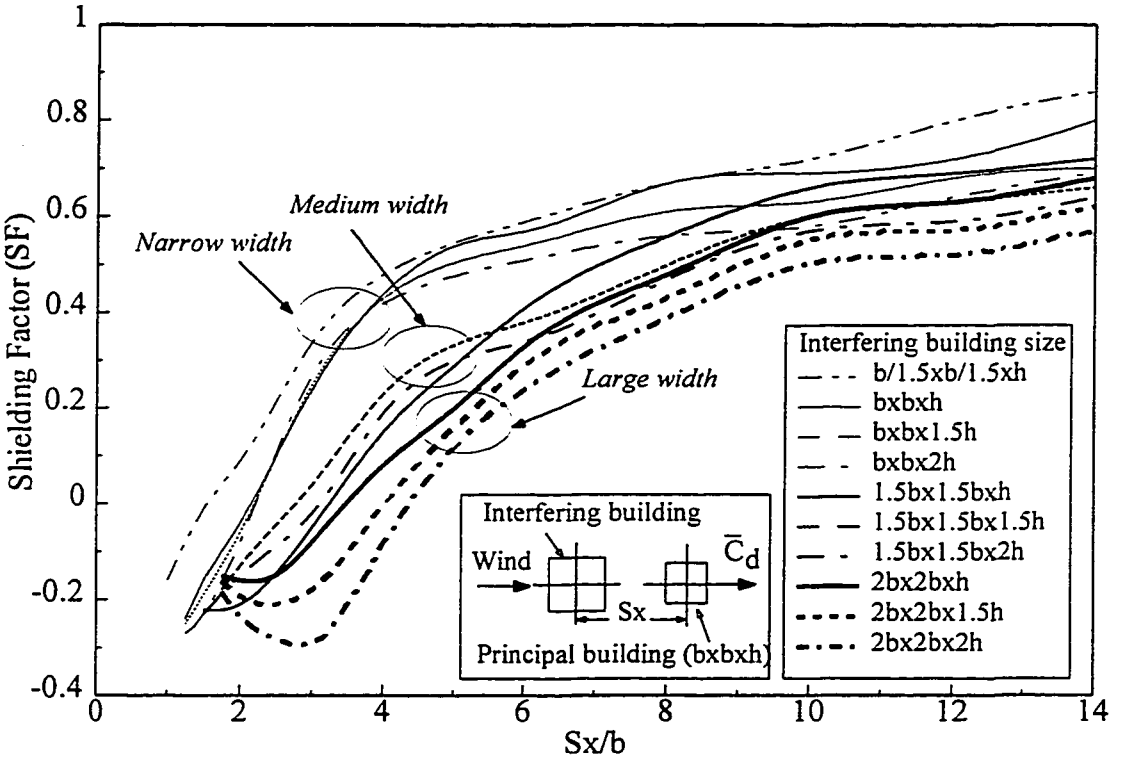

Figure 7.25 Shielding Factors for interfering buildings of various sizes.

Shielding is more sensitive to upstream building width than to its height. This is evident, for instance, from the curve representing SF for an interfering building size of 2b x 2b x h,

which lies below the b x b x 2h curve, indicating a lower SF or drag (higher shielding) for the building with larger width. Moreover, the curves with similar interfering building cross-sections show similar trends, and have therefore been bunched together into three sets: i) narrow width (b x b), ii) medium width (1.5b x 1.5b) and iii) large width (2b x 2b), where b is the width of the principal building. Each set comprises three interfering building heights of h, 1.5h and 2h, where h is the height of the principal building. The data for each of the three groups is modelled separately, for open terrain. The effects of the suburban and urban terrain are incorporated later from Figure 7.20.

Shielding Factor (*SF*) for open exposure in tandem position (Sy = 0) can be expressed as a function of the building geometries and spacing in a normalized form as,

$$SF = f(\frac{Sx}{b_p}, \frac{b_i}{b_p}, \frac{h_i}{h_p}) \tag{7.2}$$

where Sx = centre-to-centre spacing between the principal and interfering building, b_p and b_i are the widths of the principal and interfering buildings, respectively and h_p and h_i are the heights of the principal and interfering buildings respectively. A normalized separation variable, s, combining and relating Sx and the building geometries is defined as,

$$s = \frac{Sx}{b_p}\left[\frac{b_r^2 + h_r^2}{b_r\, h_r}\right] \tag{7.3}$$

where,

$$b_r = \frac{b_i}{b_p} \tag{7.4}$$

$$h_r = \frac{h_i}{h_p} \tag{7.5}$$

The above equations were a result of the evaluation of several different criteria for normalization, and provided the best correlation among the data. Thus, three appropriately normalized data sets for s versus SF were prepared for modelling.

Several empirical expressions relating SF and s, based on polynomial, logarithmic and exponential fit were evaluated to describe the above data. Results of the polynomial fit were satisfactory and those of the logarithmic and exponential fit unsatisfactory. Additional trials revealed that the complex relationships among the data, especially for the medium and large building sets, could be better described by using a combination of more than one exponential. Suresh Kumar and Stathopoulos (1997) suggest an equation that is a combination of two exponentials for predicting pressure spectra on low building roofs, each exponential controlling the shape of the spectra at different frequency regions. The equation is optimized to yield the best fit. Thus, an equation of the form $SF = a_1 e^{b_1 s} + a_2 e^{b_2 s} + c$, where a_1, a_2, b_1, b_2 and c are constants, is used to fit the three data sets. Least squares optimization is done by using the Levenberg-Marquardt algorithm available as a standard routine in MATLAB (Grace 1994), a technical environment enabling numeric computation and visualization.

Using the above methodology, three equations shown below representing the shielding effects of the upstream building on a downstream building are obtained. The goodness of fit is evaluated by computing the square root of the average of the sum squared errors (*SSE*), a low value signifying a better fit.

1) Interfering building of *narrow width* ($b_i = b_p$; $h_p \le h_i \le 2h_p$):

$$SF = 0.7 - 1.6\, e^{-0.18s} \qquad (SSE = 0.10) \qquad (7.6)$$

2) Interfering building of *medium width* ($b_i = 1.5b_p$; $h_p \leq h_i \leq 2h_p$):

$$SF = 1.9\ e^{-0.01s} - 2.0\ e^{-0.07s} - 0.5 \qquad (SSE = 0.06) \tag{7.7}$$

3) Interfering building of *large width* ($b_i = 2.0b_p$; $h_p \leq h_i \leq 2h_p$):

$$SF = 1.9\ e^{-0.01s} - 2.0\ e^{-0.06s} - 0.5 \qquad (SSE = 0.06) \tag{7.8}$$

The range of building sizes for which the curves are applicable are shown above in parentheses. A linear interpolation can be used to calculate SF for other building sizes lying between the given limits. The experimental data alongwith the fitted curves is shown in Figure 7.26. The narrow and medium size interfering building curves (Figure 7.26(a)) and 7.26(b)) fit the data reasonably well. The large section interfering building curve (Figure 7.26(c)) shows a satisfactory fit, considering the random fluctuations in the data, especially in the smaller abscissa range. Figure 7.26(a) also shows some literature results taken from Sakamoto and Haniu (1988); the results are quite close to the present predictions. These curves are for open exposure. For calculating SF for suburban and urban exposures, the above values of SF at a particular location should be multiplied by appropriate Exposure Factors (E_f), evaluated using Figure 7.20, and given in Table 7.8.

Table 7.8 Exposure Factors (E_f) for shielding by buildings of various sizes in suburban and urban exposures.

Sx/b			*E_f*	
Narrow width	Medium width	Large width	Suburban	Urban
≤ 2.5	≤ 3	≤ 4	1.5	1.7
2.5 to 4.0	3.0 to 5.0	4.0 to 6.0	1.1	1.2
4.0 to 6.0	5.0 to 7.0	6.0 to 8.0	1.0	1.1
> 6	>7.0	>8.0	1.1	1.2

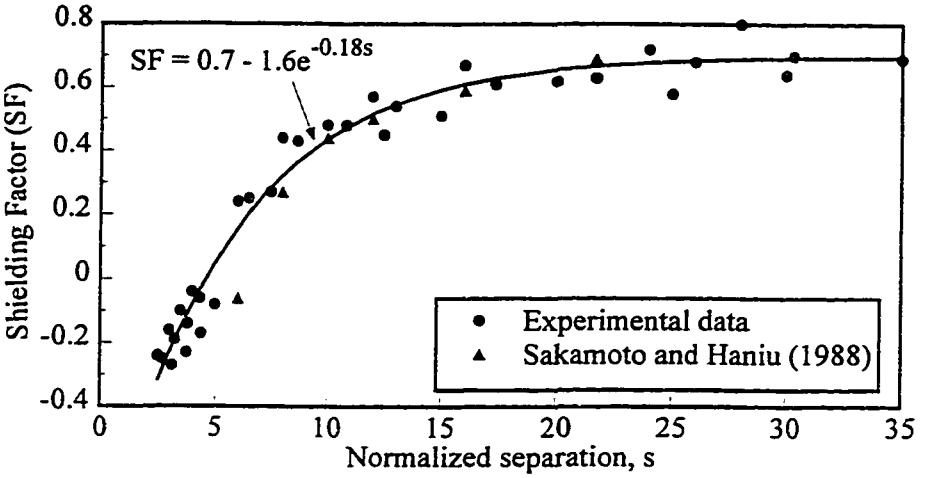

(a) Interfering building of narrow width

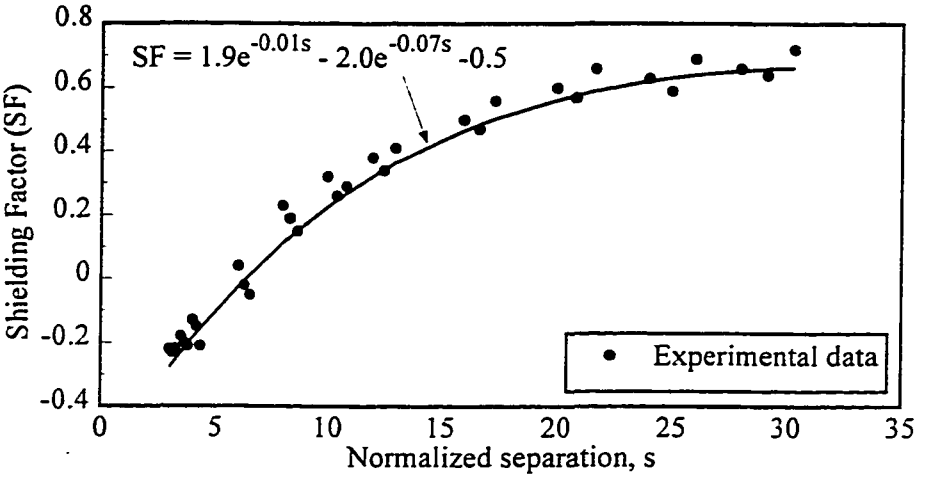

(b) Interfering building of medium width

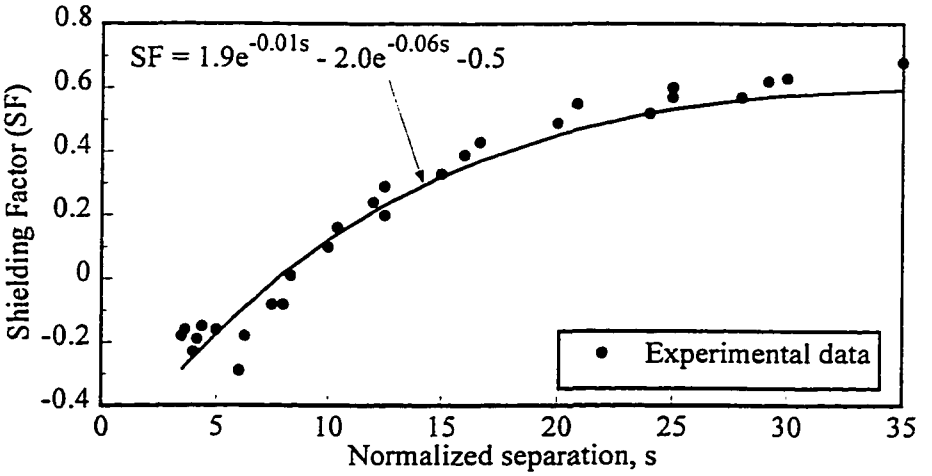

(c) Interfering building of large width

Figure 7.26 Empirical curves for prediction of Shielding Factors.

The above equations can be used to obtain a good estimate of the shielding effects of upstream buildings of sizes up to twice that of the principal building for various upstream exposures.

7.6 Peak loads

The experimental results presented above provide either the mean or the fluctuating component of the wind loads due to interference. For design of civil engineering structures, peak values of the loads are usually required and these can be obtained using the method suggested by Davenport (1964), wherein the peak response, $\hat{x}$ of a random variable, x is given by,

$$\hat{x} = \bar{x} + g\sigma_x \tag{7.9}$$

where $\bar{x}$ = mean value of x; g = statistical peak factor (3.5 to 4.5) and σ_x = standard deviation of x.

Presenting the interference effects results in terms of separate and disjointed mean and fluctuating values, is useful in many ways since it provides a detailed view of the interference effects and the related interference mechanisms, the shielding phenomenon and the dynamic effects. However, the mean and fluctuating components, viewed separately, do not give a clear idea about the peak loads. This can create confusion, especially in cases where an interfering building location may create high fluctuating loads on the principal building, but may provide low mean loads. Thus, evaluating peak loads is very important.

A value of $g = 3.8$ is commonly used to predict the hourly peak values in the analysis of force balance model test results (Isyumov et al. 1992). Zhang et al. (1994) suggest that for peak torsional moments, the value of g remains unchanged with or without interfering

models because the probability distribution of the torsional peak responses of the building both with and without the interfering building is essentially a Gaussian process. For interference effects problems, which are essentially normally distributed, Melbourne and Sharp (1977) suggest a peak factor of 3.7.

Peak values of wind loads can also be obtained directly through experiments and an extreme value analysis of the data. The whole process can be quite tedious and time consuming, especially for interference effects studies that involve a large number of building configurations and wind conditions. For the present study, equation 7.9 is used and a peak factor of 3.7 is chosen for calculating the peak drag and lift due to interference.

The mean and fluctuating force data for various wind directions shown in Figures 7.1 to 7.4 is combined by using equation 7.9 with a value of $g = 3.7$, to obtain peak drag and lift Interference Factors. The values of peak force coefficients for the isolated case are also calculated similarly.

Figure 7.27 shows the peak Interference Factor contours for drag for various wind directions. As evident from the figure, increases in peak drag are virtually non-existent. For example, compared to the high increases (up to 70%) in fluctuating drag in Figure 7.3(d), the increases in peak in the corresponding situation of Figure 7.27(d) are insignificant. In fact, the peak drag decreases for most interfering building locations. This is mainly due to the small contribution of mean drag (see Figure 7.1(d)) to the peak loads; recall from previous discussion that interference effects are responsible for shielding (lowering of mean drag). Thus, in terms of peak drag, the most noticeable effect is the significant decrease in drag and suction for close proximity locations of the interfering building.

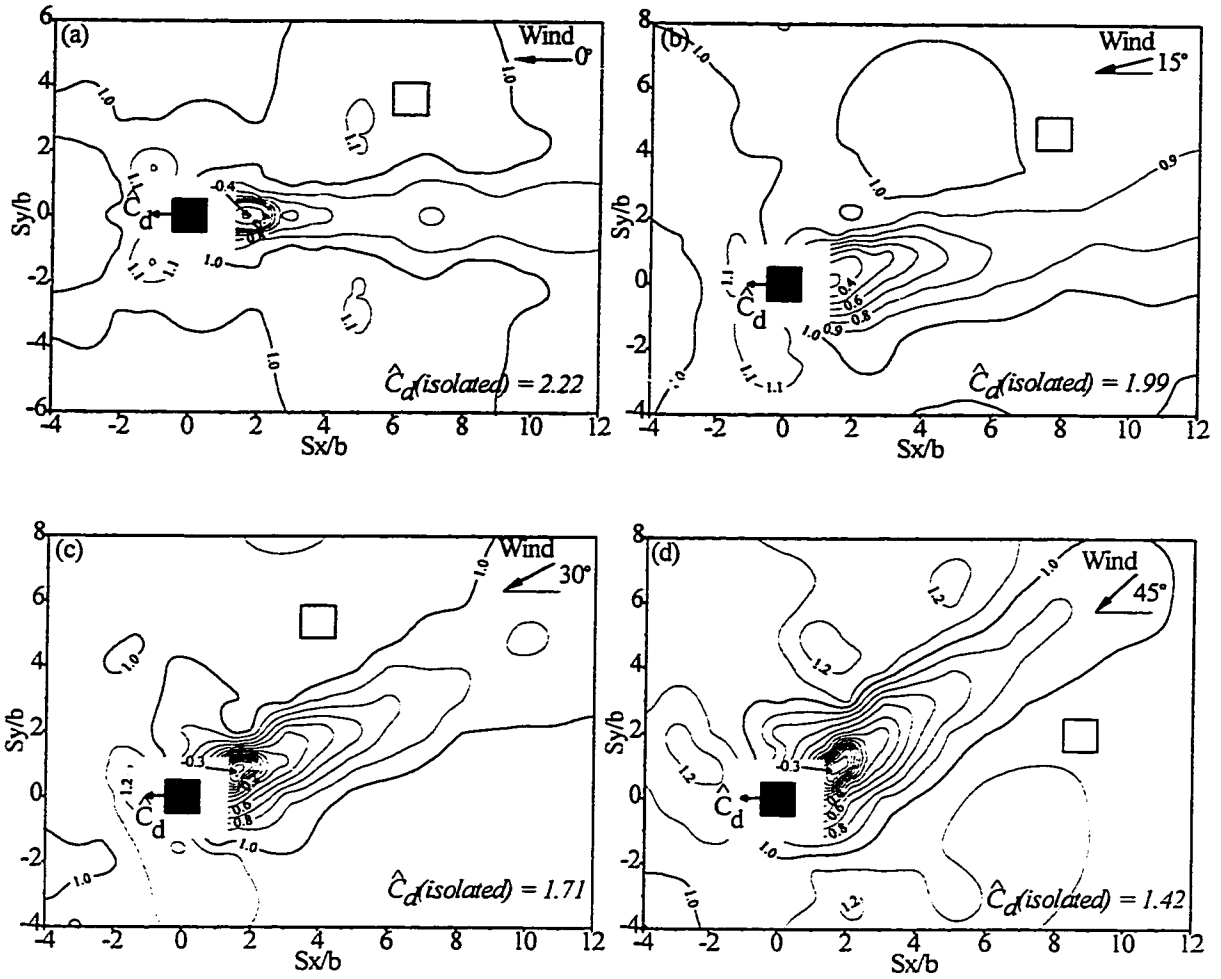

Figure 7.27 Effect of angle of attack of wind on peak drag IF.

The increases in peak lift are quite significant. This is evident from Figure 7.28 that shows the peak lift Interference Factors. Several interesting observations can be made from this figure. The spread in the range of peak lift is large, from negative to positive. For example, in Figure 7.28(b), peak lift IF ranges from -1.4 to 1.8. The negative values are due to the wide range of negative mean lift in Figure 7.2(b). Unlike peak drag which does not show any significant increase, the increases in peak lift (up to 80%) are high. The 45° wind angle produces the lowest increases in peak lift, and 15° and 75° the highest.

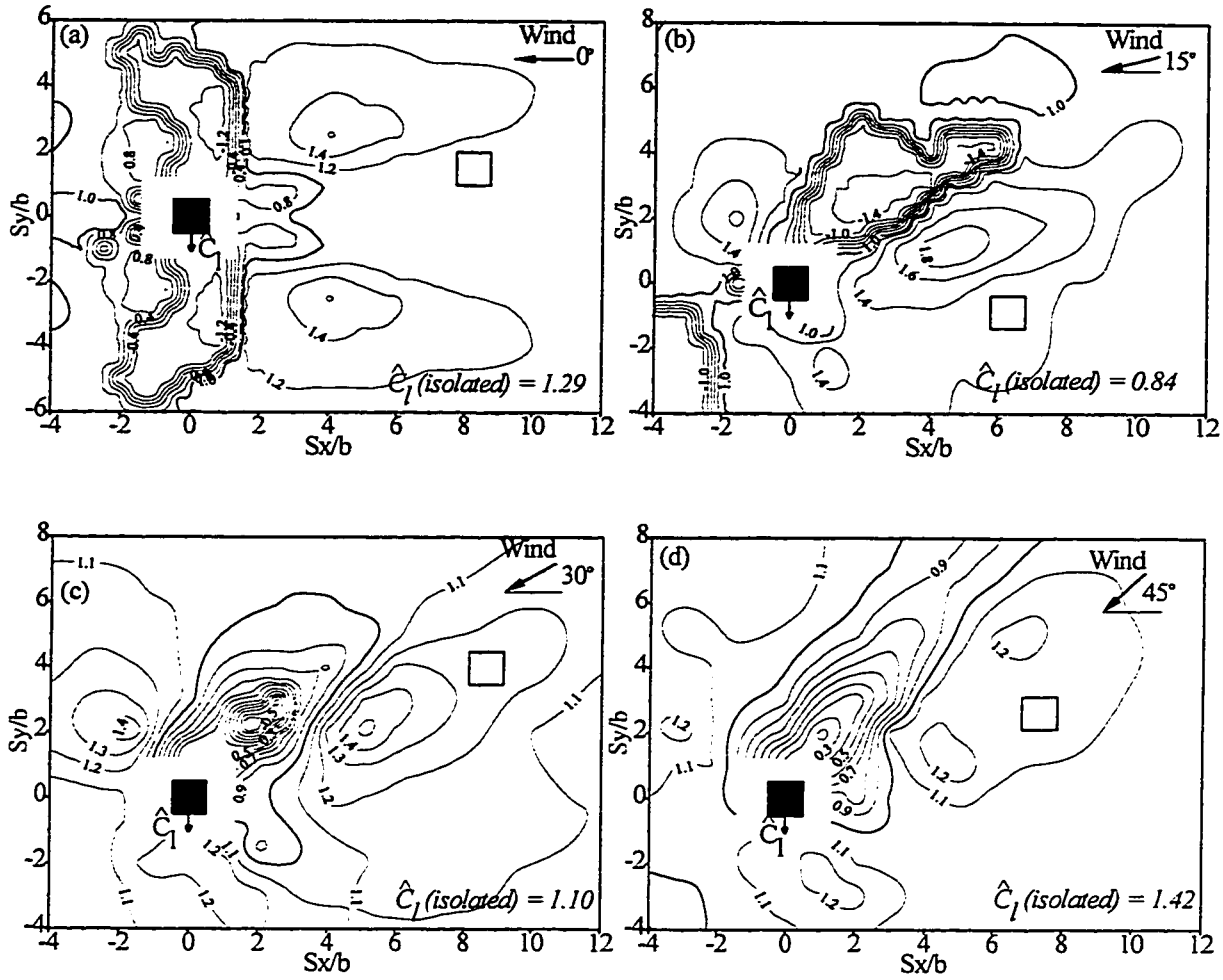

Figure 7.28 Effect of angle of attack of wind on peak lift IF.

Overall effects of wind direction on peak forces, in terms of extreme interference effects and directional probabilities, were also evaluated as done in section 7.1.5, and the results are shown in Appendix B.

7.7 Summary

The results of a detailed and comprehensive experimental study on the effects of wind direction, interfering building size and upstream exposure on wind-induced interference effects were presented, analyzed and discussed. The complexities of the relationships

among the various variables notwithstanding, overall trends were identified and general guidelines defining interfering effects were established. Thus, extreme effect contours for wind direction, Size Influence Grids for building sizes and Exposure Influence Grids for upstream exposures were set-up from a design stand-point. Shielding effects were modelled by means of simple empirical equations.

The proposed simplified guidelines and equations will provide the designer a blanket coverage for a broad range of situations as is the general norm in conventional standard provisions. The detailed contours would allow the designer, if need arises, to target specific situations as well.

The results and the associated discussions presented in this chapter help in a better understanding of the phenomenon of interference and the general guidelines presented give an overall view, helpful in preliminary design. The knowledge base generated and assimilated will form the basis of the wind design adviser, described in the next chapter, that incorporates Neural Network for modelling and generalization and Knowledge-Based System for organizing and accessing the above knowledge.

People have an extravagant capacity for generalization, of which this statement is, of course, a perfect example. However, without this ability all knowledge would have to be learnt as separate items or unique cases.

-Soren Brunak and Benny Lautrup, Neural Networks - Computers with Intuition (1988)

8

Modelling Wind-Induced Interference Effects Using Neural Networks and the Development of a Wind Design Adviser

8.1 Introduction

The previous chapters presented the results of a detailed and systematic experimental program on wind-induced interference effects. The experimental effort has generated a large quantity of valuable data that has been used to explain the phenomenon of interference. A thorough analysis of this data yielded concrete trends that helped set up generalized guidelines and recommendations. Empirical equations were also derived for simpler interference phenomena like shielding involving a minimum number of variables, i.e. building geometry and the along-wind spacing between buildings. However, a complete solution of interference problems requires, in addition to the above variables, the incorporation of other important variables like the spacing between buildings in the across-wind direction, incident wind direction and upstream exposure conditions. The present study addresses these issues by means of interference effects contours shown in chapter 6 and chapter 7. The seemingly unlimited interference situations were pruned down drastically because of complexity as well as time and economic considerations. Such a simplification, while compromising the scope of the study, does produce acceptable solutions to a significant, reasonably wide range of interference cases.

Good engineering judgement and careful simplification can only go that far however. A pertinent question therefore arises: what about the cases not tested, at least the ones lying between the limits set for the experimental program ? A linear interpolation, though

desirable, would be an oversimplification. Moreover, an examination of the data shows the relationships among input and output variables to be highly non-linear and complex. One can easily understand the futility of the traditional data modelling methods, for example multivariate, non-linear regression, in solving the problems of interference. Thus, the much needed generalization still remains elusive.

Khanduri et al. (1995a and 1997b) suggest that Neural Networks (NN), an off-shoot of the research in the field of artificial intelligence, may expand the solution of wind interference problems to more cases than those currently covered by limited wind tunnel data. A NN model based on limited interference effects data derived from previous studies did a good job of predicting interference effects for new cases not used in the development of the model. Eventhough the model considered the effects of only two inputs (along-wind and across-wind spacings between two identical buildings) on interference effects, the results were persuasive enough to conclude that NNs hold great promise as a viable and complementary alternative to extensive wind tunnel experiments. Thus, NNs are suitable for situations where data interactions are too complex for an analytical solution. A brief review of NNs has been presented in section 2.5.

In this chapter, the interference effect data generated in the present study is used to model interference effects using NNs. The model is exhaustive in that it includes all the relevant parameters covered in this study, viz. building geometries, spacing between them, incident wind direction and upstream exposure conditions. It is subjected to rigorous acceptance tests on completely new sets of data not used for the development of the NN model. The process of applying NN methodology is generally iterative and does not follow a fixed formula or set of rules. Researchers are striving to formulate general rules and

criteria that would greatly ease the application of NN methodology to a wide variety of problems. This chapter presents the lessons learnt from the present NN development and guidelines for further work.

Since NNs are not based on explicit rules, they are devoid of a logical reasoning process. Thus, the lack of an explanation capability constitutes the main drawback of NNs. In order to be useful to the building designer, the numbers generated by the NN model have to be put in proper perspective, i.e. analyzed and followed by a succinct explanation about their implications on design. Therefore, NETWIND, a NN based design advisor for wind-induced interference effects has been developed. NETWIND integrates the NN model with the useful knowledge-base developed in this study, to provide valuable assistance to designers at the preliminary design stage. The schematic of the proposed system is shown in Figure 8.1 which is reproduced, for easy reference in this chapter, from Figure 1.

8.2 Generalization Using Neural Networks

The main source of knowledge on interference effects remains detailed wind tunnel experiments. The complex nature of the problem and the large amount of variables involved make it impossible to test all building interference situations. The experimental approach adopted so far has been to minimize the number of test configurations and to keep them simple while searching for limiting conditions. The generalization of results thus obtained to various other building configurations and wind conditions still remains elusive.

As explained previously, NNs have been successfully used to model simple wind interference problems. NN attempt to mimic the human thought process to solve complex

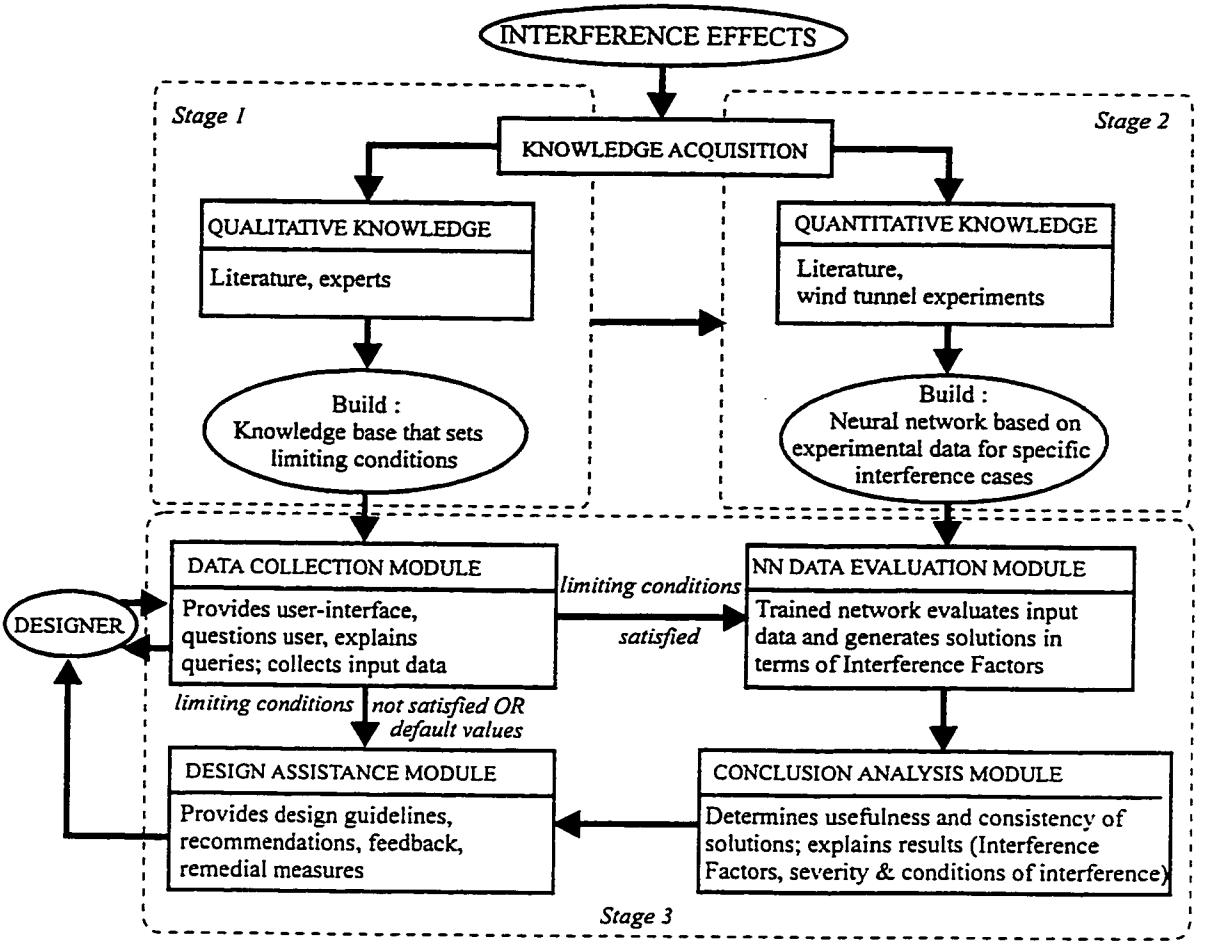

Figure 8.1 Schematic of the proposed integrated wind design adviser

multivariate and non-linear problems with incomplete or confusing information. A NN is composed of many interconnected processing elements that operate in parallel, in a way quite similar to the function of neurons in the human brain to encode information. NN representations are capable of developing functional relationships from discrete values of input-output quantities obtained from computational approaches or experimental results. This generalization property makes it possible to train a network on a representative set of input-output examples (also known as training patterns or training sets) and get good results for new inputs without training the network on all possible input-output examples.

Because of proven capabilities at pattern mapping, classification and optimization even with fuzzy, chaotic or incomplete information, NN have been successfully used to model experimental data for tasks ranging from the prediction of concrete strength to the hysteretic modelling of steel structures. Neural networks have been reported in a number of civil engineering applications (see Flood and Kartam 1994).

8.2.1 Neural Networks - an overview

Neural networks are composed of several layers of simple elements operating in parallel. Each layer has a weighted input vector and an output vector. Layers whose outputs becomes the final network output are called *output* layers, all other layers are called *hidden* layers. The first set of neurons referred to as input layer perform no computations and serve only as distribution points. The network function is determined largely by the connections between neurons or processors. Each processor accepts a set of inputs from other processors and computes an output which is propagated to connected processors. Networks are *trained* with available test examples to recognize input patterns and produce appropriate output responses. Each connection is associated with a measure of the strength of the connection, called its *weight*, which is used to modify the signals. For a given neural architecture, it is the weight of the connections between the processors which determines the output. Changing the strength or weight of connections with experience (new examples) is akin to learning, the memory of a network being embedded in the strength of the connections. An elementary backpropagation neuron with n inputs and weighted connections is shown in Figure 8.2.

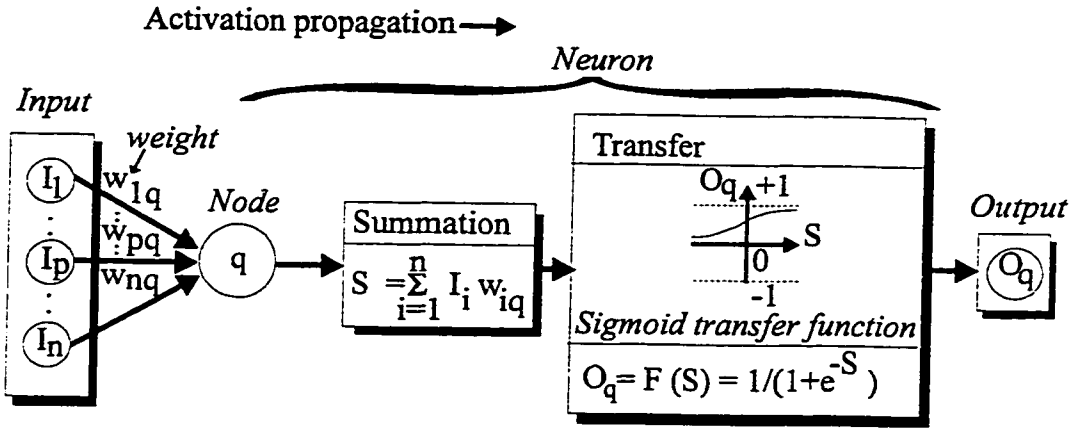

Figure 8.2 The basic neuron model and the feedforward phase

The activity pattern in a hidden layer follows an encoding of the significant features of the input. The collective activity of all the hidden units (neurons or nodes) determines the behaviour of a network. Hidden units work as internal representations for the inputs, and outputs are generated from these internal representations rather than by the original example pattern. Thus, an appropriate output pattern can be generated from any input-output pattern by employing an adequate number of hidden units. There are currently no universal rules for selecting the number of hidden nodes and layers. These vary from problem to problem and are generally fixed after several trials with the network. A network may not get trained to the acceptable level of error with too few hidden nodes, whereas with too many hidden nodes, the network may work a bit better but not generalize well. It then becomes merely a look-up table and also tends to increase training time and the size of weight matrices in the solution. Generally one hidden layer is enough for most problems, but for very complex, fuzzy and highly non-linear problems, more than one hidden layers might be required to capture the significant features in the data.

The changing of interconnection patterns and the setting of weights that determine the strength of a connection is done by *training* the network to exhibit the correct behaviour. One of the most common training algorithms is known as the Generalized Delta Rule or *backpropagation* (Rumelhart et al. 1986). Backpropagation Neural Networks (BPNN) require long training times and can get trapped in local minima instead of finding the global minimum error surface. Specht (1991) has propounded an alternative NN algorithm known as the *General Regression Neural Network* (GRNN) that resolves these problems and has been found to work well for non-linear regression problems. GRNN can reduce network training time while dramatically improving its performance (Caudill 1994). GRNN is a one-pass learning algorithm with a highly parallel structure that provides estimates of continuous variables and converges to the underlying regression surface. As opposed to the normal regression analysis that requires a prior knowledge of the form of regression function, GRNN requires no such assumption and instead, bases its results on the probability density function of the observed data. The network architecture is similar to the one described above, except that GRNNs can have only one hidden layer with one hidden node for each of the training patterns, i.e. input-output examples in the network.

The present study uses and compares both these algorithms for modelling wind interference problems. The following sub-sections briefly describe the BPNN and GRNN algorithms.

8.2.1.1 The BPNN architecture and the network training process

The backpropagation process is briefly described below and illustrated in Figure 8.3. It is

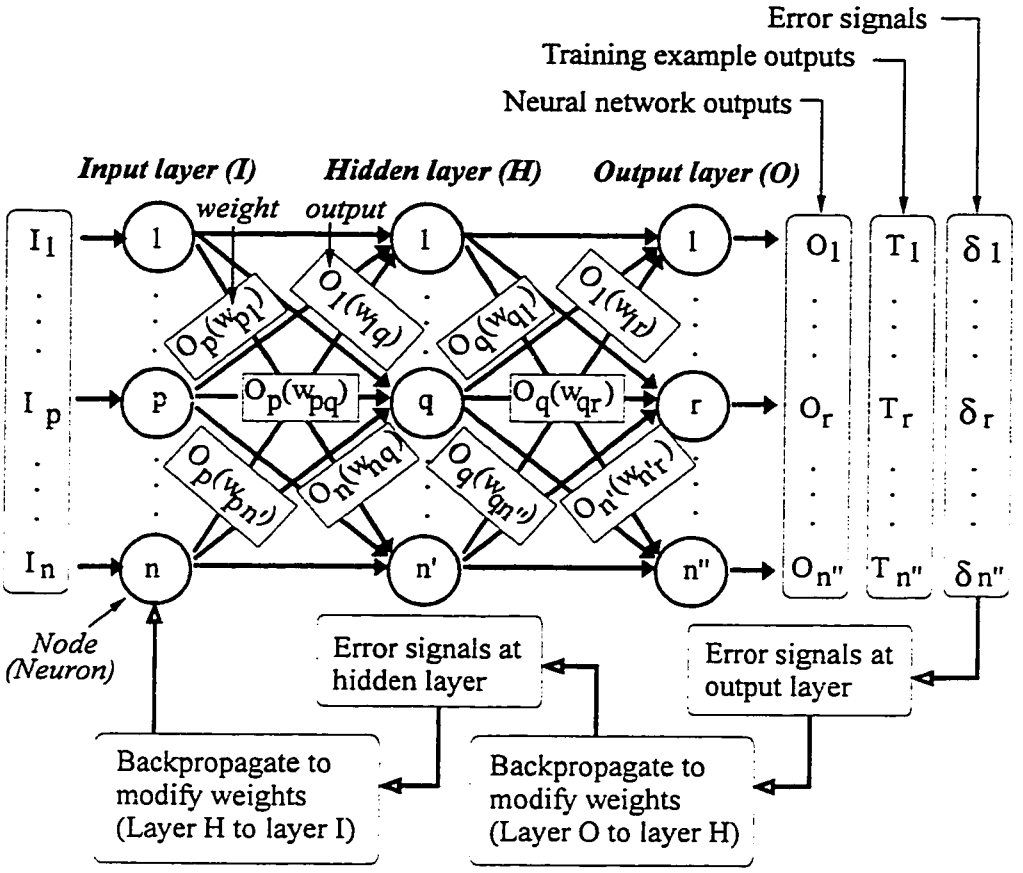

Figure 8.3 Overall BPNN architecture and the backpropagation phase

assumed for simplicity the NN to be composed of only three layers: input-hidden-output. The application of the generalized delta rule for training a network involves two phases. In the first (feedforward) phase, each input is weighted with an appropriate weight w (initialized to small random numbers, usually between -1 and 1) and the products are summed up at each neuron (node) of the network. This summation S of the weighted inputs at each neuron of the network is then modified by an activation or transfer function F shown in Figure 8.2, thereby generating an output signal O. A continuous, non-linear logistic or sigmoid (meaning S-shaped) transfer function is commonly used, mainly because it meets the differentiability requirement of the backpropagation algorithm. The

sigmoid transfer function forces the output to lie between 0 and 1 as the neuron's net input (S) goes from negative to positive infinity. The summation is continued up to the output layer of the network, the outputs of each layer serving as inputs to subsequent layers. The transfer function (see Figure 8.2) is given by :

$$F(S) = \frac{1}{(1+e^{-S})} \tag{8.1}$$

In the second (backpropagation) phase, the error between output of the network and the training set is propagated backwards through the network where it is used to adjust the weights according to the generalized delta rule proposed by Rumelhart et al. (1986). The algorithm makes a small adjustment to the strength of each connection in such a manner that each alternative reduces the total network error in the direction of the steepest descent of the error. This is called the gradient descent method. Derivatives of the error are calculated for the network's output layer and then backpropagated through the network until all the weights are adjusted and the sum squared error of the network is within acceptable limits. The backpropagation process is briefly described below and illustrated in Figure 8.3.

At the output layer, the error (δ_r) between the actual network output (say O_r at the r^{th} neuron) and the desired or training example output (say T_r at the r^{th} neuron) is calculated by multiplying the difference between T_r and O_r by the derivative of the transfer function $\partial F(S_r)/\partial S_r = O_r(1-O_r)$. Thus,

$$\delta_r = (T_r - O_r)\{O_r(1 - O_r)\} \tag{8.2}$$

This error is backpropagated from the output layer where it is used to adjust the weights

of connections between the hidden layer and the output layer according to the generalized delta rule (Rumelhart et al. 1986) as follows:

$$\Delta W_{qr} = \eta \delta_r O_q \tag{8.3}$$

$$W_{qr}(m+1) = W_{qr}(m) + \Delta W_{qr} \tag{8.4}$$

where η is the training rate coefficient; δ_r is the error for neuron r in the output layer; O_q is the value of output for neuron q (hidden layer); $W_{qr}(m)$ is the value of weight of connection from neuron q in the hidden layer to neuron r in the output layer at iteration m, before adjustment and $W_{qr}(m+1)$ is the value of weight at iteration $m+1$, after adjustment.

The training rate coefficient (η) serves to adjust the size of the average weight change, and is typically set between 0.01 to 1.0 (Wasserman 1989). The larger this coefficient, the larger the changes in the weights and more rapid the learning. However, in some cases, large training rates often lead to oscillation of weight changes and the model does not converge to a solution. Errors at the output layer are backpropagated to the hidden layers preceding the output layer and the weight adjustments for the connections from the hidden layer to the input layer are made as follows :

$$\delta_q = \{\sum_{i=1}^{n''} \delta_i W_{qi}\}\{O_q(1-O_q)\} \tag{8.5}$$

$$\Delta W_{pq} = \eta \delta_q O_p \tag{8.6}$$

$$W_{pq}(m+1) = W_{pq}(m) + \Delta W_{pq} \tag{8.7}$$

where δ_q is the error for neuron q in the hidden layer; δ_i is the error for neuron i in the

output layer; W_{qi} is the value of weight of connection from neuron q in the hidden layer to neuron i in the output layer; n'' is the number of neurons in the output layer; O_p is the value of output for neuron p (input layer); $W_{pq}(m)$ is the value of a weight from neuron p in the input layer to neuron q in the hidden layer at iteration m before adjustment and $W_{pq}(m+1)$ is the value of weight at iteration $m+1$, after adjustment.

The above steps are repeated for all training examples and the square of all the errors between the network and training examples outputs are added up. For a network trained on l examples, each having n outputs the average mean square error E is calculated as follows:

$$E = \frac{1}{2l}\sum_{j=1}^{l}\sum_{i=1}^{n}(T_{ij} - O_{ij})^2 \qquad (8.8)$$

where T_{ij} is the i^{th} output of the j^{th} training example set; O_{ij} is the network output at the i^{th} output neuron of the j^{th} training example set.

The entire training process is repeated until the behaviour of the network is satisfactory, i.e. the average mean square error E is less than or equal to a user-defined threshold. After being trained on a large number of cases, a network will not only be able to map the input and output patterns of the training examples, it will also perform well on many cases which were not present in the training set, i.e. it will display some abilities to generalize.

8.2.1.2 The GRNN architecture and the network training process

General Regression Neural Networks (GRNN) are known for their ability to train quickly on sparse data sets. GRNNs are especially useful for continuous function approximation,

can have multidimensional input, and fit closely multidimensional surfaces through data (Specht 1991).

A GRNN is essentially a three-layer network with one hidden neuron for each training pattern. There are no training parameters such as training rate etc. as in BPNN, but there is a *smoothing factor* that is applied after the network is trained.

GRNNs work by measuring how far a given sample pattern (or training example) is from other patterns in the training set in N dimensional space, where N is the number of inputs in the problem. When a new pattern is presented to the network, that input pattern is compared in N - dimensional space to all of the patterns in the training set to determine how far in distance it is from those patterns. The output that is predicted by the network is a proportional amount of all of the outputs in the training set. The proportion is based upon how far the new pattern is from the given patterns in the training set. For example, if a new pattern is in a cluster with other patterns in the training set, the output for the new pattern is going to be very close to the other patterns in the cluster around it. The GRNN algorithm (Specht 1991) is briefly described below.

As shown in Figures 8.2 and 8.3, every input node is connected to a hidden node. At such a hidden node (say q), the difference of each input and the corresponding weight is computed. Then the sum of the squares of these differences across all the weights is calculated to correspond to the input function for the qth hidden layer neuron I_q. This net input is finally modified though a non-linear activation function of the type:

$$F(I_q) = e^{\left(\frac{-I_q}{2\omega^2}\right)} \tag{8.9}$$

where ω is a smoothing constant that defines the smoothness of the regression surface. In

general, a larger value of ω produces a smoother curve and a smaller value generates a detailed curve. Thus, greater generalization (closer to a simple mean of the training sample output) is obtained with larger values of ω and a more accurate fit for smaller values of ω; an intermediate value will provide the best generalization. The outputs of the hidden nodes are passed on to the output layer also referred to as summation layer. Here a dot product is performed of the weight vector (set to the training set output values) and a vector composed of the outputs from the hidden layer. This product is divided by the summation of the hidden layer output values to yield the final network output. When the size of the training set becomes very large (generally greater than 2000 samples), data clustering is required and this modifies somewhat the calculation of the final network output (see Specht 1991 and Caudill 1994). No data clustering is used in this study.

8.3 Development of Neural Network Model For Wind Interference Problems - General Requirements

Neural networks exhibit several characteristics that make them suitable to study interference effects in wind engineering :

- Training teaches a network to capture significant features or relationships in the data. Thus a trained network is capable of exhibiting such relationships in new related data.
- The ability of neural networks to perform a computation when trained with examples makes them applicable in situations where a model is needed, yet no currently acceptable theory exists for describing the input/output pattern.
- "Fault tolerance" due to their distributed nature, i.e. provide reasonable response when presented with incomplete or noisy input.

The complete NN modelling process is iterative and requires considerable judgement in the selection of the training and testing data sets, definition of the network architecture and the termination criteria for a training session. The main objective is to develop a model that generalizes the data patterns well, rather than memorize them, and must be able to give the correct response for previously unknown input. Several NN architectures are trained and the final decision regarding the exact number of hidden nodes and hidden layers is taken only after testing each network configuration with new input. The network that gives the best response with new input is finally selected. This constitutes the "real test" for the NN since it confirms the generalization capability of a particular NN model.

In order to model wind-induced interference effects, five NN models are developed in section 8.4 to 8.6 to predict the Shielding Factors (SF), mean drag Interference Factors (IF) and lift coefficients as well as dynamic drag and lift IFs. The simpler Shielding Factor model is developed as a starting point to "test the waters" and to compare with the regression equations suggested in chapter 7. At the end of the NN development phase, conclusions are drawn and suggestions formulated for subsequent NN developments in section 8.7.

Three main steps are necessary for the successful development of a NN: selection of a suitable NN development environment, network training, and Network testing or validation. These steps are described in the next sub-sections.

8.3.1 NN development environment

A number of neural network development tools are commercially available (see Neural Network 1995). The performance of network modelling and training using such programs

depends not only on the type of the NN paradigm but also on several other criteria like ease of data interface, speed of training, memory requirements, interface with external programs and general user-friendliness.

Exploratory NN models developed for this study (Khanduri et al. 1995a) used an early version (1988) of NeuroShell, a neural network development software. Although adequate for simple applications, it supports only a single hidden layer which renders it unsuitable for large and complex problems. Other limitations are a poor user-interface and no post-processing facilities like detailed statistics, graphs etc. NN toolbox of MATLAB (Demuth and Beale 1994) gives the user a good choice of several transfer functions, up to three hidden layers and includes powerful functions to speed up and optimize training. However, it lacks general user-friendliness in that an intimate knowledge of MATLAB functions and programming is required for pre- and post-processing the network. The latest version of NeuroShell (NeuroShell2 1996) combines the computing power of MATLAB with extensive post-network and data analysis facilities which ease the development of NNs. It includes powerful GRNN and the choice of several network architectures with an easy interface with popular spreadsheet software. Its ability to generate NN source code in C and Visual Basic helps in the integration and customization of the NN models with other external programs.

Thus, NeuroShell2 (1996) gives a good balance of the general requirements of this project. Furthermore, several software reviews have presented NeuroShell favourably (see Entsminger 1991 and Hillman 1990). NeuroShell2 requires the system developer to:

- define the network inputs and outputs,
- extract data suitable for training and testing sets,
- select a network paradigm (BPNN, GRNN etc.),
- fix the neural network architecture i.e. define the number of hidden nodes and layers, and
- select a training termination criterion.

The entire NN development is carried out using NeuroShell2 in Microsoft Windows 95™ environment, on an IBM® PC compatible with Intel® 166 MHz Pentium™ processor with 32MB RAM.

8.3.2 Network input and output

A NN is only as good as the data it is supposed to represent and finding data that can represent broadly the important "events" in a problem requires considerable effort. Eventhough a NN might be fairly simple to program, thorough data checking, sorting and processing (using statistical tools, if needed) is an essential prerequisite to an efficient NN model development. As seen before, wind interference effects depend on several parameters. In order to train and test the network, it is necessary to develop a data set consisting of IF or force coefficient values in relation to the various relevant parameters. Data for NN development is taken from the experimental results presented in chapters 6 and 7. This data constitutes the quantitative knowledge derived from experimental results as shown in the top box (dotted line) of Figure 8.1. Thus in all, eight variables are considered as input and one as output for the neural network model, as given below:

a) Input variables:

- Incident wind direction, θ
- Longitudinal turbulence intensity, I_v of the approach wind at building height
- Width of the principal building, b_p
- Width of the interfering building, b_i
- Height of the principal building, h_p
- Height of the interfering building, h_i
- Centre-to-centre spacing, *Sx* between the buildings along the X-axis and
- Centre-to-centre spacing, *Sy* between the buildings along the Y-axis.

b) Output variable:

- Interference Factor *IF*, for mean and fluctuating drag and fluctuating lift, or mean lift coefficient $\overline{C}_l$. IF (as already explained - see equation 3.11) represents the increase or decrease in wind loads on a building due to the presence of an adjacent interfering building.

In the case of the Shielding Factor NN model, the incident wind direction θ is fixed at 0°, the upstream exposure is open, i.e. $I_v = 7\%$, and buildings are arranged in tandem, i.e. $Sy = 0$, in keeping with the empirical formulation of chapter 7. Therefore, the input variables are reduced to the geometries of the buildings and the spacing between them along the X-axis.

Simplifying the information presented to a NN enhances its performance, and helps it to "learn" the relationships among the data more effectively. For instance, in case of building geometries, the salient information is the relative width ratio or the relative height ratio between the interfering and the principal building. Thus, it makes better

sense to supply two variables (b_i / b_p and h_i / h_p) instead of four (b_p, b_i, h_p, h_i). This makes the work of the NN easier, since the number of input variables is reduced as well as an additional information regarding the relative importance (inherent in the ratios) of the variables is now available to the NN. Similarly, the centre-to-centre spacings between the buildings, *Sx* and *Sy*, are normalized by the width b_p of the principal building. Thus, the total number of input variables presented to the NN are reduced to six (three in case of the Shielding Factor model).

8.3.3 Network training and testing

After deciding on network input/output and preparing data for the NN model, the network is ready to be trained on the input-output examples in the data set. Training the network on the entire data is not a good idea, because the NN model developed in this manner might not work well on new sets of data not present in the training data set. Moreover, models developed in this manner generally end up either resembling a "look-up table" (lack of generalization), or overfitting the data. To avoid this situation, two suitable data sets are extracted from the overall database, one for training the network and the other for testing its generalization capability. Thus, the network is trained on a representative sample of the data and tested on another sample not present in the training data set. Once again, a caveat exists: networks trained this way may master the training patterns but fail when presented with new data. It is inconvenient to interrupt the training cycle several times to test accuracy of the network in order to determine when the training is to be stopped, especially when the data set and the network are large. Thus, the network might "overtrain" and the model will "memorize" the patterns instead of

smoothly interpolating among them. If the data is "noisy", the network will also tend to learn noise, if overtrained.

A solution to this problem lies in the *calibration* option of NeuroShell2 that automates the training-testing cycle. Calibration trains on the training set and computes an average error factor for it during training. But very often at intervals (number of training patterns processed) specified by the user, it reads the test set and computes an average error for it as well. The network can be saved every time a low test set error is encountered. Thus, calibration limits overtraining and helps develop an optimal network.

After the network model is calibrated to a satisfactory level of accuracy, it is further tested to see how well it has learned the data patterns and to verify if it can predict correctly IF values for previously unknown input. This is done using a completely new set of data such that no single item from this new data set is present in the data used for training and testing the network. Thus, when using calibration, the training and testing data sets are both involved in training of the network. However, the NN model is said to have generalized well if it works well on previously "unseen" input-output examples. Therefore, a third data set, known as the *production set*, is extracted from the entire database. This production set actually represents new data not yet "seen" by the network. NN output is computed for input from the above data set and compared with actual output from the same data set to check the accuracy of predictions. Network is trained further if it does not give satisfactory results on the production set. If further training does not improve performance, the network is redesigned by changing the number of hidden nodes and/or hidden layers or by using an altogether new NN paradigm, and trained again.

The following statistical criteria (Neuroshell2 1996) are used to evaluate "goodness of the fit":

a) R squared: This is the main criterion used for evaluating "goodness of fit" of the model. R squared (or R^2) is a statistical indicator usually applied to regression analysis. It compares the accuracy of the model to the accuracy of a trivial benchmark model wherein the prediction is just the mean of all samples. A perfect fit would result in a R^2 value of 1, a very good fit near 1 and a very poor fit near 0. If the NN model predictions are worse than those predicted by simply using the mean of the sample outputs, the R^2 value will be 0. R squared is defined as

$$R^2 = 1 - \frac{SSE}{SS_{yy}} \tag{8.10}$$

where,

$$SSE = \Sigma(y - \hat{y})^2 \tag{8.11}$$

$$SS_{yy} = \Sigma(y - \bar{y})^2 \tag{8.12}$$

where y is the actual value, $\hat{y}$ is the predicted value of y, and $\bar{y}$ is the mean of the y values.

b) Mean Squared Error (MSE): This the mean over all patterns of the square of the actual value minus the predicted value. Thus,

$$MSE = \frac{SSE}{N_{pat}} \tag{8.13}$$

where N_{pat} is the number of data patterns (or examples) used.

c) Mean Absolute Error: This is the mean over all patterns of the absolute value of the actual value minus the predicted value. Thus mean absolute error $|\bar{E}|$ is given by,

$$|\overline{E}| = \frac{|y - \hat{y}|}{N_{pat}} \tag{8.14}$$

d) Maximum Absolute Error: This is the maximum of the absolute value of actual minus predicted values of all patterns. Thus maximum absolute error $|\hat{E}|$ is given by,

$$|\hat{E}| = |y - \hat{y}| \tag{8.15}$$

e) Percent within 5%, 5% to 10%, 10% to 20%, 20% to 30% and over 30%: These represent the percent of network answers that are within the specified percentage of the actual answers used to train the network. If the actual answer is 0, the percentage cannot be computed (due to division by 0) and the pattern is not included in the group. For this reason (and rounding) the total computed percentages may not add up to 100.

The number of input-output data patterns for the training, testing and production sets depends on the quantity and type of data, the complexity of the problem, and can only be fixed after a few training trials with the data. Generally, around 20% of the overall data selected at random is reserved for the test set and 10% for the production set. Table 8.1 gives the various data patterns (or sets) extracted for this study.

Table 8.1 Number of data patterns processed for various NN models

NN model	*Overall data*	*Training set*	*Testing set*	*Production set*
Shielding Factor	112	74	22	16
Mean Drag	1387	972	277	138
Mean Lift	1199	901	179	119
Fluctuating Drag	1528	1040	260	228
Fluctuating Lift	1409	917	281	211

Total number of data sets used: 5635

8.3.4 Selection of NN paradigm and architecture

Based on previous NN development for interference effects (Khanduri et al. 1997b and Khanduri et al. 1995a), BPNN with one hidden layer seems be an appropriate paradigm and architecture for this study. However, many problems respond differently to different types of networks and architectures and there is no way to tell in advance exactly which type of network will work best for a particular problem. Further, it should be noted that the aforementioned NN developments were of an exploratory nature and comprised of a small data set (27 training patterns) with only two input variables and one output. A single hidden layer with 6 to 15 hidden nodes did the job in that case.

The problem at hand is larger (except for the Shielding Factor model) and more complicated since the number of input variables has now increased threefold and the maximum number of training patterns increased by about 30 to 40 times (see Table 8.1 above). A simple educated guess suggests that the above architecture (and maybe the paradigm as well) may not be sufficient to model the present data sets. However, backpropagation remains the paradigm of choice, since it is the most widely used, time-tested and successful algorithm for most engineering applications. It has been suggested (Caudill 1991) that BPNNs do not cope well with training sets that are large, either in the size of each input pattern or in the number of examples in the training set, and especially with non-monotonic functions. It is clear from the results presented in chapters 6 and 7 that Interference Factors are non-monotonic (a monotonic function increases or decreases continuously with its argument), especially in case of fluctuating loads. Thus, it would be wise to select alternative NN paradigms, in case backpropagation fails to do the job. The advantages of General Regression Neural Networks have been stated before. NeuroShell2

(1996) presents the GRNN as the most powerful paradigm for continuous function approximation. Therefore, BPNN and GRNN have been used for modelling data in this study.

In order to decide on the overall BPNN architecture, a range of configurations of hidden nodes are considered and the one that most closely models the data is selected. As explained before, an appropriate output pattern can be generated from any input-output pattern by designing a network having the correct number of hidden units. Generally one hidden layer is sufficient for most problems, but for very complex and highly non-linear problems, more than one hidden layer might be required to model the data correctly. It has been suggested (Chester 1990) that in NNs with a single hidden layer, the neurons interact with each other globally, making it difficult to improve approximation at one point without worsening it elsewhere. This problem can be overcome by using two hidden layers. It may also be necessary, in the present study, to use more than one hidden layers, which will only become clear after adequate experimentation with network development.

There are currently no standard rules for selecting the number of hidden nodes. For single layer NNs, Caudill (1988) suggests using twice the number of input nodes plus one as the number of hidden nodes whereas Rogers (1994) proposes as initial guess for the number of nodes in the hidden layer the sum of the nodes in the input and the output layers. More recently, Khanduri et al. (1995b) suggest that for NN modelling of wind-induced interference effects, a good guess on the number of hidden nodes would be twice the sum of input and output nodes. NeuroShell (1996) uses as default number of hidden nodes the average of the number of input and output nodes plus the square root of the

number of training patterns. Thus, the criteria for fixing the number of hidden nodes seem to vary from problem to problem and are generally fixed after several trials with the network. A network may not get trained to the acceptable level of error with too few hidden nodes, whereas with too many hidden nodes, the network may work a bit better, but does not generalize well. It then becomes merely a look-up table and also tends to increase training time and the size of weight matrices in the solution.

8.3.5 Selection of NN training termination criteria

In order to avoid overtraining or undertraining the network, it is important to know precisely when to stop the training. For BPNN, the termination criterion is generally based upon a threshold value of acceptable error (for example, MSE = 0.001) for the testing data set. However, many a time the network never gets trained to the given threshold error, and in this circumstance the training is terminated based on a number of training events or iterations in which the network shows no improvement. The exact threshold error or the number of training events varies from problem to problem and can only be decided after adequate experimentation with the problem at hand.

In NeuroShell2 (1996), GRNN uses a genetic algorithm (see Kennedy 1995) to find appropriate individual smoothing factor adjustments for each input as well as an overall smoothing factor. A genetic algorithm works by selective breeding of a population of "individuals", each of which is a potential solution to the problem. In this case, a potential solution is a set of smoothing factors, and the genetic algorithm seeks to breed an individual that minimizes the mean squared error of the test set. After testing all of the individuals in the pool, a new "generation" of individuals (smoothing factors) is produced

for testing. The algorithm uses a "fitness" measure to determine which of the individuals in the population survive and reproduce. The training is terminated when there have been 20 successive reproductions (generations) of the whole population, but none has produced an individual that improved the mean squared error by at least 1%.

Having defined the general requirements and guidelines, the training and testing of specific NN models for wind-induced interference effects can now proceed.

8.4 Development of NN model for Shielding Factors

Shielding Factor (SF) was defined and modelled empirically in chapter 7. SF will be modelled once again, this time using NN. This exercise will serve as an exploratory test as well as compare and contrast the empirical modelling with NN modelling. The various statistics of the input-output data patterns are shown in Table 8.2.

Table 8.2 Statistics of Shielding Factor (SF) data

Statistics	*Inputs*			*Output*
	b_i / b_p	h_i / h_p	Sx / b_p	*SF*
Minimum	0.667	1.000	1.000	-0.290
Maximum	2.000	2.000	14.000	0.860
Mean	1.376	1.442	6.028	0.271
Standard Dev.	0.463	0.418	4.178	0.344

The number of training, testing and production data sets are given in Table 8.1. A network with an input layer consisting of 3 input nodes (b_i / b_p, h_i / h_p and Sx / b_p), one hidden layer and an output layer with one output node representing IF for mean drag is selected. The number of hidden nodes, N_h are set to the default value suggested by NeuroShell2 (1996) and given by,

$$N_h = \frac{(N_i + N_o)}{2} + \sqrt{N_{trn}} \qquad (8.16)$$

where N_i, N_o and N_{trn} are the number of input nodes, number of output nodes and number of training patterns. Based on equation 8.16, the number of hidden nodes is set to 11 as an initial trial.

While training, the mean squared error (MSE) of the training and testing data patterns is monitored. The MSE for both data sets decreases rapidly, until a point in time when the decrease in the MSE of the training set slows down. The training is terminated when no appreciable improvement in the testing data set MSE (= 0.0006) is observed for 40,000 training events. The network weights are saved at this point. The saved network is applied to the production set that contains 16 data patterns (see Table 8.1) not "seen" yet by the network. A R^2 value of 0.978 is obtained, which is quite satisfactory.

To see if the network performance improves by increasing the number of hidden nodes, the number of hidden nodes is increased to 15, but the performance deteriorates a bit. It is thus decided to decrease the number of hidden nodes. As a second trial, the number of hidden nodes N_h is fixed using the formula suggested by Khanduri et al. (1995b):

$$N_h = 2*(N_i + N_o) \qquad (8.17)$$

Thus, 8 hidden nodes are selected for the second trial. The training process is again repeated afresh and the network is saved based on a criteria similar to the first trial. The network performance somewhat improves as compared to 11 hidden nodes. Thus, it is decided to decrease the number of hidden nodes steadily till the best response is obtained. The hidden nodes are set to 7, 6, 5 and 4.

Figure 8.4 shows the performance of the NN with different numbers of hidden nodes. Network with 5 hidden nodes is the clear winner since it gives the highest R^2 for the overall data, the training set, the testing set and the production set.

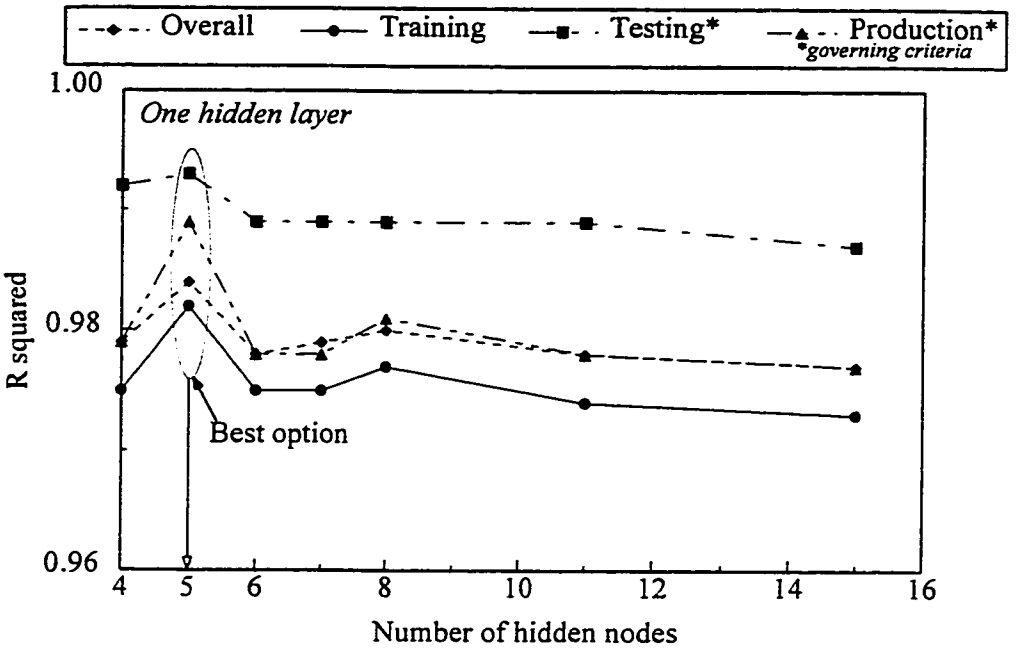

Figure 8.4 Selection of the most suitable NN architecture for modelling Shielding Factors

Figure 8.5 shows the scatter plot comparing the Observed (experimental) and Predicted (NN) values of SF with 5 hidden nodes. The diagonal is the line of maximum correlation between the two graphed variables. Data points close to this line indicate a strong relationship between observed and predicted outputs, or in other words, a good prediction. Table 8.3 shows the NN statistics for the various architectures used. The network with 5 hidden nodes gives the largest number of correct responses in all categories (see *"Percent within..."*). Thus, a single layer NN with 5 hidden nodes provides the best modelling of wind-induced shielding effects. Consequently, the formula

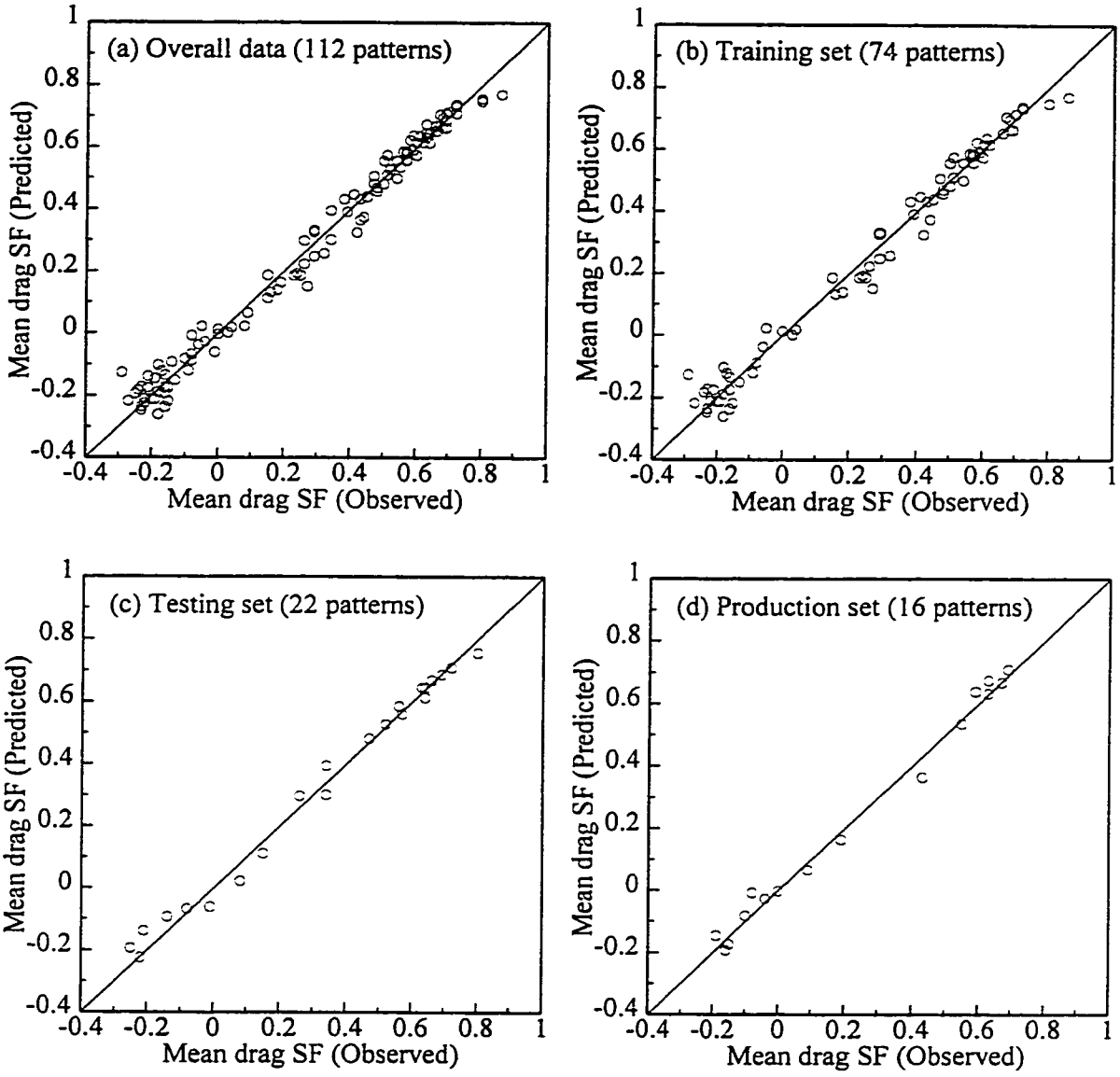

Figure 8.5 NN modelling of Shielding Factors (SF) with 5 hidden nodes BPNN - Comparisons between Observed (experimental) and Predicted (Neural network) results

Table 8.3 NN modelling of Shielding Factors: Statistics of NN simulations for a single layer BPNN with different number of hidden nodes.

: *Best option.*

Number of Hidden Nodes	**4**	**5**	**6**	**7**	**8**	**11**	**15**
Data set	*Overall statistics: Complete set (112 patterns processed)*						
R squared:	0.979	0.984	0.978	0.979	0.980	0.978	0.977
Mean squared error:	0.002	0.002	0.003	0.002	0.002	0.003	0.003
Mean absolute error:	0.038	0.033	0.038	0.037	0.038	0.039	0.040
Max. absolute error:	0.154	0.164	0.164	0.159	0.154	0.171	0.148
Percent within 5%:	36	38	37	35	31	36	37
Percent within 5% to 10%:	16	11	19	21	21	19	15
Percent within 10% to 20%:	18	23	8	13	13	11	12
Percent within 20% to 30%:	13	13	12	13	13	13	8
Percent over 30%:	16	14	23	16	20	21	27
Data set	*Training set (74 patterns processed)*						
R squared:	0.975	0.982	0.975	0.975	0.977	0.974	0.973
Mean squared error:	0.003	0.002	0.003	0.003	0.003	0.003	0.003
Mean absolute error:	0.041	0.036	0.040	0.041	0.040	0.041	0.043
Max. absolute error:	0.154	0.164	0.164	0.159	0.154	0.171	0.148
Percent within 5%:	32	36	36	32	28	34	36
Percent within 5% to 10%:	18	12	20	22	23	20	16
Percent within 10% to 20%:	20	24	9	15	18	14	14
Percent within 20% to 30%:	9	11	9	9	9	11	8
Percent over 30%:	19	15	23	20	20	20	24
Data set	*Testing set (22 patterns processed)*						
R squared:	0.992	0.993	0.989	0.989	0.989	0.989	0.987
Mean squared error:	0.001	0.001	0.001	0.001	0.001	0.001	0.002
Mean absolute error:	0.024	0.023	0.028	0.029	0.028	0.027	0.030
Max. absolute error:	0.064	0.063	0.085	0.072	0.076	0.084	0.095
Percent within 5%:	55	55	50	50	50	55	45
Percent within 5% to 10%:	9	23	14	5	14	14	14
Percent within 10% to 20%:	14	5	5	18	5	5	9
Percent within 20% to 30%:	18	14	9	9	14	9	5
Percent over 30%:	5	5	23	18	18	18	27
Data set	*Production set (16 NEW patterns processed)*						
R squared:	0.979	0.989	0.978	0.978	0.981	0.978	0.977
Mean squared error:	0.002	0.001	0.003	0.002	0.002	0.003	0.003
Mean absolute error:	0.041	0.028	0.041	0.042	0.039	0.042	0.042
Max. absolute error:	0.104	0.072	0.107	0.108	0.103	0.122	0.117
Percent within 5%:	25	25	19	19	19	19	25
Percent within 5% to 10%:	19	13	19	19	19	19	13
Percent within 10% to 20%:	13	25	6	13	6	6	6
Percent within 20% to 30%:	19	25	25	31	31	25	13
Percent over 30%:	19	6	25	13	19	25	38

Note: Percentages may not add up to 100 due to truncation errors (see section 8.3.3).

for the number of hidden nodes N_h , that relates the number of input nodes and output nodes by a simple expression, is now revised to:

$$N_h = 2*N_i - N_o \tag{8.18}$$

where N_i and N_o are the number of input and output nodes, respectively.

It would be worthwhile to compare the performance of NN with the results of the empirical regression equations for the same problem, suggested in chapter 7. Table 8.4 compares the results of the above NN modelling with the empirical equations. The statistics for the empirical equation are an average of the three equations (Equations 7.6, 7.7 and 7.8) that were suggested for buildings of narrow, medium and large widths. The statistics for NN are the overall statistics for the 5 hidden node NN model taken from Table 8.3.

Table 8.4 Shielding Factors - Comparison of empirical and NN predictions

Statistics	*Empirical*	*NN*
R squared	0.967	0.984
Mean squared error	0.003	0.002
Mean absolute error	0.049	0.033

It can be seen from the above table that the NN gives a better performance than empirical regression based on the Levenberg-Marquardt algorithm (Grace 1994). This is significant in that, unlike the NN model which considers only 65% of the overall data for training, the entire data was used for developing the empirical equations. Moreover, NN gives better results than regression even for the data not used in the training of the network (see statistics in Table 8.3 for the *Production set*).

The above comparison reinforces the suggestion of Khanduri et al. (1995b) that NN models consistently provide a better mapping of the input variables as compared to multiple non-linear regression analysis of up to the fourth order.

8.5 Development of NN Models for Mean Drag and Mean Lift Interference Effects

Mean drag and lift data sets are much bigger than the Shielding Factor data (see Table 8.1) modelled above. Also, in addition to b_i / b_p, h_i / h_p and Sx / b_p, the input variables now include Sy / b_p, the incident angle θ and the longitudinal turbulence intensity of wind, I_v as well. The various statistics of the input-output data patterns for mean loads are shown in Table 8.5.

Table 8.5 Statistics of Mean Drag and Mean Lift data

Statistics	*Inputs*						*Output*
	$\theta/45°$	I_v	b_i/b_p	h_i/h_p	Sx/b_p	Sy/b_p	
				Mean Drag			IF
Minimum	0.00	0.07	0.67	1.00	-4.00	-6.00	-0.31
Maximum	1.00	0.25	2.00	2.00	14.00	8.00	1.36
Mean	0.15	0.08	1.22	1.27	3.31	1.37	0.83
Standard Dev.	0.30	0.04	0.40	0.36	4.66	2.23	0.27
				Mean Lift			$\overline{C}_l$
Minimum	0.00	0.07	0.67	1.00	-4.00	-6.00	-0.35
maximum	1.00	0.25	2.00	2.00	12.00	8.00	1.61
Mean	0.17	0.08	1.19	1.22	2.81	1.67	0.13
Standard Dev.	0.32	0.04	0.38	0.37	4.01	2.69	0.29

Owing to the increase in the size and complexity of the data set, it is expected that the formula suggested for the number of hidden nodes in equation 8.18 may not work in this case, and even the number of hidden layers may have to be increased. However, as an initial

guess for modelling mean drag IF, a single hidden layer with the number of hidden nodes set at 13, as per equation 8.18 is used.

As expected, the network response is poor. The mean squared error (MSE) for the test gets stuck at 0.0044 and makes no progress thereafter. This MSE is inadequate in modelling the IFs satisfactorily, for the R^2 value for the training, testing and production sets is 0.79, 0.77 and 0.78, respectively, rather unpersuasive for good predictions. An R^2 value over 0.90 is deemed to be acceptable.

As the next trial, the value of hidden nodes is increased to 35, the value calculated as per equation 8.16. An immediate improvement in the NN performance is obtained. The network is trained several times by varying the number of hidden nodes around this value and the performance of the network monitored closely. The best results are obtained with 34 hidden nodes. The R^2 for all data categories, except the test set, is above 0.90. Some extreme and intermediate cases, with the number of hidden nodes set to 7, 15, 20 and 40, were also checked but the performance of the network worsened.

Although results for the single layer, 34-hidden nodes architecture are quite satisfactory, it was decided to check if the behaviour of the network would improve by increasing the number of hidden layers to two. The total number of hidden nodes is kept the same (34), but distributed equally between the two hidden layers, so that each hidden layer now has 17 nodes. A significant improvement in the results is obtained, especially in the percentage of predicted output within 10% of the actual output for the production set ("unseen data"), which increases to 79% from 67% for the single hidden layer architecture. After several trials with different numbers of hidden nodes, the 2-hidden layers architecture with 17 nodes in each layer is retained.

Further improvement possibilities are explored using the General Regression Neural Network (GRNN) architecture. As explained before, the number of hidden nodes in GRNN is set to the number of training patterns, 972 in this case (see Table 8.1). GRNN squarely beats both the above tested architectures in all performance criteria. This is a significant development, for GRNN is a fairly new concept, yet to acquire the popularity and acceptance of BPNN for engineering applications. The performance of the three NN architectures for modelling mean drag IF is compared in Figure 8.6. The figure shows that GRNN is the best architecture for modelling wind-induced IF for mean drag.

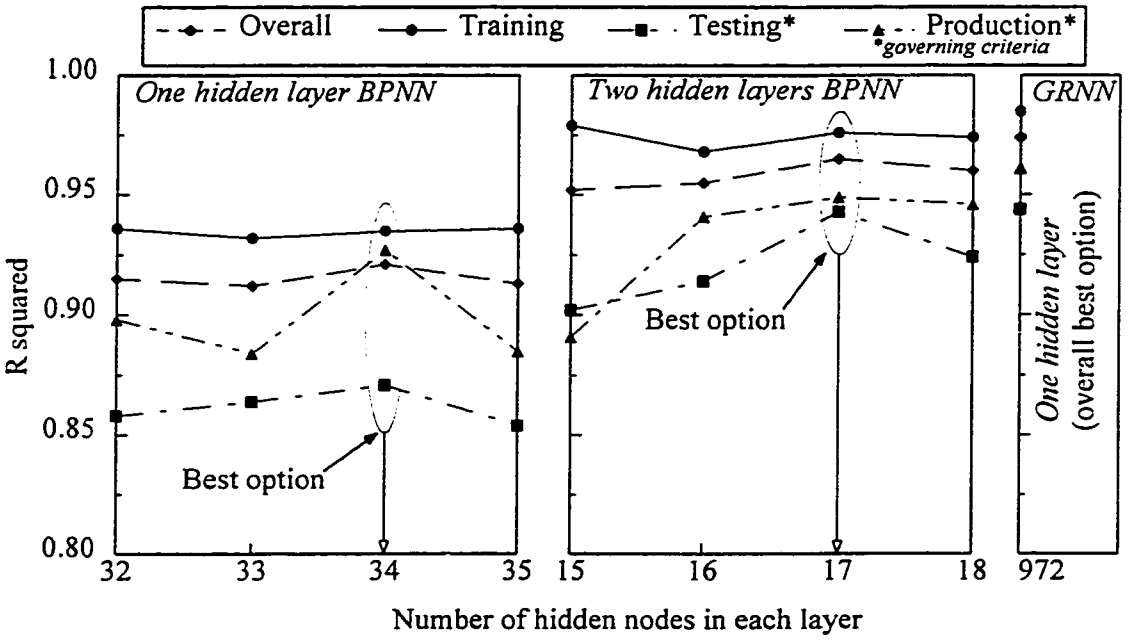

Figure 8.6 Selection of the most suitable NN architecture for modelling mean drag interference effects

Figure 8.7 shows the scatter graph for the GRNN model. The detailed statistics of NN simulations for the above NN architectures are shown in Table 8.6. It should be noted that

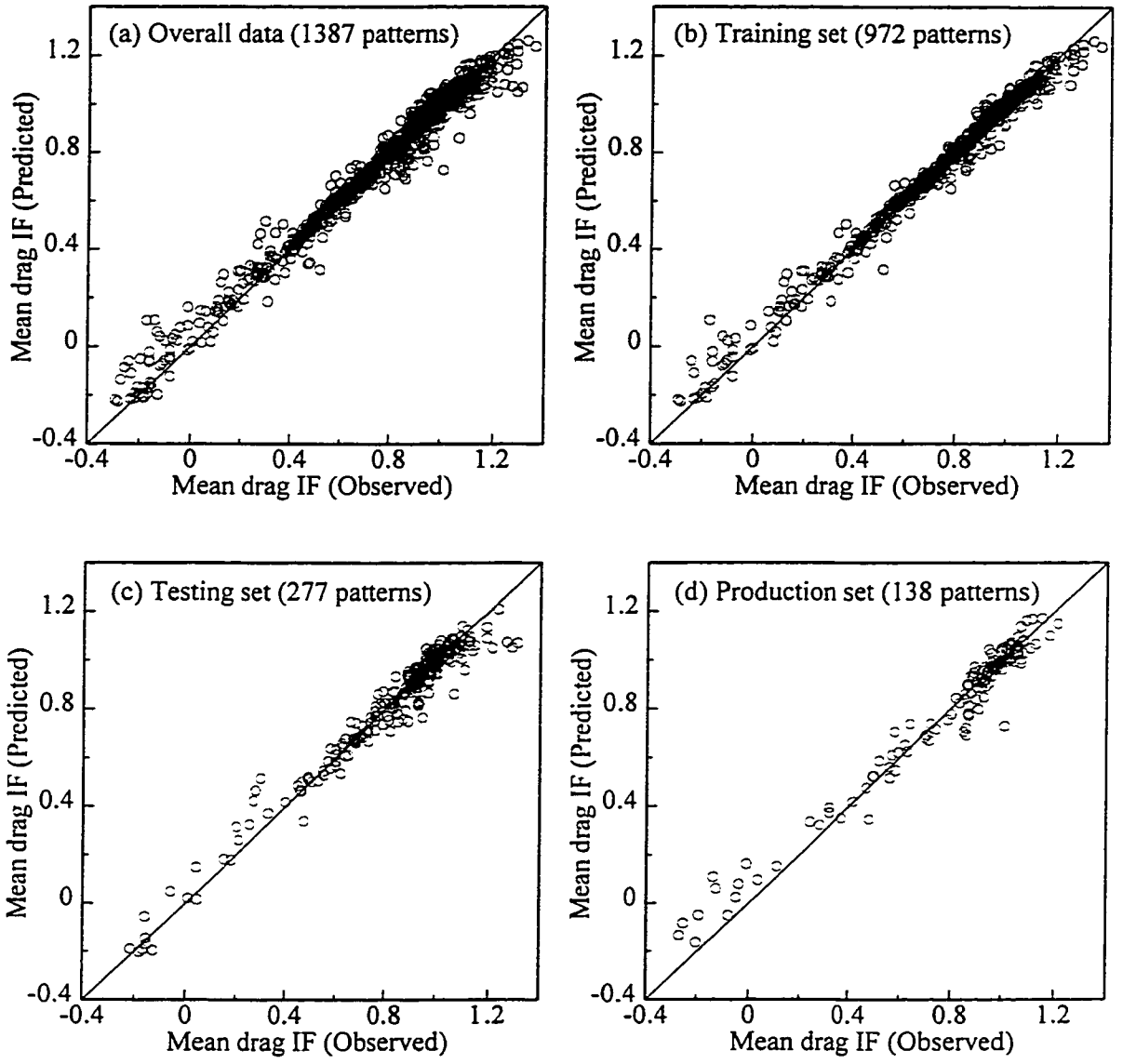

Figure 8.7 NN modelling of mean drag Interference Factors (IF) with GRNN - Comparisons between Observed (experimental) and Predicted (Neural Network) results

Table 8.6 NN modelling of mean drag interference effects: Statistics of NN simulations with various NN architectures.

▨ : *Best option in each category.*

Architecture	**Backpropagation**								**GRNN**
Number of hidden layers	***One***				***Two***				***One***
Number of hidden nodes	32	33	▨ 34	35	15	16	▨ 17	18	972
Data set	*Overall statistics: Complete set (1387 patterns processed)*								
R squared:	0.915	0.912	0.921	0.913	0.952	0.955	0.965	0.960	0.974
Mean squared error:	0.007	0.007	0.006	0.007	0.004	0.004	0.003	0.003	0.002
Mean absolute error:	0.059	0.060	0.056	0.059	0.036	0.042	0.037	0.038	0.027
Max. absolute error:	0.484	0.706	0.551	0.473	1.082	0.477	0.391	0.590	0.394
Percent within 5%:	48	47	50	50	71	63	69	66	79
Percent within 5% to 10%:	28	27	27	25	19	23	20	20	11
Percent within 10% to 20%:	15	17	13	15	6	9	7	8	5
Percent within 20% to 30%:	3	4	4	5	1	2	1	1	1
Percent over 30%:	6	5	6	5	3	4	3	3	4
Data set	*Training set (972 patterns processed)*								
R squared:	0.936	0.932	0.935	0.936	0.979	0.968	0.976	0.974	0.985
Mean squared error:	0.005	0.005	0.005	0.005	0.002	0.002	0.002	0.002	0.001
Mean absolute error:	0.052	0.053	0.051	0.051	0.029	0.036	0.031	0.033	0.019
Max. absolute error:	0.484	0.417	0.458	0.452	0.252	0.276	0.269	0.254	0.278
Percent within 5%:	51	51	53	55	77	67	73	70	85
Percent within 5% to 10%:	29	27	28	24	16	22	18	19	8
Percent within 10% to 20%:	14	15	12	13	4	7	5	7	3
Percent within 20% to 30%:	3	3	3	4	1	1	1	1	1
Percent over 30%:	4	4	4	4	2	3	2	2	3
Data set	*Testing set (277 patterns processed)*								
R squared:	0.858	0.864	0.871	0.854	0.902	0.914	0.943	0.924	0.944
Mean squared error:	0.012	0.011	0.01	0.012	0.008	0.007	0.005	0.006	0.005
Mean absolute error:	0.076	0.075	0.068	0.078	0.055	0.055	0.046	0.052	0.043
Max. absolute error:	0.426	0.487	0.551	0.473	0.642	0.477	0.322	0.486	0.394
Percent within 5%:	41	40	45	36	57	53	62	58	68
Percent within 5% to 10%:	27	24	25	28	24	26	21	22	16
Percent within 10% to 20%:	18	23	19	20	11	13	10	12	10
Percent within 20% to 30%:	5	7	4	9	2	2	3	3	1
Percent over 30%:	8	7	8	7	6	6	4	5	5
Data set	*Production set (138 NEW patterns processed)*								
R squared:	0.898	0.884	0.927	0.885	0.891	0.941	0.949	0.946	0.961
Mean squared error:	0.012	0.013	0.008	0.013	0.013	0.007	0.006	0.006	0.005
Mean absolute error:	0.074	0.077	0.068	0.08	0.053	0.054	0.053	0.048	0.047
Max. absolute error:	0.433	0.706	0.316	0.42	1.082	0.397	0.391	0.590	0.283
Percent within 5%:	46	38	38	41	58	52	52	55	62
Percent within 5% to 10%:	17	28	29	22	23	22	27	25	17
Percent within 10% to 20%:	18	19	14	20	9	15	9	11	9
Percent within 20% to 30%:	5	4	9	7	1	1	2	2	3
Percent over 30%:	13	12	9	9	8	9	9	7	9

Note: Percentages may not add up to 100 due to truncation errors (see secion 8.3.3).

GRNN, while producing better predictions than BPNN, requires more computational effort. Typical network training time (CPU) for a two-layers BPNN is about 30 minutes, whereas, GRNN requires about 45 minutes for modelling mean drag IF.

Mean lift data is also modelled similarly. Figure 8.8 shows the performance of a single-layer BPNN, 2-layers BPNN and GRNN architectures. Based on this figure, a 35-hidden nodes single layer and a two-hidden layers with 17 hidden nodes in each layer are the best architectures in each category. This time, GRNN, while producing excellent results in the overall, training set and testing set category, lags behind the two-hidden layers BPNN in the production set category. Figure 8.9 shows the scatter plot for the GRNN model. Table 8.7 shows the detailed statistics of NN simulations for mean lift.

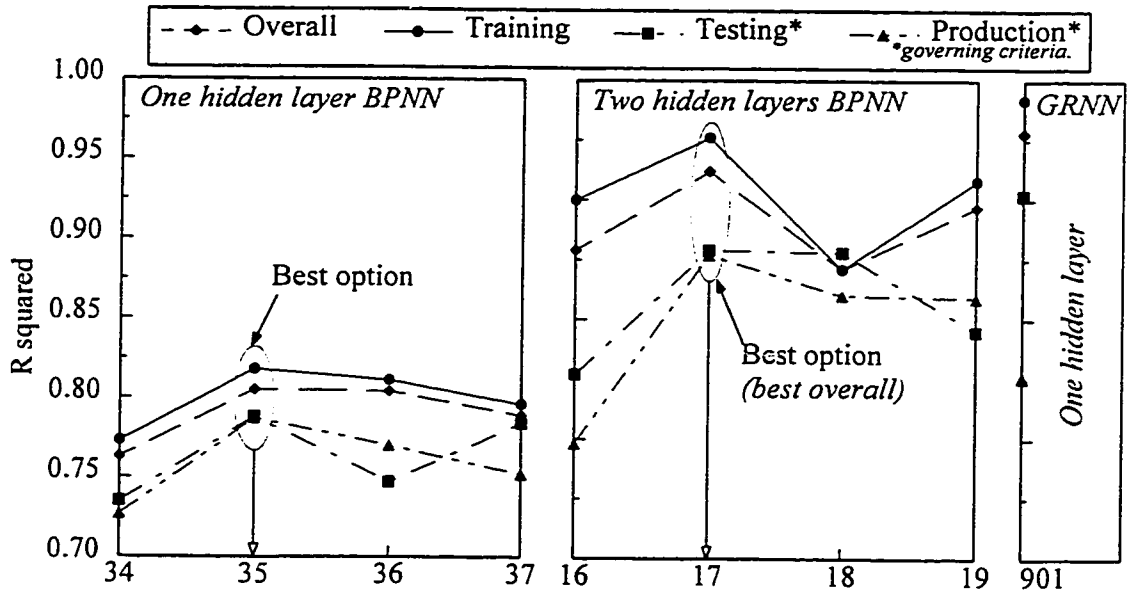

Figure 8.8 Selection of the most suitable NN architecture for modelling mean lift interference effects

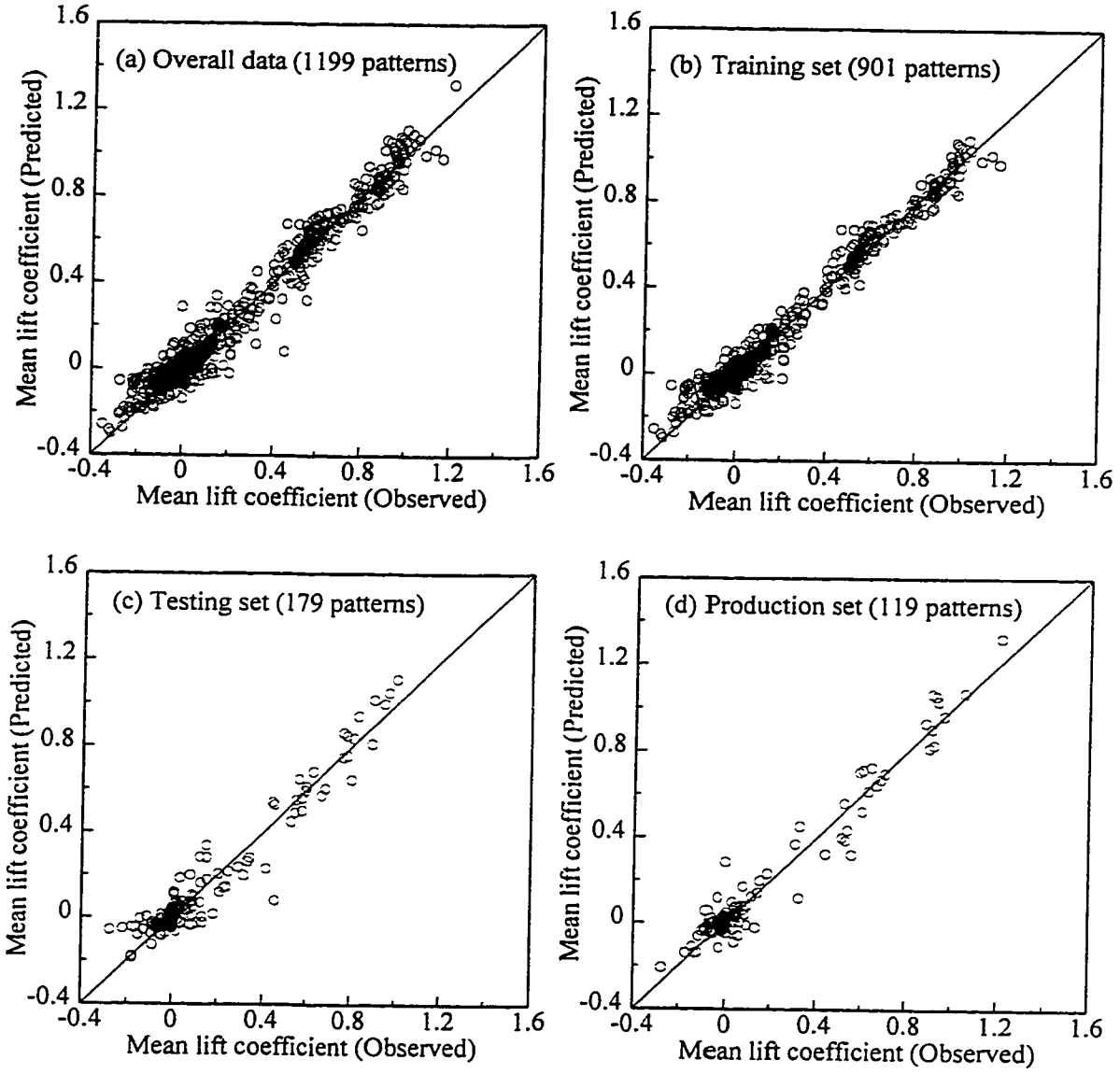

Figure 8.9 NN modelling of mean lift coefficient with GRNN - Comparisons between Observed (experimental) and Predicted (Neural Network) results

Table 8.7 NN modelling of mean lift interference effects: Statistics of NN simulations with various NN architectures.

: *Best option in each category.*

Architecture	**Backpropagation**								**GRNN**
Number of hidden layers	***One***				***Two***				***One***
Number of hidden nodes	34	35	36	37	16	17	18	19	901
Data set	*Overall statistics: Complete set (1199 patterns processed)*								
R squared:	0.763	0.805	0.804	0.789	0.929	0.962	0.921	0.947	0.978
Mean squared error:	0.020	0.016	0.016	0.017	0.006	0.003	0.007	0.004	0.002
Mean absolute error:	0.093	0.086	0.080	0.086	0.047	0.035	0.049	0.042	0.017
Max. absolute error:	1.092	0.707	1.188	1.118	0.625	0.409	0.834	0.586	0.449
Percent within 5%:	3	4	6	6	10	12	10	9	32
Percent within 5% to 10%:	5	4	5	5	7	9	8	7	12
Percent within 10% to 20%:	8	8	8	8	9	12	9	9	11
Percent within 20% to 30%:	7	7	5	5	6	7	7	6	7
Percent over 30%:	66	66	66	65	56	49	56	58	28
Data set	*Training set (901 patterns processed)*								
R squared:	0.773	0.818	0.811	0.796	0.950	0.976	0.921	0.958	0.992
Mean squared error:	0.019	0.015	0.016	0.017	0.004	0.002	0.007	0.003	0.001
Mean absolute error:	0.091	0.083	0.079	0.085	0.041	0.030	0.049	0.039	0.010
Max. absolute error:	1.092	0.707	1.188	1.118	0.452	0.230	0.834	0.357	0.449
Percent within 5%:	4	4	5	6	12	14	10	11	38
Percent within 5% to 10%:	6	3	5	4	7	9	7	7	12
Percent within 10% to 20%:	7	8	8	8	10	12	9	9	11
Percent within 20% to 30%:	7	6	5	6	6	8	7	6	6
Percent over 30%:	65	66	66	65	54	47	55	56	21
Data set	*Testing set (179 patterns processed)*								
R squared:	0.735	0.788	0.747	0.784	0.877	0.929	0.928	0.895	0.952
Mean squared error:	0.018	0.015	0.017	0.015	0.008	0.005	0.005	0.007	0.004
Mean absolute error:	0.096	0.081	0.093	0.083	0.058	0.047	0.045	0.053	0.034
Max. absolute error:	0.475	0.450	0.473	0.497	0.466	0.369	0.460	0.361	0.409
Percent within 5%:	2	4	4	3	7	8	11	3	14
Percent within 5% to 10%:	2	3	3	7	5	6	8	7	8
Percent within 10% to 20%:	9	8	7	6	6	12	9	9	11
Percent within 20% to 30%:	8	8	4	6	8	5	5	7	10
Percent over 30%:	69	68	70	69	65	60	57	65	47
Data set	*Production set (119 NEW patterns processed)*								
R squared:	0.727	0.787	0.770	0.752	0.848	0.927	0.910	0.909	0.876
Mean squared error:	0.028	0.022	0.024	0.026	0.016	0.008	0.009	0.009	0.007
Mean absolute error:	0.104	0.097	0.084	0.097	0.075	0.054	0.054	0.055	0.043
Max. absolute error:	0.735	0.526	0.792	0.729	0.625	0.409	0.670	0.586	0.426
Percent within 5%:	4	14	4	7	6	8	11	9	13
Percent within 5% to 10%:	4	7	9	9	10	10	8	8	13
Percent within 10% to 20%:	10	7	9	11	11	17	12	8	10
Percent within 20% to 30%:	8	3	5	3	4	8	4	8	4
Percent over 30%:	65	61	64	62	61	48	57	58	47

Note: Percentages may not add up to 100 due to truncation errors (see section 8.3.3).

8.6 Development of NN Models for Fluctuating Load Interference Factors

Fluctuating load IFs are non-monotonic in nature and are thus more complex to model than mean load interference effects. The various statistics of the input-output data patterns for fluctuating loads are shown in Table 8.8.

The networks were trained as done for mean loads. Figures 8.10 and 8.11 show the performance of a single-layer, 2-layers BPNN and GRNN architectures for fluctuating drag and fluctuating lift, respectively. Thus, for fluctuating drag the best BPNN architectures are, one-hidden layer with 32 nodes and two-hidden layers with 14 nodes in each layer and for fluctuating lift, one hidden layer with 33 nodes and two-hidden layers with 17 nodes in each

Table 8.8 Statistics of Fluctuating Drag and Fluctuating Lift data

Statistics	*Inputs*						*Output*
	$\theta/45°$	I_v	b/b_p	h/h_p	Sx/b_p	Sy/b_p	
	Fluctuating Drag						IF
Minimum	0.00	0.07	0.67	1.00	-6.00	-6.00	0.55
Maximum	1.00	0.25	2.00	2.00	14.00	8.00	1.79
Mean	0.17	0.08	1.21	1.20	3.41	1.54	1.15
Standard Dev.	0.32	0.04	0.39	0.35	4.53	2.63	0.18
	Fluctuating Lift						IF
Minimum	0.00	0.07	0.67	1.00	-6.00	-7.00	0.44
maximum	1.00	0.25	2.00	2.00	12.00	8.00	1.82
Mean	0.17	0.09	1.18	1.21	3.04	1.77	1.10
Standard Dev.	0.32	0.05	0.37	0.36	4.33	2.99	0.22

layer. But, GRNN is the overall winner in both cases and gives a much better prediction of the so-called "unseen" production set data than the BPNN architectures. Figures 8.12 and 8.13 show the scatter plots for fluctuating drag and fluctuating lift, with the GRNN model. Tables 8.9 and 8.10 show the detailed statistics of the NN simulations with various NN architectures for fluctuating drag and fluctuating lift, respectively.

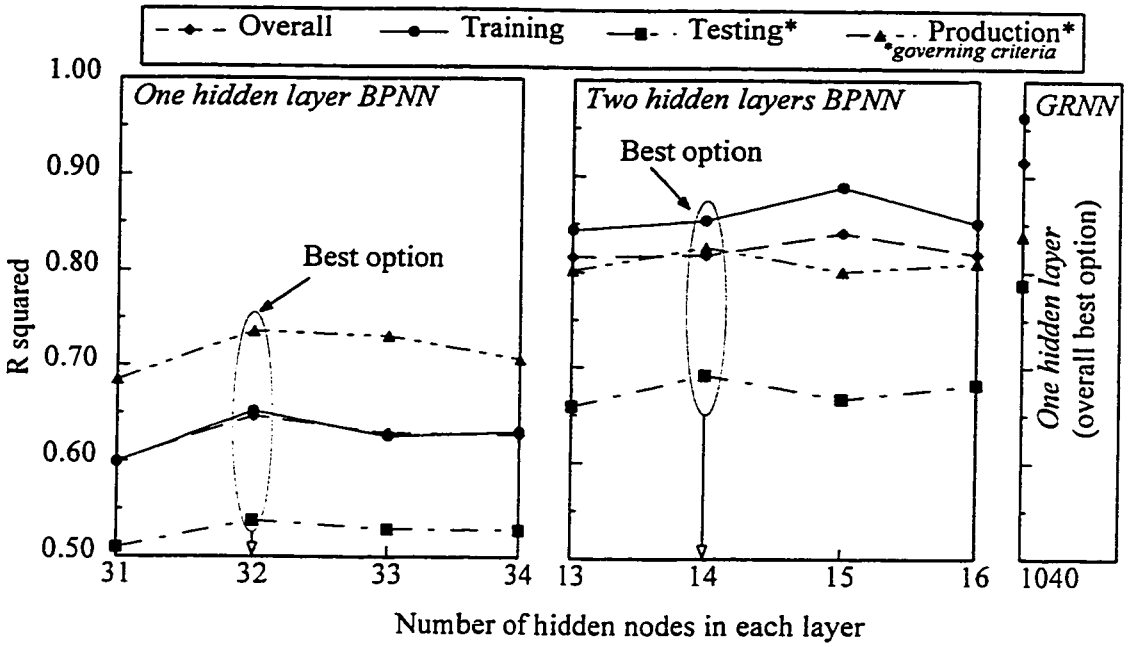

Figure 8.10 Selection of the most suitable NN architecture for modelling fluctuating drag interference effects

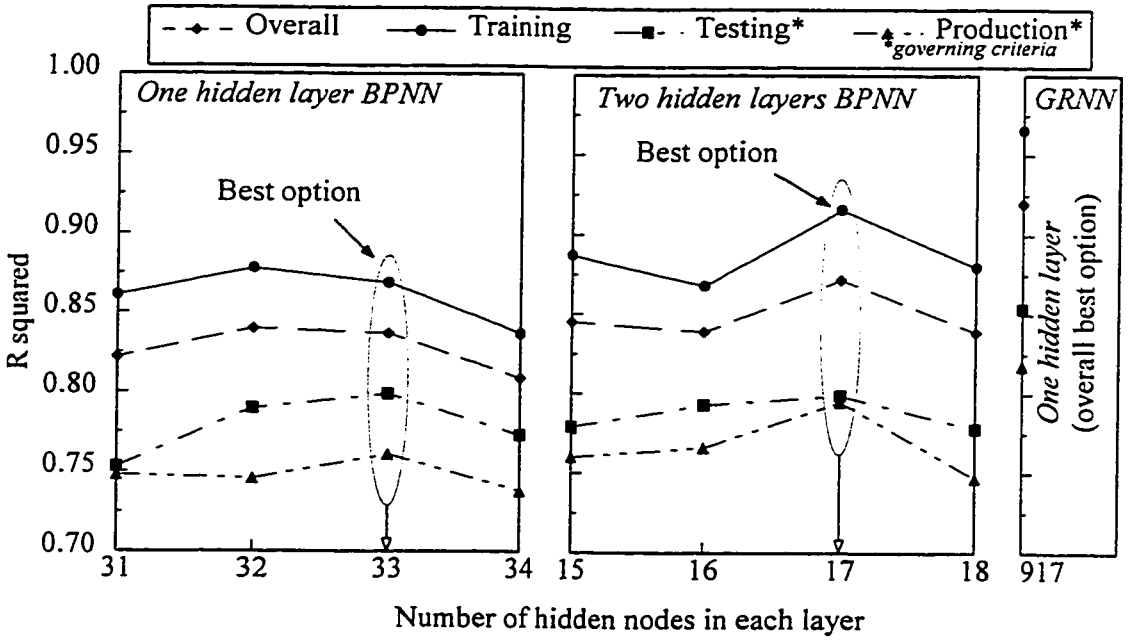

Figure 8.11 Selection of the most suitable NN architecture for modelling fluctuating lift interference effects

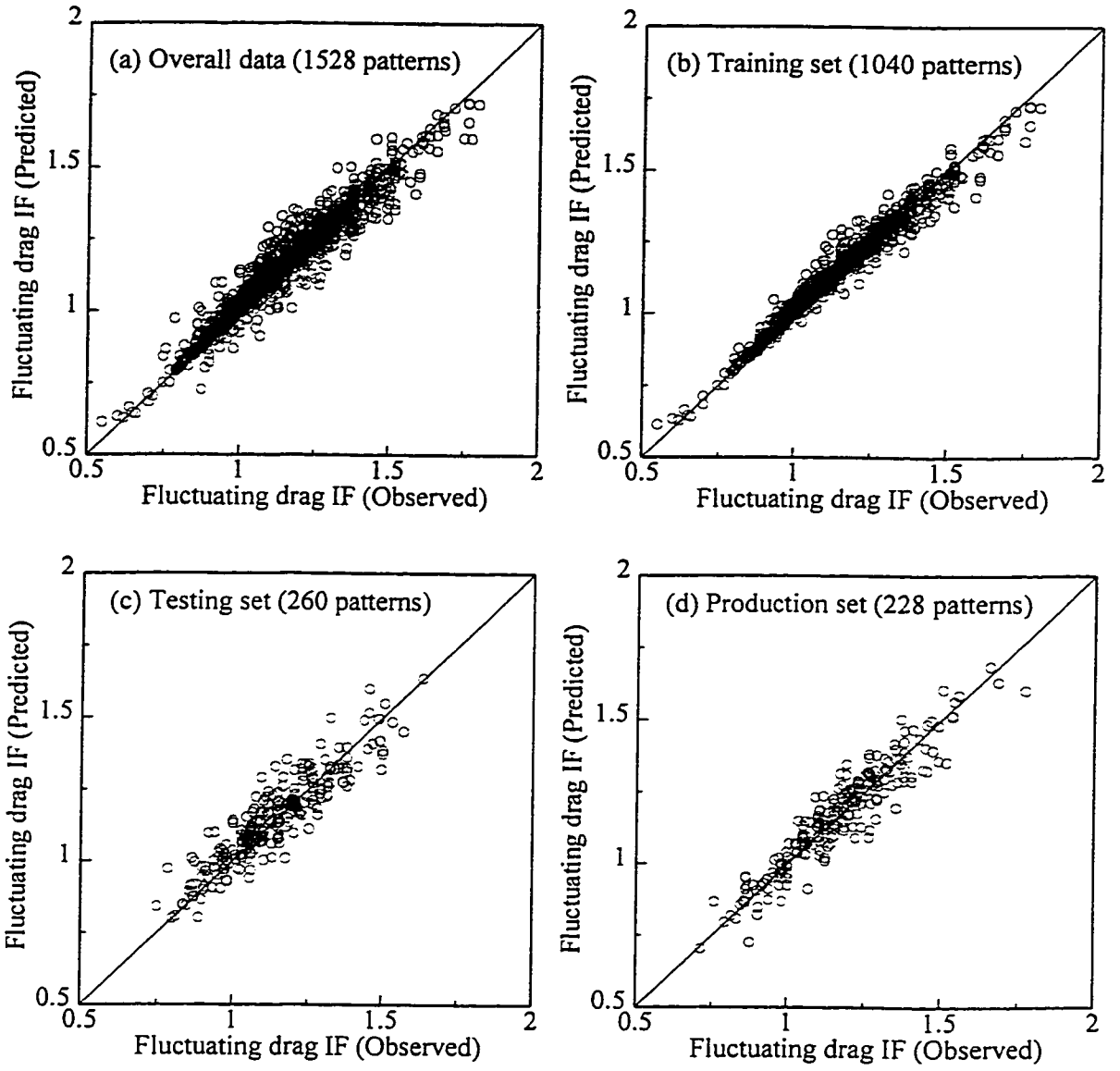

Figure 8.12 NN modelling of fluctuating drag Interference Factors (IF) with GRNN - Comparisons between Observed (experimental) and Predicted (Neural Network) results

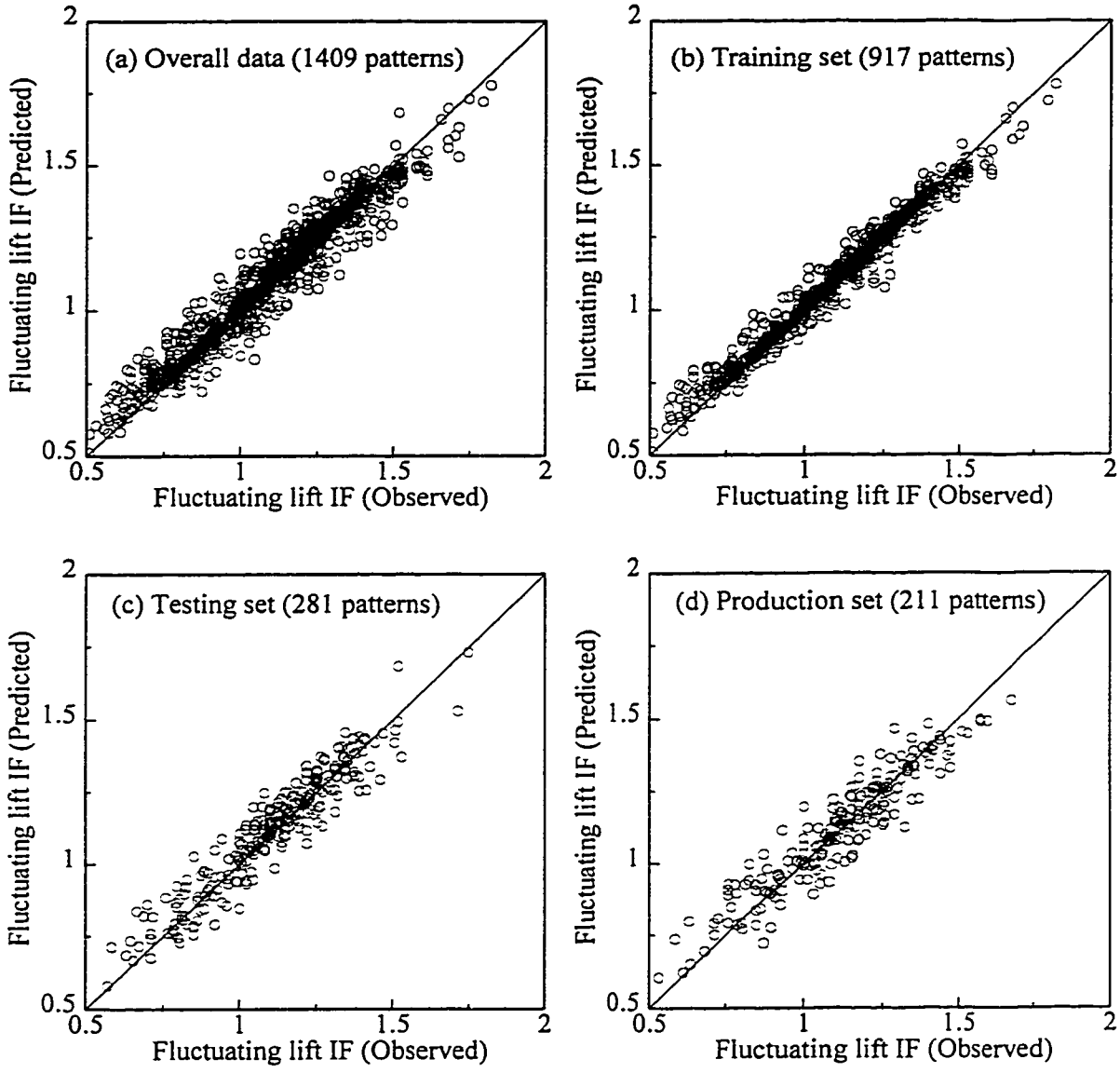

Figure 8.13 NN modelling of fluctuating lift Interference Factors (IF) with GRNN - Comparisons between Observed (experimental) and Predicted (Neural Network) results

Table 8.9 NN modelling of fluctuating drag interference effects: Statistics of NN simulations with various NN architectures.

▨ : *Best option in each category.*

Architecture	**Backpropagation**								**GRNN**
Number of hidden layers	***One***				***Two***				***One***
Number of hidden nodes	31	▨ 32	33	34	13	▨ 14	15	16	1040
Data set	*Overall statistics: Complete set (1528 patterns processed)*								
R squared:	0.600	0.647	0.629	0.628	0.816	0.818	0.841	0.819	0.916
Mean squared error:	0.013	0.011	0.012	0.012	0.006	0.006	0.005	0.006	0.003
Mean absolute error:	0.082	0.077	0.079	0.077	0.057	0.057	0.052	0.057	0.032
Max. absolute error:	0.486	0.532	0.470	0.540	0.445	0.315	0.327	0.291	0.322
Percent within 5%:	49	50	48	52	61	61	65	61	84
Percent within 5% to 10%:	27	28	31	26	27	27	25	28	12
Percent within 10% to 20%:	20	18	17	18	11	10	9	11	4
Percent within 20% to 30%:	3	2	2	2	1	1	1	1	0
Percent over 30%:	1	1	1	1	0	0	0	0	0
Data set	*Training set (1040 patterns processed)*								
R squared:	0.599	0.652	0.626	0.631	0.844	0.854	0.889	0.851	0.962
Mean squared error:	0.013	0.011	0.012	0.012	0.005	0.005	0.004	0.005	0.001
Mean absolute error:	0.082	0.077	0.079	0.077	0.053	0.051	0.044	0.052	0.021
Max. absolute error:	0.486	0.505	0.470	0.511	0.322	0.315	0.253	0.291	0.272
Percent within 5%:	49	50	48	52	64	65	71	64	92
Percent within 5% to 10%:	27	29	32	27	27	25	23	27	6
Percent within 10% to 20%:	19	18	17	18	8	8	6	8	1
Percent within 20% to 30%:	3	3	2	2	1	1	0	0	0
Percent over 30%:	1	1	1	1	0	0	0	0	0
Data set	*Testing set (260 patterns processed)*								
R squared:	0.510	0.538	0.529	0.528	0.659	0.692	0.667	0.682	0.787
Mean squared error:	0.014	0.013	0.014	0.014	0.010	0.009	0.010	0.009	0.006
Mean absolute error:	0.087	0.083	0.085	0.081	0.073	0.070	0.074	0.075	0.057
Max. absolute error:	0.486	0.532	0.447	0.540	0.445	0.304	0.327	0.272	0.316
Percent within 5%:	46	45	47	51	50	54	51	47	63
Percent within 5% to 10%:	26	30	28	23	31	27	27	31	26
Percent within 10% to 20%:	23	20	20	21	17	17	19	18	10
Percent within 20% to 30%:	4	4	5	4	2	1	3	3	1
Percent over 30%:	1	1	1	1	1	1	0	0	0
Data set	*Production set (228 NEW patterns processed)*								
R squared:	0.685	0.736	0.731	0.707	0.802	0.826	0.801	0.810	0.838
Mean squared error:	0.010	0.009	0.009	0.010	0.006	0.006	0.007	0.006	0.005
Mean absolute error:	0.077	0.070	0.071	0.073	0.064	0.058	0.062	0.060	0.052
Max. absolute error:	0.334	0.324	0.312	0.360	0.252	0.230	0.273	0.257	0.322
Percent within 5%:	50	50	53	53	55	59	56	60	68
Percent within 5% to 10%:	26	34	25	28	29	30	32	27	21
Percent within 10% to 20%:	21	14	21	18	14	11	11	11	10
Percent within 20% to 30%:	1	0	0	1	1	1	1	2	0
Percent over 30%:	1	1	1	1	0	0	0	0	0

Note: Percentages may not add up to 100 due to truncation errors (see section 8.3.3).

Table 8.10 NN modelling of fluctuating lift interference effects: Statistics of NN simulations with various NN architectures.

: *Best option in each category.*

Architecture	**Backpropagation**								GRNN
Number of hidden layers	***One***				***Two***				***One***
Number of hidden nodes	31	32	33	34	15	16	17	18	917
Data set	*Overall statistics: Complete set (1409 patterns processed)*								
R squared:	0.822	0.840	0.837	0.809	0.845	0.839	0.872	0.839	0.920
Mean squared error:	0.009	0.008	0.008	0.010	0.008	0.008	0.006	0.008	0.004
Mean absolute error:	0.072	0.067	0.068	0.072	0.066	0.066	0.059	0.067	0.039
Max. absolute error:	0.390	0.412	0.412	0.417	0.449	0.522	0.381	0.376	0.383
Percent within 5%:	49	54	54	51	53	55	60	53	77
Percent within 5% to 10%:	28	26	26	27	28	25	24	27	14
Percent within 10% to 20%:	17	15	16	16	15	15	13	15	6
Percent within 20% to 30%:	4	3	3	3	3	3	2	4	2
Percent over 30%:	2	2	2	3	2	2	1	1	1
Data set	*Training set (917 patterns processed)*								
R squared:	0.861	0.878	0.869	0.837	0.887	0.868	0.916	0.880	0.966
Mean squared error:	0.007	0.006	0.007	0.008	0.006	0.007	0.004	0.006	0.002
Mean absolute error:	0.063	0.058	0.060	0.065	0.056	0.060	0.049	0.057	0.025
Max. absolute error:	0.316	0.305	0.412	0.398	0.293	0.374	0.311	0.340	0.258
Percent within 5%:	54	60	58	54	59	59	65	57	87
Percent within 5% to 10%:	29	25	25	27	27	24	25	27	9
Percent within 10% to 20%:	13	11	13	14	12	13	9	12	3
Percent within 20% to 30%:	2	2	2	3	2	3	1	2	1
Percent over 30%:	1	1	1	1	1	1	0	1	0
Data set	*Testing set (281 patterns processed)*								
R squared:	0.753	0.790	0.799	0.773	0.779	0.793	0.799	0.778	0.854
Mean squared error:	0.013	0.011	0.011	0.012	0.012	0.011	0.011	0.012	0.080
Mean absolute error:	0.089	0.082	0.080	0.080	0.081	0.077	0.075	0.081	0.063
Max. absolute error:	0.324	0.311	0.386	0.417	0.449	0.522	0.381	0.376	0.330
Percent within 5%:	40	42	46	47	44	49	49	47	57
Percent within 5% to 10%:	26	29	28	28	29	25	25	27	26
Percent within 10% to 20%:	23	23	19	17	19	17	17	17	11
Percent within 20% to 30%:	6	4	2	3	4	5	5	6	2
Percent over 30%:	5	3	5	5	5	4	4	4	5
Data set	*Production set (211 NEW patterns processed)*								
R squared:	0.748	0.746	0.761	0.738	0.760	0.766	0.795	0.747	0.818
Mean squared error:	0.013	0.013	0.012	0.013	0.012	0.012	0.010	0.013	0.009
Mean absolute error:	0.088	0.088	0.085	0.088	0.086	0.080	0.078	0.087	0.067
Max. absolute error:	0.390	0.412	0.368	0.404	0.355	0.432	0.270	0.347	0.383
Percent within 5%:	40	40	45	42	39	45	50	42	57
Percent within 5% to 10%:	28	28	25	24	32	29	22	37	2
Percent within 10% to 20%:	22	23	23	26	22	18	24	24	14
Percent within 20% to 30%:	7	6	4	3	5	6	3	4	4
Percent over 30%:	2	3	3	4	3	2	0	1	2

Note: Percentages may not add up to 100 due to truncation errors (see section 8.3.3).

8.7 NN Development - Lessons Learnt

Having successfully modelled wind-induced interference effects on buildings using neural networks, several useful conclusions can be derived. These conclusions can serve as guidelines for future NN development, not only on wind-induced interference effects, but also in other areas of wind engineering as well as other applications of a similar nature. These guidelines are stated below:

- One of the major problems facing NN application developers is deciding the number of hidden nodes in a BPNN. For an approximate calculation of the number of hidden nodes N_h, the following two criteria are suggested:

  $$N_h = 2N_i - N_o \tag{8.19}$$

  for number of training data patterns < 200 and $N_i < 5$, and

  $$N_h = \frac{(N_i - N_o)}{2} + \sqrt{N_{trn}} \tag{8.20}$$

  for number of training data patterns > 500 and $N_i > 5$.

  where, N_i, N_o and N_{trn} are the number of input nodes, number of output nodes and number of training patterns. For larger problems, relating the number of hidden nodes with the number of training patterns seems to make sense since in general, the complexity of a NN depends, among other things, on the size of the network training data set. A safe approach would be to begin with three possibilities: Equation 8.19, Equation 8.20 and a value between the two. The worst is eliminated and training resumes on the network, varying N_h around the two remaining values till the value with the lowest acceptable mean squared error (MSE) on the test set is determined. This best configuration is then saved.

- Watch out for networks trapped in local minima. At times, the network may yield scant betterment in the MSE as it goes on and on for several thousand learning events. The only solution in this case is patience. The network (especially large ones) may resume producing regularly decreasing MSE values once again, seemingly in "one great burst of energy". This is true especially for large networks. Therefore, the simulation should be allowed to run for a while before deciding to stop, for the actual behaviour may be lost due to a momentary loss of patience. Moreover with calibration (see section 8.3.3), the danger of overtraining is eliminated.
- Usually one hidden layer is enough for small BPNNs and for monotonic data. More than one hidden layers may be required for large, complex and noisy data. However, the number of hidden layers should be increased only after exhausting all logical possibilities with a single layer. If two hidden layers are required, the number of hidden nodes in each layer is approximately equal to half the number of hidden nodes for the best one-hidden layer configuration.
- GRNN gives a better performance than BPNN. However, there are two drawbacks to GRNN: first the long training times, and second the large number of weights which are generated due to the large number of hidden nodes (= the number of training patterns) in the hidden layer. Computer programs generated using the above weights tend to be very bulky so that compiling and linking such programs with other commercial software becomes quite tedious. The C programming language code generated by NeuroShell2 (1996) for the GRNN model for mean drag IF is about 10,000 lines long. GRNN can be used as a benchmark model against which the performance of BPNN is evaluated. Thus

the training termination criterion of BPNN can be based upon the minimum error reached by a GRNN for a particular network.

- NN represents a better alternative to regression, especially for developing models involving several variables with complex, non-linear relationships.

8.8 Development of an Integrated Building Design Adviser

The detailed experimental study helped generate a database on wind-induced interference effects on buildings. This data was modelled using NN methodology. Thus, for a given sets of relevant input variables, the NN model can provide appropriate output in terms of numbers dubbed Interference Factors. To an expert in wind engineering in general and wind interference effects in particular, these numbers provide a lot of meaningful information with respect to the susceptibility of a building to interference effects. However to the uninitiated, the wealth of information held in these numbers is lost. Thus, to make the NN output meaningful to the building design practitioner, it is important to explain the significance of NN output for building design assistance.

As explained in section 2.5, while NNs help model and acquire knowledge gained form experiments and observations, Knowledge-Based Systems (KBS) can help organize and make this knowledge available in a meaningful fashion. The use of KBS has been well demonstrated and has matured over the years: they are now commonly applied and accepted in the field of engineering design. The advantages and shortcomings of both NN and KBS technologies have been stated in Table 2.1. KBS are essentially computer programs that can capture and manipulate knowledge acquired from human experts in a particular domain and

generate solutions to problems based on a logical reasoning process. NN, on the other hand, generate knowledge through training on data examples and are suitable for situations where data interactions are too complex for an analytical solution. Thus, combining the useful features of both KBS and NN to solve complex engineering problems seems to be a sound proposition.

Khanduri et al. (1995c and 1996) suggest a three-stage integration process between experimental and computerized approaches for solving wind interference problems. This integration process is shown in Figure 8.1, and includes three main stages:

Stage 1: Acquisition of qualitative knowledge through literature and experts,

Stage 2: Acquisition of quantitative knowledge through wind tunnel experiments, and

Stage 3: Modelling and interpretation of the above knowledge and design assistance through NN and KBS.

Having completed the first two stages and part of the third stage (NN modelling), the final step which now remains is the integration of the NN model with the Knowledge-Base to develop a Hybrid Knowledge-Based Design Adviser for wind-induced interference effects. Such an integration will reduce the time required to capture experience from training a NN, as opposed to encoding rules for all possible cases in a KBS. System acceptance is also potentially greater in practical design situations when a reasonable set of questions is asked to the user via a KBS than queries for vague ranges of NN values (Hillman 1990). Such a design adviser will be able to provide useful design advice on wind interference effects at the preliminary design stages.

8.9 NETWIND - A Hybrid Knowledge-Based Design Adviser For Wind-Induced Interference Effects on Buildings

A hybrid knowledge-based design adviser called NETWIND ("NET" highlights the Neural NETwork aspect) is developed to assist the building design process for wind-induced interference effects. NETWIND contains over 3,600 lines of computer code written in C and runs on an IBM PC compatible in a DOS environment. C is the programming language of choice because of ease of integration of various modules with the NN module containing the C-code generated by NeuroShell2 (1996). The modular nature of NETWIND allows for a great degree of independence among the four modules shown in Figure 8.1 such that each can also be used as a "stand-alone" program with minor modifications in the code. The three KBS modules (data collection, conclusion-analysis and design assistance) as well as the integration code between these modules and the NN module is written from scratch in C rather than using a commercial Expert System shell. The main reasons for this customization are ease of integration of the three modules with the NN module, tailoring of the software to the specific requirements of this project, greater portability of the program to other systems and platforms as well as the ease of incorporation of future developments and modifications to NETWIND. The development of the four modules making up NETWIND is explained in the following sub-sections.

8.9.1 The data collection module

During the development phase, qualitative knowledge on interference effects is gathered from literature and experts that helps build a data collection knowledge base, setting

limiting conditions on the data input by the user. On the basis of a detailed analysis of the experimental results of this study general guidelines were formulated in chapters 6 and 7. These guidelines will help build the data collection knowledge base for wind interference effects.

The data collection module (DCM) acts as a pre-processor to the NN data evaluation module, that is built by training on examples generated through wind tunnel experiments, and queries the user for data. It also checks and validates the data within the constraints imposed by the system.

NETWIND operates under certain constraints defined and set up during the exploratory and detailed experiments. These constraints guide the DCM in sorting out and filtering the correct input for NETWIND. It also looks out for erroneous and out-of-range input values and warns the user accordingly. For instance, it checks the spacing between buildings given by the user to see if building footprints overlap - an impossible situation. The various constraints imposed on the input data are:

- Wind direction θ: 0° to 45°
- Longitudinal turbulence intensity I_v of wind at building height: 7% to 25%
- Ratio of interfering and principal building widths b_i/b_p: 2/3 to 2.0
- Ratio of interfering and principal building heights h_i/h_p: 1.0 to 2.0
- Centre-to-centre spacing Sx between buildings along X-axis: $-4b_p$ to $14b_p$
- Centre-to-centre spacing Sy between buildings along Y-axis: $-6b_p$ to $8b_p$

A typical NETWIND data collection session is shown below (user responses are shown in bold text). The complete C-code for this module is given in Appendix C, section C.2.

```
DATA INPUT SCREEN

Use Uniform system of units (suggestion: use metres for length)

Wind direction (0 to 45 degrees, wind from right to left): 0
Longitudinal turbulence intensity of wind (7% to 25%): 7
Principal building width (square): 20
Interfering building width (square): 20
Principal building height (height/width = 3 to 5): 80
Interfering building height (height/width = 2 to 8): 80
Centre-to-centre spacing between buildings along X-axis: 70
Centre-to-centre spacing between buildings along Y-axis: 60

Proceed to RESULTS and ANALYSIS screen ? (Y/N):
```

8.9.2 NN data evaluation module

If the limiting conditions regarding the geometries and arrangement of the interfering buildings and characteristics of wind and upstream terrain are satisfied, the NN module evaluates the input data and generates solutions (interference factor values) to be passed on to the post-processor, which is the KBS conclusion-analysis module.

Input values from the DCM are passed on to the data evaluation module (DEM). This module is the *knowledge acquisition* arm of NETWIND. The knowledge pertaining to wind-induced interference effects is stored in the weights of the NN models. The DEM is made up of four C-functions that represent the NN models for mean drag, mean lift, fluctuating drag and fluctuating lift interference effects. Each of these functions were generated in NeuroShell2 (1996) and interfaced with the other NETWIND modules. The functions evaluate input and calculate the Interference Factors or force coefficients (for mean lift) using the network weights. The output from this module is passed directly to the conclusion-analysis module where it is analyzed and then presented to the designer with relevant explanations. It is to be noted here that the four NN functions are the best two-hidden layers architectures developed for mean and fluctuating loads, and not the GRNN

architecture. This was done because the C-code for the GRNN architecture is very lengthy (about 10,000 lines for each function). Thus compilation and interfacing of the four huge functions with other modules is very tedious, involving splitting NN functions into various sub-functions and interfacing them in a proper fashion. As reported in sections 8.5 and 8.6, the accuracy of predictions obtained with the two-hidden layers BPNN architecture is comparable to predictions generated by GRNNs, albeit with less computational effort. The functions used in this module are given in Appendix C, section C.3.

8.9.3 The conclusion-analysis module

Since the interference factor values may not have much meaning to a user uninitiated in the various aspects and terms of wind engineering, this module analyzes the NN output and explains the results in terms of the severity and conditions of interference. It also explains to the designer the implications of the resulting increase or decrease in wind loads on the affected building due to a particular configuration. To explain a NN solution, the KBS conclusion-analysis module backward chains from the network solution to the actual user input, constructing a chain of reasons to justify a particular solution.

The conclusion-analysis module (CAM) analyzes and evaluates the output values (IF) generated by the DEM. With the IF values in hand, the CAM backward chains through a set of rules to search for probable reasons for the particular output generated by the NN module. In Expert Systems jargon, this process is known as *backward chaining* (Parsaye and Chignell 1988). It also suggests a set of remedial actions that may be helpful in decreasing interference effects for the particular input values. A typical CAM rule for mean drag interference effects is outlined below:

```
If IF <= -0.15{
   Then {
         High suction on the windward face of the principal building.

         Probable reasons:
         a) Buildings very close in tandem
         b) Interfering building of larger width than principal building
         c) Incident wind angle < 15 degrees
         d) Buildings in open exposure

         Possible remedies:
         a) Increase tandem spacing between buildings to at least 3bp
         b) Locate interfering building sideways (Sy > bp)
         c) Reduce width of interfering building
         d) Reorient buildings with incident wind angle > 15 degrees
         e) Locate buildings in more turbulent suburban or urban exposures
   }

}
```

The remedial measures suggested by NETWIND are linked in general to the 'probable reasons' for a particular response. The order in which the remedies are presented range from the most effective to the least effective and most difficult to implement. For example, changing the upstream exposure to reduce interference effects would entail a change in the building site - an inconvenient, generally unacceptable and costly proposition. This option is therefore presented as the last resort. However, the remedial measures have to be viewed in light of the importance of a particular attribute (say building width) to the designer. Therefore NETWIND presents the designer with an opportunity to interact with the program in order to rank the effectiveness of specific remedies. This interaction is made possible in the design assistance module discussed in the following sub-section. The detailed IF-THEN-ELSE rules used in this module are shown in Appendix C, section C.4.

8.9.4 The design assistance module

The conclusion-analysis module leads to the KBS design assistance module. It suggests design guidelines and recommendations to the designer, for instance to go ahead with wind load modifications based on the values given by the DEM and CAM or to conduct detailed wind tunnel tests owing to the complexity and severity of the interference effects. This module also deals directly with any data that does not conform to the limiting conditions as well as default pre-set values, serving as a simple teaching/learning tool. It explains to the designer the implications of the selected building configuration on the wind loads. The KBS design assistance module can also suggests a range of remedial measures in cases where interference effects are particularly predominant. It may suggest, for example, reorientation of a building or a change in its geometry, keeping in view the user's specific requirements and the importance assigned by the user to a particular attribute.

If NETWIND identifies significant interference effects, it offers requisite design assistance to the designer. NETWIND performs simple sensitivity analysis to assess the effect of a small change in input parameters on interference effects. Thus, each input variable is changed one at a time with others frozen, while NETWIND evokes the DEM module that runs through a set of input variables to compute IF values. Each IF value is compared with a threshold value for acceptability. Input parameters that meet the IF acceptance criterion are retained and presented to the user. For example, less than 30% increase in fluctuating loads is acceptable for design as reported in section 2.7. Similarly, acceptance criteria are set up for mean loads depending upon spacing between buildings and incident wind angle. In this way the user is provided with a set of design alternatives. The complete C-code for the design assistance module is given in Appendix C, section C.5.

In order to select an acceptable building configuration, the user can exercise his engineering judgement while using NETWIND's conclusion-analysis sub-module. This sub-module uses the *Importance Factors* assigned by the user to each input and combines them with a *Modification Factor* to calculate an *Evaluation Factor* for each alternative. The Importance Factor (I) is a percentage value (0% to 100%) assigned by the user to each input variable. A high value of I implies a higher importance, meaning that a change in that variable is less acceptable. The Modification Factor (M) represents the modification required to a particular variable to decrease interference effects to an acceptable level. This is the absolute difference between the original and the modified value of a variable. The values of I and M are normalized to lie in the same range, i.e. between 0 and 1. The Evaluation Factor (E) is given by:

$$E = \sum_{i=1}^{n} I_i M_i \tag{8.21}$$

where i is the number of input variables. Since the aim is to have the least modification in the variables within the constraints (I) set by the user, a low value of E signifies the best alternative and is selected. The C-code for calculating the utility values is shown in Appendix C, section C.6.

A typical NETWIND consultation screen for this module is shown in Table 8.11. The last column gives the Evaluation Factor E. Since centre-to-centre spacing Sx along the X-axis has the least importance (20%) i.e. is the easiest parameter to change, the alternatives with modification in Sx have the lowest E and are thus the preferred alternatives. It appears that the change in building geometry does not help in reducing interference effects for this

Table 8.11 NETWIND consultation screens for design assistance

```
NETWIND DESIGN ASSISTANCE SCREEN

Input relative importance (0% to 100%) you would ascribe to each
input variable. Give a higher % to the variable you want modified
the least.

1) Principal building width: 100
2) Interfering building width: 60
3) Principal building height: 100
4) Interfering building height: 40
5) Centre-to centre spacing between buildings along X-axis: 20
6) Centre-to centre spacing between buildings along Y-axis: 40
7) Incident wind angle: 30

Press any key to view NETWIND alternatives....
```

NETWIND ALTERNATIVES
(Note: E is Evaluation Factor: select the alternative with low E)

Fluctuating Lift

Angle (°)	Iv (%)	bp (m)	bi (m)	hp (m)	hi (m)	Sx (m)	Sy (m)	IF	E
Original data									
0.0	7.0	20.0	20.0	80.0	80.0	70.0	60.0	1.48	-
NETWIND alternatives									
0.0	7.0	20.0	20.0	80.0	80.0	35.0	60.0	1.26	0.05
0.0	7.0	20.0	20.0	80.0	80.0	155.0	60.0	1.29	0.05
0.0	7.0	20.0	20.0	80.0	80.0	140.0	95.0	1.18	0.07
0.0	7.0	20.0	20.0	80.0	80.0	40.0	45.0	1.21	0.07
30.0	7.0	20.0	20.0	80.0	80.0	70.0	60.0	1.19	0.08
0.0	7.0	20.0	20.0	80.0	80.0	70.0	90.0	1.27	0.10
0.0	7.0	20.0	20.0	80.0	80.0	70.0	35.0	1.22	0.10

particular case and hence geometry changes do not show up in the list of alternatives. A complete NETWIND consultation example is shown in Appendix C, section C.7.

8.10 Summary

This chapter is the culmination of a detailed research on wind-induced interference effects on buildings. Experimental and computerized approaches to deal with the problem of wind-

induced interference effects are integrated in a meaningful fashion. The data-base generated through wind tunnel experiments has been successfully modelled using neural networks. Several neural network architectures are examined and critically analyzed and general guidelines on developing successful NN applications are suggested. The NN models developed can be used to predict interference effects on buildings taking into account several variables within a good practical range. Overall, the NN development demonstrates the fact that meaningful relationships can be established within complex engineering processes for which currently no acceptable theory or empirical generalizations exist.

Finally, NETWIND, a hybrid knowledge-based wind design adviser for interference effects is developed. NETWIND uses the NN model developed in this study for knowledge acquisition and integrates it with a knowledge base as a front-end to the NN module, for data collection and knowledge structuring, and as post-processor for conclusion analysis and for providing design guidelines. Such a hybrid system will constitute a practical tool at early design stages, enabling the evaluation and refinement of close-to-optimum building configurations.

"Computer systems are becoming commonplace: indeed they are almost ubiquitous...But these computer systems, while increasingly affecting our lives, are rigid, complex and incapable of rapid change. To help us and our organizations cope with the unpredictable eventualities of an ever-more volatile world, these systems need capabilities that will let them adapt readily to change. They need to be intelligent."

- Barbara Grosz and Randall Davis, "A Report to ARPA (Advanced Research Project Agency) on Twenty-First Century Intelligent Systems", in AI Magazine, 15(3):10-20, 1994.

9

Closure

9.1 Concluding Remarks

A detailed and comprehensive study of wind-induced interference effects on buildings has been carried out. Research developments in this area were critically analyzed and results of various studies were compared in order to stress the need to model these effects. Keeping this in view, an extensive experimental program was developed to study the wind flow mechanisms and to quantify the extent of wind load modification on buildings due to interference effects. Based on the results of detailed experiments that consider various relevant parameters, general guidelines and limiting conditions have been formulated and critical interference effects situations identified. Empirical modelling and consequent generalizations suggested to account for interference effects have paved the way for simple design guidelines, thus leading eventually to codification.

A hybrid knowledge-based design adviser, incorporating Neural Network approach for knowledge acquisition has been developed. This design adviser facilitates accounting properly for wind-induced interference effects throughout the building design process. The Neural Network model is based on the experimental results gathered during the present study. It demonstrates that meaningful relationships can be established to model complex engineering processes for which currently no acceptable theory or empirical generalizations exist. Thus, Neural Networks offer a viable alternative to extensive wind tunnel testing and can help generalize limited wind tunnel results. The hybrid knowledge-based design adviser

developed will constitute a practical tool at early design stages, enabling the evaluation and refinement of close-to-optimum building configurations, saving valuable time and costs which is especially pertinent whenever scale models are to be built for subsequent wind-tunnel testing.

9.2 Research Contributions

The overall research, owing to the enormity of the experimental effort as well due to the complexity of the problem, was indeed challenging. The main challenge was to capture and present the complex inter-relationships among the various variables involved in a simple, yet comprehensive fashion. The contributions of this study towards a better overall understanding of wind-induced interference effects as well as in the integration of experimental and computerized approaches to provide valuable design assistance can be summarized as follows:

- A comprehensive review of research developments in the area of wind-induced interference effects to highlight the seriousness of the problem. A thorough analysis and comparison of the results of previous limited studies to identify their diverse nature and to stress the need for a systematic experimental program to model these effects.
- Fabrication of a three-component force-balance for quick, preliminary estimates of wind interference effects.
- A thorough investigation of mean and fluctuating forces and spectra for a single, free-standing building to provide a reference for the study. Suggestion of empirical equations for the estimation of mean and fluctuating force coefficients on tall buildings, taking into account wind direction and upstream exposure conditions.

- Detailed experimental study to generate a comprehensive data-base on wind-induced interference effects on buildings that includes information on mean and fluctuating loads as well as the wind load interference excitation spectra. Inclusion of most relevant parameters like incident wind direction, upstream exposure, building geometries and spacing between them. Accounting for the effects of immediate surroundings, to demonstrate the reduction of interference effects in city-centre environments.
- Analysis of the experimental results to evaluate peak loads and to account for wind directionality including the meteorological climate model.
- Detailed study and analysis of various interference mechanisms to identify specific interference zones of importance (proximity, interaction and passive) around a building.
- Identification of overall trends and establishment of generalized design guidelines on interference effects in terms of Interference Influence Grids, Interference Spectral Diagrams, Extreme Effect Contours for wind direction, Exposure Influence Grids for upstream exposure and Size Influence Grids for various interfering building sizes.
- Empirical modelling and derivation of easy-to-use regression equations for shielding effects due to upstream buildings of various sizes.
- Modelling and generalization of the data-base constituted by the experimental program on interference effects using Neural Networks, taking into account most relevant parameters. Detailed study and analysis of various Neural Network architectures and suggestions of thumb-rules for the development of Neural Network models.
- Integration of knowledge-based approach and Neural Network generalization to develop a hybrid Knowledge-Based Design Adviser for interference effects in order to provide design assistance at an early design stage.

- Provision in the design adviser of useful advice to explain the severity of interference for various building configurations, probable causes and remedial measures to recover from problematic wind interference situations.
- Incorporation of sensitivity analysis in the design adviser to suggest alternative building configurations that reduce interference effects.
- Evaluation of various feasible alternatives to suggest the best one to the designer, based on the importance assigned to different attributes by the designer.

9.3 Recommendations For Further Work

The present study, though the first of its kind in its detailed and comprehensive treatment of wind-induced interference effects on buildings and the use of Neural Network technology for modelling, generalization and design assistance, has only managed to survey the tip of the iceberg. However, it is hoped that this study will act as a catalyst to more vigorous research activities in the area of wind-interference, which will lead to a steady stream of innovations and improvements. Based on the limitations of the present study, a number of improvements to the present approach can be envisaged and further research avenues, most of which are aimed towards a better generalization, can be suggested. These may be summarized as follows:

- Incorporation of additional parameters like building shape, beginning with the most common ones like rectangular and circular, may help obtain a more complete generalization.

- The present study has discounted the effect of relatively shorter (than the principal building) interfering buildings based on a few previous studies that suggested their insignificance. Including this category will help in a better generalization.
- Although increasing the number of buildings is expected to decrease interference, the effects of small groups of three or four interfering buildings is still not clear. Even a single additional building is bound to increase experimental effort substantially, but a judicious selection of the testing cases and setting limiting conditions based on the results of the present study will help reduce the experimental effort to a great extent.
- Area averaging was employed in the present study to obtain overall drag and lift forces, as well as to reduce experimental time as opposed to sampling and obtaining local loads at each pressure tap. While this approach is adequate to evaluate the extent and magnitude of interference effects, the results cannot be directly applied to obtain the distribution of wind loads on the entire facade of a building which is important for the design of the building envelope (cladding) as well as for the assessment of ventilation-driven heat losses of a building. Understandably, carrying out such an investigation is extremely time intensive. However, conducting a detailed investigation of local loads, only for the critical cases found in this study (refer to the IIGs for instance), would be in order.
- The comparisons of interference effect results with those of full-scale studies would make for a valuable study. Obtaining comparable full-scale test results for tall buildings is not easy. However, comparisons with full-scale results have been traditionally used to validate wind tunnel results and constitute the "real test" of the accuracy of experimental results.

- Once additional parameters are included in the interference effect model, the Neural Network weights need to be updated to reflect the increased scope of the model. Interestingly, the network need not be trained all over again, but training may proceed from where the present Neural Network model ended. In this way, the old memory (weights) will not be lost but merely updated to include the effects of new data and additional parameters.
- Several enhancements can be envisaged in the Knowledge-Based Design Adviser. The inclusion of "fuzziness" in predictions would add practicality to the results. Thus, instead of a single, sharp demarcation between safe and unsafe conditions (for example, IF < 1.30 is deemed to be safe), evaluating the safety of a configuration with respect to a "critical corridor" (say IF between 1.25 and 1.35) would be more realistic. Since interference effects depend on several variables, each affecting wind loads in its own unique way and each with a varying degree of importance to the designer, a multi-objective decision analysis would help arrive at an alternative that has the highest utility value or, in other words, is most satisfying to the designer. Other useful enhancements would be the incorporation of graphics and menus to increase user-friendliness.

As for the future, one hopes that researchers, in planning their areas of study, will keep the eventual consumers of the fruits of their labours predominantly in mind, not only in terms of the objectives but also in terms of the manner in which the results are presented.

- K. C. Antony, Wind Engineering - The Personal View of a Practising Engineer, Proceedings of The Fourth International Conference on Wind Effects on Buildings and Structures, Heathrow, UK (1975).

References

Akins, R. E. (1992). "Effects of Turbulence on Mean Force and Moment Coefficients", *Journal of Wind Engineering and Industrial Aerodynamics*", 41-44, 701-712.

Allen, R. H. (1987). "Expert Systems in Structural Engineering : Works in Progress", *Journal of Computing in Civil Engineering*, ASCE, 1(4), Paper No. 21871, 312-319.

ANSI (1982). "Minimum Design Loads for Buildings and Other Structures", ANSI A58.1-1982, *American National Standard Institute*, Inc., New York, NY, USA.

Armitt, J. (1980). "Wind Loading on Cooling Towers", *Journal of Structural Division*, ASCE, 106(ST3), 623-641.

Bailey, A. and Vincent, N. D. G. (1943). "Wind-Pressure on Buildings Including Effects of Adjacent Buildings", *Journal of Institution of Civil Engineers*, 20, 243-275.

Bailey, P. A. and Kwok, K. C. S. (1985). "Interference Excitation of Twin Tall Buildings", *Journal of Wind Engineering and Industrial Aerodynamics*, Vol. 21, 323-338.

Baines, W. D. (1963). "Effect of Velocity Distribution on Wind Loads and Flow Patterns on Buildings", *Proceedings of The International Conference on Wind Effects on Buildings and Structures (Symposium No. 16)*, Vol. I, National Physical laboratories, Teddington, England, 197-223.

Bearman, P. W. (1978). "Turbulence Effects on Bluff Body Mean Flow", *Proceedings of The Third US National Conference on Wind Engineering Research*, Gainesville, FL, USA, 265-272.

Bédard, C. and Gowri, K. (1990). "Automating Building Design Process with KBES", *Journal of Computing in Civil Engineering*, ASCE, 4(2), Paper No. 24496, 69-83.

Bédard, C. and Ravi, M. (1991). "Knowledge-Based Approach to Overall Configuration of Multi-storey Office Buildings", *Journal of Computing in Civil Engineering*, ASCE, 5(4), Paper No. 26307, 336-353.

Bennett, J., Creary, L., Englemore, R. and Melosh, R. (1978). "*SACON: A Knowledge-Based Consultant for Structural Analysis*", Technical Report STAN-CS-78-699, Stanford University, CA, USA.

Blessmann, J. and Riera, J. D. (1979). "Interaction Effects on Neighbouring Tall Buildings", *Proceedings of the Fifth International Conference on Wind Engineering*, Fort Collins, CO, USA, 381-395.

Blessmann, J. and Riera, J. D. (1985). "Wind Excitation of Neighbouring Tall Buildings", *Journal of Wind Engineering and Industrial Aerodynamics*, Vol. 18, 91-103.

Blessmann, J. (1985). "Buffeting Effects of Neighbouring Tall Buildings", *Journal of Wind Engineering and Industrial Aerodynamics*, Vol. 18, 105-110.

Buchanan, B. G. and Feigenbaum, E. A. (1978). "DENDRAL and Meta DENDRAL: Their Applications Dimension", *Artificial Intelligence*, Vol.11.

Caudill, M. (1988). "Neural Networks Primer: Part 3", *AI Expert*, 19-23.

Caudill, M. (1990). "Using Neural Nets: Hybrid Expert Networks", *AI Expert*, 49-54.

Caudill, M. (1991). "Avoiding The Great Backpropagation Trap", *AI Expert*, 29-35.

Caudill, M. (1994). "GRNN and Bear It", *Using Neural Networks, AI Expert*, Miller Freeman Inc., San Francisco, CA, USA, 47-52.

Courchesne, J. and Laneville, A. (1980). "An Experimental Evaluation of Drag Coefficient For Rectangular Cylinders Exposed to Grid Turbulence", *Journal of Fluids Engineering, ASME*, 104, 523-527.

Chen, W. and Reed, D. (1990). "Structural Safety Assessment", *Journal of Wind Engineering and Industrial Aerodynamics*, 36, 1259-1268.

Chen, S. S. and Shah, K. (1992). "Neural Networks in Dynamic Analysis of Bridges", *Proceedings of The Eight Conference on Computing in Civil Engineering and Geographical Information Systems Symposium*, Dallas, TX, USA, 1058-1065.

Chester, D. L. (1990). "Why Two Hidden Layers Are Better Than One", *Proceedings of the International Conference on Neural Networks*, January 15-19, Washington, DC, USA, I-265-I-268.

Davenport, A. G. (1961). "The Spectrum of Horizontal Gustiness Near The Ground in High Winds", *Quarterly Journal of The Royal Meteorological Society*, 87(372).

Davenport, A. G. (1964). "Note on the Distribution of the Largest Value of a Random Function with Application to Gust Loading", *Proceedings of The Institution of Civil Engineers, London*, 28, 187-196.

Davenport, A. G. (1967). "Gust Loading Factors", *Journal of Structural Division, ASCE*, 93(ST3).

Demuth, H. and Beale, M. (1994). "Neural Network Tool Box for Use With MATLAB, The Mathworks Inc., Nantick MA, USA.

Duda, R. O., Nilsson, N. J. and Raphel, B. (1979). "State of Technology in Artificial Intelligence", In Peter Wegner (Ed.) *Research Directions in Software Technology*, Cambridge, MA, MIT Press.

English, E. C. (1985). "Shielding Factors From Wind-Tunnel Studies of Mid-Rise and High-Rise Structures", *Proceedings of The Fifth US National Conference on Wind Engineering*, Texas Tech University, Lubbock, TX, USA, 4A-49-4A-56.

English, E. C. (1990). "Shielding Factors From Wind-Tunnel Studies of Prismatic Structures", *Journal of Wind Engineering and Industrial Aerodynamics*, 36, 611-619.

English, E. C. (1993). "Shielding Factors for Paired Rectangular Prisms : An Analysis of Along-Wind Mean Response Data from Several Sources", *Proceedings of The Seventh US National Conference on Wind Engineering*, University of California, Los Angeles, CA, USA, 193-201.

ESDU (1979). "Mean Fluid Forces and Moments on Rectangular Prisms", *Engineering Sciences data Unit*, Item Number 80003 (with Amendment A May 1986).

Entsminger, G. (1991). "Neural-Network Creativity", *AI Expert*, May, 1991, 19-24.

Farell, C. and Sitheeq, M. M. (1993). "Wind Pressure Distribution on Sheltered Buildings: An Analysis of Existing Data For Application to Infiltration Loss Estimates", *Proceedings of The Seventh US National Wind Engineering Conference*, University of California, LA, USA, 223-232.

Flood, I. and Kartam, N. (1994). "Neural Networks in Civil Engineering I : Principles and Understanding and II: Systems and Applications", *Journal of Computing in Civil Engineering*, ASCE, 8(2), 131-162.

Garrett(Jr), J. H. (1992). "Neural Networks and Their Applicability Within Civil Engineering", *Proceedings of The Eight ASCE National Conference on Computing in Civil and Geographic Information Systems Symposium, Dallas, TX*, USA, 1155-1162.

Gowda, B. H. L. and Sitheeq, M. M. (1993). "Interference Effects on the Wind Pressure Distribution on Prismatic Bodies in Tandem Arrangement", *Indian Journal of Technology*, 31, 485-495.

Grace, A. (1994). *Optimization Toolbox for use with MATLAB*, The Mathworks Inc., Nantick, MA, USA.

Gumley, S. J. (1983). "Tubing Systems For Pneumatic Averaging of Fluctuating Pressures", *Journal of Wind Engineering and Industrial Aerodynamics*, 12, 189-228.

Gunaratnam, D. J. and Gero, J. S. (1993). "Neural Network Learning in Structural Engineering Applications", *Proceedings of The Fifth ASCE International Conference on Computing in Civil and Building Engineering*, Anaheim, CA, USA, 1448-1455.

Hajela, P. and Berke, L. (1992). "Neural Networks in Structural Analysis and Design: An Overview", *Computing Systems in Engineering*, 3(1-4), 525-538.

Harris, C. L. (1934). "Influence of Neighbouring Structures on the Wind Pressure on Tall Buildings", *Bureau of Standards, Journal of Research*, Vol. 12, Research Paper RP 637, 103-118.

Hillman, D. (1990). "For Novices and Professionals Alike NeuroShell v. 3.2", *AI Expert*, September, 1990, 61-64.

Ho, T. C. E., Surry, D. and Davenport A. G. (1990). "The Variability of Low Building Wind Loads due to Surrounding Obstructions", *Journal of Wind Engineering and Industrial Aerodynamics*, 36, 161-170.

Holmes, J. D. And Best, R. J. (1979). "A Wind-Tunnel Study of Wind Pressures on Grouped Tropical Houses", *Report 5/79, Department of Civil and Systems Engineering, James Cook University of North Queensland*, Townsville, Queensland, Australia.

Holmes, J. D. (1994). "Wind Pressures on Tropical Housing", *Journal of Wind Engineering and Industrial Aerodynamics*, 63, 105-123.

Hussain, M., and Lee, B. E. (1980). "A Wind Tunnel Study of the Mean Pressure Forces Acting on a Large Group of Low-Rise Buildings", *Journal of Wind Engineering and Industrial Aerodynamics*, 6, 207-225.

Irwin, H. P. A. H., Cooper, K. R. and Girard, R. (1979). "Correction of Distortion Effects Caused by Tubing Systems in Measurements of Fluctuating Pressures", *Journal of Wind Engineering and Industrial Aerodynamics*, 5, 93-107.

Issa, R. A. (1992). "Predicting Tower Guy Pretension Using a Neural Network", *Proceedings of The Eight ASCE Conference on Computing in Civil Engineering and Geographical Information Systems Symposium*, Dallas, TX, USA, 1074-1081.

Isyumov, N. and Davenport, A. G. (1975). "The Ground Level Wind Environment in Built-up Areas", *Proceedings of The Fourth International Conference on Wind Effects on Buildings and Structures*, Heathrow, UK, 403-421.

Isyumov, N. (1982). "The Aeroelastic Modelling of Tall Buildings", *International Workshop on Wind Tunnel Modelling for Civil Engineering Applications* (Ed. T. A. Reinhold), Cambridge University Press, IV.1-1 - IV.1-40.

Isyumov, N. and Poole, M. (1983). "Wind Induced Torque on Square and Rectangular Building Shapes", *Journal of Wind Engineering and Industrial Aerodynamics*, 13, 183-196.

Isyumov, N., Fediw, A. A., Colaco, J. and Banavalkar, P. V. (1992). "Performance of a Tall Building Under Wind Action", *Journal of Wind Engineering and Industrial Aerodynamics*, 41-44, 1053-1064.

Jozwiak, P., Kacprzyck, J. and Zuranski, J. A. (1993). "Wind Tunnel Investigation of Interference Effects on Pressure Distribution On a Building", *Proceedings of The First IAWE European and African Regional Conference*, Guernsey (Ed. N. J. Cook), 105-112.

Kamarthi, S. V., Sanvido, V. E. and Kumara, S. R. T. (1992). "NEUROFORM - Neural Network System for Vertical Formwork Selection", *Journal of Computing in Civil Engineering*, ASCE, 6(2), Paper No. 416, 178-199.

Karakatsanis, A. (1985). "FLODER: A Floor Designer Expert System", MSc. Thesis, Department of Civil Engineering, Carnegie-Mellon University, Pittsburgh, PA, USA.

Kareem, A. (1982). "Fluctuating Wind Loads on Buildings", Journal of Engineering Mechanics Division, ASCE, 108(EM6), 1086-1102.

Kareem, A. and Cermak, J. S. (1984). "Pressure Fluctuations on a Square Building Model in Boundary-Layer Flow", *Journal of Wind Engineering And Industrial Aerodynamics*, 16, 17-41.

Kareem A. (1987). "The Effects of Aerodynamic Interference on the Dynamic Response of Prismatic Structures", *Journal of Wind Engineering and Industrial Aerodynamics*, 25, 365-372.

Kareem, A. and Allen, R. H. (1990). "Development of Knowledge Based Systems in Wind Engineering", *Journal of Wind Engineering and Industrial Aerodynamics*, 36, 1245-1258.

Kartam, N., Flood, I. and Tongthong, T. (1993). "Artificial Neural Networks and Knowledge Based Systems : Complementary AI Techniques for Civil Engineering", *Proceedings of The Fifth ASCE International Conference on Computing in Civil and Building Engineering*, Anaheim, CA, USA, 1398-1403.

Kelnhofer, Wm. J. (1971). "Influence of a Neighbouring Building on Flat Roof Wind Loading", *Proceedings of the Third International Conference on Wind Effects on Buildings and Structures*, Tokyo, Japan, 221-230.

Kennedy, S. (1995). "Genetic Algorithms: Digital Darwinism", *Hitchhiker's Guide to Artificial Intelligence, AI Expert*, Miller Freeman Publication, SanFrancisco, CA, USA, 29-36.

Khanduri, A. C., Stathopoulos, T. and Bédard, C. (1997a). "Wind-Induced Interference Effects on Buildings - A Review of The State-of-The Art" *Journal of Engineering Structures* (in press).

Khanduri, A. C., Bédard, C. and Stathopoulos, T. (1997b). "Modelling of Wind-Induced Interference Effects Using Backpropagation Neural Networks" *Journal of Wind Engineering and Industrial Aerodynamics* (in press).

Khanduri, A. C., Stathopoulos, T. and Bédard, C. (1996). "Modelling Wind-Induced Interference Effects - Integrating Experimental and Computerized Approaches", *The 1996 CSCE Annual Conference*, Edmonton, Alberta, Canada, May 29-June 1, 588-599.

Khanduri, A. C., Bédard, C. and Stathopoulos, T. (1995a). "Neural Network Modelling of Wind-Induced Interference Effects", *Proceedings of the Ninth International Conference on Wind Engineering*, New Delhi, India, January 9-13, 1341-1352.

Khanduri, A. C., Bédard, C. and Stathopoulos, T. (1995b). "Modelling Wind-Induced Interference Effects-Building Design With a Hybrid KBS Approach", *Proceedings of The Sixth International Conference on Computing in Civil and Building Engineering*, Berlin, Germany, July 12-15, 221-228.

Khanduri, A. C., Bédard, C. and Stathopoulos, T. (1995c). "Development of a Hybrid KBS for Design Applications in Wind Engineering", *Proceedings of The ASCE Structures Congress XIII*, Boston, MA, USA, April 2-5, 1427-1431.

Kwok, K. C. S. (1989). "Interference Effects on Tall Buildings", *Recent Advances in Wind Engineering, Proceedings of the Second Asia-Pacific Symposium in Wind Engineering, Vol. I*, Beijing, China, 446-453.

Laneville, A., Gartshore, I.S. and Parkinson, G. V. (1975). "An Explanation of Some Effects of Turbulence on Bluff Bodies", *Proceedings of The Fourth International Conference on Wind Effects on Buildings and Structures*, London, UK, 333-340.

Lawson, T. V. and Penwarden, A. D. (1975). The Effects of Wind on People in the Vicinity of Buildings , *Proceedings of The Fourth International Conference on Wind Effects on Buildings and Structures*, Heathrow, UK, 605-622.

Lee, B. E. (1975). "The Effect of Turbulence on The Surface Pressure Field of a Square prism", *Journal of Fluid Mechanics*, 69(2), 263-282.

Lee, B. E. and Fowler, G. R. (1975). "The Mean Wind Forces Acting on a Pair of Square Prisms", *Building Science*, 10, 107-110.

Lee B. E. (1989). "Wind Loading on Low-Rise Buildings", *Recent Advances in Wind Engineering, Proceedings of the Second Asia-Pacific Symposium in Wind Engineering, Vol. I*, Beijing, China, 54-64.

Liu, H. (1991). "*Wind Engineering : A Handbook for Structural Engineers*", Prentice Hall, Inc., Englewood Cliffs, NJ, USA.

Maher, M. L. (1984). "HI-RISE: A Knowledge-Based Expert System for The Preliminary Design of High Rise Buildings", *Ph.D. Thesis, Department of Civil Engineering, Carnegie-Mellon University*, Pittsburgh, PA, USA.

Mc Laren, F. G., Sherratt, A. F. C. and Morton, A. S. (1971). "The Interference between Bluff Sharp-Edged Cylinders in Turbulent Flows Representing Models of Two Tower Buildings Close Together", *Building Science*, 6, 273-274.

Melbourne, W. H. and Sharp, D. B. (1976). " Effect of Upwind Buildings on the Response of Tall Buildings", *Proceedings of The Regional Conference on Tall Buildings*, Hong Kong, 174-191.

Moselhi, O., Hegazy, T. and Fazio, P. (1991). "Neural Networks as Tools in Construction", *Construction Engineering and Management*, ASCE, 117(4), 606-625.

NBCC (1985). "Supplement to The National Building Code of Canada, 1985", Associate Committee on National Building Code, *National Research Council of Canada*, Ottawa, Ontario, Canada.

Neural Network (1995). "Neural Network Resource Guide", *Neural Network Special Report '95, AI Expert*, Miller Freeman Inc., San Francisco, CA, USA.

NeuroShell2 (1996). *Neural Network Development Shell*, Ward Systems Group, Inc., Executive Park West, 5 Hillcrest Drive, Frederick, MD 21702, USA.

Parsaye, K. and Chignell, M. (1988). "Expert System for Experts", John Wiley and Sons Inc., New York, NY, USA.

Paterson, D. A. and Papenfuss, A. T. (1993). "Computation of Wind Flows around two Tall Buildings", *Journal of Wind Engineering and Industrial Aerodynamics*, 50, 69-74.

Peterka, J. A. and Cermak, J. E. (1976). "Adverse Wind Loading Induced by Adjacent Buildings", *Journal of Structural Division*, ASCE, 102(ST3), 533-548.

Rao, G. N., Grobler, F. and Kim, S. (1993). "Conceptual Cost Estimating : A Hybrid Neural-Expert System Approach", *Proceedings of The Fifth ASCE International Conference on Computing in Civil and Building Engineering*, Anaheim, CA, USA, 423-430.

Reed, D. A. (1990). "Expert Systems in Wind Engineering", *Journal of Wind Engineering and Industrial Aerodynamics*, 33, 487-494.

Rehak, D., Howard, H. C. And Sriram, D. (1985). "Architecture of an Integrated-Based Environment for Structural Engineering Applications", *Knowledge Engineering in Computer-Aided Design*, Elsevier North-Holland, Inc., Amsterdam, Netherlands, 89-117.

Reich, Y. and Fenves, S. J. (1989). "The Potential of Machine Learning Techniques for Expert Systems", *Artificial Intelligence for Engineering Design, Analysis and Manufacturing*, 3(3), 175-193.

Reinhold, T. A., Tielman, H. W. and Maher, F. C. (1977). "Interaction of Square Prisms in Two Flow Fields", *Journal of Wind Engineering And Industrial Aerodynamics*, 2, 223-241.

Reinhold, T. A. and Sparks, P. R. (1980). "The Influence of an Upstream Structure on the Dynamic Response of a Square-Section Tall Building", *Proceedings of The Fourth Colloquium on Industrial Aerodynamics, Part II*, Aachen, Germany, 223-235.

Rogers, J. L. (1994). "Simulating Structural Analysis with Neural Networks", *Journal of Computing in Civil Engineering*, ASCE, 8(2), 252-265.

Rumelhart, D. E., Hinton, G. E. and Williams, R. J. (1986). "Learning Internal Representations by Error Propagation", in D. E. Rumelhart and J. L. Mc Clelland (eds.), *Parallel Distributed Processing: Explorations in The Microstructures of Cognition, Vol. 1: Foundations*, MIT Press, Cambridge, MA, USA.

Ruscheweyh, H. P. (1979). "Dynamic Response of High Rise Buildings Under Wind Action with Interference Effects from Surrounding Buildings of Similar Size", *Proceedings of the Fifth International Conference on Wind Engineering*, Fort Collins, CO, 725-734.

SAA (1989). "Minimum Design Loads on Structures (SAA Loading Code), Part 2 : Wind Loads", AS 1170.2-1989, *Standards Association of Australia*, North Sydney, Australia.

Saathoff, P. J. and Melbourne, W. H. (1987). "Freestream Turbulence And Wind Tunnel Blockage Effects on Streamwise Surface Pressures, *Journal of Wind Engineering And Industrial Aerodynamics*, 26, 353-370.

Sakamoto, H., Haniu, H. and Obata, Y. (1987). "Fluctuating Forces Acting on Two Square Prisms in a Tandem Arrangement", *Journal of Wind Engineering and Industrial Aerodynamics*, 26, 85-103.

Sakamoto, H. and Haniu, H. (1988). "Aerodynamic Forces Acting on Two Square Prisms Placed Vertically in a Turbulent Boundary Layer", *Journal of Wind Engineering and Industrial Aerodynamics*, 31, 41-66.

Sandri, P. And Mehta, K. C. (1995). "Using a Backpropagation Neural Network for Predicting Wind-Induced damage to Buildings", *Proceedings of the Ninth International Conference on Wind Engineering*, New Delhi, India, January 9-13, 1989-1999.

Sanni, R. A., Surry, D. and Davenport, A. G. (1992). "Wind Loading on Intermediate Height Buildings", *Canadian Journal of Civil Engineering*, 19, 148-163.

Saunders, J. W. and Melbourne, W. H. (1979). "Buffeting Effects of Upwind Buildings", *Proceedings of the Fifth International Conference on Wind Engineering*, Fort Collins, CO, 593-605.

Sayers, A. T. (1991). "Steady State Pressure and Force Coefficients for Group of three Equispaced Square Cylinders Situated in a Cross Flow", *Journal of Wind Engineering and Industrial Aerodynamics*, 37, 197-208.

Sharpe, R., Marksjo, B., Holmes, J. D., Fitchett and Ho, F. (1990). "Wind Loads on Building Expert System - WINDLOADER", *Journal of Wind Engineering and Industrial Aerodynamics*, 36, 1269-1277.

Shortliffe, E. H. (1976). "*Computer-Based Medical Consultation: MYCIN*", Elsevier, New York, NY, USA.

Simiu , E. and Scanlan, R. H. (1986). *Wind Effects on Structures*, Second Edition, John Wiley and Sons, New York, USA.

Smith, D. A., Mehta, K. C., McDonald, J. R. And Cheshire, R. H. (1995). "Wind Resistance Categorization of Buildings with a Knowledge-Based System", *Proceedings of the Ninth International Conference on Wind Engineering*, New Delhi, India, January 9-13, 2000-2010.

Sockel, H. and Krönke, I. (1992). "Investigation of The Accuracy of The Pneumatic Averaging Technique", *Journal of Wind Engineering and Industrial Aerodynamics*, 41-44, 1829-1839.

Soliman, B. F. (1976). "Effect of Building Group Geometry on Wind Pressure and Properties of Flow", *Report No. BS 29, Department of Building Science, University of Sheffield*, Sheffield, UK.

Specht, D. F. (1991). "A General Regression Neural Network", *IEEE Transactions on Neural Networks*, 2(6), 568-576.

Stathopoulos, T., Surry, D. and Davenport, A. G. (1981). "Effective Wind Loads on Flat Roofs", *Journal of Structural Division, ASCE*, 107(ST2), 281-298.

Stathopoulos, T. (1984a). "Adverse Wind Loads on Low Buildings Due to Buffeting", *Journal of Structural Engineering*, ASCE, 110(10), 2374-2392.

Stathopoulos, T. (1984b). "Design And Fabrication of a Wind Tunnel for Building Aerodynamics", *Journal of Wind Engineering and Industrial Aerodynamics*, 16, 361-376.

Suresh Kumar, K. and Stathopoulos, T. (1997). "Power Spectra of Wind Pressures on Low Building Roofs", *Proceedings of The Second European and African Conference on Wind Engineering*, Genova, Italy, June 22-26, 1997 (in press).

Surry, D. and Mallais, W. (1983). "Adverse Local Wind Loads Induced by Adjacent Buildings", *Journal of Structural Engineering*, ASCE, 109(3), 816-820.

Surry, D. and Stathopoulos, T. (1978). "An Experimental Approach to the Economical Measurement of Spatially-Averaged Wind Loads", *Journal of Industrial Aerodynamics*, 2, 385-397.

Surry, D. Stathopoulos, T. and Davenport, A. G. (1983). "Simple Measurement Techniques For Area Wind Loads", *Journal of Engineering Mechanics, ASCE*, 109(4), 1058-1071.

Sykes, D. M. (1983). "Interference Effects on the Response of a Tall Building Model", *Journal of Wind Engineering and Industrial Aerodynamics*, 11, 365-380.

Taniike, Y. and Inaoka, H. (1988). "Aeroelastic Behaviour of Tall Buildings in Wakes", *Journal of Wind Engineering and Industrial Aerodynamics*, 28(1), 317-327.

Taniike, Y. (1991). "Turbulence Effect on Mutual Interference of Buildings", *Journal of Engineering Mechanics*, ASCE, 117(3), 443-456.

Taniike, Y. (1992). "Interference Mechanism for Enhanced Wind Forces on Neighbouring Tall Buildings", *Journal of Wind Engineering and Industrial Aerodynamics*, 42, 1073-1083.

Thoroddsen, S. T., Cermak, J. E. and Peterka, J. A. (1985). "Mean and Dynamic Wind Loading caused by an Upwind Structure", *Proc. The Fifth US National Conference on Wind Engineering*, Texas Tech University, Lubbock, TX, USA, 4A-73-4A-80.

Thoroddsen, S. T., Cermak, J. E. and Peterka, J. A. (1987). "Uncertainties in Wind Loads caused by Adjacent Buildings", Dynamics of Structures, *Proceedings of The ASCE Structures Congress '87 related to Dynamics of Structures*, Orlando, FL, USA, 540-555.

Tschanz, T. (1982). "The Base Balance Measurement Technique And Applications To Dynamic Wind Loading of Structures", *Ph.D. Thesis, Department of Engineering Science, The University of Western Ontario*, London, Canada.

Tsutsumi, J., Katayama, T. and Nishida, M. (1992). "Wind Tunnel Tests of Wind Pressure on Regularly Aligned Buildings", *Journal of Wind Engineering and Industrial Aerodynamics*, 41-44, 1799-1810.

Vickery, B. J. (1966). "Fluctuating Lift And Drag on a Long Cylinder of Square Cross-Section in a Smooth And in a Turbulent Stream", *Journal of Fluid Mechanics*, 25(3), 484-494.

Vickery, B. J. (1968). "Load Fluctuations in Turbulent Flow", *Journal of Engineering Mechanics Divisions, ASCE*, 94(EM1), 31-46.

Wasserman, P. D. (1988). "*Neural Computing, Theory and Practice*", First Edition, Van Nostrand Reinhold, New York, NY, USA.

Waterman, D. A. (1985). "*A Guide to Expert Systems*", Addison Wesley Publishing Co., Inc., Reading, MA, USA.

Whitbread, R. E. (1975). "The Measurement of Non-Steady Wind Forces On Small-Scale Building Models", *Proceedings of The Fourth International Conference On Wind Engineering*, Heathrow, UK, 567-574.

Wiren, B. G. (1983). "Effects of Surrounding Buildings on Wind Pressure Distributions and Ventilative Heat Loss for a Single-Family House", *Journal of Wind Engineering and Industrial Aerodynamics*, 15, 15-20.

Wiren, B. G. (1985). "Effects of Surrounding Buildings on Wind Pressure Distributions and Ventilative Heat Loss for a Single-Family House, Part I : 1 1/2 - Storey Detached Houses", *Publication Bulletin M85:19, The National Swedish Institute for Building Research.*

Wu, H., Stathopoulos, T. and Bédard, C. (1993). "Computer-based Building Design and Pedestrian-level Wind Conditions", *Proceedings of The Fifth ASCE International Conference on Computing in Civil and Building Engineering*, Anaheim, CA, USA, 1167-1174.

Wu, H. (1994). "Pedestrian-Level Wind Environment Around Buildings", *Ph.D Thesis, Centre For Building Studies, Concordia University*, Montreal, Canada.

Wu, X. and Ghaboussi, J. (1992). "Neural Network-based Modelling of Composite Material with Emphasis on Reinforced Concrete", *Proceedings of The Eighth ASCE National Conference on Computing in Civil Engineering and Geographical Information Systems Symposium*, Dallas, TX, USA, 1179-1186.

Yahyai, M., Kumar, K., Krishna, P. and Pande, P. K. (1992). "Aerodynamic Interference in Tall Rectangular Buildings", *Journal of Wind Engineering and Industrial Aerodynamics*, 41, 859-866.

Yamamoto, K. and Sakai, M. (1993). "An Application of Neural Networks to Hysteretic Modelling of Steel Structures", *Proceedings of The Fifth International Conference on Computing in Civil and Building Engineering*, Anaheim, CA, USA, 961-964.

Zhang, W. J., Xu, Y. L. and Kwok, K. C. S. (1993). "Torsional Response of Eccentric Tall Buildings with Interference Effects", *Proceedings of The Seventh US National Conference on Wind Engineering*, University of California, Los Angeles, CA, USA, 899-908.

Zhang, W. J., Kwok, K. C. S. and Xu, Y. L.(1994), "Aeroelastic Torsional Behaviour of Tall Buildings in Wakes", *Journal of Wind Engineering and Industrial Aerodynamics*, 51, 229-248.

Appendix A

Structural Response Due to Time-Dependent Loads

This Appendix presents certain elementary results of structural dynamics theory and derives, on their basis, expressions for the response of a single-degree-of-freedom structure subjected to distributed stationary random loads (Simiu and Scanlan 1986).

Consider the system represented in Figure A.1 consisting of a single mass m at B and the member AB assumed to have negligible mass. The displacement $x(t)$ of the mass m is opposed by a restoring force supplied by the member AB and a damping force due to the internal friction that develops within the system during its motion. It is assumed that the restoring force is linear, i.e. proportional to the displacement $x(t)$, and the damping is viscous, i.e. proportional to the velocity dx/dt. The motion of the mass, from Newton's second law, is described as,

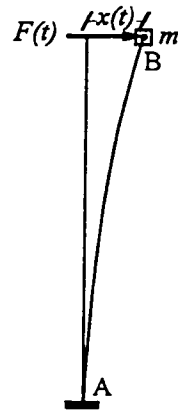

Figure A.1 A single-degree-of-freedom system

$$m\ddot{x} + c\dot{x} + kx = F(t) \tag{A.1}$$

where, $F(t)$ is the time-dependent load acting on the mass, k is the stiffness of the member AB and c is the coefficient of viscous damping. The dot denotes differentiation with respect to time. The above equation can be written in the form,

$$\ddot{x} + 2\zeta(2\pi n_1)\dot{x} + (2\pi n_1)^2 x = \frac{F(t)}{m} \tag{A.2}$$

where,

$$n_1 = \frac{1}{2\pi}\sqrt{\frac{k}{m}} \tag{A.3}$$

and

$$\zeta = \frac{c}{2\sqrt{km}} \tag{A.4}$$

Here, n_1 and ζ are known as the natural frequency and the damping ratio of the system, respectively. The denominator of ζ is known as the critical damping coefficient and can be shown to be the value of damping coefficient beyond which the free motion of the system is non-oscillatory. The damping ratio is expressed as percentage of critical damping.

For a harmonic load given by,

$$F(t) = F_0 \cos 2\pi nt \tag{A.5}$$

the steady-state solution of equation A.2 is,

$$x(t) = F_0 H(n) \cos(2\pi nt - \phi) \tag{A.6}$$

where,

$$\phi = \tan^{-1}\frac{2\zeta(n/n_1)}{1 - (n/n_1)^2} \tag{A.7}$$

$$H(n) = \frac{1}{4\pi^2 n_1^2 m\left\{\left[1-(n/n_1)^2\right]^2 + 4\zeta^2 (n/n_1)^2\right\}^{1/2}} \qquad \text{(A.8)}$$

The quantity $H(n)$ is known as the *mechanical admittance* of the system.

When the load $F(t)$ is generated by a stationary process with spectral density $S_f(n)$, the spectral density of response can be derived to be,

$$S_x(n) = H^2(n) S_f(n) \qquad \text{(A.9)}$$

The variance of deflection (or response) is given by,

$$\sigma_x^2 = \int_0^\infty S_x(n) \qquad \text{(A.10)}$$

Appendix B

Effect of Wind Directionality on Peak Loads

This Appendix presents the effects of wind directionality on peak interference factors (see Section 7.1.5). The contours for maximum peak drag and lift IFs for all wind directions are shown in Figure B.1. The results of the analysis based on the climatic model are shown in Figure B.2.

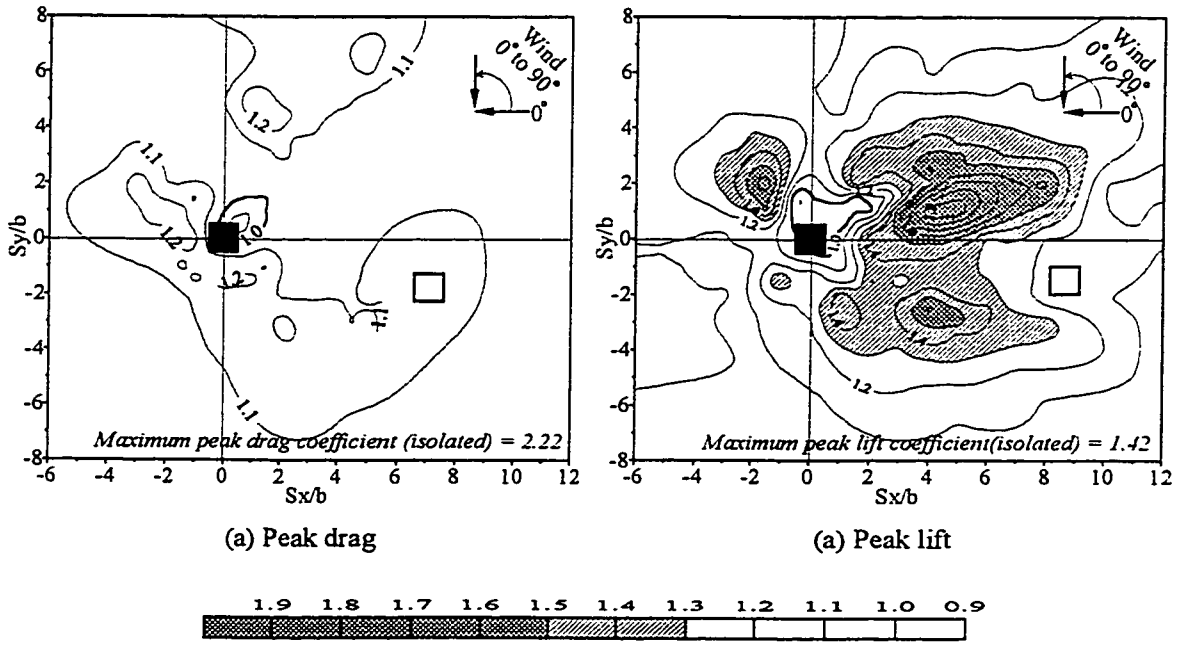

(a) Peak drag

(a) Peak lift

Figure B.1 Maximum IF contours for peak loads for all wind directions

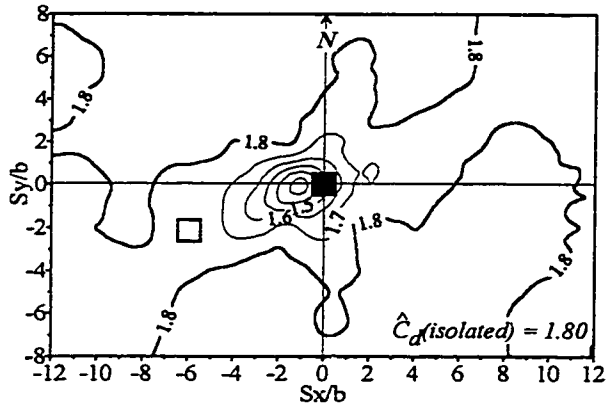

(a) Peak drag coefficient

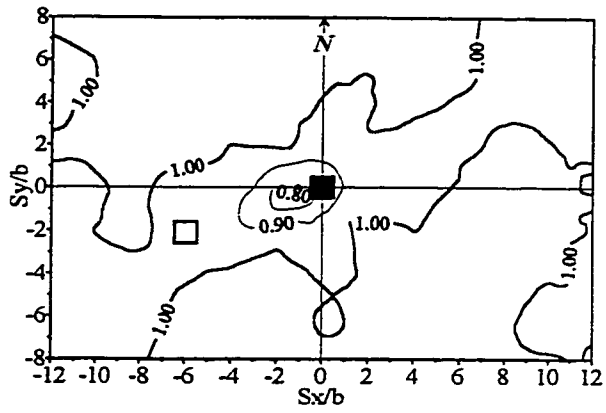

(b) Peak drag Interference Factors (IF)

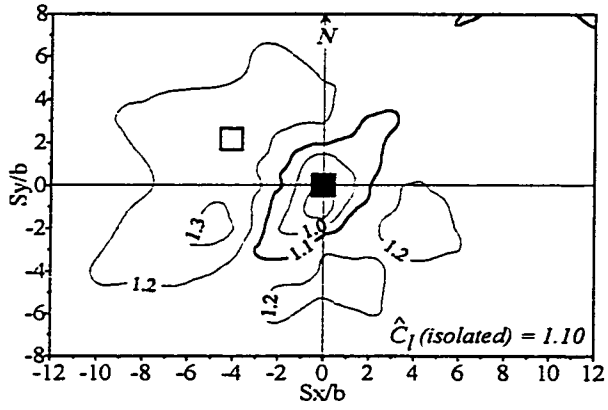

(c) Peak lift coefficient

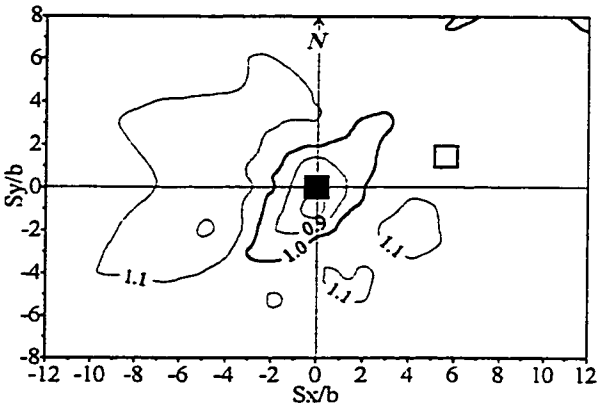

(d) Peak lift Interference Factors (IF)

Figure B.2 Average peak drag and lift due to interference weighted by directional probabilities (24 wind directions) for Montreal

Appendix C

C source code for NETWIND - A Hybrid Knowledge-Based Design Adviser for Wind-Induced Interference Effects on Buildings

C.1 The main program

```
/** Main for NETWIND **/
#include <stdio.h>
#include <math.h>
main()
{
int op1, op2, op3, op4;
double angle, Iv, bp, bi, hp, hi, b, h, sx, sy, IFmx, IFmy, IFsx, IFsy;
char op, repeat, start, in, proceed;
clrscr();
printf("\n          *****Welcome to NETWIND ver1.0 1997*****\n\n");
printf("\n                    Developed by: Atul C. Khanduri\n\n");
printf("NETWIND is a Neural Network based design adviser for\n"
"evaluating the effects of adjacent buildings on the wind-induced\n"
"loads on a building, generally known as INTERFERENCE EFFECTS.\n"
"The present version of NETWIND works best for two buildings of\n"
"different relative sizes in various upstream exposures with a\n"
"0 degree wind, normal to the building face. Cases of oblique winds\n"
"work well for two similar buildings, in open exposure. Any other\n"
"case while producing generally acceptable results, may also generate\n"
"erroneous responses. Care should be exercised when presenting such\n"
"cases to NETWIND.\n\n"
"For details on interference effects refer the following material:\n\n"
"Khanduri, A. C. (1997). Evaluation and Generalization of Wind-Induced\n"
"Interference Effects on Buildings: Integrating Experimental and\n"
"Computerized Approaches. Ph.D. Thesis, Centre for Building Studies,\n"
"Concordia University, Montreal, Canada.\n\n");
printf("Do you want to proceed (Y/N): ");
start = getche();
if(start == 'Y' || start == 'y'){
    clrscr();
    printf("\nYou will now be asked to input data into NETWIND.\n"
    "NETWIND expects the following inputs:\n\n"
    "1) Incident wind angle in degrees (wind direction is assumed from\n"
    "   left to right of the computer screen). Wind angle can vary from\n"
    "   0 to 45 degrees.\n"
    "2) Upstream exposure: Choice between two modes of input:\n"
    "   a) Select: open, suburban or urban exposures or\n"
    "   b) Input: Longitudinal turbulence intensity of wind at building height(%)\n"
    "3) Width of the building on which interference effects are to be evaluated\n"
    "   (Principal building). The present version of NETWIND assumes square plan)\n"
    "4) Width of the adjacent building (Interfering building)\n"
    "5) Height of the principal building\n"
    "6) Height of the adjacent building\n\n"
    "NETWIND performs validation checks for erroneous inputs and also ensures that\n"
```

```
    "inputs lie within the range that can be handled by it.\n\n");
    printf("Press any key to continue....\n");
    getch(); clrscr();
    printf("\n\nNETWIND output:\n\n"
    "NETWIND invokes its Neural Network interference effects model to calculate\n"
    "INTERFERENCE FACTORS (ratio of wind load on the principal building with\n"
    "interference due to adjacent building, to the wind loads on it in isolated\n"
    "condition. The results are analyzed by the Conclusion-Analysis module that\n"
    "explains the severety of interference effects. Finally, the Design Assistance\n"
    "module evaluates, if needed, another set of alternatives that reduce\n"
    "interference effects.\n\n");
    printf("Press any key to continue....\n");
    getch(); clrscr();
    again:;
        clrscr();
        printf("\n\n\nDo you want to INPUT data or QUIT ? (Y/Q): ");
        in = getche();
        if(in == 'Q' || in == 'q') goto finish;
        input(&angle, &Iv, &bp, &bi, &hp, &hi, &b, &h, &sx, &sy); /** Data collection module **/
        printf("\n\nProceed to RESULTS and ANALYSIS screen ? (Y/N): ");
        proceed = getche();
        if(proceed == 'N' || proceed == 'n') goto again;
        NNmeanx(angle, Iv, b, h, sx, sy, &IFmx);/** NN mean drag module **/
        NNmeany(angle, Iv, b, h, sx, sy, &IFmy);/** NN mean lift module **/
        NNsigmax(angle, Iv, b, h, sx, sy, &IFsx);/** NN fluctuating drag module **/
        NNsigmay(angle, Iv, b, h, sx, sy, &IFsy);/** NN fluctuating lift module **/
        concl(IFmx, IFmy, IFsx, IFsy, angle, &op1, &op2, &op3, &op4); /* Conclusion analysis module */
        if(op1 != 0 || op2 != 0 || op3 != 0 || op4 != 0){
            printf("\nDo you want NETWIND to implement necessary changes ? (Y/N): ");
            op = getche();
            if(op == 'Y' || op == 'y'){
                clrscr();
                assist(op1, op2, op3, op4, angle, Iv, b, h, sx, sy, bp, bi, hp, hi, IFmx, IFmy, IFsx, IFsy);
                /** Design assistance module **/
                printf("\nDo you want to run NETWIND with new inputs or QUIT? (Y/Q): ");
                repeat = getche();
                if(repeat == 'Y' || repeat == 'y') goto again;
            }
            else if(op == 'N' || op == 'n'){
                printf("\nPress any key to continue....\n");
                getch();
                printf("\nDo you want to run NETWIND with new inputs or QUIT? (Y/Q):");
                repeat = getche();
                if(repeat == 'Y' || repeat == 'y') goto again;
            }
        }
        else if(op1 == 0 && op2 == 0 && op3 == 0 && op4 == 0){
            printf("\nPress any key to continue....\n");
            getch();
            printf("Do you want to run NETWIND with new inputs or QUIT? (Y/Q): ");
            repeat = getche();
            if(repeat == 'Y' || repeat == 'y') goto again;
        }
    }
    finish:;
    clrscr();
    printf("\n\n\n\n\n**Thank you for using NETWIND. Outputs are stored in file: NETWIND.OUT**\n");
    printf("\n\nPRESS ANY KEY TO RETURN TO DOS\n");
    getch(); clrscr();
}
```

C.2 The Data Collection Module

```
/** Data Collection Module **/
#include <stdio.h>
#include <math.h>
input(angle, Iv, bp, bi, hp, hi, b, h, sx, sy)
double *angle, *Iv, *bp, *bi, *hp, *hi, *b, *h, *sx, *sy;
{
double sx1, sx2, sy1, sy2, sxx, syy, lap;
char start;
clrscr();
printf("DATA INPUT SCREEN:\n\n");
printf("Use uniform system of units  (suggestion: use metres for length)\n\n");
for(;;){
    printf("Wind direction (0 to 45 degrees, wind from right to left): ");
    scanf("%lf", angle);
    if(*angle >= 0.0 && *angle <= 45.0) break;
    else printf("\n**OUT OF RANGE! Angle must lie\n"
    "between 0 and 45 degrees**\n\n");
}
for(;;){
    printf("Longitudinal turbulence intensity of wind (7% to 25%): ");
    scanf("%lf", Iv);
    if(*Iv >= 7 && *Iv <= 25) break;
    else printf("\n**OUT OF RANGE! Use a longitudinal turbulence\n"
    "intensity between 7% and 25%**\n\n");
}
for(;;){
    printf("Principal building width (square): ");
    scanf("%lf", bp);
    printf("Interfering building width (square): ");
    scanf("%lf", bi);
    *b = (*bi)/(*bp);
    if(*b >= 0.667 && *b <= 2.0) break;
    else printf("\n**OUT OF RANGE! Ratio of interfering to principal\n"
    "building width must be between 0.667 to 2 (inclusive) **\n\n");
}
for(;;){
    for(;;){
        printf("Principal building height (height/width = 3 to 5): ");
        scanf("%lf", hp);
        if((*hp)/(*bp) >= 3 && (*hp)/(*bp) <= 5) break;
        else printf("\n**OUT OF RANGE! Ratio of principal building height\n"
        "to width must be between 3 to 5 (inclusive)**\n");
    }
    for(;;){
        printf("Interfering building height (height/width = 2 to 8): ");
        scanf("%lf", hi);
        if((*hi)/(*bi) >= 2 && (*hi)/(*bi) <=8) break;
        else printf("\n**OUT OF RANGE! Ratio of interfering building height\n"
        "to width must be between 2 to 8 (inclusive)**\n");
    }
    *h = (*hi)/(*hp);
    if(*h >= 1.0 && *h <= 2.0) break;
```

```
    else printf("\n**OUT OF RANGE! Ratio of interfering building to principal\n"
    "building height must be between 1 to 2 (inclusive) **\n\n");
}
for(;;){
    for(;;){
        printf("Centre-to-centre spacing between buildings along X-axis: ");
        scanf("%lf", sx);
            *sx = *sx/(*bp);
            sx1 = (*bp)*14;
            sx2 = (*bp)*-4;
            if(*sx >= -4.0 && *sx <= 14) break;
            else printf("\n**OUT OF RANGE! Reduce spacing to lie\n"
            "between %5.2lf, and %5.2lf**\n\n", sx2, sx1);
    }
    for(;;){
        printf("Centre-to-centre spacing between buildings along Y-axis: ");
        scanf("%lf", sy);
        *sy = *sy/(*bp);
        sy1 = (*bp)*8;
        sy2 = (*bp)*-6;
        if(*sy >= -6.0 && *sy <= 8) break;
        else printf("\n**OUT OF RANGE! Reduce spacing to lie\n"
        "between %5.2lf, and %5.2lf**\n\n", sy2, sy1);
    }
    lap = ((*bp) + (*bi))/2.0; /** check for building overlap **/
    sxx = (*sx)*(*bp);
    syy = (*sy)*(*bp);
    if((sxx == 0 && syy <= lap ))
    printf("\nIMPOSSIBLE SITUATION! Buildings overlapping or\n"
    "touching each other. Check spacing.\n\n");
    else if(syy == 0 && sxx <= lap)
    printf("\nIMPOSSIBLE SITUATION! Buildings overlapping or\n"
    "touching each other. Check spacing.\n\n");
    else if(sxx > 0 && syy > 0 && sxx <= lap && syy <= lap)
    printf("\nIMPOSSIBLE SITUATION! Buildings overlapping or\n"
    "touching each other. Check spacing.\n\n");
    else break;
}}
```

C.3 Neural Network Data Evaluation Module

C.3.1 Neural Network model for Predicting Mean Drag IF

```
/* This code fires the neural network for predicting mean drag IF*/
/* The network has 6 input nodes, one output node, 2 hidden layers with 17 nodes in each layer*/
/* This code is designed to be simple and fast for porting to any machine. Therefore all code and weights */
/* are inline without looping or data storage which might be harder to port between compilers. */

#include <math.h>
 NNmeanx(angle, Iv, b, h, sx, sy, IFmx)
double angle, Iv, b, h, sx, sy, *IFmx;
{
```

```
 double netsum, feature2[17], feature3[17], inarray[6], outarray[1];
/* inarray[0] is Angle, inarray[1] is Iv , inarray[2] is b, inarray[3] is h, */
/* inarray[4] is Sx , inarray[5] is Sy, outarray[0] is IFmx */

inarray[0] = angle/45.0; inarray[1] = Iv/100.0; inarray[2] = b; inarray[3] = h;inarray[4] = sx;inarray[5] = sy;

if (inarray[0]< 0) inarray[0] =  0; if (inarray[0]> 1) inarray[0] =  1; inarray[0] =  2 * inarray[0] -1;
if (inarray[1]< .07) inarray[1] =  .07; if (inarray[1]> .25) inarray[1] =  .25;
inarray[1] =  2 * (inarray[1] -  .07) / .18 -1;
if (inarray[2]< .667) inarray[2] =  .667; if (inarray[2]> 2) inarray[2] =  2;
inarray[2] =  2 * (inarray[2] -  .667) / 1.333 -1;
if (inarray[3]< 1) inarray[3] =  1; if (inarray[3]> 2) inarray[3] =  2; inarray[3] =  2 * (inarray[3] -  1) -1;
if (inarray[4]<-4) inarray[4] = -4; if (inarray[4]> 14) inarray[4] =  14;
inarray[4] =  2 * (inarray[4] +  4) / 18 -1; if (inarray[5]<-6) inarray[5] = -6;
if (inarray[5]> 8) inarray[5] =  8;inarray[5] =  2 * (inarray[5] +  6) / 14 -1;

netsum =  5.426034; netsum += inarray[0] *  5.643956; netsum += inarray[1] *  1.129651;
netsum += inarray[2] *  3.148004; netsum += inarray[3] *  .4201554; netsum += inarray[4] * -11.22922;
netsum += inarray[5] * -13.21265; feature2[0] = 1 / (1 + exp(-netsum));

netsum = -.95164; netsum += inarray[0] * -1.201404; netsum += inarray[1] *  1.196379;
netsum += inarray[2] * -.4296919; netsum += inarray[3] *  1.949706; netsum += inarray[4] * -9.354192;
netsum += inarray[5] *  24.5662; feature2[1] = 1 / (1 + exp(-netsum));

netsum =  3.590785; netsum += inarray[0] *  3.574342; netsum += inarray[1] * -4.754134;
netsum += inarray[2] * -2.058782; netsum += inarray[3] *  8.166539E-02;
netsum += inarray[4] *  11.37787; netsum += inarray[5] *  7.203399; feature2[2] = 1 / (1 + exp(-netsum));

netsum = -13.26854; netsum += inarray[0] * -13.16067; netsum += inarray[1] * -2.451614;
netsum += inarray[2] * -3.814862; netsum += inarray[3] *  27.04425; netsum += inarray[4] *  5.856436;
netsum += inarray[5] *  25.22646; feature2[3] = 1 / (1 + exp(-netsum));

netsum =  2.684604; netsum += inarray[0] *  2.601014; netsum += inarray[1] * -7.688723;
netsum += inarray[2] *  4.082613; netsum += inarray[3] * -.9416943; netsum += inarray[4] * -9.291237;
netsum += inarray[5] *  69.44304; feature2[4] = 1 / (1 + exp(-netsum));

netsum =  .8298084; netsum += inarray[0] *  .6133345; netsum += inarray[1] *  2.029215;
netsum += inarray[2] * -5.586653; netsum += inarray[3] * -.1711287; netsum += inarray[4] *  2.576559;
netsum += inarray[5] *  .7476215; feature2[5] = 1 / (1 + exp(-netsum));

netsum = -1.914387; netsum += inarray[0] * -2.121764; netsum += inarray[1] *  4.240619;
netsum += inarray[2] * -1.184918;netsum += inarray[3] * -4.333227E-02;
netsum += inarray[4] * -4.934216; netsum += inarray[5] *  6.495207; feature2[6] = 1 / (1 + exp(-netsum));

netsum =  30.37047; netsum += inarray[0] *  29.83824; netsum += inarray[1] *  2.856343;
netsum += inarray[2] *  .8844358; netsum += inarray[3] *  .4131839; netsum += inarray[4] * -2.475326;
netsum += inarray[5] * -32.5012; feature2[7] = 1 / (1 + exp(-netsum));

netsum =  .2209278; netsum += inarray[0] * -4.604933E-02; netsum += inarray[1] *  1.346202;
netsum += inarray[2] *  .5902432; netsum += inarray[3] *  4.743054; netsum += inarray[4] * -5.092134;
netsum += inarray[5] * -7.072847; feature2[8] = 1 / (1 + exp(-netsum));

netsum =  2514.582; netsum += inarray[0] *  2514.453; netsum += inarray[1] *  7.476143;
netsum += inarray[2] *  .6562786; netsum += inarray[3] * -.4779786; netsum += inarray[4] * -10.64312;
netsum += inarray[5] * -11.02275; feature2[9] = 1 / (1 + exp(-netsum));

netsum = -3.004354; netsum += inarray[0] * -2.766107; netsum += inarray[1] * -.1793359;
netsum += inarray[2] * -.7701458; netsum += inarray[3] * -1.053158; netsum += inarray[4] * -1.4924;
netsum += inarray[5] *  9.806155; feature2[10] = 1 / (1 + exp(-netsum));

netsum =  21.5638; netsum += inarray[0] *  21.40949; netsum += inarray[1] *  .6804734;
netsum += inarray[2] * -.7534396; netsum += inarray[3] *  4.469105; netsum += inarray[4] *  3.235188;
netsum += inarray[5] *  13.12603; feature2[11] = 1 / (1 + exp(-netsum));
```

```
 netsum =  .4590361; netsum += inarray[0] *  .3970347; netsum += inarray[1] *  4.357385;
netsum += inarray[2] * -.5295236; netsum += inarray[3] *  .1315186; netsum += inarray[4] * -11.86261;
netsum += inarray[5] *  9.084569; feature2[12] = 1 / (1 + exp(-netsum));
 netsum =  .3874907; netsum += inarray[0] *  .17911; netsum += inarray[1] * -.5515376;
netsum += inarray[2] *  12.88551; netsum += inarray[3] *  .4988762; netsum += inarray[4] * -5.859687;
netsum += inarray[5] * -19.21034; feature2[13] = 1 / (1 + exp(-netsum));

netsum = -.5620068; netsum += inarray[0] * -.3465756; netsum += inarray[1] *  6.406243;
netsum += inarray[2] * -9.027111E-02; netsum += inarray[3] *  .1189464;
netsum += inarray[4] * -14.90439; netsum += inarray[5] *  8.116454; feature2[14] = 1 / (1 + exp(-netsum));

netsum =  1.065341; netsum += inarray[0] *  1.326822; netsum += inarray[1] * -5.936304;
netsum += inarray[2] *  1.726392; netsum += inarray[3] *  .7836199; netsum += inarray[4] *  9.15772;
netsum += inarray[5] * -30.10819; feature2[15] = 1 / (1 + exp(-netsum));

netsum =  2.389933; netsum += inarray[0] *  2.546365; netsum += inarray[1] * -.3973462;
netsum += inarray[2] * -2.345482; netsum += inarray[3] *  .7180923; netsum += inarray[4] * -2.030955;
netsum += inarray[5] *  20.81105; feature2[16] = 1 / (1 + exp(-netsum));

netsum = -8.300262E-02; netsum += feature2[0] *  .1842481; netsum += feature2[1] *  1.094063;
netsum += feature2[2] * -2.645932; netsum += feature2[3] *  .8526106;
netsum += feature2[4] * -1.669922; netsum += feature2[5] * -.4030522;
netsum += feature2[6] * -.3126844; netsum += feature2[7] *  2.248683;
netsum += feature2[8] * -.1960233; netsum += feature2[9] * -12.1354;netsum += feature2[10] * -.8245318;
netsum += feature2[11] * -2.381898; netsum += feature2[12] *  11.44163;
netsum += feature2[13] *  .1226753; netsum += feature2[14] * -5.272793;
netsum += feature2[15] *  .3052878; netsum += feature2[16] * -5.227429;
feature3[0] = 1 / (1 + exp(-netsum));

netsum =  3.9375; netsum += feature2[0] *  4.051121; netsum += feature2[1] * -4.431974;
netsum += feature2[2] * -.330805; netsum += feature2[3] *  1.43195; netsum += feature2[4] * -.7721025;
netsum += feature2[5] *  .6738524; netsum += feature2[6] *  3.958757; netsum += feature2[7] *  2.010976;
netsum += feature2[8] *  .5847387; netsum += feature2[9] *  .9940304;netsum += feature2[10] * -3.978002;
netsum += feature2[11] * -1.939378; netsum += feature2[12] * -2.857481;
netsum += feature2[13] * -5.592762; netsum += feature2[14] * -5.838791;
netsum += feature2[15] *  .3019072; netsum += feature2[16] * -.8913267;
feature3[1] = 1 / (1 + exp(-netsum));

netsum = -3.989914; netsum += feature2[0] * -3.903541; netsum += feature2[1] * -.6488837;
netsum += feature2[2] *  3.293183; netsum += feature2[3] *  .236702; netsum += feature2[4] * -1.0071;
netsum += feature2[5] *  1.968387; netsum += feature2[6] *  10.85572; netsum += feature2[7] * -14.71759;
netsum += feature2[8] *  9.794748; netsum += feature2[9] *  13.33312; netsum += feature2[10] *  5.286163;
netsum += feature2[11] *  .4617356; netsum += feature2[12] *  4.391747;
netsum += feature2[13] *  6.764881; netsum += feature2[14] *  44.49934;
netsum += feature2[15] * -6.294193; netsum += feature2[16] * -7.379649;
feature3[2] = 1 / (1 + exp(-netsum));

netsum = -1.153597; netsum += feature2[0] * -1.113753; netsum += feature2[1] * -1.286859;
netsum += feature2[2] *  .4908625; netsum += feature2[3] *  .1581635; netsum += feature2[4] *  1.111784;
netsum += feature2[5] *  .5844223; netsum += feature2[6] *  .1121373; netsum += feature2[7] *  .2674604;
netsum += feature2[8] * -8.383422; netsum += feature2[9] * -.8380387;
netsum += feature2[10] * -1.414823; netsum += feature2[11] *  .9184062;
netsum += feature2[12] *  .4525327; netsum += feature2[13] * -1.063202;
netsum += feature2[14] *  3.553144;  netsum += feature2[15] * -1.219928;
netsum += feature2[16] *  1.320815; feature3[3] = 1 / (1 + exp(-netsum));

netsum = -.209841; netsum += feature2[0] * -.2680518; netsum += feature2[1] * -.2264647;
netsum += feature2[2] * -1.470798; netsum += feature2[3] *  .4868768;netsum += feature2[4] * -.5239337;
netsum += feature2[5] * -10.69993; netsum += feature2[6] * -6.40336; netsum += feature2[7] *  3.562177;
netsum += feature2[8] *  1.415007; netsum += feature2[9] * -7.607525; netsum += feature2[10] * -1.529;
netsum += feature2[11] * -1.174056; netsum += feature2[12] * -.5138053;
netsum += feature2[13] * -.2530025; netsum += feature2[14] *  .3690992;
netsum += feature2[15] *  4.683806; netsum += feature2[16] * -1.737179;
```

```
feature3[4] = 1 / (1 + exp(-netsum));

netsum =  5.716781; netsum += feature2[0] *  5.532424; netsum += feature2[1] * -2.803895;
netsum += feature2[2] *  3.271209; netsum += feature2[3] * -12.65413;netsum += feature2[4] * -4.136511;
netsum += feature2[5] *  5.680575; netsum += feature2[6] * -1.211416; netsum += feature2[7] * -5.595252;
netsum += feature2[8] * -6.40752; netsum += feature2[9] * -.8940904;netsum += feature2[10] *  1.698879;
netsum += feature2[11] *  5.620651; netsum += feature2[12] *  3.467931;
netsum += feature2[13] * -18.44639; netsum += feature2[14] * -3.251668;
netsum += feature2[15] *  2.126926; netsum += feature2[16] * -8.622111;
feature3[5] = 1 / (1 + exp(-netsum));

netsum =  3.438589; netsum += feature2[0] *  3.493266; netsum += feature2[1] *  2.789222;
netsum += feature2[2] * -3.22863; netsum += feature2[3] * -7.684339; netsum += feature2[4] *  4.372654;
netsum += feature2[5] * -2.289676; netsum += feature2[6] * -1.981996;netsum += feature2[7] *  7.709759;
netsum += feature2[8] * -3.217479; netsum += feature2[9] * -7.403054;
netsum += feature2[10] *  1.671525; netsum += feature2[11] *  2.310564;
netsum += feature2[12] * -4.830167; netsum += feature2[13] *  8.959752;
netsum += feature2[14] * -4.59551; netsum += feature2[15] *  .7190802;
netsum += feature2[16] * -1.655946; feature3[6] = 1 / (1 + exp(-netsum));

netsum = -1.646541; netsum += feature2[0] * -1.889565; netsum += feature2[1] *  .1745782;
netsum += feature2[2] * -5.807692; netsum += feature2[3] *  13.16492; netsum += feature2[4] *  .9588081;
netsum += feature2[5] *  2.944967; netsum += feature2[6] *  11.93871; netsum += feature2[7] *  8.248969;
netsum += feature2[8] *  1.209046; netsum += feature2[9] *  2.387471;netsum += feature2[10] * -.2666026;
netsum += feature2[11] * -12.94359; netsum += feature2[12] * -.3562957;
netsum += feature2[13] *  1.152106; netsum += feature2[14] * -4.254176;
netsum += feature2[15] * -14.56163;netsum += feature2[16] * -1.5068;feature3[7] = 1 / (1 + exp(-netsum));

netsum = -7.763846; netsum += feature2[0] * -7.775364; netsum += feature2[1] *  15.58298;
netsum += feature2[2] *  3.535256; netsum += feature2[3] *  5.233077; netsum += feature2[4] *  9.623768;
netsum += feature2[5] *  .6881822; netsum += feature2[6] * -9.061026; netsum += feature2[7] * -6.33579;
netsum += feature2[8] * -4.328033;netsum += feature2[9] * -.1507146;
netsum += feature2[10] *  9.671589; netsum += feature2[11] * -5.611124;
netsum += feature2[12] * -14.79592; netsum += feature2[13] *  5.996681;
netsum += feature2[14] *  27.3382; netsum += feature2[15] * -.1358684;
netsum += feature2[16] *  4.031231; feature3[8] = 1 / (1 + exp(-netsum));

netsum = -3.657245; netsum += feature2[0] * -3.567923; netsum += feature2[1] *  14.3096;
netsum += feature2[2] * -2.614325E-02; netsum += feature2[3] * -.4127991;
netsum += feature2[4] * -1.205254; netsum += feature2[5] *  2.622378;netsum += feature2[6] * -3.614318;
netsum += feature2[7] * -1.261189; netsum += feature2[8] *  5.15147; netsum += feature2[9] *  .2949581;
netsum += feature2[10] *  6.183877; netsum += feature2[11] * -.7647554;
netsum += feature2[12] * -13.9743; netsum += feature2[13] *  15.84844;
netsum += feature2[14] *  3.180513; netsum += feature2[15] *  3.863262;
netsum += feature2[16] *  4.975611;feature3[9] = 1 / (1 + exp(-netsum));

netsum =  .3490862; netsum += feature2[0] *  .7181826; netsum += feature2[1] * -1.421861;
netsum += feature2[2] *  .5153818; netsum += feature2[3] * -.3166228;
netsum += feature2[4] * -2.001251; netsum += feature2[5] *  .3929093; netsum += feature2[6] *  1.939252;
netsum += feature2[7] *  .8257256; netsum += feature2[8] * -1.056042; netsum += feature2[9] *  .766843;
netsum += feature2[10] * -4.001426; netsum += feature2[11] * -.2560946;
netsum += feature2[12] * -5.12244; netsum += feature2[13] *  1.104428;
netsum += feature2[14] *  2.193245; netsum += feature2[15] * -.1177414;
netsum += feature2[16] *  .479585; feature3[10] = 1 / (1 + exp(-netsum));

netsum = -.5970222; netsum += feature2[0] * -.9191513; netsum += feature2[1] *  .0112832;
netsum += feature2[2] *  .4325827; netsum += feature2[3] * -.1956099;netsum += feature2[4] * -.3896076;
netsum += feature2[5] *  .9310904; netsum += feature2[6] *  .0510413; netsum += feature2[7] * -3.338203;
netsum += feature2[8] *  .1187898; netsum += feature2[9] *  1.157771; netsum += feature2[10] *  .3519571;
netsum += feature2[11] *  2.223212; netsum += feature2[12] * -1.064003;
netsum += feature2[13] * -.6210651; netsum += feature2[14] *  .8592824;
netsum += feature2[15] * -1.014339; netsum += feature2[16] * -2.757166E-02;
feature3[11] = 1 / (1 + exp(-netsum));
```

```
netsum =  .1194835; netsum += feature2[0] *  .5419418; netsum += feature2[1] * -.1858121;
netsum += feature2[2] * -.2700156; netsum += feature2[3] * -.1549768;netsum += feature2[4] * -1.479093;
netsum += feature2[5] * -1.148649; netsum += feature2[6] *  14.33199;
netsum += feature2[7] *  8.427829E-02; netsum += feature2[8] * -10.78358;
netsum += feature2[9] *  14.959; netsum += feature2[10] * -.1045304; netsum += feature2[11] *  1.786357;
netsum += feature2[12] *  2.218387; netsum += feature2[13] *  .3609074;
netsum += feature2[14] * -5.742524; netsum += feature2[15] * -.6681755;
netsum += feature2[16] *  .3824788;feature3[12] = 1 / (1 + exp(-netsum));

netsum = -4.427272E-02; netsum += feature2[0] * -1.411389E-02; netsum += feature2[1] *  .2844273;
netsum += feature2[2] * -.2269448; netsum += feature2[3] * -1.503406;netsum += feature2[4] *  .1550518;
netsum += feature2[5] *  1.253663; netsum += feature2[6] * -.7128375;netsum += feature2[7] * -.6464944;
netsum += feature2[8] * -1.005381; netsum += feature2[9] * -.2812601;
netsum += feature2[10] *  .0293147; netsum += feature2[11] *  .4370428;
netsum += feature2[12] *  .6165105; netsum += feature2[13] *  .6623625;
netsum += feature2[14] *  5.575562; netsum += feature2[15] * -.2223711;
netsum += feature2[16] *  .7060705; feature3[13] = 1 / (1 + exp(-netsum));

netsum = -6.214553; netsum += feature2[0] * -6.49475; netsum += feature2[1] *  21.37661;
netsum += feature2[2] * -2.544259;netsum += feature2[3] * -9.429055; netsum += feature2[4] *  5.706001;
netsum += feature2[5] *  .4139959; netsum += feature2[6] *  8.699655; netsum += feature2[7] * -2.006581;
netsum += feature2[8] * -14.103; netsum += feature2[9] * -13.11593; netsum += feature2[10] *  15.37325;
netsum += feature2[11] *  8.119346; netsum += feature2[12] * -10.68998;
netsum += feature2[13] * -7.081314; netsum += feature2[14] *  11.34192;
netsum += feature2[15] *  5.401464; netsum += feature2[16] *  8.337749;
feature3[14] = 1 / (1 + exp(-netsum));

netsum = -3.804518; netsum += feature2[0] * -3.603461; netsum += feature2[1] * -1.937518;
netsum += feature2[2] *  2.78337; netsum += feature2[3] * -.1688556; netsum += feature2[4] * -1.60117;
netsum += feature2[5] * -5.36975; netsum += feature2[6] *  81.07878; netsum += feature2[7] *  .9030642;
netsum += feature2[8] * -9.457049;netsum += feature2[9] *  3.031073;netsum += feature2[10] *  .2916116;
netsum += feature2[11] * -.350528; netsum += feature2[12] * -.5767872;
netsum += feature2[13] * -2.992942; netsum += feature2[14] *  17.84223;
netsum += feature2[15] * -5.507989; netsum += feature2[16] *  2.856563;
feature3[15] = 1 / (1 + exp(-netsum));

netsum = -2.362669; netsum += feature2[0] * -1.921806; netsum += feature2[1] *  .2215194;
netsum += feature2[2] * -5.277424; netsum += feature2[3] *  3.803922; netsum += feature2[4] *  .9072934;
netsum += feature2[5] *  1.169902; netsum += feature2[6] *  .8656368; netsum += feature2[7] *  1.152453;
netsum += feature2[8] *  .1821053;netsum += feature2[9] * -1.420535;netsum += feature2[10] *  .2441307;
netsum += feature2[11] * -3.584478; netsum += feature2[12] *  .3818257;
netsum += feature2[13] *  .6807297; netsum += feature2[14] *  2.484864;
netsum += feature2[15] * -1.167441; netsum += feature2[16] *  .2534138;
feature3[16] = 1 / (1 + exp(-netsum));

netsum = -1.300247; netsum += feature3[0] * -1.383361; netsum += feature3[1] * -.6095772;
netsum += feature3[2] *  .2724209; netsum += feature3[3] *  .4932613; netsum += feature3[4] * -1.035979;
netsum += feature3[5] * -.2267601; netsum += feature3[6] *  .168013; netsum += feature3[7] * -.5079883;
netsum += feature3[8] *  .5978275;netsum += feature3[9] *  .6717989;netsum += feature3[10] *  2.523436;
netsum += feature3[11] *  .294795; netsum += feature3[12] * -.5213724;
netsum += feature3[13] *  .2968957; netsum += feature3[14] *  .2141894;
netsum += feature3[15] *  .2629796; netsum += feature3[16] *  .8003103;
outarray[0] = 1 / (1 + exp(-netsum));
outarray[0] =  1.65 *  (outarray[0] - .1) / .8  + -.29;
if (outarray[0]<-.29) outarray[0] = -.29;
if (outarray[0]> 1.36) outarray[0] =  1.36;
*IFmx = outarray[0];
}
```

C.3.2 Neural Network model for Predicting Mean Lift Coefficient

```
/* This code fires the neural network for predicting mean lift coefficient */
/* The network has 6 input nodes, one output node, 2 hidden layers with 17 nodes in each layer */
/* This code is designed to be simple and fast for porting to any machine.Therefore all code and weights*/ /*
are inline without looping or data storage which might be harder to port between compilers. */

#include <math.h>
 NNmeany(angle, Iv, b, h, sx, sy, IFmy)
double angle, Iv, b, h, sx, sy, *IFmy;
{
double netsum, feature2[17], feature3[17], inarray[6], outarray[1];
/* inarray[0] is Angle, inarray[1] is Iv ,  inarray[2] is b, inarray[3] is h, */
/* inarray[4] is Sx , inarray[5] is Sy, outarray[0] is IFmy */

inarray[0] = angle/45.0; inarray[1] = Iv/100.0; inarray[2] = b; inarray[3] = h;inarray[4] = sx;inarray[5] = sy;

if (inarray[0]< 0) inarray[0] =  0; if (inarray[0]> 1) inarray[0] =  1; inarray[0] =  2 * inarray[0] -1;
if (inarray[1]< .07) inarray[1] =  .07; if (inarray[1]> .25) inarray[1] =  .25;
inarray[1] =  2 * (inarray[1] -  .07) / .18 -1;
if (inarray[2]< .667) inarray[2] =  .667; if (inarray[2]> 2) inarray[2] =  2;
inarray[2] =  2 * (inarray[2] -  .667) / 1.333 -1;
if (inarray[3]< 1) inarray[3] =  1; if (inarray[3]> 2) inarray[3] =  2; inarray[3] =  2 * (inarray[3] -  1) -1;
if (inarray[4]<-4) inarray[4] = -4; if (inarray[4]> 12) inarray[4] =  12;
inarray[4] =  2 * (inarray[4] +  4) /16 - 1;if (inarray[5]<-6) inarray[5] = -6; if (inarray[5]> 8) inarray[5] =  8;
inarray[5] =  2 * (inarray[5] +  6) / 14 -1;

netsum = -3.409414; netsum += inarray[0] * -3.191493; netsum += inarray[1] * -1.243875;
netsum += inarray[2] *  .1189888; netsum += inarray[3] * -.1570665; netsum += inarray[4] * -2.593052;
netsum += inarray[5] *  .1127802; feature2[0] = 1 / (1 + exp(-netsum));

netsum =  71.61603; netsum += inarray[0] *  71.36627; netsum += inarray[1] *  10.93101;
netsum += inarray[2] * -.9768978; netsum += inarray[3] * -.102241; netsum += inarray[4] * -13.83116;
netsum += inarray[5] *  1.228578; feature2[1] = 1 / (1 + exp(-netsum));

netsum = -3.939688; netsum += inarray[0] * -3.956131; netsum += inarray[1] * -.9313214;
netsum += inarray[2] * -.60203; netsum += inarray[3] * -.7148401; netsum += inarray[4] *  6.002186;
netsum += inarray[5] *  1.447774; feature2[2] = 1 / (1 + exp(-netsum));

netsum = -23.57881; netsum += inarray[0] * -23.47093; netsum += inarray[1] * -1.423359;
netsum += inarray[2] * -7.304638; netsum += inarray[3] *  .2143439; netsum += inarray[4] *  4.861237;
netsum += inarray[5] * -43.01623; feature2[3] = 1 / (1 + exp(-netsum));

netsum =  9.496904; netsum += inarray[0] *  9.413313; netsum += inarray[1] *  5.330538;
netsum += inarray[2] *  11.09498; netsum += inarray[3] *  3.4055; netsum += inarray[4] *  2.305651;
netsum += inarray[5] * -10.90993; feature2[4] = 1 / (1 + exp(-netsum));

netsum = -.5041121; netsum += inarray[0] * -.7205865; netsum += inarray[1] * -.172676;
netsum += inarray[2] *  .2151404; netsum += inarray[3] * -.5846136; netsum += inarray[4] * -1.892695;
netsum += inarray[5] * -.6332822; feature2[5] = 1 / (1 + exp(-netsum));

netsum = -3.637677; netsum += inarray[0] * -3.845051; netsum += inarray[1] *  .8612718;
netsum += inarray[2] * -1.208538; netsum += inarray[3] *  .0469361; netsum += inarray[4] *  1.476875;
netsum += inarray[5] * -.1946259; feature2[6] = 1 / (1 + exp(-netsum));
```

```
 netsum = -53.55109; netsum += inarray[0] * -54.08332; netsum += inarray[1] * -13.72867;
netsum += inarray[2] * -26.87209; netsum += inarray[3] * -10.97447; netsum += inarray[4] * -3.21626;
netsum += inarray[5] * -8.733092; feature2[7] = 1 / (1 + exp(-netsum));

netsum = -5.495933; netsum += inarray[0] * -5.762908; netsum += inarray[1] *  1.187024;
netsum += inarray[2] * -6.229853; netsum += inarray[3] *  .5557837; netsum += inarray[4] * -1.861424;
netsum += inarray[5] *  4.471185; feature2[8] = 1 / (1 + exp(-netsum));

netsum = -1.995918; netsum += inarray[0] * -2.124886; netsum += inarray[1] * -.1563947;
netsum += inarray[2] * -.8975261; netsum += inarray[3] * -.4808972; netsum += inarray[4] * -1.287982;
netsum += inarray[5] *  1.802122; feature2[9] = 1 / (1 + exp(-netsum));

netsum = -.4090929; netsum += inarray[0] * -.1708466; netsum += inarray[1] *  8.710465;
netsum += inarray[2] *  .1925494; netsum += inarray[3] * -.6579962; netsum += inarray[4] * -13.79645;
netsum += inarray[5] *  15.7069; feature2[10] = 1 / (1 + exp(-netsum));

netsum = -1.466134; netsum += inarray[0] * -1.620442; netsum += inarray[1] *  1.889196E-02;
netsum += inarray[2] *  .4933942; netsum += inarray[3] * -.7219498; netsum += inarray[4] * -.8716218;
netsum += inarray[5] *  .6183653; feature2[11] = 1 / (1 + exp(-netsum));

netsum =  3.198575; netsum += inarray[0] *  3.136574; netsum += inarray[1] * -4.689206E-02;
netsum += inarray[2] * -1.341358; netsum += inarray[3] * -.4961716; netsum += inarray[4] *  16.3535;
netsum += inarray[5] * -16.00493; feature2[12] = 1 / (1 + exp(-netsum));

netsum =  260.2872; netsum += inarray[0] *  260.0789; netsum += inarray[1] *  1.456361;
netsum += inarray[2] *  15.15424; netsum += inarray[3] * -1.374572; netsum += inarray[4] *  3.474412;
netsum += inarray[5] * -134.7016; feature2[13] = 1 / (1 + exp(-netsum));

netsum = -.1133982; netsum += inarray[0] *  .1020299; netsum += inarray[1] *  4.40924;
netsum += inarray[2] * -.1300482; netsum += inarray[3] * -8.297043E-02;
netsum += inarray[4] * -9.914862;netsum += inarray[5] * -5.721687; feature2[14] = 1 / (1 + exp(-netsum));

netsum = -.9963812; netsum += inarray[0] * -.7348978; netsum += inarray[1] * -.3623974;
netsum += inarray[2] * -7.212708E-02;netsum += inarray[3] *  2.06471; netsum += inarray[4] * -1.198873;
netsum += inarray[5] * -1.125763; feature2[15] = 1 / (1 + exp(-netsum));

netsum = -1.461934; netsum += inarray[0] * -1.305502; netsum += inarray[1] * -.1608762;
netsum += inarray[2] *  1.970749E-02;netsum += inarray[3] *  .9608573;netsum += inarray[4] *  2.246938;
netsum += inarray[5] *  8.511233; feature2[16] = 1 / (1 + exp(-netsum));

netsum =  21.98466; netsum += feature2[0] *  22.25191; netsum += feature2[1] *  9.794468E-03;
netsum += feature2[2] *  655.501; netsum += feature2[3] *  13.48367; netsum += feature2[4] * -12.01737;
netsum += feature2[5] * -.2043335; netsum += feature2[6] *  314.9749; netsum += feature2[7] *  50.47223;
netsum += feature2[8] *  189.7054; netsum += feature2[9] * -3.482806E-03;
netsum += feature2[10] * -14.81476; netsum += feature2[11] *  .1701109;
netsum += feature2[12] *  3.507198; netsum += feature2[13] * -4.830043;
netsum += feature2[14] * -27.65129; netsum += feature2[15] *  4.365238;
netsum += feature2[16] * -6.029491; feature3[0] = 1 / (1 + exp(-netsum));

netsum = -9.441715E-02; netsum += feature2[0] *  1.920301E-02; netsum += feature2[1] * -1.158897;
netsum += feature2[2] *  6.005142; netsum += feature2[3] *  10.49917; netsum += feature2[4] * -1.615091;
netsum += feature2[5] * -4.247871; netsum += feature2[6] * -8.783886; netsum += feature2[7] *  .258846;
netsum += feature2[8] *  1.22469; netsum += feature2[9] * -1.355146; netsum += feature2[10] *  36.03907;
netsum += feature2[11] * -1.658714; netsum += feature2[12] *  9.988897;
```

```
netsum += feature2[13] *  3.301749; netsum += feature2[14] * -7.266922;
netsum += feature2[15] * -1.162612; netsum += feature2[16] *  4.656372;
feature3[1] = 1 / (1 + exp(-netsum));

netsum =  2.209667; netsum += feature2[0] *  2.29604; netsum += feature2[1] * -1.385601;
netsum += feature2[2] *  2.673238; netsum += feature2[3] *  26.52488; netsum += feature2[4] * -7.08518;
netsum += feature2[5] * -3.065511; netsum += feature2[6] * -131.386; netsum += feature2[7] * -118.1533;
netsum += feature2[8] *  3.434504; netsum += feature2[9] * -.7411524;
netsum += feature2[10] * -2.331223; netsum += feature2[11] * -.8347864;
netsum += feature2[12] *  12.67055; netsum += feature2[13] * -1.384228;
netsum += feature2[14] * -2.255741; netsum += feature2[15] * -23.42797;
netsum += feature2[16] *  6.712746; feature3[2] = 1 / (1 + exp(-netsum));

netsum = -1.663667; netsum += feature2[0] * -1.623822; netsum += feature2[1] *  2.66046;
netsum += feature2[2] *  1.480116; netsum += feature2[3] * -18.06391; netsum += feature2[4] *  2.88328;
netsum += feature2[5] *  2.034111; netsum += feature2[6] * -22.02661; netsum += feature2[7] *  2.980034;
netsum += feature2[8] *  5.842053; netsum += feature2[9] * -1.011701;
netsum += feature2[10] * -264.1354; netsum += feature2[11] * -1.094831;
netsum += feature2[12] *  .1758808; netsum += feature2[13] *  .1161178;
netsum += feature2[14] *  9.142639; netsum += feature2[15] * -12.4;
netsum += feature2[16] * -3.596925; feature3[3] = 1 / (1 + exp(-netsum));

netsum = -2.585648; netsum += feature2[0] * -2.643859; netsum += feature2[1] * -2.667191;
netsum += feature2[2] * -7.893235;netsum += feature2[3] *  3.204524; netsum += feature2[4] * -1.675052;
netsum += feature2[5] *  .1581337; netsum += feature2[6] *  8.31107; netsum += feature2[7] * -.0686762;
netsum += feature2[8] *  1.199956; netsum += feature2[9] * -3.280892E-02;
netsum += feature2[10] *  13.85341; netsum += feature2[11] *  9.994907E-02;
netsum += feature2[12] *  .9920209; netsum += feature2[13] *  9.393542;
netsum += feature2[14] *  11.47211; netsum += feature2[15] * -.6574687;
netsum += feature2[16] *  .5734611; feature3[4] = 1 / (1 + exp(-netsum));

netsum =  .3176911; netsum += feature2[0] *  .1333349; netsum += feature2[1] * -.749083;
netsum += feature2[2] *  .3869866; netsum += feature2[3] *  2.750682; netsum += feature2[4] *  4.7707;
netsum += feature2[5] *  4.216469E-02; netsum += feature2[6] *  .274802;
netsum += feature2[7] *  .2990669; netsum += feature2[8] * -.620822;
netsum += feature2[9] * -3.486796E-02; netsum += feature2[10] * -2.00889;
netsum += feature2[11] *  .3208063; netsum += feature2[12] *  .1214016;
netsum += feature2[13] * -3.525733;  netsum += feature2[14] *  .1757359;
netsum += feature2[15] * -.9428302; netsum += feature2[16] *  .9099593;
feature3[5] = 1 / (1 + exp(-netsum));

netsum = -1.439373; netsum += feature2[0] * -1.384696; netsum += feature2[1] * -5.645583;
netsum += feature2[2] * -8.315351;netsum += feature2[3] * -4.612312; netsum += feature2[4] *  .3228945;
netsum += feature2[5] * -2.661298;netsum += feature2[6] * -2.123009; netsum += feature2[7] *  .5246561;
netsum += feature2[8] *  .8434981;netsum += feature2[9] * -1.358192;netsum += feature2[10] *  2.028425;
netsum += feature2[11] * -.5387276; netsum += feature2[12] *  1.766374;
netsum += feature2[13] * -1.327582; netsum += feature2[14] *  6.21976;
netsum += feature2[15] * -1.201128; netsum += feature2[16] *  .3338804;
feature3[6] = 1 / (1 + exp(-netsum));

netsum =  .2270532; netsum += feature2[0] * -1.597217E-02; netsum += feature2[1] *  .1794217;
netsum += feature2[2] * -1.068656; netsum += feature2[3] * -1.315658;netsum += feature2[4] *  5.518153;
netsum += feature2[5] *  .4774743; netsum += feature2[6] * -.3707425; netsum += feature2[7] *  .188641;
netsum += feature2[8] *  .170696; netsum += feature2[9] * -.3279836;netsum += feature2[10] * -3.749949;
```

```
netsum += feature2[11] *  .2619099; netsum += feature2[12] * -.8932151;
netsum += feature2[13] * -4.187588E-02; netsum += feature2[14] *  1.557627;
netsum += feature2[15] * -1.116206; netsum += feature2[16] *  .8174236;
feature3[7] = 1 / (1 + exp(-netsum));

netsum =  .3655963; netsum += feature2[0] *  .3540785; netsum += feature2[1] * -4.330989;
netsum += feature2[2] * -252.8454; netsum += feature2[3] * -108.5673;netsum += feature2[4] *  .8392894;
netsum += feature2[5] *  2.938286; netsum += feature2[6] * -8.771436;netsum += feature2[7] * -196.3515;
netsum += feature2[8] * -3.063646;netsum += feature2[9] *  .7786877;netsum += feature2[10] *  7.141585;
netsum += feature2[11] * -.2673817; netsum += feature2[12] * -5.585548;
netsum += feature2[13] * -4.749362; netsum += feature2[14] *  8.577057;
netsum += feature2[15] * -4.331275; netsum += feature2[16] *  .4559188;
feature3[8] = 1 / (1 + exp(-netsum));

netsum = -.7490611; netsum += feature2[0] * -.6597397; netsum += feature2[1] *  1.565566;
netsum += feature2[2] *  1.758264; netsum += feature2[3] *  55.28933; netsum += feature2[4] * -1.987263;
netsum += feature2[5] * -8.076057E-02; netsum += feature2[6] *  7.327705;
netsum += feature2[7] * -1.55309; netsum += feature2[8] *  2.66824;
netsum += feature2[9] *  8.850194E-02; netsum += feature2[10] * -.4046198;
netsum += feature2[11] * -.2747653; netsum += feature2[12] *  1.454221;
netsum += feature2[13] * -1.784502; netsum += feature2[14] *  2.506942;
netsum += feature2[15] * -2.533293; netsum += feature2[16] *  .7612424;
feature3[9] = 1 / (1 + exp(-netsum));

netsum = -2.442927E-02; netsum += feature2[0] *  .344667; netsum += feature2[1] *  19.29774;
netsum += feature2[2] *  9.199359; netsum += feature2[3] *  975.6089; netsum += feature2[4] * -5.788594;
netsum += feature2[5] * -9.7416; netsum += feature2[6] *  6.452041; netsum += feature2[7] * -3.665535;
netsum += feature2[8] *  .9197361; netsum += feature2[9] * -3.319864E-02;
netsum += feature2[10] *  2.70205; netsum += feature2[11] *  .2989487;
netsum += feature2[12] *  .8362848; netsum += feature2[13] *  39.52069;
netsum += feature2[14] *  43.85501; netsum += feature2[15] * -1.177928;
netsum += feature2[16] *  .1170564;feature3[10] = 1 / (1 + exp(-netsum));

netsum = -.181978; netsum += feature2[0] * -.5041069; netsum += feature2[1] *  11.01427;
netsum += feature2[2] *  15.50456; netsum += feature2[3] * -.1754171; netsum += feature2[4] *  84.73843;
netsum += feature2[5] * -1.417683;netsum += feature2[6] *  1.897596; netsum += feature2[7] * -3.321378;
netsum += feature2[8] * -3.672336; netsum += feature2[9] * -3.145789E-02;
netsum += feature2[10] * -.9096288; netsum += feature2[11] *  .1263328;
netsum += feature2[12] * -11.60814; netsum += feature2[13] * -151.1183;
netsum += feature2[14] * -9.518965; netsum += feature2[15] *  5.457663;
netsum += feature2[16] *  3.280402; feature3[11] = 1 / (1 + exp(-netsum));

netsum =  .2066833; netsum += feature2[0] *  .6291389; netsum += feature2[1] *  .3487742;
netsum += feature2[2] * -1.100214;netsum += feature2[3] * -1.456651; netsum += feature2[4] *  .6887835;
netsum += feature2[5] *  .1624159;netsum += feature2[6] * -.1050742; netsum += feature2[7] * -.1583839;
netsum += feature2[8] *  .3826949; netsum += feature2[9] *  .3627937;
netsum += feature2[10] *  5.011055E-03; netsum += feature2[11] *  2.146612E-02;
netsum += feature2[12] *  .12971; netsum += feature2[13] * -.4708502;
netsum += feature2[14] *  .2674436; netsum += feature2[15] *  .1464488;
netsum += feature2[16] *  .9214792; feature3[12] = 1 / (1 + exp(-netsum));

netsum = -.4021382; netsum += feature2[0] * -.3719796; netsum += feature2[1] * -1.605079;
netsum += feature2[2] * -1.765702;netsum += feature2[3] * -.0224565; netsum += feature2[4] *  2.676246;
netsum += feature2[5] *  3.868871; netsum += feature2[6] *  .2713934; netsum += feature2[7] * -.6232998;
```

```
netsum += feature2[8] * -2.529772; netsum += feature2[9] * -.5894892;
netsum += feature2[10] * -1.138928; netsum += feature2[11] * -.4091205;
netsum += feature2[12] * -.8064309; netsum += feature2[13] * -1.101806;
netsum += feature2[14] * -19.27215; netsum += feature2[15] *  .3979027;
netsum += feature2[16] *  .473321; feature3[13] = 1 / (1 + exp(-netsum));

netsum = -3.746956; netsum += feature2[0] * -4.027164; netsum += feature2[1] * -.7737001;
netsum += feature2[2] * -2.828376; netsum += feature2[3] *  1.901808; netsum += feature2[4] *  2.267383;
netsum += feature2[5] * -2.224894;netsum += feature2[6] * -48.06786; netsum += feature2[7] *  6.944082;
netsum += feature2[8] * -4.624728;netsum += feature2[9] * -2.38311; netsum += feature2[10] *  10.05116;
netsum += feature2[11] * -.5914407; netsum += feature2[12] *  3.933043;
netsum += feature2[13] *  .422413; netsum += feature2[14] * -.8687955;
netsum += feature2[15] * -6.008258; netsum += feature2[16] *  4.25731;
feature3[14] = 1 / (1 + exp(-netsum));

netsum = -7.025997; netsum += feature2[0] * -6.82494; netsum += feature2[1] * -1.172834;
netsum += feature2[2] *  1.454357; netsum += feature2[3] *  4.069937; netsum += feature2[4] *  8.700971;
netsum += feature2[5] *  5.502646E-03; netsum += feature2[6] * -.4555604;
netsum += feature2[7] *  5.853171; netsum += feature2[8] *  6.966273E-02;
netsum += feature2[9] *  8.979424E-02; netsum += feature2[10] * -2.367011;
netsum += feature2[11] * -1.345811; netsum += feature2[12] * -4.42798;
netsum += feature2[13] * -4.685797;  netsum += feature2[14] *  2.768926;
netsum += feature2[15] *  3.739944; netsum += feature2[16] * -5.75929;
feature3[15] = 1 / (1 + exp(-netsum));

netsum = -1.661608; netsum += feature2[0] * -1.220749; netsum += feature2[1] * -.6661804;
netsum += feature2[2] * -2.762789;netsum += feature2[3] * -152.5842; netsum += feature2[4] * -.3821257;
netsum += feature2[5] * -2.364557;netsum += feature2[6] * -17.86898; netsum += feature2[7] *  5.310775;
netsum += feature2[8] * -1.831967; netsum += feature2[9] * -1.506387;
netsum += feature2[10] *  3.239048; netsum += feature2[11] * -1.072615;
netsum += feature2[12] *  4.463168; netsum += feature2[13] * -.8064213;
netsum += feature2[14] *  .2074858; netsum += feature2[15] *  .1098837;
netsum += feature2[16] * -.3780876; feature3[16] = 1 / (1 + exp(-netsum));

netsum = -.2023443; netsum += feature3[0] * -.2854584; netsum += feature3[1] * -.5041612;
netsum += feature3[2] *  .632741; netsum += feature3[3] *  .6220419; netsum += feature3[4] * -.1951409;
netsum += feature3[5] * -.2396716;netsum += feature3[6] *  7.688838; netsum += feature3[7] * -.2619227;
netsum += feature3[8] *  .8785699;netsum += feature3[9] *  .5186343;netsum += feature3[10] * -.2430233;
netsum += feature3[11] *  .1584135; netsum += feature3[12] * -.3976248;
netsum += feature3[13] *  .5879129; netsum += feature3[14] *  .6953321;
netsum += feature3[15] *  6.691236; netsum += feature3[16] *  1.178057;
outarray[0] = 1 / (1 + exp(-netsum));

 outarray[0] =  1.959 *  (outarray[0] - .1) / .8  + -.349;
if (outarray[0]<-.349) outarray[0] = -.349;
if (outarray[0]> 1.61) outarray[0] =  1.61;
 *IFmy = outarray[0];
}
```

C.3.3 Neural Network model for Predicting Fluctuating Drag IF

```
/* This code fires the neural network for predicting fluctuating drag IF*/
/* The network has 6 input nodes and one output node, 2 hidden layers with 14 nodes in each layer */
/* This code is designed to be simple and fast for porting to any machine . Therefore all code and weights */
/* are inline without looping or data storage which might be harder to port between compilers. */

#include <math.h>
 NNsigmax(angle, Iv, b, h, sx, sy, IFsx)
double angle, Iv, b, h, sx, sy, *IFsx;
{
 double netsum, feature2[14], double feature3[14], double inarray[6], double outarray[1];
/* inarray[0] is Angle, inarray[1] is Iv , inarray[2] is b, inarray[3] is h, */
/* inarray[4] is Sx , inarray[5] is Sy, outarray[0] is IFsx */

inarray[0] = angle/45.0; inarray[1] = Iv/100.0; inarray[2] = b; inarray[3] = h;inarray[4] = sx;inarray[5] = sy;

if (inarray[0]< 0) inarray[0] =  0; if (inarray[0]> 1) inarray[0] =  1; inarray[0] =  2 * inarray[0] -1;
if (inarray[1]< .07) inarray[1] =  .07; if (inarray[1]> .25) inarray[1] =  .25;
inarray[1] =  2 * (inarray[1] -  .07) / .18 -1;
if (inarray[2]< .667) inarray[2] =  .667; if (inarray[2]> 2) inarray[2] =  2;
inarray[2] =  2 * (inarray[2] -  .667) / 1.333 -1;
if (inarray[3]< 1) inarray[3] =  1; if (inarray[3]> 2) inarray[3] =  2; inarray[3] =  2 * (inarray[3] -  1) -1;
if (inarray[4]<-6) inarray[4] = -6; if (inarray[4]> 14) inarray[4] =  14;
inarray[4] =  2 * (inarray[4] +  6) /20 - 1; if (inarray[5]<-6) inarray[5] = -6;
if (inarray[5]> 8) inarray[5] =  8;inarray[5] =  2 * (inarray[5] +  6) / 14 -1;

netsum =  1.20805; netsum += inarray[0] *  1.389696; netsum += inarray[1] *  3.747058;
netsum += inarray[2] *  1.022878; netsum += inarray[3] *  .5132967; netsum += inarray[4] * -26.9788;
netsum += inarray[5] * -2.382929; feature2[0] = 1 / (1 + exp(-netsum));

netsum =  2.478925; netsum += inarray[0] *  2.149764; netsum += inarray[1] *  1.597753;
netsum += inarray[2] *  9.218743; netsum += inarray[3] *  2.59077; netsum += inarray[4] *  10.96746;
netsum += inarray[5] *  1.149267; feature2[1] = 1 / (1 + exp(-netsum));

netsum =  174.3468; netsum += inarray[0] *  174.2857; netsum += inarray[1] * -.2241132;
netsum += inarray[2] * -.9439262; netsum += inarray[3] * -.3931135; netsum += inarray[4] *  9.945068;
netsum += inarray[5] *  19.50452; feature2[2] = 1 / (1 + exp(-netsum));

netsum =  .1642886; netsum += inarray[0] * -.1022856; netsum += inarray[1] *  .9639274;
netsum += inarray[2] *  3.30385; netsum += inarray[3] *  1.746314; netsum += inarray[4] * -9.432745;
netsum += inarray[5] *  11.58623; feature2[3] = 1 / (1 + exp(-netsum));

netsum =  3.406643; netsum += inarray[0] *  3.144025; netsum += inarray[1] * -13.87746;
netsum += inarray[2] *  .8681836; netsum += inarray[3] *  1.427674; netsum += inarray[4] *  14.97046;
netsum += inarray[5] *  58.29533; feature2[4] = 1 / (1 + exp(-netsum));

netsum = -20.61761; netsum += inarray[0] * -20.806; netsum += inarray[1] * -17.98771;
netsum += inarray[2] * -10.6213; netsum += inarray[3] * -8.148485; netsum += inarray[4] *  34.3442;
netsum += inarray[5] * -.5184844; feature2[5] = 1 / (1 + exp(-netsum));

netsum = -474.765; netsum += inarray[0] * -474.3821; netsum += inarray[1] * -3.244617;
netsum += inarray[2] *  3.727103; netsum += inarray[3] * -2.249237; netsum += inarray[4] * -7.106648;
netsum += inarray[5] *  73.94875; feature2[6] = 1 / (1 + exp(-netsum));
```

```
netsum = -2.493529; netsum += inarray[0] * -2.763691; netsum += inarray[1] *  3.686451;
netsum += inarray[2] *  .4702337; netsum += inarray[3] *  .3705728; netsum += inarray[4] * -1.561085;
netsum += inarray[5] * -9.554892; feature2[7] = 1 / (1 + exp(-netsum));

netsum =  .117388; netsum += inarray[0] * -.304866; netsum += inarray[1] * -2.099214;
netsum += inarray[2] *  6.227221; netsum += inarray[3] *  6.362922; netsum += inarray[4] * -12.20159;
netsum += inarray[5] * -13.58041; feature2[8] = 1 / (1 + exp(-netsum));

netsum = -.3462435; netsum += inarray[0] * -.7914051; netsum += inarray[1] *  2.057255;
netsum += inarray[2] * -.5098069; netsum += inarray[3] *  1.143024; netsum += inarray[4] *  7.842332;
netsum += inarray[5] * -4.507905; feature2[9] = 1 / (1 + exp(-netsum));

netsum = -1.893931; netsum += inarray[0] * -1.993049; netsum += inarray[1] *  3.280659;
netsum += inarray[2] * -2.11765; netsum += inarray[3] * -1.706038; netsum += inarray[4] * -.2285572;
netsum += inarray[5] *  .1108782; feature2[10] = 1 / (1 + exp(-netsum));

netsum =  3.453593; netsum += inarray[0] *  3.164954; netsum += inarray[1] * -2.050394;
netsum += inarray[2] * -1.366089E-02; netsum += inarray[3] *  7.051506E-02;
netsum += inarray[4] *  4.494117; netsum += inarray[5] * -9.233224; feature2[11] = 1 / (1 + exp(-netsum));

netsum = -3.502324; netsum += inarray[0] * -3.609626; netsum += inarray[1] *  3.425473E-02;
netsum += inarray[2] * -5.102934; netsum += inarray[3] *  8.364184; netsum += inarray[4] * -16.44497;
netsum += inarray[5] * -.2238104; feature2[12] = 1 / (1 + exp(-netsum));

netsum =  242.5442; netsum += inarray[0] *  242.5788; netsum += inarray[1] *  12.66628;
netsum += inarray[2] *  2.72647; netsum += inarray[3] *  .9879422; netsum += inarray[4] * -7.689018;
netsum += inarray[5] * -144.0078; feature2[13] = 1 / (1 + exp(-netsum));

netsum =  11.95408; netsum += feature2[0] *  12.02724; netsum += feature2[1] * -5.287333;
netsum += feature2[2] *  1.573893;netsum += feature2[3] * -17.60161; netsum += feature2[4] * -.4505034;
netsum += feature2[5] * -6.816415;netsum += feature2[6] * -.9242731; netsum += feature2[7] *  21.89444;
netsum += feature2[8] * -4.565635; netsum += feature2[9] *  .5623548;
netsum += feature2[10] * -.5744507; netsum += feature2[11] * -.2526899;
netsum += feature2[12] *  5.182776; netsum += feature2[13] * -4.577964;
feature3[0] = 1 / (1 + exp(-netsum));

netsum = -2.539844; netsum += feature2[0] * -2.493499; netsum += feature2[1] *  2.040028;
netsum += feature2[2] * -.4673971; netsum += feature2[3] *  10.12327; netsum += feature2[4] *  2.928389;
netsum += feature2[5] * -1.199849;netsum += feature2[6] * -8.713886E-02; netsum += feature2[7] * -28.9;
netsum += feature2[8] * -8.084008; netsum += feature2[9] * -.6294707;
netsum += feature2[10] * -5.091599; netsum += feature2[11] *  .7626099;
netsum += feature2[12] *  2.716516; netsum += feature2[13] * -.3660978;
feature3[1] = 1 / (1 + exp(-netsum));

netsum =  1.918388; netsum += feature2[0] *  1.944701; netsum += feature2[1] *  2.159621;
netsum += feature2[2] * -1.431164; netsum += feature2[3] * -3.496638; netsum += feature2[4] * -1.65798;
netsum += feature2[5] *  .3682027; netsum += feature2[6] * -.3783498; netsum += feature2[7] *  55.61106;
netsum += feature2[8] * -7.897944;netsum += feature2[9] * -10.9327; netsum += feature2[10] *  .9213243;
netsum += feature2[11] *  .8119825; netsum += feature2[12] *  .4217039;
netsum += feature2[13] * -5.783743; feature3[2] = 1 / (1 + exp(-netsum));

netsum = -94.34023; netsum += feature2[0] * -94.80325; netsum += feature2[1] * -2.196241;
netsum += feature2[2] *  4.223174; netsum += feature2[3] *  22.08274; netsum += feature2[4] * -5.628299;
```

```
netsum += feature2[5] *  32.66164; netsum += feature2[6] *  29.02589; netsum += feature2[7] * -35.07125;
netsum += feature2[8] * -3.471447; netsum += feature2[9] *  8.362792;
netsum += feature2[10] * -8.549549E-02; netsum += feature2[11] * -3.39619;
netsum += feature2[12] *  2.742441; netsum += feature2[13] *  65.59381;
feature3[3] = 1 / (1 + exp(-netsum));

netsum = -9.019506; netsum += feature2[0] * -8.614139; netsum += feature2[1] *  6.232363;
netsum += feature2[2] * -2.431525; netsum += feature2[3] *  16.20409; netsum += feature2[4] *  .2837894;
netsum += feature2[5] * -1.015313;netsum += feature2[6] * -.5336202; netsum += feature2[7] *  1.387059;
netsum += feature2[8] *  506.5494;netsum += feature2[9] *  1.981066;netsum += feature2[10] *  4.230393;
netsum += feature2[11] *  4.397417;netsum += feature2[12] *  139.45;netsum += feature2[13] *  2.170991;
feature3[4] = 1 / (1 + exp(-netsum));

netsum = -2.253678; netsum += feature2[0] * -2.51159; netsum += feature2[1] * -.8251243;
netsum += feature2[2] * -1.249243;netsum += feature2[3] *  .8854095; netsum += feature2[4] * -.4584546;
netsum += feature2[5] * -.2913869;netsum += feature2[6] *  .6821151; netsum += feature2[7] * -1.089791;
netsum += feature2[8] * -.1336867; netsum += feature2[9] * -.2774635;
netsum += feature2[10] * -1.049702; netsum += feature2[11] *  3.164295;
netsum += feature2[12] * -6.193014E-02; netsum += feature2[13] * -.7910458;
feature3[5] = 1 / (1 + exp(-netsum));

netsum = -3.127104; netsum += feature2[0] * -3.449508; netsum += feature2[1] * -3.444319;
netsum += feature2[2] * -.7422214; netsum += feature2[3] * -3.476655;
netsum += feature2[4] *  8.794951E-02; netsum += feature2[5] *  .115592;
netsum += feature2[6] *  5.030956; netsum += feature2[7] *  11.37568; netsum += feature2[8] * -19.73276;
netsum += feature2[9] *  .9170184;netsum += feature2[10] *  38.25433;netsum += feature2[11] *  .468016;
netsum += feature2[12] * -10.84694; netsum += feature2[13] *  11.41008;
feature3[6] = 1 / (1 + exp(-netsum));

netsum = -1.4587; netsum += feature2[0] * -1.338176; netsum += feature2[1] * -.4473642;
netsum += feature2[2] * -1.624758; netsum += feature2[3] *  .367549; netsum += feature2[4] * -.4664221;
netsum += feature2[5] * -.3603213; netsum += feature2[6] *  .6520985;netsum += feature2[7] * -1.357607;
netsum += feature2[8] * -.3011418; netsum += feature2[9] * -.4994008;
netsum += feature2[10] * -.5199615; netsum += feature2[11] *  3.111704;
netsum += feature2[12] * -1.919584E-02; netsum += feature2[13] * -.6159054;
feature3[7] = 1 / (1 + exp(-netsum));

netsum = -1.068969; netsum += feature2[0] * -.8856944; netsum += feature2[1] *  .8734049;
netsum += feature2[2] *  1.487651; netsum += feature2[3] *  2.01983; netsum += feature2[4] * -2.531518;
netsum += feature2[5] * -.6818703; netsum += feature2[6] *  1.081514;netsum += feature2[7] * -10.45501;
netsum += feature2[8] *  7.20897; netsum += feature2[9] * -3.890713;netsum += feature2[10] * -52.91467;
netsum += feature2[11] *  2.805081; netsum += feature2[12] *  33.14056;
netsum += feature2[13] * -3.032446; feature3[8] = 1 / (1 + exp(-netsum));

netsum = -2.451468; netsum += feature2[0] * -2.250339; netsum += feature2[1] * -.5231699;
netsum += feature2[2] * -.1635088; netsum += feature2[3] *  4.485424;netsum += feature2[4] * -.2910785;
netsum += feature2[5] * -5.273783; netsum += feature2[6] * -4.466717;netsum += feature2[7] * -5.460445;
netsum += feature2[8] *  3.824427; netsum += feature2[9] *  .888444; netsum += feature2[10] *  3.726739;
netsum += feature2[11] *  .7021886; netsum += feature2[12] * -7.927748;
netsum += feature2[13] *  .0234571; feature3[9] = 1 / (1 + exp(-netsum));
 netsum =  1.798404; netsum += feature2[0] *  1.386184; netsum += feature2[1] *  .3951239;
netsum += feature2[2] * -4.108757; netsum += feature2[3] * -4.792764;netsum += feature2[4] *  1.782916;
netsum += feature2[5] *  5.644722; netsum += feature2[6] *  8.766236; netsum += feature2[7] *  77.51235;
netsum += feature2[8] * -21.53361; netsum += feature2[9] *  17.25458;netsum += feature2[10] *  136.1916;
```

```
netsum += feature2[11] * -.5702398; netsum += feature2[12] * -5.604276;
netsum += feature2[13] *  2.832377; feature3[10] = 1 / (1 + exp(-netsum));

netsum =  .6389452; netsum += feature2[0] *  .5702786; netsum += feature2[1] * -.4295131;
netsum += feature2[2] * -.7895747; netsum += feature2[3] * -3.44917; netsum += feature2[4] * -1.44736;
netsum += feature2[5] *  2.00375; netsum += feature2[6] *  .3501926; netsum += feature2[7] * -1.762709;
netsum += feature2[8] *  2.293572; netsum += feature2[9] * -.374153; netsum += feature2[10] *  1.046286;
netsum += feature2[11] * -.1464832; netsum += feature2[12] * -2.068316;
netsum += feature2[13] * -2.381713; feature3[11] = 1 / (1 + exp(-netsum));

netsum = -1.871579; netsum += feature2[0] * -1.554174; netsum += feature2[1] * -3.724299;
netsum += feature2[2] *  5.206225E-02; netsum += feature2[3] *  2.39131;
netsum += feature2[4] * -.7389356; netsum += feature2[5] *  8.663327;netsum += feature2[6] * -.6234229;
netsum += feature2[7] * -11.29407; netsum += feature2[8] * -6.357502;netsum += feature2[9] * -.5295238;
netsum += feature2[10] * -12.75168; netsum += feature2[11] *  .5928643;
netsum += feature2[12] *  3.081871; netsum += feature2[13] *  2.803325;
feature3[12] = 1 / (1 + exp(-netsum));

netsum = -.7964826; netsum += feature2[0] * -.8693236; netsum += feature2[1] *  .4577513;
netsum += feature2[2] * -3.971766; netsum += feature2[3] *  .9086901;netsum += feature2[4] * -.3297983;
netsum += feature2[5] * -.6847123; netsum += feature2[6] *  1.024968;netsum += feature2[7] * -12.38481;
netsum += feature2[8] *  .1298577; netsum += feature2[9] * -.5033534;
netsum += feature2[10] * -2.553259; netsum += feature2[11] *  1.071767;
netsum += feature2[12] *  .9703329;  netsum += feature2[13] *  1.504226;
feature3[13] = 1 / (1 + exp(-netsum));

netsum = -.2505203; netsum += feature3[0] * -.2125981; netsum += feature3[1] *  .3572012;
netsum += feature3[2] *  .5431378; netsum += feature3[3] *  .381394; netsum += feature3[4] * -.3939942;
netsum += feature3[5] *  1.315949; netsum += feature3[6] * -.2747229; netsum += feature3[7] *  1.684937;
netsum += feature3[8] *  .2599323; netsum += feature3[9] *  1.13917; netsum += feature3[10] * -.2981;
netsum += feature3[11] *  .3574841; netsum += feature3[12] *  .2033706;
netsum += feature3[13] *  .453217; outarray[0] = 1 / (1 + exp(-netsum));

 outarray[0] =  1.244 *  (outarray[0] - .1) / .8  +  .55;
if (outarray[0]< .55) outarray[0] =  .55;
if (outarray[0]> 1.794) outarray[0] =  1.794;
*IFsx = outarray[0];
}
```

C.3.4 Neural Network model for Predicting Fluctuating Lift IF

```
/* This code fires the neural network for predicting fluctuating lift IF*/
/* The network has 6 input nodes and one output node, 2 hidden layers with 17 nodes in each layer */
/* This code is designed to be simple and fast for porting to any machine. Therefore all code and weights */
/* are inline without looping or data storage which might be harder to port between compilers. */

#include <math.h>
 NNsigmay(angle, Iv, b, h, sx, sy, IFsy)
double angle, Iv, b, h, sx, sy, *IFsy;
{
 double netsum, feature2[17], feature3[17], inarray[6], outarray[1];
```

```
/* inarray[0] is Angle, inarray[1] is Iv ,  inarray[2] is b, inarray[3] is h, */
/* inarray[4] is Sx , inarray[5] is Sy, outarray[0] is IFsy */

inarray[0] = angle/45.0; inarray[1] = Iv/100.0; inarray[2] = b; inarray[3] = h;inarray[4] = sx;inarray[5] = sy;

if (inarray[0]< 0) inarray[0] =  0; if (inarray[0]> 1) inarray[0] =  1; inarray[0] =  2 * inarray[0] -1;
if (inarray[1]< .07) inarray[1] =  .07; if (inarray[1]> .25) inarray[1] =  .25;
inarray[1] =  2 * (inarray[1] -  .07) / .18 -1;
if (inarray[2]< .667) inarray[2] =  .667; if (inarray[2]> 2) inarray[2] =  2;
inarray[2] =  2 * (inarray[2] -  .667) / 1.333 -1;
if (inarray[3]< 1) inarray[3] =  1; if (inarray[3]> 2) inarray[3] =  2; inarray[3] =  2 * (inarray[3] -  1) -1;
if (inarray[4]<-6) inarray[4] = -6; if (inarray[4]> 12) inarray[4] =  12;
inarray[4] =  2 * (inarray[4] +  6) / 18 -1; if (inarray[5]<-7) inarray[5] = -7;
if (inarray[5]> 8) inarray[5] =  8;inarray[5] =  2 * (inarray[5] +  7) / 15 -1;

netsum = -.5234975; netsum += inarray[0] * -.4691809; netsum += inarray[1] *  .1698853;
netsum += inarray[2] *  .8053327; netsum += inarray[3] * -.138877; netsum += inarray[4] *  1.61182;
netsum += inarray[5] *  2.25602; feature2[0] = 1 / (1 + exp(-netsum));

netsum =  2.755499; netsum += inarray[0] *  2.478295; netsum += inarray[1] *  5.768715;
netsum += inarray[2] * -3.851286; netsum += inarray[3] * -1.228571; netsum += inarray[4] *  1.4733;
netsum += inarray[5] *  3.672381; feature2[1] = 1 / (1 + exp(-netsum));

netsum =  2.215848; netsum += inarray[0] *  2.173425; netsum += inarray[1] *  2.861951;
netsum += inarray[2] *  5.727424; netsum += inarray[3] *  1.081417; netsum += inarray[4] *  2.278805;
netsum += inarray[5] * -24.95615; feature2[2] = 1 / (1 + exp(-netsum));

netsum =  1.058541; netsum += inarray[0] *  1.157305; netsum += inarray[1] *  3.737079;
netsum += inarray[2] *  4.629634; netsum += inarray[3] * -.4150238; netsum += inarray[4] *  7.483263;
netsum += inarray[5] * -1.253475; feature2[3] = 1 / (1 + exp(-netsum));

netsum =  1.010261; netsum += inarray[0] *  1.067956; netsum += inarray[1] * -1.078159;
netsum += inarray[2] * -.1674923; netsum += inarray[3] *  .3500696; netsum += inarray[4] * -.8621936;
netsum += inarray[5] * -.764094; feature2[4] = 1 / (1 + exp(-netsum));

netsum = -4.162245; netsum += inarray[0] * -4.452683; netsum += inarray[1] *  3.080859;
netsum += inarray[2] * -1.984687; netsum += inarray[3] * -1.287967; netsum += inarray[4] * -2.3214;
netsum += inarray[5] *  12.04685; feature2[5] = 1 / (1 + exp(-netsum));

netsum =  .6603913; netsum += inarray[0] *  .5818408; netsum += inarray[1] *  .2737159;
netsum += inarray[2] * -1.009881; netsum += inarray[3] *  1.055253; netsum += inarray[4] *  15.84988;
netsum += inarray[5] *  8.816561; feature2[6] = 1 / (1 + exp(-netsum));

netsum =  1.57948; netsum += inarray[0] *  .938163; netsum += inarray[1] *  1.422397;
netsum += inarray[2] *  3.393803; netsum += inarray[3] *  1.638334; netsum += inarray[4] *  2.221265;
netsum += inarray[5] *  2.544474; feature2[7] = 1 / (1 + exp(-netsum));

netsum = -.2290078; netsum += inarray[0] * -.6869594; netsum += inarray[1] *  .6691074;
netsum += inarray[2] * -.6062338; netsum += inarray[3] * -.0492705; netsum += inarray[4] *  2.152192;
netsum += inarray[5] *  .8311747; feature2[8] = 1 / (1 + exp(-netsum));

netsum = -30.34255; netsum += inarray[0] * -30.4757; netsum += inarray[1] *  .5271954;
netsum += inarray[2] * -20.22071; netsum += inarray[3] * -16.06137; netsum += inarray[4] * -57.68306;
netsum += inarray[5] * -5.745067; feature2[9] = 1 / (1 + exp(-netsum));
```

```
netsum = -5.0862; netsum += inarray[0] * -4.779646; netsum += inarray[1] * -2.99588;
netsum += inarray[2] *  6.298084; netsum += inarray[3] *  8.360859; netsum += inarray[4] * -6.261894;
netsum += inarray[5] *  .3431876; feature2[10] = 1 / (1 + exp(-netsum));

netsum =  11.56519; netsum += inarray[0] *  11.41277; netsum += inarray[1] * -3.922804;
netsum += inarray[2] * -18.07987; netsum += inarray[3] * -1.793761; netsum += inarray[4] * -20.26226;
netsum += inarray[5] * -81.85622; feature2[11] = 1 / (1 + exp(-netsum));

netsum =  .2213712; netsum += inarray[0] *  6.346229E-02; netsum += inarray[1] *  .5804648;
netsum += inarray[2] *  .2518557; netsum += inarray[3] *  .2617642; netsum += inarray[4] * -1.224525;
netsum += inarray[5] * -5.95516; feature2[12] = 1 / (1 + exp(-netsum));

netsum =  2.228709; netsum += inarray[0] *  2.022827; netsum += inarray[1] *  5.765227;
netsum += inarray[2] * -1.672433; netsum += inarray[3] * -.7071466; netsum += inarray[4] * -4.728745;
netsum += inarray[5] *  25.56511; feature2[13] = 1 / (1 + exp(-netsum));

netsum =  .5139022; netsum += inarray[0] *  .7535684; netsum += inarray[1] *  2.054381;
netsum += inarray[2] *  3.453411; netssum += inarray[3] *  2.437324 netsum += inarray[4] * -10.66794;
netsum += inarray[5] *  8.164324; feature2[14] = 1 / (1 + exp(-netsum));

netsum =  .2468642; netsum += inarray[0] *  .4270723; netsum += inarray[1] *  2.067193E-02;
netsum += inarray[2] *  20.50154; netsum += inarray[3] * -.4521952; netsum += inarray[4] * -13.325;
netsum += inarray[5] * -10.36703; feature2[15] = 1 / (1 + exp(-netsum));

netsum =  842.5016; netsum += inarray[0] *  842.6636; netsum += inarray[1] *  1.537167;
netsum += inarray[2] * -1.620075; netsum += inarray[3] *  1.637372; netsum += inarray[4] *  2.510219;
netsum += inarray[5] *  7.830803; feature2[16] = 1 / (1 + exp(-netsum));

netsum =  7.002063E-02; netsum += feature2[0] *  .3679131; netsum += feature2[1] * -1.428476;
netsum += feature2[2] * -2.721658; netsum += feature2[3] *  8.027017;
netsum += feature2[4] *  1.318986E-02; netsum += feature2[5] * -5.436129;
netsum += feature2[6] *  1.033891; netsum += feature2[7] *  5.029002; netsum += feature2[8] *  1.580846;
netsum += feature2[9] *  .4013727; netsum += feature2[10] * -4.486714;
netsum += feature2[11] * -.5517701; netsum += feature2[12] * -.7865537;
netsum += feature2[13] *  3.876369; netsum += feature2[14] * -4.353261;
netsum += feature2[15] *  8.244522; netsum += feature2[16] * -.5972756;
feature3[0] = 1 / (1 + exp(-netsum));

netsum =  9.969191E-02; netsum += feature2[0] *  .3989961; netsum += feature2[1] *  7.154096E-02;
netsum += feature2[2] *  .4786238; netsum += feature2[3] *  .1266692; netsum += feature2[4] * -.4363723;
netsum += feature2[5] *  .3977933; netsum += feature2[6] * -.6353419; netsum += feature2[7] *  .2943768;
netsum += feature2[8] *  .4364567;netsum += feature2[9] *  .1224003;netsum += feature2[10] * -.7071894;
netsum += feature2[11] * -1.273798; netsum += feature2[12] * -.7181405;
netsum += feature2[13] * -.4059735; netsum += feature2[14] * -8.797991E-02;
netsum += feature2[15] *  .6126429; netsum += feature2[16] * -.2738469;
feature3[1] = 1 / (1 + exp(-netsum));

netsum =  1.602875; netsum += feature2[0] *  1.670547; netsum += feature2[1] *  7.480943;
netsum += feature2[2] *  3.687899; netsum += feature2[3] * -64.68496; netsum += feature2[4] *  .560288;
netsum += feature2[5] *  6.107778; netsum += feature2[6] * -11.92393; netsum += feature2[7] *  5.126218;
netsum += feature2[8] *  1.403501; netsum += feature2[9] * -1.391626;
netsum += feature2[10] * -2.460809; netsum += feature2[11] * -.2026062;
netsum += feature2[12] * -13.29282; netsum += feature2[13] *  1.549342;
```

```
netsum += feature2[14] * -.2416277; netsum += feature2[15] * -3.881628;
netsum += feature2[16] *  1.148356; feature3[2] = 1 / (1 + exp(-netsum));

netsum = -5.142202E-02; netsum += feature2[0] * -.1727207; netsum += feature2[1] * -.5746776;
netsum += feature2[2] * -2.037428;netsum += feature2[3] * -.5974432; netsum += feature2[4] *  .4750788;
netsum += feature2[5] * -.2466601;netsum += feature2[6] *  .6111555; netsum += feature2[7] * -.0342424;
netsum += feature2[8] * -.2902392; netsum += feature2[9] * -7.665923E-02;
netsum += feature2[10] *  6.358673E-02; netsum += feature2[11] * -.149095;
netsum += feature2[12] *  3.588614E-02; netsum += feature2[13] *  .6465396;
netsum += feature2[14] *  3.162854E-02; netsum += feature2[15] * -.1510507;
netsum += feature2[16] * -.2563983; feature3[3] = 1 / (1 + exp(-netsum));

netsum =  .3053924; netsum += feature2[0] *  .1947398; netsum += feature2[1] *  1.348557;
netsum += feature2[2] *  11.34401; netsum += feature2[3] *  8.803256;
netsum += feature2[4] *  3.708697E-02; netsum += feature2[5] * -3.527278;
netsum += feature2[6] * -1.092865; netsum += feature2[7] * -7.353796;
netsum += feature2[8] * -8.396819E-02; netsum += feature2[9] * -3.645407;
netsum += feature2[10] * -1.914687; netsum += feature2[11] * -6.970372;
netsum += feature2[12] *  1.13331; netsum += feature2[13] *  2.060375;
netsum += feature2[14] *  .757682; netsum += feature2[15] *  11.65749;
netsum += feature2[16] *  1.706749; feature3[4] = 1 / (1 + exp(-netsum));

netsum =  .2162886; netsum += feature2[0] * -8.960922E-03; netsum += feature2[1] * -3.342413;
netsum += feature2[2] * -.6366304;netsum += feature2[3] * -2.353294; netsum += feature2[4] *  3.302991;
netsum += feature2[5] * -1.721979; netsum += feature2[6] *  .1667166;  netsum += feature2[7] *  3.80031;
netsum += feature2[8] * -.1438652; netsum += feature2[9] * -.1764546;
netsum += feature2[10] *  .2919473;  netsum += feature2[11] * -.1111337;
netsum += feature2[12] * -.6179213;  netsum += feature2[13] *  3.875433;
netsum += feature2[14] * -7.913342; netsum += feature2[15] *  140.9931;
netsum += feature2[16] * -4.04722; feature3[5] = 1 / (1 + exp(-netsum));

netsum =  .7173901; netsum += feature2[0] *  .7412454; netsum += feature2[1] *  5.100038;
netsum += feature2[2] * -1091.127;netsum += feature2[3] * -208.8495; netsum += feature2[4] * -5.966786;
netsum += feature2[5] *  3.599876;netsum += feature2[6] * -2.446052E-02;
netsum += feature2[7] * -5.999775; netsum += feature2[8] *  .8340796; netsum += feature2[9] *  .6500478;
netsum += feature2[10] *  19.38442; netsum += feature2[11] *  12.58616;
netsum += feature2[12] * -26.35854; netsum += feature2[13] * -.9804661;
netsum += feature2[14] *  26.33802; netsum += feature2[15] * -205.1707;
netsum += feature2[16] * -4.261616;feature3[6] = 1 / (1 + exp(-netsum));

netsum =  .19152; netsum += feature2[0] *  2.591019E-02; netsum += feature2[1] *  2.191121;
netsum += feature2[2] *  3.808081; netsum += feature2[3] *  .8459163; netsum += feature2[4] * -.2145392;
netsum += feature2[5] *  .2220641; netsum += feature2[6] * -.4109038; netsum += feature2[7] *  .2661347;
netsum += feature2[8] *  .426264; netsum += feature2[9] * -9.472127E-02;
netsum += feature2[10] *  1.309234; netsum += feature2[11] *  .6558262;
netsum += feature2[12] *  2.487461; netsum += feature2[13] * -.8638321;
netsum += feature2[14] *  5.298436E-03; netsum += feature2[15] *  .3162168;
netsum += feature2[16] * -.1954974; feature3[7] = 1 / (1 + exp(-netsum));
netsum =  7.688728E-02; netsum += feature2[0] * -2.06829E-03; netsum += feature2[1] *  1.594982;
netsum += feature2[2] * -23.49134; netsum += feature2[3] *  .3797363;
netsum += feature2[4] * -2.386399E-02; netsum += feature2[5] * -2.348327;
netsum += feature2[6] * -.6814575; netsum += feature2[7] *  1.409646;
netsum += feature2[8] * -2.840193E-02; netsum += feature2[9] *  8.782143;
netsum += feature2[10] * -.6004543; netsum += feature2[11] * -.7114358;
```

```
netsum += feature2[12] * -59.21994; netsum += feature2[13] * -.894133;
netsum += feature2[14] *  7.199222; netsum += feature2[15] * -.5676019;
netsum += feature2[16] *  .7227787; feature3[8] = 1 / (1 + exp(-netsum));

netsum = -.8661603; netsum += feature2[0] * -.8915868; netsum += feature2[1] * -.6327117;
netsum += feature2[2] *  7.471171; netsum += feature2[3] * -2.538476; netsum += feature2[4] *  1.318736;
netsum += feature2[5] *  .5776473; netsum += feature2[6] *  5.057993; netsum += feature2[7] * -5.054674;
netsum += feature2[8] * -3.703466; netsum += feature2[9] *  1.281765;
netsum += feature2[10] * -.2073815; netsum += feature2[11] *  .8858638;
netsum += feature2[12] *  .7494262;  netsum += feature2[13] *  1.156769;
netsum += feature2[14] * -3.645156; netsum += feature2[15] * -.5264646;
netsum += feature2[16] *  4.254569; feature3[9] = 1 / (1 + exp(-netsum));

netsum =  .1859055; netsum += feature2[0] *  .5558855; netsum += feature2[1] * -21.25051;
netsum += feature2[2] * -8.825708;netsum += feature2[3] *  155.3734; netsum += feature2[4] * -.6828206;
netsum += feature2[5] * -.3857552;netsum += feature2[6] *  4.255913; netsum += feature2[7] * -1.515691;
netsum += feature2[8] *  .2510208; netsum += feature2[9] *  5.668711;
netsum += feature2[10] * -1.095104; netsum += feature2[11] * -2.230436;
netsum += feature2[12] * -.115444; netsum += feature2[13] * -11.87648;
netsum += feature2[14] *  .2785862; netsum += feature2[15] *  262.594;
netsum += feature2[16] *  3.456178; feature3[10] = 1 / (1 + exp(-netsum));

netsum = -5.542992; netsum += feature2[0] * -6.007411; netsum += feature2[1] * -2.645458;
netsum += feature2[2] *  2.698593; netsum += feature2[3] * -5.788582; netsum += feature2[4] *  4.335444;
netsum += feature2[5] *  3.586174; netsum += feature2[6] *  35.61002; netsum += feature2[7] *  3.139076;
netsum += feature2[8] * -2.298276; netsum += feature2[9] *  .6948254;
netsum += feature2[10] * -.6817574; netsum += feature2[11] *  .1232711;
netsum += feature2[12] *  .1083438;  netsum += feature2[13] * -1.495962;
netsum += feature2[14] *  7.476014; netsum += feature2[15] * -.6315138;
netsum += feature2[16] *  1.866294; feature3[11] = 1 / (1 + exp(-netsum));

netsum = -.2175986; netsum += feature2[0] *  .2797127; netsum += feature2[1] *  6.333447E-02;
netsum += feature2[2] * -.1700054; netsum += feature2[3] *  5.942731E-02;
netsum += feature2[4] * -.3534243;netsum += feature2[5] *  .1894018; netsum += feature2[6] * -1.150056;
netsum += feature2[7] *  .1840184; netsum += feature2[8] *  .2159043; netsum += feature2[9] *  .2546629;
netsum += feature2[10] * -.8154136; netsum += feature2[11] * -.1000001;
netsum += feature2[12] *  .231395; netsum += feature2[13] * -4.211837E-02;
netsum += feature2[14] *  1.865774; netsum += feature2[15] *  1.577592E-02;
netsum += feature2[16] *  1.399653;feature3[12] = 1 / (1 + exp(-netsum));

netsum =  6.514765E-02; netsum += feature2[0] *  1.082969E-02; netsum += feature2[1] *  30.92208;
netsum += feature2[2] * -100.7583; netsum += feature2[3] *  5.168296; netsum += feature2[4] *  2.568679;
netsum += feature2[5] * -5.009957;netsum += feature2[6] *  5.277859; netsum += feature2[7] * -1.461174;
netsum += feature2[8] * -9.180321; netsum += feature2[9] * -11.79341;
netsum += feature2[10] * -.4839785; netsum += feature2[11] *  .3909915;
netsum += feature2[12] *  35.83482; netsum += feature2[13] *  2.457625;
netsum += feature2[14] * -.2552994; netsum += feature2[15] * -4.182423;
netsum += feature2[16] *  1.320164; feature3[13] = 1 / (1 + exp(-netsum));

netsum =  .1701123; netsum += feature2[0] * -.1992278; netsum += feature2[1] * -.3552467;
netsum += feature2[2] *  .1905437;netsum += feature2[3] * -.2452044; netsum += feature2[4] * -.1363172;
netsum += feature2[5] *  .17702; netsum += feature2[6] *  .5386735; netsum += feature2[7] * -.221677;
netsum += feature2[8] * -.2718283; netsum += feature2[9] *  .2827173;
netsum += feature2[10] *  .2275754; netsum += feature2[11] *  .1476722;
```

```
netsum += feature2[12] * .4336105;  netsum += feature2[13] * .5825009;
netsum += feature2[14] * -7.061563E-02; netsum += feature2[15] * -.2403713;
netsum += feature2[16] * .1039118; feature3[14] = 1 / (1 + exp(-netsum));

netsum = .0206196; netsum += feature2[0] * .1186698; netsum += feature2[1] * -.3846875;
netsum += feature2[2] * .1975343; netsum += feature2[3] * .4378715;
netsum += feature2[4] * 9.219401E-02; netsum += feature2[5] * 3.562687E-02;
netsum += feature2[6] * .486899; netsum += feature2[7] * .1914994;
netsum += feature2[8] * -.2074439; netsum += feature2[9] * .1435558;
netsum += feature2[10] * .1822895; netsum += feature2[11] * -.1260806;
netsum += feature2[12] * -9.015924E-02; netsum += feature2[13] * .1243092;
netsum += feature2[14] * .228945; netsum += feature2[15] * -.2592478;
netsum += feature2[16] * .2844225; feature3[15] = 1 / (1 + exp(-netsum));

netsum = .2155805; netsum += feature2[0] * .614311; netsum += feature2[1] * 3.382054;
netsum += feature2[2] * -12.56947;netsum += feature2[3] * -.5967454; netsum += feature2[4] * -.4205863;
netsum += feature2[5] * -.4395705;netsum += feature2[6] * -.6581645; netsum += feature2[7] * .8704508;
netsum += feature2[8] * .594275; netsum += feature2[9] * -.3935435; netsum += feature2[10] * .6661645;
netsum += feature2[11] * -1.300843; netsum += feature2[12] * 14.10187;
netsum += feature2[13] * -3.723258; netsum += feature2[14] * -.3625298;
netsum += feature2[15] * 1.588313; netsum += feature2[16] * -4.730013;
feature3[16] = 1 / (1 + exp(-netsum));

netsum = -.3197201; netsum += feature3[0] * -.5649142; netsum += feature3[1] * -.9160964;
netsum += feature3[2] * -.6728038; netsum += feature3[3] * .6194019; netsum += feature3[4] * .4816841;
netsum += feature3[5] * .6550974;netsum += feature3[6] * -.4620157; netsum += feature3[7] * -.5947516;
netsum += feature3[8] * .4916807; netsum += feature3[9] * .4552884;
netsum += feature3[10] * -.5162541; netsum += feature3[11] * .5893487;
netsum += feature3[12] * -.487336;  netsum += feature3[13] * .4061059;
netsum += feature3[14] * .3011003; netsum += feature3[15] * .3437203;
netsum += feature3[16] * -.5962353; outarray[0] = 1 / (1 + exp(-netsum));

outarray[0] = 1.380834 * (outarray[0] - .1) / .8 + .439166;
if (outarray[0]< .439166) outarray[0] = .439166;
if (outarray[0]> 1.82) outarray[0] = 1.82;
*IFsy = outarray[0];
}
```

C.4 The Conclusion-Analysis Module

```
/* This function is the post-processor to NETWIND's Neural Network interference effects prediction
module. The function uses its Knowledge Base to process the numerical outputs of the NN module */

concl(IFmx, IFmy, IFsx, IFsy, angle, op1, op2, op3, op4)
double IFmx, IFmy, IFsx, IFsy, angle;
int *op1, *op2, *op3, *op4;
{
float percent;
*op1 = 0; *op2 = 0; *op3 = 0; *op4 = 0;
/* angle is incident wind angle, IFmx is IF for mean drag, Ifmy is mean lift coefficient, */
/* IFsx is fluctuating drag IF, IFsy is fluctuating lift IF */
```

```
clrscr();
printf("RESULTS AND ANALYSIS\n\n");
printf("1. MEAN DRAG:\n");
if(IFmx <= -0.15){
    printf("**High Suction**! (IF = %4.2lf)\n", IFmx);
    printf("\nProbable Reasons:\n");
    printf(" a) Buildings very close in tandem\n"
        "b) Interfering building of larger width than principal building\n"
        "c) Incident wind angle < 15 degrees\n"
        "d) Buildings in open exposure\n");

    printf("\nPossible Remedies:\n");
    printf(" a) Increase tandem spacing between buildings to at least 3*bp\n"
        "b) Locate interfering building sideways (Sy > bp)\n"
        "c) Reduce the width of interfering building\n"
        "d) Reorient buildings with wind angle > 15 degrees\n"
        "e) Locate buildings in more turbulent suburban/urban exposures\n\n");
    *op1 = 1;
    printf("\nMORE....Mean Lift....Press any key to continue....\n");
    getch();
    clrscr();
}
else if(IFmx >-0.15 && IFmx < 0){
    printf("**Mild Suction** (IF = %4.2lf)\n", IFmx);
    printf("\nProbable Reasons:\n");
    printf(" a) Buildings in close tandem arrangement (wind angle <= 15 degres)\n"
        "  or close staggered arrangement (wind angle > 15 degrees)\n"
        "b) Interfering building of larger width than principal building\n"
        "c) Incident wind angle < 15 degrees\n"
        "d) Buildings in open or suburban exposures\n");

    printf("\nPossible Remedies:\n");
    printf("The situation is not serious. No changes required.\n\n");
    printf("\nMORE....Mean Lift....Press any key to continue....\n");
    getch();
    clrscr();
}
else if(IFmx >= 0.0 && IFmx < 0.5){
    percent = (1.0 - IFmx)*100.0;
    printf("**High Shielding** %3.0f percent decrease in mean drag (IF = %4.2lf)\n", percent, IFmx);
    printf("\nProbable Reasons:\n");
    printf( "a) Buildings in moderately close tandem arrangement (wind angle <= 15 degres)\n"
        "  or in moderately close staggered arrangement (wind angle > 15 degrees)\n"
        "b) Interfering building wider or/and taller than principal building\n"
        "c) Incident wind angle < 15 degrees\n"
        "d) Buildings in low turbulence open or suburban exposures\n"
        "e) Buildings in urban exposure but in close tandem arrangement\n\n");

    printf("\nPossible Remedies:\n");
    printf("Shielding is desirable since it reduces overall drag on the principal building\n"
        "Therefore no changes are required.\n\n");
    printf("\nMORE....Mean Lift....Press any key to continue....\n");
    getch();
    clrscr();
```

```
}
else if(IFmx >= 0.5 && IFmx < 0.7){
    percent = (1.0 - IFmx)*100.0;
    if(percent >= 1.0)
    printf("**Moderate Shielding** %3.0f percent decrease in mean drag (IF = %4.2lf)\n",
    percent, IFmx);
    else if(percent < 1.0)
    printf("**Complete Shielding** No change in isolated building mean drag (IF = %4.2lf)\n", percent,
IFmx);
    printf("\nProbable Reasons:\n");
    printf("a) Buildings in moderately close tandem arrangement\n"
        "  or in moderately close staggered arrangement\n"
        "b) Interfering building downstream\n"
        "c) Interfering building wider or/and taller than principal building\n"
        "d) Incident wind angle < 15 degrees\n"
        "e) Buildings in open, suburban or urban exposures\n");

    printf("\nPossible Remedies:\n");
    printf("Shielding is desirable since it reduces overall drag on the principal building.\n"
    "Therefore no changes required.\n");
    printf("\nMORE....Mean Lift....Press any key to continue....\n");
    getch();
    clrscr();
}
else if(IFmx > 1.3){
    percent = (IFmx - 1.0)*100.0;
    printf("**High Drag!** %3.0f percent increase in mean drag (IF = %4.2lf)\n", percent, IFmx);
    printf("\nProbable Reasons:\n");
    printf("a) Interfering building located downstream\n"
        "b) Interfering building of larger width and height than principal building\n"
        "c) Buildings in open exposure\n");

    printf("\nPossible Remedies:\n");
    printf("a) Move interfering building near downstream tandem location\n"
        "b) Move interfering building to a side of principal building\n"
        "c) Reduce the width or/and height of interfering building\n"
        "d) Reorient buildings with wind angle > 15 degrees\n"
        "e) Locate buildings in more turbulent suburban/urban exposures\n");
    *op1 = 2;
    printf("\nMORE....Mean Lift....Press any key to continue....\n");
    getch();
    clrscr();
}
else{
    printf("IF = %4.2lf\n", IFmx);
    if(IFmx < 1.0){
        percent = (1.0 - IFmx)*100.0;
        printf("SAFE. %3.0f percent decrease in mean drag.\n"
        "No significant interference effects.\n\n", percent);
    }
    else if(IFmx > 1.0){
        percent = (IFmx - 1.0)*100.0;
        printf("SAFE. Only %3.0f percent increase in mean drag.\n"
        "No significant interference effects.\n\n", percent);
```

```
    }
  }
  printf("\n2. MEAN LIFT:\n");
  if(IFmy <= -0.20){
     printf("**High Lift Suction**! (Cl = %4.2lf)\n", IFmy);
     printf("\nProbable Reasons:\n");
     printf("a) Buildings arranged side-by-side (for wind angles < 15 degrees)\n"
          "  or in close staggered arrangements (for wind angles >15 degrees)\n"
          "b) Interfering building wider or/and taller than principal building\n"
          "c) Buildings in open exposure\n");

     printf("\nPossible Remedies:\n");
     printf("a) Move buildings away from each other\n"
          "b) Reduce the width or/and height of interfering building\n"
          "c) Reorient buildings with wind angle > 20 degrees\n"
          "d) Locate buildings in more turbulent suburban/urban exposures\n\n");
     *op2 = 1;
  }
  else if(IFmy > 0.20 && angle <= 15){
     printf("**High Lift Pressure**! (Cl = %4.2lf)\n", IFmy);
     printf("\nProbable Reasons:\n");
     printf("a) Interfering building in downstream (more probable)\n"
          "or upstream staggered locations\n"
          "b) Low angle of attack of wind ( <= 15 degrees)\n"
          "c) Interfering building wider or/and taller than principal building\n"
          "d) Buildings in open exposure\n");

     printf("\nPossible Remedies:\n");
     printf("a) Move buildings away from each other\n"
          "b) Bring interfering building in-line (tandem) with principal building\n"
          "c) Reduce the width or/and height of interfering building\n"
          "d) Locate buildings in more turbulent suburban/urban exposures\n\n");
     *op2 = 2;
  }
  else if(IFmy > 0.75 && angle > 15 && angle <= 30){
     printf("**High Lift Pressure**! (Cl = %4.2lf)\n", IFmy);
     printf("\nProbable Reasons:\n");
     printf("a) Interfering building in downstream (more probable)\n"
          "or upstream staggered locations\n"
          "b) Medium angle of attack of wind (15 to 30 degrees)\n"
          "c) Interfering building wider or/and taller than principal building\n"
          "d) Buildings in open exposure\n");

     printf("\nPossible Remedies:\n");
     printf("a) Move buildings away from each other\n"
          "b) Bring interfering building in-line (tandem) with principal building\n"
          "c) Reduce the width or/and height of interfering building\n"
          "d) Reorient buildings with a low wind angle\n"
          "e) Locate buildings in more turbulent suburban/urban exposures\n\n");
     *op2 = 3;
  }
  else if(IFmy > 1.10 && angle > 30 && angle <= 45){
     printf("**High Lift Pressure**! (Cl = %4.2lf)\n", IFmy);
     printf("\nProbable Reasons:\n");
```

```
    printf("a) Interfering building in downstream (more probable)\n"
        "or upstream staggered locations\n"
        "b) High angle of attack of wind ( >= 30 degrees)\n"
        "c) Interfering building wider or/and taller than principal building\n"
        "d) Buildings in open exposure\n");

    printf("\nPossible Remedies:\n");
    printf("a) Move buildings away from each other\n"
        "b) Bring interfering building in-line (tandem) with principal building\n"
        "c) Reduce the width or/and height of interfering building\n"
        "d) Reorient buildings with wind angle < 30 degrees\n"
        "e) Locate buildings in more turbulent suburban/urban exposures\n\n");
    *op2 = 4;
}
else if(angle <= 15 && *op2 == 0){
    printf("Cl = %4.2lf\n", IFmy);
    printf("SAFE. No significant interference effects.\n\n");
}
else if(angle > 15 && *op2 == 0){
    printf("Cl = %4.2lf\n", IFmy);
    printf("SAFE. No significant interference effects for this wind angle.\n\n");
}

printf("\nMORE....Fluctuating loads....Press any key to continue....\n");
getch();
clrscr();
printf("3. FLUCTUATING DRAG:\n");
if(IFsx > 1.3 && IFsx <= 1.5){
    percent = (IFsx - 1.0)*100.0;
    printf("**High Fluctuating Drag**! %3.0f percent increase in fluctuating drag (IF = %4.2lf)\n", percent,
IFsx);
    printf("High fluctuating drag should be of considerable concern, especially in terms\n"
        "of serviceability requirements of the building. A comprehensive wind\n"
        "tunnel model testing is recommended\n\n");
    printf("\nProbable Reasons:\n");
    printf("a) Upstream interfering building in wake-interaction region.\n"
        "  (Sx = 2bp to 10bp, Sy = 0 to 5bp for wind angles < 30 degrees)\n"
        "  (Sx = 2bp to 8bp, Sy = 3bp to 8bp for wind angles > 30 degrees)\n"
        "b) Interfering buildings downstream in close proximity region\n"
        "  (Sx = -1.5bp to -2.5bp, Sy = 0 to 2bp)  (less probable).\n"
        "c) Interfering building wider or/and taller than principal building\n"
        "d) Buildings in open exposure\n");

    printf("\nPossible Remedies:\n");
    printf("a) Move buildings away from the wake-interaction region.\n"
        "  Position interfering building towards the side of principal building\n"
        "b) Reduce the width or/and height of interfering building\n"
        "c) Reorient buildings with wind angle > 20 degrees\n"
        "d) Locate buildings in more turbulent suburban/urban exposures\n");
    *op3 = 1;
    printf("\nMORE....Press any key to continue....\n");
    getch();
    clrscr();
}
```

```
  else if(IFsx > 1.5){
      percent = (IFsx - 1.0)*100.0;
      printf("**Very High Fluctuating Drag**! %3.0f percent increase in\n"
      "fluctuating drag(IF = %4.2lf)\n", percent, IFsx);
      printf("This increase is well outside the safety margin used in normal design.\n"
      "A mandatory wind tunnel model testing is recommended\n");
      printf("\nProbable Reasons:\n");
      printf("a) Upstream interfering building in wake-interaction region.\n"
          "  (Sx = 2bp to 10bp, Sy = 0 to 5bp for wind angles < 30 degrees)\n"
          "  (Sx = 2bp to 8bp, Sy = 3bp to 8bp for wind angles > 30 degrees)\n"
          "b) Interfering buildings downstream in close proximity region\n"
          "   (Sx = -1.5bp to -2.5bp, Sy = 0 to 2bp)  (less probable).\n"
          "c) Interfering building wider or/and taller than principal building\n"
          "d) Buildings in open exposure\n");

      printf("\nPossible Remedies:\n");
      printf("a) Move buildings away from the wake-interaction region.\n"
          "   Position interfering building towards the side of principal building\n"
          "b) Reduce the width or/and height of interfering building\n"
          "c) Reorient buildings with wind angle > 20 degrees\n"
          "d) Locate buildings in more turbulent suburban/urban exposures\n");
      *op3 = 2;
      printf("\nMORE....Press any key to continue....\n");
      getch();
      clrscr();
  }
  else{
      printf("IF = %4.2lf\n", IFsx);
      if(IFsx < 1.0){
          percent = (1.0 - IFsx)*100.0;
          printf("SAFE. %3.0f percent decrease in fluctuating drag.\n"
          "No significant interference effects.\n\n", percent);
      }
      else if(IFsx > 1.0){
          percent = (IFsx - 1.0)*100.0;
          printf("SAFE. Only %3.0f percent increase in fluctuating drag.\n"
          "No significant interference effects.\n\n", percent);
      }
  }
  printf("4. FLUCTUATING LIFT:\n");
  if(IFsy > 1.3 && IFsy <= 1.5){
      printf("**High Fluctuating Lift**! (IF = %4.2lf)\n", IFsy);
      printf("High fluctuating lift should be of considerable concern, especially in terms\n"
          "of serviceability requirements of the building. A comprehensive wind\n"
          "tunnel model testing is recommended\n");
      printf("\nProbable Reasons:\n");
      printf("a) Upstream interfering building in wake-interaction region.\n"
          "(Sx = 2bp to 8bp, Sy = 2bp to 6bp)\n"
          "b) Interfering building wider or/and taller than principal building\n"
          "c) Buildings in open exposure\n");

      printf("\nPossible Remedies:\n");
      printf( "a) Move buildings away from the wake-interaction region.\n"
          "b) Position interfering building towards the side of principal building\n"
```

```
        "c) Locate interfering building close to principal building\n"
        "d) Locate buildings in more turbulent suburban/urban exposures\n");
    *op4 = 1;
    printf("\nMORE....Press any key to continue....\n");
    getch();
    clrscr();
}
else if(IFsy > 1.5){
    printf("**Very High Fluctuating Lift**! (IF = %4.2lf)\n", IFsy);
    printf("This increase is well outside the safety margin used in normal design.\n"
        "A mandatory wind tunnel model testing is recommended\n");
    printf("\nProbable Reasons:\n");
    printf("a) Upstream interfering building in wake-interaction region.\n"
        "(Sx = 2bp to 8bp, Sy = 2bp to 6bp\n"
        "b) Interfering building wider or/and taller than principal building\n"
        "c) Buildings in open exposure\n");

    printf("\nPossible Remedies:\n");
    printf("a) Move buildings away from the wake-interaction region\n"
        "b) Position interfering building towards the side of principal building\n"
        "c) Locate interfering building close to principal building\n"
        "d) Locate buildings in more turbulent suburban/urban exposures\n");
    *op4 = 2;
    printf("\nMORE....Press any key to continue....\n");
    getch();
    clrscr();
}
else{
    printf("IF = %4.2lf\n", IFsy);
    if(IFsy < 1.0){
        percent = (1.0 - IFsy)*100.0;
        printf("\nSAFE. %3.0f percent decrease in fluctuating lift.\n"
        "No significant interference effects.\n\n", percent);
    }
    else if(IFsy > 1.0){
        percent = (IFsy - 1.0)*100.0;
        printf("\nSAFE. Only %3.0f percent increase in fluctuating lift.\n"
        "No significant interference effects.\n\n", percent);
    }
}}
```

C.5 The Design Assistance Module

```
/** Design Assistance Module **/
#include <stdio.h>
#include <math.h>
assist(op1, op2, op3, op4, angle, Iv, b, h, sx, sy, bp, bi, hp, hi, IFmx, IFmy, IFsx, IFsy)
int op1, op2, op3, op4;
double angle, Iv, b, h, sx, sy, bp, bi, hp, hi, IFmx, IFmy, IFsx, IFsy;
{
double wbp, wbi, whp, whi, wsx, wsy, wang, sum;
```

```
double v1, v2, v3, v4, v5, v6, v7, v8, v9, v10, v11;
printf("\nNETWIND has used Neural Networks and its  Knowledge Base to  evaluate\n"
"the effects of various input parameters on interference effects. The following\n"
"guidelines have been used in arriving at the best configurations  presented on\n"
"the next screen:\n\n"
"MEAN DRAG: -0.15 <= IF < 1.30\n"
"MEAN LIFT: For wind angles <= 15 degrees: -0.20 <= Cl <= 0.20\n"
"          For wind angles between 15 and 30 degrees: Cl <= 0.75\n"
"          For wind angles > 30 degrees: Cl <= 1.10\n"
"FLUCTUATING DRAG: IF < 1.30\n"
"FLUCTUATING LIFT: IF < 1.30\n\n"
"Symbols used:\n"
"Angle: Incident wind angle;  Iv: Longitudinal turbulence intensity of wind \n"
"bp: Width of principal building; bi: Width of interfering building\n"
"hp: Height of principal building; hi: Height of interfering building\n"
"Sx: Centre-to-centre distance between the buildings along the horizontal axis\n"
"Sy: Centre-to-centre distance between the buildings along the vertical axis\n"
"IF: Interference Factor; Cl: Mean lift.\n\n");
printf("Press any key to continue....\n");
getch();
clrscr();
printf("NETWIND selects the best option based on the relative importance\n"
"or the rigidity of various input variables to design.\n"
"INPUT the percentage weight (0 to 100) you would ascribe to each variable.\n"
"Give a higher weight to the input variable you want modified the least.\n\n"
"IMPORTANCE FACTORS:\n\n");

printf("Principal building width: ");
scanf("%lf", &wbp);
printf("Interfering building width: ");
scanf("%lf", &wbi);
printf("Principal building height: ");
scanf("%lf", &whp);
printf("Interfering building height: ");
scanf("%lf", &whi);
printf("Centre-to-centre spacing in horizontal direction (X-axis): ");
scanf("%lf", &wsx);
printf("Centre-to-centre spacing in vertical direction (Y-axis): ");
scanf("%lf", &wsy);
printf("Incident wind angle: ");
scanf("%lf", &wang);
/** Normalization **/
sum = wbp + wbi + whp + whi + wsx + wsy + wang;
wbp = wbp/sum; wbi = wbi/sum; whp = whp/sum; whi = whi/sum;
wsx = wsx/sum; wsy = wsy/sum; wang = wang/sum;
printf("Press any key to go to DESIGN ASSISTANCE SCREEN....\n");
getch();
clrscr();
if(op1 == 1 || op1 == 2)
assistmx(wbp, wbi, whp, whi, wsx, wsy, wang, angle, Iv, b, h, sx, sy, bp, bi, hp, hi, IFmx);
if(op2 == 1 || op2 == 2 || op2 == 3 || op2 == 4)
assistmy(wbp, wbi, whp, whi, wsx, wsy, wang, angle, Iv, b, h, sx, sy, bp, bi, hp, hi, IFmy);
if(op3 == 1 || op3 == 2)
assistsx(wbp, wbi, whp, whi, wsx, wsy, wang, angle, Iv, b, h, sx, sy, bp, bi, hp, hi, IFsx);
```

```
if(op4 == 1 || op4 == 2)
assistsy(wbp, wbi, whp, whi, wsx, wsy, wang,angle, Iv, b, h, sx, sy, bp, bi, hp, hi, IFsy);
}
```

C.5.1 The design assistance sub-module for mean drag

```
/** Design Assistance Sub-Module for Mean Drag **/
#include <stdio.h>
#include <math.h>
assistmx(wbp, wbi, whp, whi, wsx, wsy, wang, angle, Iv, b, h, sx, sy, bp, bi, hp, hi, IFmx)
double wbp, wbi, whp, whi, wsx, wsy, wang; /** weights of attributes **/
double angle, Iv, b, h, sx, sy, bp, bi, hp, hi, IFmx;
{
double angle1, b1, b2, h1, h2, sx1, sy1;
angle1 = angle; b1 = b; h1 = h; sx1 = sx; sy1 = sy; b2 = bp; h2 = hp;
    printf("MEAN DRAG:\n");
    printf("\n Angle    Iv    bp    bi    hp    hi    Sx    Sy    IF  E\n\n");
    printf("Original data:\n");
    printf(" %7.1lf  %7.1lf %7.2lf %7.2lf %7.2lf %7.2lf %7.2lf %7.2lf\n",
    angle, Iv, bp, bi, hp, hi, sx*bp, sy*bp, IFmx);
    printf("NETWIND alternatives:\n");
for(;;){
    if(sx <= 14.0){
        NNmeanx(angle, Iv, b, h, sx, sy, &IFmx);
        if(IFmx > -0.15 && IFmx < 1.30){
            utility(wbp, wbi, whp, whi, wsx, wsy, wang, angle, angle1, Iv, b, b1, b2, h, h1, h2, sx, sx1, sy,
            sy1, bp, bi, hp, hi, IFmx); /** calculates utility values of alternatives and prints results **/
            break;
        }
        else sx = sx + 0.25;
    }
    else break;
}
sx = sx1;
for(;;){
    if(sy <= 8.0){
        NNmeanx(angle, Iv, b, h, sx, sy, &IFmx);
        if(IFmx > -0.15 && IFmx < 1.30){
            utility(wbp, wbi, whp, whi, wsx, wsy, wang, angle, angle1, Iv, b, b1, b2, h, h1, h2, sx, sx1, sy,
            sy1, bp, bi, hp, hi, IFmx);
            break;
        }
        else sy = sy + 0.25;
    }
    else break;
}
sy = sy1;
for(;;){
    if(sx <= 14.0 && sy <= 8.0){
        NNmeanx(angle, Iv, b, h, sx, sy, &IFmx);
        if(IFmx > -0.15 && IFmx < 1.30){
```

```
            utility(wbp, wbi, whp, whi, wsx, wsy, wang, angle, angle1, Iv, b, b1, b2, h, h1, h2, sx, sx1, sy,
            sy1, bp, bi, hp, hi, IFmx);
            break;
        }
        else{
            sx = sx + 0.50;
            sy = sy + 0.25;
        }
    }
    else break;
}
sx = sx1;
sy = sy1;
for(;;){
    if(sx >= -5.0){
        NNmeanx(angle, Iv, b, h, sx, sy, &IFmx);
        if(IFmx > -0.15 && IFmx < 1.30){
            utility(wbp, wbi, whp, whi, wsx, wsy, wang, angle, angle1, Iv, b, b1, b2, h, h1, h2, sx, sx1, sy,
            sy1, bp, bi, hp, hi, IFmx);
            break;
        }
        else sx = sx - 0.25;
    }
    else break;
}
sx = sx1;
for(;;){
    if(sy >= -6.0){
        NNmeanx(angle, Iv, b, h, sx, sy, &IFmx);
        if(IFmx > -0.15 && IFmx < 1.30){
            utility(wbp, wbi, whp, whi, wsx, wsy, wang, angle, angle1, Iv, b, b1, b2, h, h1, h2, sx, sx1, sy,
            sy1, bp, bi, hp, hi, IFmx);
            break;
        }
        else sy = sy - 0.25;
    }
    else break;
}
sy = sy1;
for(;;){
    if(sx >= -5.0 && sy >= -6.0){
        NNmeanx(angle, Iv, b, h, sx, sy, &IFmx);
        if(IFmx > -0.15 && IFmx < 1.30){
            utility(wbp, wbi, whp, whi, wsx, wsy, wang, angle, angle1, Iv, b, b1, b2, h, h1, h2, sx, sx1, sy,
            sy1, bp, bi, hp, hi, IFmx);
            break;
        }
        else{
            sx = sx - 0.50;
            sy = sy - 0.25;
        }
    }
    else break;
}
```

```
sx = sx1;
sy = sy1;
for(;;){
    if(b >= 0.667){
        NNmeanx(angle, Iv, b, h, sx, sy, &IFmx);
        if(IFmx > -0.15 && IFmx < 1.30){
            utility(wbp, wbi, whp, whi, wsx, wsy, wang, angle, angle1, Iv, b, b1, b2, h, h1, h2, sx, sx1, sy,
            sy1, bp, bi, hp, hi, IFmx);
            break;
        }
        else b = b*0.95;
    }
    else break;
}
b = b1;
for(;;){
    if(h >= 1.0){
        NNmeanx(angle, Iv, b, h, sx, sy, &IFmx);
        if(IFmx > -0.15 && IFmx < 1.30){
            utility(wbp, wbi, whp, whi, wsx, wsy, wang, angle, angle1, Iv, b, b1, b2, h, h1, h2, sx, sx1, sy,
            sy1, bp, bi, hp, hi, IFmx);
            break;
        }
        else h = h*0.95;
    }
    else break;
}
h = h1;
for(;;){
    if(b >= 0.667 && h >= 1.0){
        NNmeanx(angle, Iv, b, h, sx, sy, &IFmx);
        if(IFmx > -0.15 && IFmx < 1.30){
            utility(wbp, wbi, whp, whi, wsx, wsy, wang, angle, angle1, Iv, b, b1, b2, h, h1, h2, sx, sx1, sy,
            sy1, bp, bi, hp, hi, IFmx);
            break;
        }
        else{
            b = b*0.95;
            h = h*0.95;
        }
    }
    else break;
}
b = b1;
h = h1;
for(;;){
    if(angle >= 0 && angle <= 45){
        NNmeanx(angle, Iv, b, h, sx, sy, &IFmx);
        if(IFmx > -0.15 && IFmx < 1.30){
            utility(wbp, wbi, whp, whi, wsx, wsy, wang, angle, angle1, Iv, b, b1, b2, h, h1, h2, sx, sx1, sy,
            sy1, bp, bi, hp, hi, IFmx);
            break;
        }
        else angle = angle + 7.5;
```

```
    }
    else break;
}
angle = angle1;
for(;;){
    if(angle >= 0 && angle <= 45){
        NNmeanx(angle, Iv, b, h, sx, sy, &IFmx);
        if(IFmx > -0.15 && IFmx < 1.30){
        utility(wbp, wbi, whp, whi, wsx, wsy, wang, angle, angle1, Iv, b, b1, b2, h, h1, h2, sx, sx1, sy, sy1,
        bp, bi, hp, hi, IFmx);
            break;
        }
        else angle = angle - 7.5;
    }
    else break;
}
angle = angle1;
printf("\nMORE....Press any key to continue....\n");
getch(); clrscr();
}
```

C.5.2 The design assistance sub-module for mean lift

```
/** Design Assistance Sub-Module for Mean Lift **/
#include <stdio.h>
#include <math.h>
assistmy(wbp, wbi, whp, whi, wsx, wsy, wang, angle, Iv, b, h, sx, sy, bp, bi, hp, hi, IFmy)
double wbp, wbi, whp, whi, wsx, wsy, wang; /** weights of attributes **/
double angle, Iv, b, h, sx, sy, bp, bi, hp, hi, IFmy;
{
double angle1, b1, b2, h1, h2, sx1, sy1;
angle1 = angle; b1 = b; h1 = h; sx1 = sx; sy1 = sy; b2 = bp; h2 = hp;
        printf("MEAN LIFT:\n");
        printf("\n Angle    Iv    bp    bi    hp    hi    Sx    Sy    IF  E\n\n");
        printf("Original data:\n");
        printf(" %7.1lf  %7.1lf %7.2lf %7.2lf %7.2lf %7.2lf %7.2lf %7.2lf %7.2lf\n",
        angle, Iv, bp, bi, hp, hi, sx*bp, sy*bp, IFmy);
        printf("NETWIND alternatives:\n");
for(;;){
    if(sx <= 14.0){
        NNmeany(angle, Iv, b, h, sx, sy, &IFmy);
        if(angle <= 15 && IFmy > -0.20 && IFmy < 0.20){
            utility(wbp, wbi, whp, whi, wsx, wsy, wang, angle, angle1, Iv, b, b1, b2, h, h1, h2, sx, sx1, sy,
            sy1, bp, bi, hp, hi, IFmy); /** calculates utility values of alternatives and prints results **/
            break;
        }
        else if(angle > 15 && angle <=30 && IFmy > -0.20 && IFmy < 0.75){
            utility(wbp, wbi, whp, whi, wsx, wsy, wang, angle, angle1, Iv, b, b1, b2, h, h1, h2, sx, sx1, sy,
            sy1, bp, bi, hp, hi, IFmy);
            break;
        }
```

```
        else if(angle > 30 && angle <=45 && IFmy > -0.20 && IFmy < 1.10){
            utility(wbp, wbi, whp, whi, wsx, wsy, wang, angle, angle1, Iv, b, b1, b2, h, h1, h2, sx, sx1, sy,
            sy1, bp, bi, hp, hi, IFmy);
            break;
        }
        else sx = sx + 0.25;
    }
    else break;
}
sx = sx1;
for(;;){
    if(sy <= 8.0){
        NNmeany(angle, Iv, b, h, sx, sy, &IFmy);
        if(angle <= 15 && IFmy > -0.20 && IFmy < 0.20){
            utility(wbp, wbi, whp, whi, wsx, wsy, wang, angle, angle1, Iv, b, b1, b2, h, h1, h2, sx, sx1, sy,
            sy1, bp, bi, hp, hi, IFmy);
            break;
        }
        else if(angle > 15 && angle <=30 && IFmy > -0.20 && IFmy < 0.75){
            utility(wbp, wbi, whp, whi, wsx, wsy, wang, angle, angle1, Iv, b, b1, b2, h, h1, h2, sx, sx1, sy,
            sy1, bp, bi, hp, hi, IFmy);
            break;
        }
        else if(angle > 30 && angle <=45 && IFmy > -0.20 && IFmy < 1.10){
            utility(wbp, wbi, whp, whi, wsx, wsy, wang, angle, angle1, Iv, b, b1, b2, h, h1, h2, sx, sx1, sy,
            sy1, bp, bi, hp, hi, IFmy);
            break;
        }
        else sy = sy + 0.25;
    }
    else break;
}
sy = sy1;
for(;;){
    if(sx <= 14.0 && sy <= 8.0){
        NNmeany(angle, Iv, b, h, sx, sy, &IFmy);
        if(angle <= 15 && IFmy > -0.20 && IFmy < 0.20){
            utility(wbp, wbi, whp, whi, wsx, wsy, wang, angle, angle1, Iv, b, b1, b2, h, h1, h2, sx, sx1, sy,
            sy1, bp, bi, hp, hi, IFmy);
            break;
        }
        else if(angle > 15 && angle <=30 && IFmy > -0.20 && IFmy < 0.75){
            utility(wbp, wbi, whp, whi, wsx, wsy, wang, angle, angle1, Iv, b, b1, b2, h, h1, h2, sx, sx1, sy,
            sy1, bp, bi, hp, hi, IFmy);
            break;
        }
        else if(angle > 30 && angle <=45 && IFmy > -0.20 && IFmy < 1.10){
            utility(wbp, wbi, whp, whi, wsx, wsy, wang, angle, angle1, Iv, b, b1, b2, h, h1, h2, sx, sx1, sy,
            sy1, bp, bi, hp, hi, IFmy);
            break;
        }
        else{
            sx = sx + 0.50;
            sy = sy + 0.25;
```

```
            }
        }
        else break;
    }
    sx = sx1;
    sy = sy1;
    for(;;){
        if(sx >= -5.0){
            NNmeany(angle, Iv, b, h, sx, sy, &IFmy);
            if(angle <= 15 && IFmy > -0.20 && IFmy < 0.20){
                utility(wbp, wbi, whp, whi, wsx, wsy, wang, angle, angle1, Iv, b, b1, b2, h, h1, h2, sx, sx1, sy,
                sy1, bp, bi, hp, hi, IFmy);
                break;
            }
            else if(angle > 15 && angle <=30 && IFmy > -0.20 && IFmy < 0.75){
                utility(wbp, wbi, whp, whi, wsx, wsy, wang, angle, angle1, Iv, b, b1, b2, h, h1, h2, sx, sx1, sy,
                sy1, bp, bi, hp, hi, IFmy);
                break;
            }
            else if(angle > 30 && angle <=45 && IFmy > -0.20 && IFmy < 1.10){
                utility(wbp, wbi, whp, whi, wsx, wsy, wang, angle, angle1, Iv, b, b1, b2, h, h1, h2, sx, sx1, sy,
                sy1, bp, bi, hp, hi, IFmy);
                break;
            }
            else sx = sx - 0.25;
        }
        else break;
    }
    sx = sx1;
    for(;;){
        if(sy >= -6.0){
            NNmeany(angle, Iv, b, h, sx, sy, &IFmy);
            if(angle <= 15 && IFmy > -0.20 && IFmy < 0.20){
                utility(wbp, wbi, whp, whi, wsx, wsy, wang, angle, angle1, Iv, b, b1, b2, h, h1, h2, sx, sx1, sy,
                sy1, bp, bi, hp, hi, IFmy);
                break;
            }
            else if(angle > 15 && angle <=30 && IFmy > -0.20 && IFmy < 0.75){
                utility(wbp, wbi, whp, whi, wsx, wsy, wang, angle, angle1, Iv, b, b1, b2, h, h1, h2, sx, sx1, sy,
                sy1, bp, bi, hp, hi, IFmy);
                break;
            }
            else if(angle > 30 && angle <=45 && IFmy > -0.20 && IFmy < 1.10){
                utility(wbp, wbi, whp, whi, wsx, wsy, wang, angle, angle1, Iv, b, b1, b2, h, h1, h2, sx, sx1, sy,
                sy1, bp, bi, hp, hi, IFmy);
                break;
            }
            else sy = sy - 0.25;
        }
        else break;
    }
    sy = sy1;
    for(;;){
        if(b >= 0.667){
```

```
        NNmeany(angle, Iv, b, h, sx, sy, &IFmy);
        if(angle <= 15 && IFmy > -0.20 && IFmy < 0.20){
            utility(wbp, wbi, whp, whi, wsx, wsy, wang, angle, angle1, Iv, b, b1, b2, h, h1, h2, sx, sx1, sy,
            sy1, bp, bi, hp, hi, IFmy);
            break;
        }
        else if(angle > 15 && angle <=30 && IFmy > -0.20 && IFmy < 0.75){
            utility(wbp, wbi, whp, whi, wsx, wsy, wang, angle, angle1, Iv, b, b1, b2, h, h1, h2, sx, sx1, sy,
            sy1, bp, bi, hp, hi, IFmy);
            break;
        }
        else if(angle > 30 && angle <=45 && IFmy > -0.20 && IFmy < 1.10){
            utility(wbp, wbi, whp, whi, wsx, wsy, wang, angle, angle1, Iv, b, b1, b2, h, h1, h2, sx, sx1, sy,
            sy1, bp, bi, hp, hi, IFmy);
            break;
        }
        else b = b*0.95;
    }
    else break;
}
b = b1;
for(;;){
    if(angle >= 0 && angle <= 45){
        NNmeany(angle, Iv, b, h, sx, sy, &IFmy);
        if(angle1 <= 15 && IFmy > -0.20 && IFmy < 0.20){
            utility(wbp, wbi, whp, whi, wsx, wsy, wang, angle, angle1, Iv, b, b1, b2, h, h1, h2, sx, sx1, sy,
            sy1, bp, bi, hp, hi, IFmy);
            break;
        }
        else if(angle1 > 15 && angle <=30 && IFmy > -0.20 && IFmy < 0.75){
            utility(wbp, wbi, whp, whi, wsx, wsy, wang, angle, angle1, Iv, b, b1, b2, h, h1, h2, sx, sx1, sy,
            sy1, bp, bi, hp, hi, IFmy);
            break;
        }
        else if(angle1 > 30 && angle <=45 && IFmy > -0.20 && IFmy < 1.10){
            utility(wbp, wbi, whp, whi, wsx, wsy, wang, angle, angle1, Iv, b, b1, b2, h, h1, h2, sx, sx1, sy,
            sy1, bp, bi, hp, hi, IFmy);
            break;
        }
        else angle = angle + 7.5;
    }
    else break;
}
angle = angle1;
for(;;){
    if(angle >= 0 && angle <= 45){
        NNmeany(angle, Iv, b, h, sx, sy, &IFmy);
        if(angle1 <= 15 && IFmy > -0.20 && IFmy < 0.20){
            utility(wbp, wbi, whp, whi, wsx, wsy, wang, angle, angle1, Iv, b, b1, b2, h, h1, h2, sx, sx1, sy,
            sy1, bp, bi, hp, hi, IFmy);
            break;
        }
        else if(angle1 > 15 && angle <=30 && IFmy > -0.20 && IFmy < 0.75){
            utility(wbp, wbi, whp, whi, wsx, wsy, wang, angle, angle1, Iv, b, b1, b2, h, h1, h2, sx, sx1, sy,
```

```
            sy1, bp, bi, hp, hi, IFmy);
            break;
        }
        else if(angle1 > 30 && angle <=45 && IFmy > -0.20 && IFmy < 1.10){
            utility(wbp, wbi, whp, whi, wsx, wsy, wang, angle, angle1, Iv, b, b1, b2, h, h1, h2, sx, sx1, sy,
            sy1, bp, bi, hp, hi, IFmy);
            break;
        }
        else angle = angle - 7.5;
    }
    else break;
}
angle = angle1;
printf("\nMORE....Press any key to continue....\n");
getch(); clrscr();
}
```

C.5.3 The design assistance sub-module for fluctuating drag

```
/** Design Assistance Sub-Module for Fluctuating Drag **/
#include <stdio.h>
#include <math.h>
assistsx(wbp, wbi, whp, whi, wsx, wsy, wang, angle, Iv, b, h, sx, sy, bp, bi, hp, hi, IFsx)
double wbp, wbi, whp, whi, wsx, wsy, wang; /** weights of attributes **/
double angle, Iv, b, h, sx, sy, bp, bi, hp, hi, IFsx;
{
double angle1, b1, b2, h1, h2, sx1, sy1;
angle1 = angle; b1 = b; h1 = h; sx1 = sx; sy1 = sy; b2 = bp; h2 = hp;

    printf("FLUCTUATING DRAG\n");
    printf("\n Angle    Iv    bp    bi    hp    hi    Sx    Sy    IF  E\n\n");
    printf("Original data:\n");
    printf(" %7.1lf  %7.1lf %7.2lf %7.2lf %7.2lf %7.2lf %7.2lf %7.2lf %7.2lf\n",
    angle, Iv, bp, bi, hp, hi, sx*bp, sy*bp, IFsx);
    printf("NETWIND alternatives:\n");
for(;;){
    if(sx <= 14.0){
        NNsigmax(angle, Iv, b, h, sx, sy, &IFsx);
        if(IFsx < 1.30){
            utility(wbp, wbi, whp, whi, wsx, wsy, wang, angle, angle1, Iv, b, b1, b2, h, h1, h2, sx, sx1, sy,
            sy1, bp, bi, hp, hi, IFsx); /** Calculates utility values of alternatives and prints results **/
            break;
        }
        else sx = sx + 0.25;
    }
    else break;
}
sx = sx1;
for(;;){
    if(sx >= -5.0){
        NNsigmax(angle, Iv, b, h, sx, sy, &IFsx);
```

```
            if(IFsx < 1.30){
                utility(wbp, wbi, whp, whi, wsx, wsy, wang, angle, angle1, Iv, b, b1, b2, h, h1, h2, sx, sx1, sy,
                sy1, bp, bi, hp, hi, IFsx);
                break;
            }
            else sx = sx - 0.25;
        }
        else break;
    }
    sx = sx1;
    for(;;){
        if(sy <= 8.0){
            NNsigmax(angle, Iv, b, h, sx, sy, &IFsx);
            if(IFsx < 1.30){
                utility(wbp, wbi, whp, whi, wsx, wsy, wang, angle, angle1, Iv, b, b1, b2, h, h1, h2, sx, sx1, sy,
                sy1, bp, bi, hp, hi, IFsx);
                break;
            }
            else sy = sy + 0.25;
        }
        else break;
    }
    sy = sy1;
    for(;;){
        if(sy >= -6.0){
            NNsigmax(angle, Iv, b, h, sx, sy, &IFsx);
            if(IFsx < 1.30){
                utility(wbp, wbi, whp, whi, wsx, wsy, wang, angle, angle1, Iv, b, b1, b2, h, h1, h2, sx, sx1, sy,
                sy1, bp, bi, hp, hi, IFsx);
                break;
            }
            else sy = sy - 0.25;
        }
        else break;
    }
    sy = sy1;
    for(;;){
        if(sx <= 14.0 && sy <= 8.0){
            NNsigmax(angle, Iv, b, h, sx, sy, &IFsx);
            if(IFsx < 1.30){
                utility(wbp, wbi, whp, whi, wsx, wsy, wang, angle, angle1, Iv, b, b1, b2, h, h1, h2, sx, sx1, sy,
                sy1, bp, bi, hp, hi, IFsx);
                break;
            }
            else{
                sx = sx + 0.50;
                sy = sy + 0.25;
            }
        }
        else break;
    }
    sx = sx1;
    sy = sy1;
    for(;;){
```

```
    if(sx >= -5.0 && sy >= -6.0){
        NNsigmax(angle, Iv, b, h, sx, sy, &IFsx);
        if(IFsx < 1.30){
            utility(wbp, wbi, whp, whi, wsx, wsy, wang, angle, angle1, Iv, b, b1, b2, h, h1, h2, sx, sx1, sy,
            sy1, bp, bi, hp, hi, IFsx);
            break;
        }
        else{
            sx = sx - 0.50;
            sy = sy - 0.25;
        }
    }
    else break;
}
sx = sx1;
sy = sy1;
for(;;){
    if(b >= 0.667){
        NNsigmax(angle, Iv, b, h, sx, sy, &IFsx);
        if(IFsx < 1.30){
            utility(wbp, wbi, whp, whi, wsx, wsy, wang, angle, angle1, Iv, b, b1, b2, h, h1, h2, sx, sx1, sy,
            sy1, bp, bi, hp, hi, IFsx);
            break;
        }
        else b = b*0.95;
    }
    else break;
}
b = b1;
for(;;){
    if(h >= 1.0){
        NNsigmax(angle, Iv, b, h, sx, sy, &IFsx);
        if(IFsx < 1.30){
            utility(wbp, wbi, whp, whi, wsx, wsy, wang, angle, angle1, Iv, b, b1, b2, h, h1, h2, sx, sx1, sy,
            sy1, bp, bi, hp, hi, IFsx);
            break;
        }
        else h = h*0.95;
    }
    else break;
}
h = h1;
for(;;){
    if(b >= 0.667 && h >= 1.0){
        NNsigmax(angle, Iv, b, h, sx, sy, &IFsx);
        if(IFsx < 1.30){
            utility(wbp, wbi, whp, whi, wsx, wsy, wang, angle, angle1, Iv, b, b1, b2, h, h1, h2, sx, sx1, sy,
            sy1, bp, bi, hp, hi, IFsx);
            break;
        }
        else{
            b = b*0.95;
            h = h*0.95;
        }
```

```
    }
    else break;
}
b = b1;
h = h1;
for(;;){
    if(angle >= 0 && angle <= 45){
        NNsigmax(angle, Iv, b, h, sx, sy, &IFsx);
        if(IFsx < 1.30){
            utility(wbp, wbi, whp, whi, wsx, wsy, wang, angle, angle1, Iv, b, b1, b2, h, h1, h2, sx, sx1, sy,
            sy1, bp, bi, hp, hi, IFsx);
            break;
        }
        else angle = angle + 7.5;
    }
    else break;
}
angle = angle1;
for(;;){
    if(angle >= 0 && angle <= 45){
        NNsigmax(angle, Iv, b, h, sx, sy, &IFsx);
        if(IFsx < 1.30){
            utility(wbp, wbi, whp, whi, wsx, wsy, wang, angle, angle1, Iv, b, b1, b2, h, h1, h2, sx, sx1, sy,
            sy1, bp, bi, hp, hi, IFsx);
            break;
        }
        else angle = angle - 7.5;
    }
    else break;
}
angle = angle1;

printf("\nMORE....Press any key to continue...\n");
getch(); clrscr();
}
```

C.5.4 The design assistance sub-module for fluctuating lift

```
/** Design Assistance Sub-Module for Fluctuating Lift **/
#include <stdio.h>
#include <math.h>
assistsy(wbp, wbi, whp, whi, wsx, wsy, wang, angle, Iv, b, h, sx, sy, bp, bi, hp, hi, IFsy)
double wbp, wbi, whp, whi, wsx, wsy, wang; /** weights of attributes **/
double angle, Iv, b, h, sx, sy, bp, bi, hp, hi, IFsy;
{
double angle1, b1, b2, h1, h2, sx1, sy1;
angle1 = angle; b1 = b; h1 = h; sx1 = sx; sy1 = sy; b2 = bp; h2 = hp;
    printf("FLUCTUATING LIFT\n");
    printf("\n  Angle    Iv    bp    bi    hp    hi    Sx    Sy    IF  E\n\n");
    printf("Original data:\n");
    printf(" %7.1lf  %7.1lf %7.2lf %7.2lf %7.2lf %7.2lf %7.2lf %7.2lf %7.2lf\n",
```

```
    angle, Iv, bp, bi, hp, hi, sx*bp, sy*bp, IFsy);
    printf("NETWIND alternatives:\n");
 for(;;){
    if(sx <= 14.0){
        NNsigmay(angle, Iv, b, h, sx, sy, &IFsy);
        if(IFsy < 1.30){
            utility(wbp, wbi, whp, whi, wsx, wsy, wang, angle, angle1, Iv, b, b1, b2, h, h1, h2, sx, sx1, sy,
            sy1, bp, bi, hp, hi, IFsy); /** calculates utility values of alternatives and prints results **/
            break;
        }
        else sx = sx + 0.25;
    }
    else break;
}
sx = sx1;
for(;;){
    if(sx >= -5.0){
        NNsigmay(angle, Iv, b, h, sx, sy, &IFsy);
        if(IFsy < 1.30){
            utility(wbp, wbi, whp, whi, wsx, wsy, wang, angle, angle1, Iv, b, b1, b2, h, h1, h2, sx, sx1, sy,
            sy1, bp, bi, hp, hi, IFsy);
            break;
        }
        else sx = sx - 0.25;
    }
    else break;
}
sx = sx1;
for(;;){
    if(sy <= 8.0){
        NNsigmay(angle, Iv, b, h, sx, sy, &IFsy);
        if(IFsy < 1.30){
            utility(wbp, wbi, whp, whi, wsx, wsy, wang, angle, angle1, Iv, b, b1, b2, h, h1, h2, sx, sx1, sy,
            sy1, bp, bi, hp, hi, IFsy);
            break;
        }
        else sy = sy + 0.25;
    }
    else break;
}
sy = sy1;
for(;;){
    if(sy >= -6.0){
        NNsigmay(angle, Iv, b, h, sx, sy, &IFsy);
        if(IFsy < 1.30){
            utility(wbp, wbi, whp, whi, wsx, wsy, wang, angle, angle1, Iv, b, b1, b2, h, h1, h2, sx, sx1, sy,
            sy1, bp, bi, hp, hi, IFsy);
            break;
        }
        else sy = sy - 0.25;
    }
    else break;
}
sy = sy1;
```

```
  for(;;){
     if(sx <= 14.0 && sy <= 8.0){
        NNsigmay(angle, Iv, b, h, sx, sy, &IFsy);
        if(IFsy < 1.30){
           utility(wbp, wbi, whp, whi, wsx, wsy, wang, angle, angle1, Iv, b, b1, b2, h, h1, h2, sx, sx1, sy,
           sy1, bp, bi, hp, hi, IFsy);
           break;
        }
        else{
           sx = sx + 0.50;
           sy = sy + 0.25;
        }
     }
     else break;
  }
  sx = sx1;
  sy = sy1;
  for(;;){
     if(sx >= -5.0 && sy >= -6.0){
        NNsigmay(angle, Iv, b, h, sx, sy, &IFsy);
        if(IFsy < 1.30){
           utility(wbp, wbi, whp, whi, wsx, wsy, wang, angle, angle1, Iv, b, b1, b2, h, h1, h2, sx, sx1, sy,
           sy1, bp, bi, hp, hi, IFsy);
           break;
        }
        else{
           sx = sx - 0.50;
           sy = sy - 0.25;
        }
     }
     else break;
  }
  sx = sx1;
  sy = sy1;
  for(;;){
     if(b >= 0.667){
        NNsigmay(angle, Iv, b, h, sx, sy, &IFsy);
        if(IFsy < 1.30){
           utility(wbp, wbi, whp, whi, wsx, wsy, wang, angle, angle1, Iv, b, b1, b2, h, h1, h2, sx, sx1, sy,
           sy1, bp, bi, hp, hi, IFsy);
           break;
        }
        else b = b*0.95;
     }
     else break;
  }
  b = b1;
  for(;;){
     if(h >= 1.0){
        NNsigmay(angle, Iv, b, h, sx, sy, &IFsy);
        if(IFsy < 1.30){
           utility(wbp, wbi, whp, whi, wsx, wsy, wang, angle, angle1, Iv, b, b1, b2, h, h1, h2, sx, sx1, sy,
           sy1, bp, bi, hp, hi, IFsy);
           break;
```

```
            }
            else h = h*0.95;
        }
        else break;
    }
    h = h1;
    for(;;){
        if(b >= 0.667 && h >= 1.0){
            NNsigmay(angle, Iv, b, h, sx, sy, &IFsy);
            if(IFsy < 1.30){
                utility(wbp, wbi, whp, whi, wsx, wsy, wang, angle, angle1, Iv, b, b1, b2, h, h1, h2, sx, sx1, sy,
                sy1, bp, bi, hp, hi, IFsy);
                break;
            }
            else{
                b = b*0.95;
                h = h*0.95;
            }
        }
        else break;
    }
    b = b1;
    h = h1;
    for(;;){
        if(angle >= 0 && angle <= 45){
            NNsigmay(angle, Iv, b, h, sx, sy, &IFsy);
            if(IFsy < 1.30){
                utility(wbp, wbi, whp, whi, wsx, wsy, wang, angle, angle1, Iv, b, b1, b2, h, h1, h2, sx, sx1, sy,
                sy1, bp, bi, hp, hi, IFsy);
                break;
            }
            else angle = angle + 7.5;
        }
        else break;
    }
    angle = angle1;
    for(;;){
        if(angle >= 0 && angle <= 45){
            NNsigmay(angle, Iv, b, h, sx, sy, &IFsy);
            if(IFsy < 1.30){
                utility(wbp, wbi, whp, whi, wsx, wsy, wang, angle, angle1, Iv, b, b1, b2, h, h1, h2, sx, sx1, sy,
                sy1, bp, bi, hp, hi, IFsy);
                break;
            }
            else angle = angle - 7.5;
        }
        else break;
    }
    angle = angle1;
    printf("\nMORE....Press any key to continue...\n");
    getch(); clrscr();
    }
```

C.6 Function for Calculating Utility Values of Alternatives

```
/** Calculates Utility Values of Feasible Alternatives **/
#include <math.h>
utility(wbp, wbi, whp, whi, wsx, wsy, wang, angle, angle1, Iv, b, b1, b2, h, h1, h2, sx, sx1, sy, sy1, bp, bi,
hp, hi, IF)
double wbp, wbi, whp, whi, wsx, wsy, wang; /** normalized weights of attributes **/
double angle, Iv, b, h, sx, sy, bp, bi, hp, hi, IF;
double angle1, b1, b2, h1, h2, sx1, sy1;
{
double sum;
double v; /** utility value **/

sum = fabs(angle-angle1) + fabs(bp-b2) + bp*fabs(b-b1) + fabs(hp-h2) + hp*fabs(h-h1) + bp*fabs(sx-sx1) +
bp*fabs(sy-sy1); /** for normalization **/
v = wang*fabs(angle-angle1)/sum + wbp*fabs(bp-b2)/sum + wbi*bp*fabs(b-b1)/sum + whp*fabs(hp-
h2)/sum + whi*hp*fabs(h-h1)/sum + wsx*bp*fabs(sx-sx1)/sum + wsy*bp*fabs(sy-sy1)/sum;

printf(" %7.1lf  %7.1lf %7.2lf %7.2lf %7.2lf %7.2lf %7.2lf %7.2lf %7.2lf %4.2lf\n", angle, Iv, bp, bi, hp, hi,
sx*bp, sy*bp, IF, v);
}
```

C.7 An Example NETWIND Consultation session

Note: User responses are shown in bold text.

```
      *****Welcome to NETWIND ver1.0 1997*****
NETWIND is a Neural Network based design adviser for
evaluating the effects of adjacent buildings on the wind-induced
loads on a building, generally known as INTERFERENCE EFFECTS.
The present version of NETWIND works best for two buildings of
different relative sizes in various upstream exposures with a
0 degree wind normal to the building face. Cases of oblique winds
work well for two similar buildings, in open exposure. Any other
case while producing generally acceptable results, may also
generate erroneous responses. Care should be exercised when
presenting such cases to NETWIND.

For details on interference effects refer the following material:

Khanduri, A. C. (1997). Evaluation and Generalization of Wind-
Induced Interference Effects on Buildings: Integrating
Experimental and Computerized Approaches. Ph.D. Thesis, Centre for
Building Studies, Concordia University, Montreal, Canada (under
preparation).

Khanduri, A. C., Stathopoulos, T. and Bedard, C. (1997). Wind-
Induced Interference Effects on Buildings: A Review of The State
of The Art. Journal of Engineering Structures (in press).

Do you want to proceed (Y/N): Y
```

```
You will now be asked to input data into NETWIND.
NETWIND expects the following inputs:
1) Incident wind angle in degrees (wind direction is assumed from
   left to right of the computer screen). Wind angle can vary
  from 0 to 45 degrees.
2) Upstream exposure: Choice between two modes of input:
   a) Select: open, suburban or urban exposures or
   b) Input: Longitudinal turbulence intensity of wind at
      building height(%)
3) Width of the building on which interference effects are to be
   evaluated (Principal building). The present version of NETWIND
   assumes square plan)
4) Width of the adjacent building (Interfering building)
5) Height of the principal building
6) Height of the adjacent building

NETWIND performs validation checks for erroneous inputs and also
ensures that inputs lie within the range that can be handled by
it.

Press any key to continue....
```

NETWIND output:

NETWIND invokes its Neural Network interference effects model to calculate INTERFERENCE FACTORS (ratio of wind load on the principal building with interference due to adjacent building, to the wind loads on it in isolated condition. The results are analyzed by the Conclusion-Analysis module that explains the severety of interference effects. Finally, the Design Assistance module evaluates, if needed, another set of alternatives that reduce interference effects.

Do you want to INPUT data or QUIT ? (Y/Q): **Y**

DATA INPUT SCREEN:

Use Uniform system of units (suggestion: use metres for length)

Wind direction (0 to 45 degrees, wind from right to left): **0**
Longitudinal turbulence intensity of wind (7% to 25%): **7**
Principal building width (square): **20**
Interfering building width (square): **20**
Principal building height (height/width = 3 to 5): **80**
Interfering building height (height/width = 2 to 8): **80**
Centre-to-centre spacing between buildings along X-axis: **70**
Centre-to-centre spacing between buildings along Y-axis: **60**

Proceed to RESULTS and ANALYSIS screen ? (Y/N): **Y**

```
RESULTS AND ANALYSIS

1. MEAN DRAG:

SAFE.  3 percent decrease in mean drag (IF = 0.97)
No significant interference effects.

MORE....Mean Lift....Press any key to continue....

2. MEAN LIFT:

SAFE.  Cl = 0.01
No significant interference effects

MORE....Fluctuating loads....Press any key to continue....
```

```
3. FLUCTUATING DRAG:

SAFE.  Only 14 percent increase in fluctuating drag (IF = 1.14)
No significant interference effects.

4. FLUCTUATING LIFT:

**HIGH FLUCTUATING LIFT**! (IF = 1.48)
High fluctuating lift should be of considerable concern, especially
in terms of serviceability requirements of the building. A
comprehensive wind tunnel model testing is recommended

Probable Reasons:
a) Upstream interfering building in wake-interaction region
   (Sx = 2bp to 8bp and Sy = 2bp to 6bp)
b) Interfering building wider and/or taller than principal
    building
c) Buildings in open exposure

Possible Remedies:
a) Move buildings away from the wake-interaction region
b) Position interfering building towards side of principal building
c) Locate interfering building close to principal building
d) Locate buildings in more turbulent suburban/urban exposures

Do you want NETWIND to implement necessary changes ? (Y/N): Y
```

NETWIND has used Neural Networks and its Knowledge Base to evaluate the effects of various input parameters on interference effects. The following guidelines have been used in arriving at the best configurations presented on the next screens:

MEAN DRAG: -0.15 <= IF < 1.30
MEAN LIFT: For wind angles <= 15 degrees: -0.20 <= Cl <= 0.20
For wind angles between 15 and 30 degrees: Cl <= 0.75
For wind angles > 30 degrees: Cl <= 1.10
FLUCTUATING DRAG: IF < 1.30
FLUCTUATING LIFT: IF < 1.30

Symbols used:
Angle: Incident wind angle; Iv: Longitudinal turbulence intensity of wind; bp: Width of principal building; bi: Width of interfering building; hp: Height of principal building; hi: Height of interfering building; Sx: Centre-to-centre distance between the buildings along the horizontal axis; Sy: Centre-to-centre distance between the buildings along the vertical axis; IF: Interference Factor Cl: Mean lift. E: Evaluation Factor

Press any key to go to NETWIND DESIGN ASSISTANCE SCREEN....

NETWIND DESIGN ASSISTANCE SCREEN

NETWIND selects the best option based on the relative importance or the rigidity of various input variables to design. INPUT the relative importance (0% to 100%) you would ascribe to each variable. Give a higher weight to the input variable you want modified the least.

IMPORTANCE FACTORS:

Input relative importance (0% to 100%) you would ascribe to each input variable. Give a higher % to the variable you want modified the least.

1) Principal building width: **100**
2) Interfering building width: **60**
3) Principal building height: **100**
4) Interfering building height: **40**
5) Centre-to centre spacing between buildings along X-axis: **20**
6) Centre-to centre spacing between buildings along Y-axis: **40**
7) Incident wind angle: **30**

Press any key to view NETWIND design alternatives....

NETWIND ALTERNATIVES
(Note: E is Evaluation Factor: select the alternative with low E)

Fluctuating Lift

Angle (°)	Iv (%)	bp (m)	bi (m)	hp (m)	hi (m)	Sx (m)	Sy (m)	IF	E
Original data									
0.0	7.0	20.0	20.0	80.0	80.0	70.0	60.0	1.48	-
NETWIND alternatives									
0.0	7.0	20.0	20.0	80.0	80.0	35.0	60.0	1.26	0.05
0.0	7.0	20.0	20.0	80.0	80.0	155.0	60.0	1.29	0.05
0.0	7.0	20.0	20.0	80.0	80.0	140.0	95.0	1.18	0.07
0.0	7.0	20.0	20.0	80.0	80.0	40.0	45.0	1.21	0.07
30.0	7.0	20.0	20.0	80.0	80.0	70.0	60.0	1.19	0.08
0.0	7.0	20.0	20.0	80.0	80.0	70.0	90.0	1.27	0.10
0.0	7.0	20.0	20.0	80.0	80.0	70.0	35.0	1.22	0.10

MORE....Press any key to continue....

Do you want to run NETWIND with new inputs or QUIT ? (Y/Q): Q

** Thank you for using NETWIND **

PRESS ANY KEY TO RETURN TO DOS